H3K9 trimethylation controls oncogenic signaling and the malignant state in mantle cell lymphoma

Azadeh Hajmirza

Communauté
UNIVERSITÉ Grenoble Alpes

THÈSE

Pour obtenir le grade de

DOCTEUR DE LA COMMUNAUTE UNIVERSITE GRENOBLE ALPES

Spécialité : **Biologie du développement - Oncogenèse**

Arrêté ministériel : 25 mai 2016

Présentée par

Azadeh HAJMIRZA

Thèse dirigée par **Pr. Mary CALLANAN**

préparée au sein de l'équipe **«Génétique et Epigénétique des cancers lymphoïdes»** Centre de Recherche Institute for Advanced Biosciences INSERM U1209-CNRS, UMR 5309

dans **l'École Doctorale Chimie et Sciences du Vivant**

H3K9 trimethylation controls oncogenic signaling and the malignant state in mantle cell lymphoma

Thèse soutenue publiquement le **« 15 décembre 2017»**, devant le jury composé de :

Pr. Dominique LEROUX
PU-PH, CHU de Grenoble / Institut pour l'Avancée des Biosciences
UGA - INSERM U 1209 - CNRS UMR 5309, Président

Pr. Jude FITZGIBBON
Directeur de recherche, Barts Cancer Institute (BCI), Rapporteur

Dr. Luisa DI STEFANO
Directeur de recherche, LBCMCP, Université Paul Sabatier, CNRS, Toulouse, Rapporteur

Dr. Saadi KHOCHBIN
Directeur de recherche, Institut pour l'Avancée des Biosciences
UGA - INSERM U 1209 - CNRS UMR 5309, Examinateur

Pr. Antoine MARTIN
Hôpital Avicenne AP-HP, Bobigny, France, Examinateur

Pr. Mary CALLANAN
PU-PH, Institut pour l'Avancée des Biosciences
UGA - INSERM U 1209 - CNRS UMR 5309, Examinatrice

Acknowledgement

I would like to especially thank all the members of the thesis jury, Pr. Dominique Leroux, Pr. Jude Fitzgibbon, Dr. Luisa Di Stefano, Dr. Saadi Khochbin, and Pr. Antoine Martin, who kindly accepted to evaluate my doctoral work.

I would like to thank Pr. Callanan for hosting me in her laboratory and supervising my PhD. Mary, it was a great honor for me to know you as a person and as a scientific and to work under your direction. I learned a lot from you during these years and the especial one that will stay with me is the attention to the details. Thank you for your trust and for providing a working environment with the freedom of developing individual creativity and autonomy.

I would like to thank the members of Pr. Callanan's team both in IAB building and in Grenoble hospital. I feel so lucky that I had the chance of working with them. Samuel, Sieme, Anouk, Patricia, and Thierry, I never felt like a foreigner between you. Thank you for being patient with me and my French, especially on my arrival, and for repeating the phrases several times when it was hard for me to understand and this with smile on your faces. Remy, Christine and Martine, thank you for your valuable inputs in the meetings and for your participation in the clinical part of the project. Thank you all for sharing your expertise and experiences with generosity and being available for questions and trouble-shootings.
Your presence also made my personal life in the institute more pleasant. Samuel, you taught me a lot about French culture, language, songs, and foods. Sieme thank you for being careful and proposing your help even before I ask for it. Anouk, thank you for the positive energy and the enthusiasm that you shared. Thank you for being available for helpful discussions each time I needed and for the inspirations. I am also grateful for your support during preparation of my thesis defense. Thierry, thanks for interesting statistical discussions and your intellectual and analytical input on my results. Also thank you for introducing me the regional mountains and beautiful spots to visit.

I would like to thank Dr. Khochbin and Dr. Rousseaux for their precious advises especially regarding to high throughput data analysis.

I would like to thank also my friends in the institute with whom we shared a lot of moments during our ‘challenge’. Sarah, I appreciated our discussions about our projects, our future, our concerns and our happiness. Thank you for your attentions and little post-its of ‘bon weekend’, ‘bon voyage’, and ‘bon vacances’, they always made me smiling. My especial thanks to Sanela for all the constructive conversations we had. Mahya, Alexander, Kate, Mathieu, Naghmeh, and Valentina, thank you for your helps, our gatherings and good memories.

I would like to acknowledge Société Française d’Hématologie (SFH) for funding last 6 months of my PhD work.

I am grateful to my parents and my family who were always encouraging me. Thank you for supporting me in my decisions and following my dreams. Thank you for helping me to be who I am and to build what I want.

Abstract

Mantle cell lymphoma (MCL) is an aggressive lymphoid cancer characterised by iterative clinical relapses and short survival. MCL displays complex genetics and hallmarks of misregulated expression of lineage specific genes. We have hypothesized that the latter might result from corruption of H3 lysine 9 trimethylation signaling, a key pathway for suppression of lineage inappropriate programs in somatic cells. By screening for H3K9me3 levels across a cohort of 120 MCL cases, we found global reductions of H3K9me3 in 1/3 of cases. This was linked to a dramatically altered H3K9me3 landscape defining two 'epigenetic subtypes' of MCL defined by distinct gene expression programs. Mechanistically, this could be linked to differential regulation of SUV39H1 and SETDB1 histone methyl transferase expression / activity respectively and activation of key cancer signatures relating to hypoxic signaling, embryonic/hematopoietic stem cell function, and B cell differentiation. In keeping with the pathological relevance of these findings, knockdown of SUV39H1 accelerated tumour growth in MCL xenografts while SETDB1 depletion induced G1/S arrest coincident to reprogramming to a pre-B cell-like phenotype. Taken together, this identifies convergence of H3K9me3 signaling pathways to essential targets for MCL disease initiation and progression.

Contents

List of figures

List of tables

Abbreviations

A

AID	Activation-Induced cytidine Deaminase
ASCT	Autologous-stem Cell Transplantation

B

B-ALL	B-cell derived Acute Lymphoblastic Leukemia
BCL-6	B-Cell Lymphoma 6
B-CLL	B cell Chronic Lymphocytic Leukemia
BCR	B-Cell Receptor
BET	Bromodomain and Extra-Terminal motif protein
BL	Burkitt Lymphoma
BRD	Bromodomain
BTK	Bruton's Tyrosine Kinase

C

CAF-1	Chromatin Assembly Factor 1
CD5	Cluster of Differentiation 5
ChIP	Chromatin Immunoprecipitation
CHX	Cyclohexemide
CLP	Common Lymphoid Progenitor
CSR	Class-Switch Recombination
CXCL12	C-X-C motif chemokine 12

D

DBR	Differentially Bound Region
DLBCL	Diffuse Large B-cell Lymphoma
DNMT	DNA methyltransferase
DSB	Double-Strand Breaks
dsRNA	Double Strand RNA
DTP	Drug-tolerant Population

E

Ebf1	Early B cell Factor
ERV	Endogenous Retroviruse
ESC	Embryonic Stem Cell

F

FAD	Flavin Adenine Dinucleotide
FDC	Follicular Dendritic Cell
FISH	Fluorescence In Situ Hybridization
FL	Follicular Lymphoma

G

GC	Germinal Center
GOF	Gain Of Function
GSEA	Gene Set Enrichment Analysis

H

HAT	Histone Acetyltransferase
HC	Heterochromatin
HDAC	Histone Deacetylases
HP1	Heterochromatin Protein 1
HSCs	Hematopoietic Stem Cells

I

ID2	Inhibitor of DNA binding 2
IDH	Isocitrate Dehydrogenase
IF	Immunofluorescent
IFN	Interferon
IgH	Immunoglobulin Heavy Chain
IGHV	Immunoglobulin Heavy-chain Variable Region
IHC	Immunohistochemistry
IKZF1	Ikaros
INCENP	Inner Centromere Protein
iPSC	Induced Pluripotent Stem Cell
IRF8	Interferon Regulatory Factor 8

J

JMJC	Jumonji C

K

KAP-1	KRAB-associated protein-1
KDM	Lysine Demethylase
KMT	Lysine Methyltransferase

L

LAD	Lamina Associated Domain
LDH	Lactic Hehydrogenase
LEF1	Lymphoid Enhancer Binding Factor 1
LINE-1	Long Interspersed Repeat Element 1
lncRNA	Long non-coding RNA
LSD1	Lysine-Specific Demethylase 1

M

MCL	Mantle Cell Lymphoma
MDM2	Mouse Double Minute 2 homolog
MDS	Myelodysplastic Syndrome
MEF	Mouse Embryonic Fibroblast

MLL	Mixed-lineage Leukemia
MLV	Murine Leukemia Virus
MM	Multiple Myeloma
MMSET	Multiple Myeloma SET-domain Protein
MPP	Multipotent Progenitor

N

NES	Nuclear Export Signal
NGS	Next-Generation Sequencing
NHL	Non-Hodgkin Lymphoma
NL	Nuclear Lamina
NSCLC	Non-small Cell Lung Cancer

O

OB	Osteoblasts
OPG	Osteoprotegerin
OS	Overall Survival

P

PAX5	Paired box protein 5
PC	Plasma Cell
PcG	Polycomb-Group Proteins
PI	Propodium Iodide
PRC1	Polycomb Repressive Complex 1
PRC2	Rpressive Complex 2
PTM	Posttranslational Modification

R

RAG1	Recombination-Activating Gene 1
RAG2	Recombination-Activating Gene 2
Rb	Retinoblasma protein
RRRs	Reprogramming Resistant Regions

S

SAHF	Senescence Associated Heterochromatin Foci
SCF	Stem Cell Factor
SET	(Su(var)3-9, Enhancer of zest, and Trithorax domain
SETDB1	SET domain bifurcated 1
SHM	Somatic Hypermutation
SIRT1	Sirtuin 1
SNT	Somatic Nuclear Transfer
SOX11	(SRY (Sex determining region Y)-box11
SOX4	Sex-determining region Y (SRY) box 4

T

TAD	Topologically Associated Domain

TE	Transposable Element
TET1	Ten-eleven Translocation dioxygenase 1
TF	Transcription Factor

U

USP7	Ubiquitin-specific-processing Protease 7

W

WES	Whole-Exome Sequencing
WGS	Whole-Genome Sequencing

X

XBP1	X-box Binding Protein 1

Z

ZFP	Zinc Finger Protein

Introduction

Chapter 1: Overview on B-cell normal development and malignancies

1.1. Hematopoiesis

In mammals, all types of blood cells are raised from a small population of pluripotent hematopoietic stem cells (HSCs), residing in the bone marrow niche of adult individuals. During blood cell development (hematopoiesis), differentiation potential of these cells become progressively restricted and leads to generation of different types of multipotent progenitors which are, in turn, capable of developing committed progenitors and all of the mature cells in the blood system, including red blood cells, megakaryocytes, myeloid cells (monocyte/macrophage and neutrophil), and lymphocytes (Figure 1). Self-renewal capacity of HSCs ensures continuous production of sufficient, but not excessive, numbers of cells of all lineages (Lampreia et al., 2017; Orkin and Zon, 2008; Wang and Wagers, 2011).

Differentiation of hematopoietic stem cells into distinct cell types with a high turn-over is fine-tuned by different regulators including cytokines, growth factors, cell cycle regulators, chromatin modifiers, and transcription factors (TFs). Perturbation of this regulatory network, especially via deregulation of hematopoietic TFs (Figure 1, red bars) impairs complete differentiation and can lead to development of hematopoietic malignancies, including different types of lymphoma and leukemia.

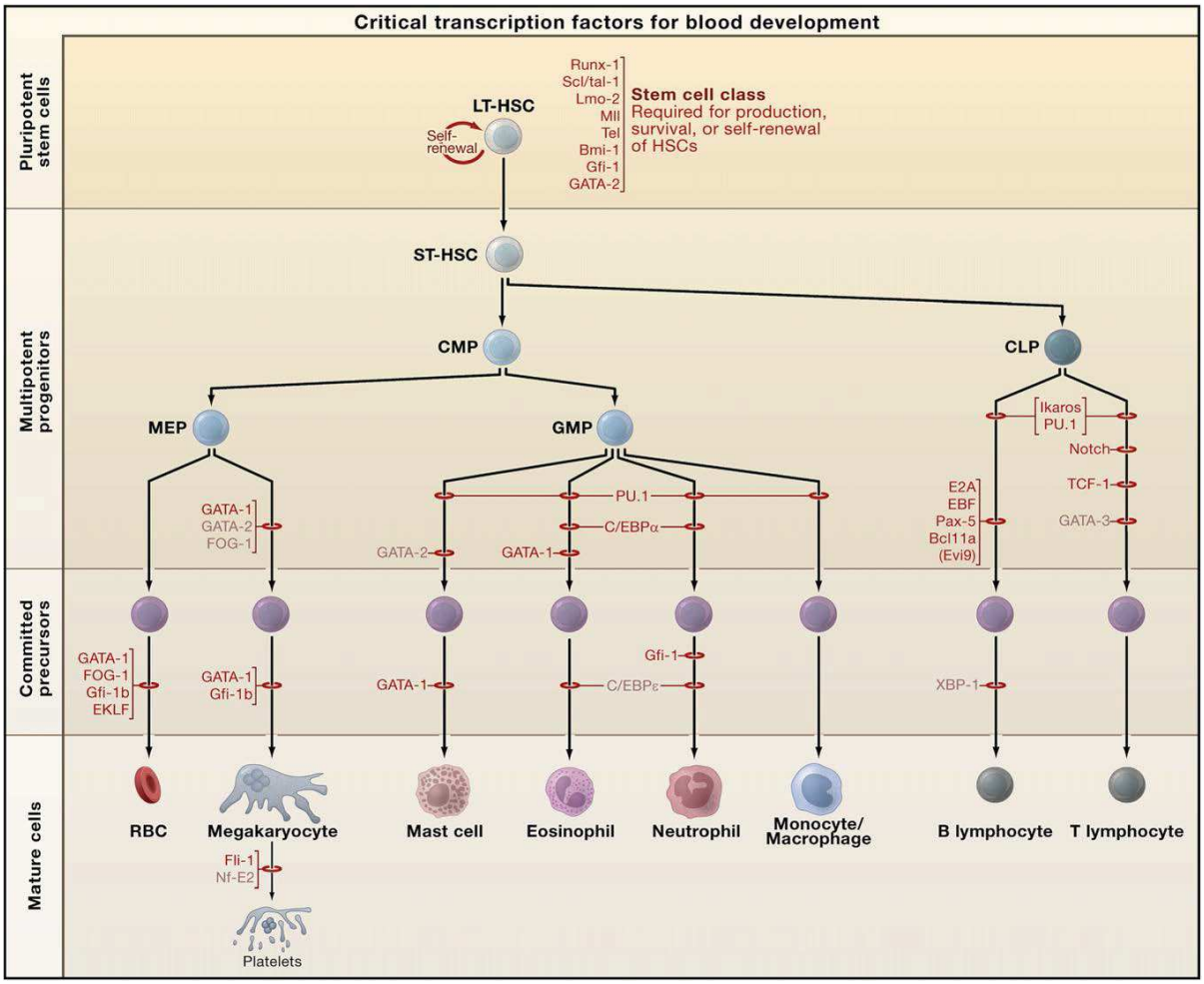

Figure 1. Schematic illustration of working model for normal hematopoiesis.
LT-HSC, long term hematopoietic stem cell; ST-HSC, short term hematopoietic stem cell; CMP, common myeloid progenitor; CLP, Common lymphoid progenitor; MEP, megakaryocyte-erythrocyte progenitor; GMP, granulocyte-monocyte progenitor. From (Orkin and Zon, 2008).

1.2. B-cell development

The development of functional B lymphocytes is a multistep and highly ordered process that relies on activation of B lineage genes as well as restriction of alternative cell fates in multipotent progenitors (MPPs). Bone marrow stromal cells create distinct microenvironments, known as niches, which together with expression of stage-specific TFs provide support for B-cell development (Matthias and Rolink, 2005), (Nagasawa, 2006). Commitment of common lymphoid progenitor (CLP) to the B-cell lineage in bone marrow is regulated by key transcription factors such as IKZF1 (IKAROS) PAX5, E2A, and LEF1 (Figure 2).

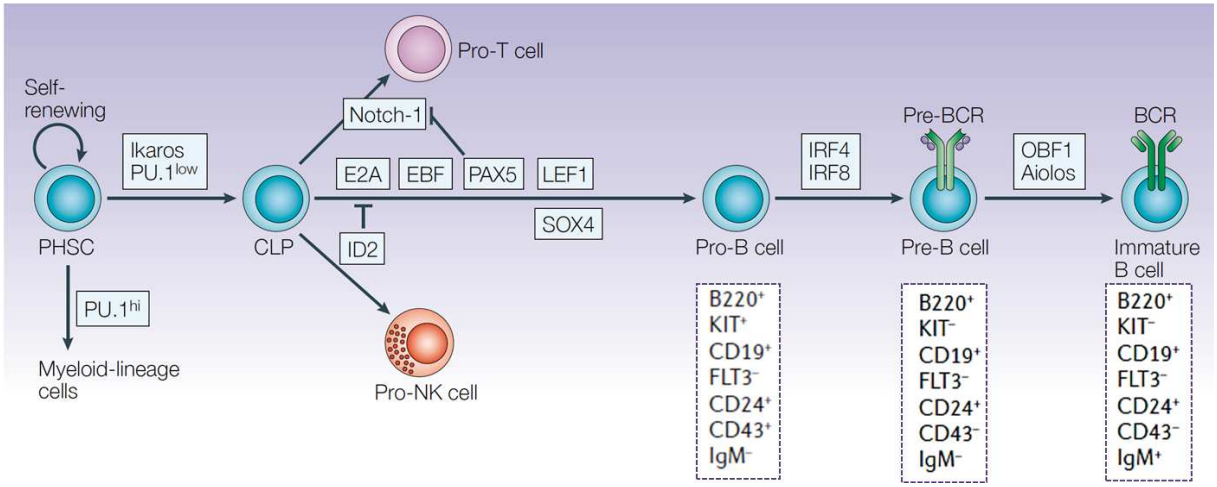

Figure 2. The genetic control of B-cell specification and commitment in the bone marrow
Key regulating transcription factors are indicated in solid boxes. Cell surface markers associated with the three main steps of early B-cell development are indicated in dashed line boxes. BCR, B-cell receptor; EBF, early B-cell factor; IRF, interferon-regulatory factor; LEF1, lymphoid-enhancer-binding factor 1; OBF1, OCT (octamer-binding transcription factor)-binding factor 1; PAX5, paired box protein 5; PHSC, pluripotent haematopoietic stem cell; SOX4, sex-determining region Y (SRY) box 4; ID2, inhibitor of DNA binding 2. Adapted from (Nagasawa, 2006) and (Matthias and Rolink, 2005).

Rearrangement of the immunoglobulin genes starts gradually at this time window in bone marrow in three distinct stages of early B cell development: VDJ rearrangement of the IGH locus takes place at pro-B cell stage, the cells that have undergone productive $V_HD_HJ_H$ rearrangement express membrane μ chains with surrogate light chains in the pre-B receptor at Pre-B stage followed by expression of cell surface immunoglobulin (i.e. IgM) formed by combination of heavy and light chains in immature B cell stage (Martin-Subero and Oakes, 2017). The endonuclease enzymes RAG1 and RAG2, encoded by recombination-activating genes 1 and two respectively, are essential for initiating V(D)J recombination by introducing DNA double-strand breaks (DSBs) in the recombination sites (Figure 3a) (Cooper, 2015), (Notarangelo et al., 2016).

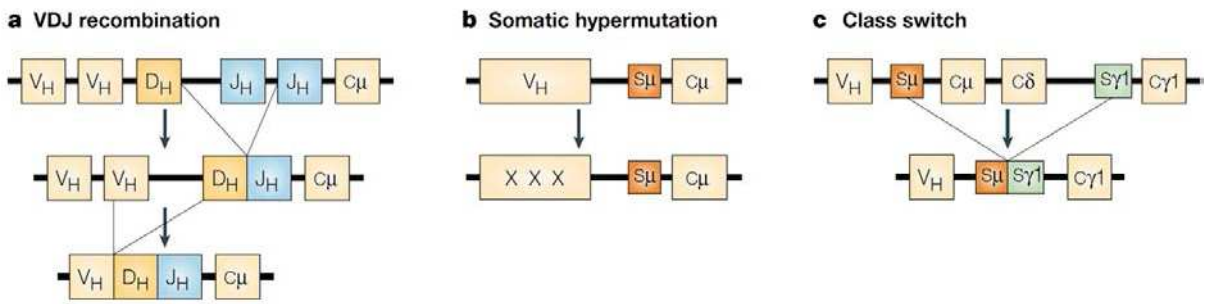

Figure 3. Molecular processes that remodel immunoglobulin genes

Immunoglobulin (Ig) genes are composed of variable (V) regions and constant (C) regions, which interact with antigen and mediate the effector functions of Igs respectively. Diverse repertoire of functional Igs are created by rearrangements in DNA segments that encode the heavy (H)- and light (L)- chain (not shown) regions of the variable genes.

a) First, during 'V(D)J recombination', B-cell precursors carry out D_H–J_H rearrangements in H-chain genes. These D_H–J_H rearrangements are followed by V_H–D_HJ_H rearrangements and result in encoding the heavy chain variable region. Pre-B-cell receptor is then expressed if the rearrangement is productive. The cells then carry out rearrangements at their L-chain loci (not shown). The V regions of the κ- and λ-light chains, alternatively, are each encoded by two gene segments — the V_L and J_L genes (not shown). The V-region of the Ig gene is ultimately connected to the C-region of the Ig gene (Cμ of IgM in diagram).

b) Somatic hypermutation in the GC leads to the introduction of point mutations, deletions or duplications in the rearranged V-region of Ig genes, denoted by 'Xs' in the figure, without affecting the downstream Cμ region.

c) Class switching results in the replacement of the originally expressed H-chain C-region gene with that of another Ig gene. In the diagram, the C-region for IgM (Cμ) and IgD (Cδ) are exchanged for the C-region of IgG (Cγ1) by recombination at the switch regions for these genes (Sμ and Sγ1, respectively). This results in an antibody with different effector functions but the same antigen-binding domain. Adapted from (Kuppers, 2005).

BCR–expressing immature B cells then leave the bone marrow to the periphery and are referred to as transitional 1 and 2 (T1 and T2) B cells, which give rise to naive mature B cells (Kurosaki et al., 2010).

These naive B cells circulate through secondary lymphoid organs, such as lymph nodes and Peyer's patches after having contact with antigen. At the outer T cell zones of secondary lymphoid tissues they receive cognate T cell help, and differentiate along one of two pathways: an extra follicular pathway, which gives rise to short lived plasmablasts (PCs), or a follicular pathway, which gives rise to germinal center (GC) founder B cells. Highly-proliferating cells in dark zone of GC, called centroblasts, undergo somatic hypermutation (SHM) of the immunoglobulin (Figure 3b) and further differentiate into centrocytes and move

to the light zone, where they undergo positive and negative selection depending on their increased or decreased affinity of their B-cell receptors, respectively.

Newly generated centrocytes that produce an unfavorable antibody undergo apoptosis and are eliminated. Selected centrocytes undergo immunoglobulin class-switch recombination (CSR) by activation-induced cytidine deaminase (AID) (Figure 3c), and eventually, they differentiate into high-affinity memory (M) and plasma cells (PCs) (Martin-Subero and Oakes, 2017).

Germinal-center events are also regulated by transcription factors such as BCL-6, IRF8, MTA3, NF-κB, BLIMP1, and XBP1.

1.2.1. Role of chemokines in B-cell maturation

Different stages of B cell maturation in bone marrow and GC also rely on chemokines which are produced by stromal cells of the respective zones (Figure 4).

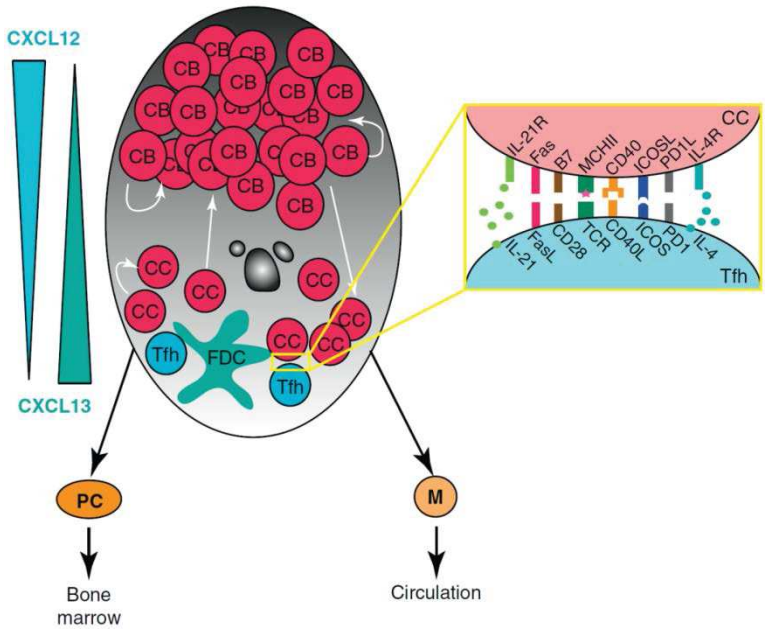

Figure 4. Germinal center regulation of B-cell differentiation.
Left: chemokine gradient within the germinal center; middle: GC reactions in dark and light zones and potential fates; right box: interaction of the B-cells with follicular helper T cells (Tfh) in the light zone of GC. CBs (centroblasts) CBs are located in the dark zone (black shading) where they proliferate and undergo SMH of their B cell receptor. CBs that migrate to the light zone (grey shading) are referred to as centrocytes (CCs). CCs downregulate CXCR4 and migrate to the light zone in response to CXCL13, which is produced by FDCs. CCs have several potential fates (arrows). These include: (i) apoptosis, if cells are unable to bind antigen and/or gain T follicular helper cell (Tfh) cell help; (ii) return to the dark zone for further proliferation and SMH; and (iii) selection to differentiate into long-lived PCs or memory B cells (M). Long-lived PCs reside in the bone marrow, whereas memory B cells can recirculate. The factors that govern CC fate or selection are not fully understood; some key interactions between CCs and Tfh cells are shown on the right. Adapted from (Zotos and Tarlinton, 2012).

For example, C-X-C motif chemokine 12 (CXCL12), stem cell factor (SCF), interleukin-7 (IL-7), receptor activator of nuclear factor κB ligand (RANKL), and osteoprotegerin (OPG), produced by bone marrow 'stromal cells', including mesenchymal stem cells/multipotent stromal cells (MSCs) and osteoblasts (OBs), are critical for early B cell development (Manilay and Zouali, 2014). Circulation of B cells between light zone and dark zone of GC is mediated by chemokine gradient. For example dark zone is more enriched for CLCX12 whereas it is reduced and replaced by CLCX13, produced by follicular dendritic cells (FDC) in the light zone (Zotos and Tarlinton, 2012). Going back to the bone marrow plasmablasts depend on IL6 to precede terminal differentiation to the plasma cells.

1.2.2. Epigenetic regulation of B-cell development

Similar to other cell types, B-cell development is also coupled to expanded epigenome changes specific to each stage. Loss of function studies in transgenic mice revealed that in addition of key TFs, epigenetic modifiers are also crucial for activation of lineage-specific genes and the repression of lineage-inappropriate genes during B cell development.

For example deficiency of polycomb-group proteins (PcG) is associated with defective development and/or function of lymphocytes. Expression of PcG genes undergoes marked changes during the various stages of B cell differentiation. Polycomb repressive complex 1 and 2 (PRC1 and PRC2) are two major complexes (PcGs) which are responsible for mono-ubiquitination of histone H2A at lysine 119 (H2AK119ub1) and methylation of histone H3 at lysine 27 (H3K27) respectively. Expression of BMI-1 and EZH2, catalytic subunits of PRC1 and PRC2 complexes respectively, alternates during the various stages of GC B-cell development (Raaphorst et al., 2001). Inactivation of the bmi-1 in the germ line of mice was associated with progressive decrease in the number of lymphoid and myeloid cells resulting in cellularity defects in bone marrow, thymus and spleen of bmi-1 $^{-/-}$ mice (van der Lugt et al., 1994).

Deficiency in Ezh2, catalytic subunit of PRC2 complex, impairs both generation of pre-B cells and immature B cells in mice bone marrow, due to reducing rearrangement of the immunoglobulin heavy chain gene (Igh), and the germinal center formation (Su et al., 2003), (Beguelin et al., 2016).

Yamaguchi et al., showed that presence of at least one of the two major histone deacetylases, HDAC1 and HDAC2, is strictly required for the B-cell development. This study showed that elimination of both enzymes at early stages of B cell development leads to a dramatic block at the pre B-cell stage, accompanied by G1 arrest and apoptosis induction (Yamaguchi et al., 2010).

Class-switch recombination (CSR) in mouse primary B cells have been showed to be associated with the accumulation of SUV4-20H enzymes and H4K20 trimethylation levels at the Sμ sites of the *IgH* locus (Rodriguez-Cortez et al., 2017).

Finally, DNA methyltransferases (DNMTs), particularly DNMT1, are also essential for hematopoiesis and B cell differentiation. DNA methylation is a dynamic epigenetic mark that undergoes extensive changes during differentiation of self-renewing stem cells. It has been shown that DNA methylation is required to maintain HSC self-renewal capacity and the homeostasis within the HSC pool. Mouse HSCs with reduced Dnmt1 activity cannot suppress key myeloerythroid regulators and give rise into myeloerythroid, but not lymphoid, progeny (Broske et al., 2009).

DNMT1 is also required later at GC forming stages. *Dnmt1* hypomorphic mice or DNA methyltransferase inhibition by Decitabine resulted in deficient/failure GC formation accompanied by increased DNA damage (Shaknovich et al., 2011).

Global DNA methylation profiles also changes during B cell development. GC B cells are predominantly hypomethylated compared to naive B cells and GC B cells also exhibit greater DNA methylation heterogeneity than naive B cells (Shaknovich et al., 2011). This massive reconfiguration of the DNA methylome in B cells also affects heterochromatin/nuclear lamina associated domains (LADs), DNA repeats and polycomb repressed regions.

Taken together, B-cell differentiation is a far complex process that relies on programed action of multiple factors in precise microenvironments and time windows. A schematic illustration of different regulatory layers during B-cell development including key TFs, microenvironmental shifts and epigenetic changes are represented in Figure 5.

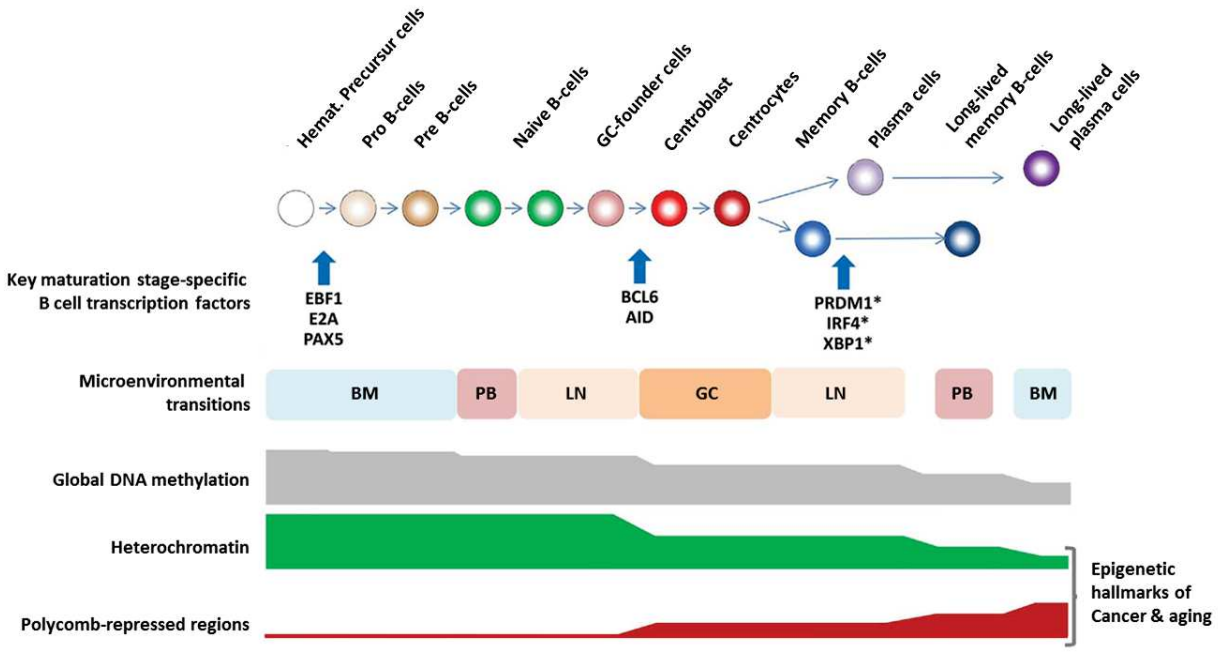

Figure 5. Integrative scheme of B cell differentiation
* Expression of these transcription factors is plasma cell specific (not related to long-lived memory B cells). Adapted from (Martin-Subero and Oakes, 2017)

1.3. B-cell malignancies are derived from disruptions in particular maturation/activation stages

Miss-regulations in different steps of B-cell differentiation, particularly gene rearrangements involved in establishment of immunoglobulin diversity and antigen response, could disturb the homeostasis of normal differentiation, proliferation and apoptosis of these cells leading to malignant transformations. B-cell malignancies, including lymphoma, leukemia, and myeloma, are frequently associated with chromosomal translocations, gene mutations, and additional genetic aberrations such as hyperploidy and aneuploidy. Most of the chromosomal translocations are due to aberrations that occur during DNA rearrangements at immunoglobulin genes, including V(D)J rearrangements in bone marrow, class-switch recombination (CSR) and somatic hyper mutations (SHM) in GC. These processes are required for B-cell receptor (BCR) formation, diversity, and affinity but represent a threat to the B-cell genome stability. The genetic aberrations in B-cell malignancies target frequently key TFs, signaling pathways, and epigenetic regulators which are important in different stages of B-cell differentiation (Table 1).

Category	Genes	Diseases
Epigenetic	CREBBP, EP300	DLBCL, FL
	EZH2, KMT2D (MLL2), KDM2B, KDM6B	DLBCL, FL, MCL
	HISTH1B/C/D/E	CLL, DLBCL, FL
	ARID1A, MEF2B, MED12	CLL, DLBCL, FL
	CHD2, SMARCA4	CLL, DLBCL
Signaling	CD79B, CARD11, IRF8, GNA13, STAT3/6, MYD88, NOTCH1, PRDM1, SGK1, TNFAIP3, TNFRSF14, TRAF3, BIRC3, PIM1	CLL, DLBCL, FL, MCL
TFs	FOXO1, EBF1, POU2F2	DLBCL
	BCL6	DLBCL
Growth, survival, genome maintenance	MYC, BCL2, FAS, PIM1, CCND1, TP53, ATM, POT1, BIRC3	CLL, DLBCL, FL, MCL
mRNA processing	SF3B1, XPO1	CLL

Table 1. Frequent mutations in B-cell lymphomas. From .*(Greiner et al., 2006; Koues et al., 2015)*

According to the stage of differentiation that is impaired, different types of B-cell neoplasms can be raised (Figure 6).

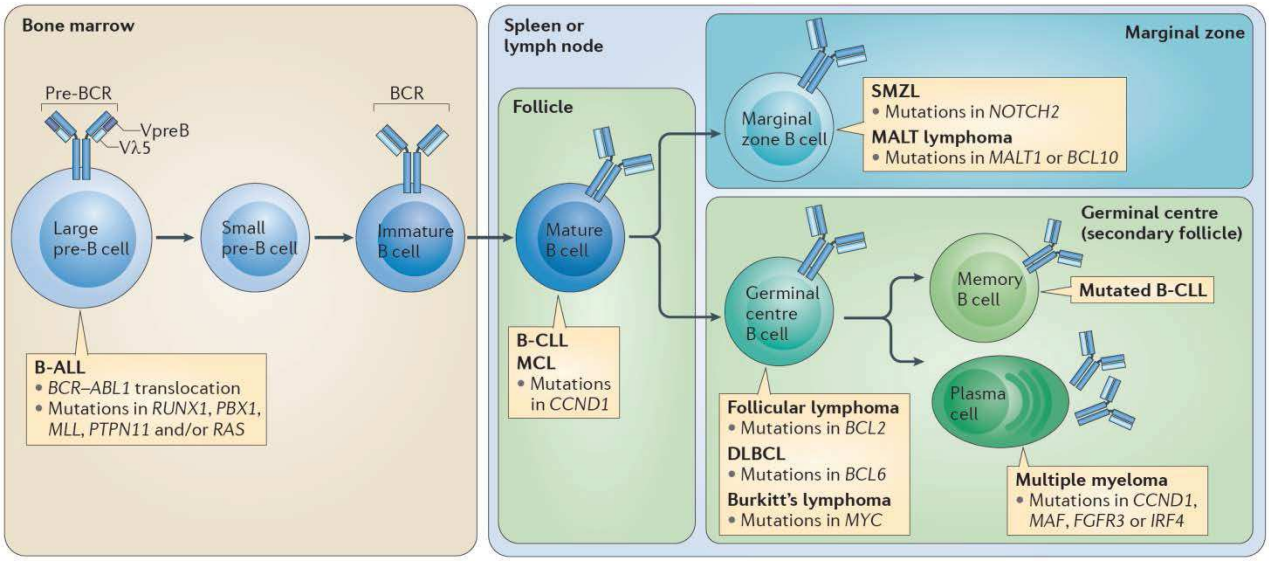

Figure 6. B cell neoplasms arise at different stages of B cell differentiation. From (Rickert, 2013).

Most frequent B-cell derived malignancies are briefly presented below.

1.3.1. Leukemia

B-ALL (B-cell derived acute lymphoblastic leukemia): accounts for the majority of ALL cases with predominance in children and adolescents. B-ALL is derived from the proliferative pro-B cell or pre‑B cell compartment in the bone marrow.

B-CLL (B cell chronic lymphocytic leukemia) is one of the most common types of adult leukemia which has often an indolent clinical course. Unmutated subtype of B-CLL derives from mature $CD5^+$ B cells whereas *IGHV*-mutated CLLs are proposed to be derived from post-GC B cells (Kipps et al., 2017), (Seifert et al., 2012). The unmutated subtype is associated with a worse clinical prognosis.

1.3.2. Myeloma

Multiple Myeloma (MM) is an incurable malignancy of plasma cells and constitutes approximately 10% of all hematological malignancies. Plasma cells are the terminally differentiated B-cells that produce disease- and infection-fighting antibodies. Myeloma cells prevent the normal production of antibodies, leading to weakened immune system and high risk to infection. Reciprocal chromosomal translocations between one of the immunoglobulin loci and various other genes, including the histone modifying enzyme MMSET (multiple myeloma SET-domain protein), also called *WHSC1* are considered to be primary oncogenic events.

1.3.3. Lymphoma

Hodgkin lymphoma (HL): Accounts for 11 % of all lymphoid malignancies, and is highly curable in most instances. It can be subdivided into a classical subtype and a less common nodular lymphocyte predominant subtype with a clonal B-cell origin (Gobbi et al., 2013; Jones et al., 2009).

Non-Hodgkin lymphoma (NHL): NHL consists a group of B cell malignancies that includes both aggressive (rapidly growing) and indolent (slow-growing) types**.** Some

examples are briefly presented below and largely reviewed in (Kuppers, 2005; Rickert, 2013; Scott and Gascoyne, 2014; Shaffer et al., 2002). Some subtypes of NHL are described below.

Diffuse large B-cell lymphoma (DLBCL): Is the most common type of NHL (30–45% of cases). DLBCLs are clinically, morphologically and molecularly heterogeneous. DLBCL is composed of the activated B cell (ABC)-derived and the GC B cell (GCB)-derived subtypes. BCL6 and BCL2 abnormalities are recurrent. 5-year overall survival (OS) is 60%.

Follicular lymphoma (FL) is a nodal B-cell lymphoma with a follicular growth pattern and represents 22% of NHLs. It is often indolent (median OS>10 years), and is mostly characterized by the overexpression of BCL-2 due to the t(14;18) translocation. Lymphoma cells morphologically and phenotypically resemble GC B cells.

Marginal-zone lymphoma/ MALT lymphoma: comprises 7–8% of all B-cell lymphomas. This lymphoma, originated from marginal zone B-cells, develops mostly in non-lymphoid tissues such as the stomach, lungs, and salivary glands. Overexpression of MALT lymphoma translocation protein 1 (MALT1) or the inhibitor of apoptosis protein 2 (IAP2)–MALT1 fusion protein as well as gastric inflammation caused by chronic Helicobacter pylori infection are considered as disease drivers for this type of lymphoma. It has mostly an indolent behavior with a 5 year OS of ~85%.

Burkitt lymphoma (BL) represents 1-2% of B-cell lymphomas with an aggressive clinical course in both children and young adults. More than 95% of the cases are associated with c-*MYC* rearrangements mostly due to the t(8;14) translocation. It is a curable lymphoma in more than 80% of cases.

Lymphoplasmacytic lymphoma is a rare form of NHL that comprises 1-2% of nodal lymphomas. It is usually indolent, with a median OS of 5-10 years. Bone marrow, lymph nodes and spleen are frequently involved. Post GC B-cells are considered as the origin of disease. Tumor-cell population is composed of small B cells, plasmacytoid lymphocytes and plasma cells. Most patients present with a serum monoclonal protein, usually of the IgM type. A subset of lymphoplasmacytic lymphomas is characterized by recurrent t(9;14),which involves the *PAX5* (paired box gene 5) and *IGHV* loci.

Mantle-cell lymphoma (MCL) is B-cell lymphoma that localizes to the mantle region of secondary follicles. MCLs comprise 6% of all NHLs, with a male predominance

and occur at a median age of 60. MCL features are presented more widely in the next chapter.

Chapter 2: General introduction of Mantle cell lymphoma

2.1. General characteristics

Mantle cell lymphoma accounts for 5–10% of non-Hodgkin lymphoma and represent a spectrum from indolent to aggressive disease with a male predominance and median age of 60 years old. MCL is raised from abnormal proliferation of B-cells in mantle zone of lymphoid follicles. The majority of MCL B-cells are similar to naïve B-cells however, less than 40% of cases could also show somatic hypermutation (SHM), a characteristic of germinal center experienced B cells. MCL is a heterogeneous disease and shows as well disparate response so the responds to the current therapies. MCL shows relatively short remission duration and frequent relapses despite the good initial responds to the standard treatments and remains almost incurable in advanced stages. This indicates the importance of therapeutic innovations that take into account the individual varieties of oncogenic factors (Martin et al., 2017; Scott and Gascoyne, 2014).

The majority of MCL cases are already in advanced stages of disease at diagnosis level and show blood, bone marrow (~60%), nodal and extranodal involvement including gastrointestinal tract involvement (Vose, 2017). Recurrent symptoms are lymph node enlargement, fever, night sweats, fatigue, loss of appetite and weight (Wang and Ma, 2014).

2.2. Diagnosis

Diagnosis is based on combination of different techniques made on lymph node, bone marrow or blood biopsies.

At morphological levels, the samples show the classic morphology of small to medium sized lymphoid cells with irregular nuclear contours, somewhat dispersed chromatin, inconspicuous nucleoli and scant cytoplasm in 80-90% of cases (Pileri and Falini, 2009). 10-20% of MCL cases present other cytological variants of MCL cells known as blastoid, pleomorphic and

small cell MCL with a high mitotic rate and more aggressive clinical evolution associated with blastoid and pleomorphic variants (Figure 7).

According to the stage of disease MCL cells invade non mantle zone regions within the lymph node and change from a mantle zone to nodular or diffuse growth pattern ending up to effacement of the organ's structure (Jares and Campo, 2008).

MCL immunophenotype is determined by immunohistochemistry (IHC) or FACS analysis (fluorescent activated cell sorting) to recognize presence of CD5, CD19, CD20, IgM, and IgD and absence of CD10 and CD23. Presence of CD20 and absence of CD23 helps distinguishing MCL from other chronic B cell malignancies such as chronic lymphocytic leukemia (CLL), which shows otherwise high similarity to MCL cells.

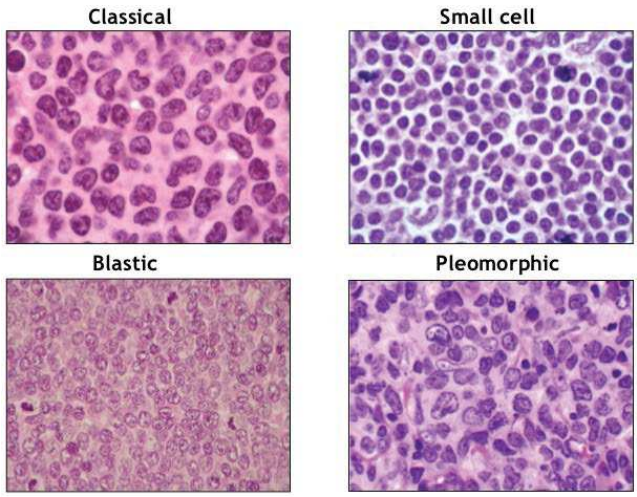

Figure 7. Morphological subtypes of MCL

At cytogenetic level, MCL is characterized by presence of t(11;14)(q13;q32) translocation in more than 95% of cases and is known as the primary oncogenic hit in MCL. This translocation takes place in bone marrow at pre-B stage of B-cell development and is detected by FISH (fluorescence *in situ* hybridization) technique. This chromosomal alteration displaces *CCND1* gene from its normal location on chr11 to the chr14q32 where its expression will be under control of regulatory elements of highly expressed *IGH* gene, located on this region. Consequently the gene product, called CYCLIN D1, which is usually undetectable in normal lymphocytes, becomes over expressed in MCL cells (Sander et al., 2016). CYCLIN D1 is a major regulator of cell cycle and participates also in cell cycle independent processes such as cell migration, DNA damage response and cell differentiation via interaction with different partners including transcription factors, chromatin-remodeling, and histone-modifying enzymes (Bienvenu et al., 2010; Fu et al., 2004; Musgrove et al., 2011).

More than 95% of MCL cases represent overexpression of *CCND1* nonetheless, a few CYCLIN D1 negative cases have been identified which show overexpression of CYCLIN D2 or D3 instead (Rosenwald et al., 2003). Cytogenetic techniques also revealed several additional abnormalities in chromosomes including deletions, gains and chromosomal aneuploidy. Sarkozy et al., showed that karyotype analysis can provide survival information at the diagnostic stage. This study showed that a complex karyotype is associated with a shorter survival time and indolent patients (iMCL), which will have a less aggressive disease evolution, could be identified at the time of diagnosis based on a less complex karyotype (Sarkozy et al., 2014).

At molecular level, the majority of MCL cases are unmutated in *IGHV* locus, however 15-40% of cases show hypermutated immunoglobulin (*IGHV*) genes. Leukemic non-nodal MCL cases with stable karyotypes and a better overall survival (OS) have frequent *IGHV* mutations (Bea and Amador, 2017).

2.3. Prognostic factors

Three main prognostic factors in MCL are the blastoid morphology, the proliferation index measured by Ki67 expression and the mantle cell lymphoma international prognostic index or MIPI score, which takes in account the age of the patient, the hemoglobin level, the lactic dehydrogenase (LDH) level, as well as the presence of leukocytosis (Sarkozy et al., 2014). According to MIPI score patients are stratified into three different groups of low, intermediate and high risk in which median survival changes is not reached (5-year OS, 60%) or is 51 months or 29 months, respectively.

2.4. Oncogenic events in MCL

The t(11;14)(q13;q32) translocation and consequent *CCND1* overexpression is the hallmark of MCL disease. However CYCLIN D1 is a weak oncogene. Eμ-Cyclin D1 transgenic mice showed only very subtle alterations in the cycling behavior of B-cell populations compared with normal mice and did not develop lymphoid tumors (Lovec et al., 1994). Also downregulation of CYCLIN D1 showed minimal inhibitory effects on cell cycle and survival of MCL cell lines (Klier et al., 2008). Thus it seems that secondary oncogenic events contribute to MCL development.

2.4.1. Recurrent chromosomal alterations in MCL

Indeed, as mentioned previously, MCL displays a high degree of genomic instability. More than 90% of MCLs display highly altered genomes harboring chromosomal translocations (with the most frequent translocation of *MYC* with *IG* genes), gains and losses of the genome such as 3q, 7p, 8q(*MYC*) and 10p (*BMI1*) gains (Bea et al., 1999) and 13q, 9p (*CDKN2A, CDKN2B*), 9q and 6q, 11q (*ATM*), and 17p (*TP53*) (Sarkozy et al., 2014) deletions. These aberrations are mostly identified by FISH, low resolution metaphase CGH, and high resolution CGH-array and SNP-array and impair several cellular pathways (BCR, BAFF-R, mTOR, WNT, and NOTCH1 signaling) involved in different cellular functions (DNA repair response, cell proliferation and cell survival) in the favor of MCL development (Royo et al., 2011; Sander et al., 2016). These altered pathways could be susceptible to targeted therapies in MCL (Figure 8).

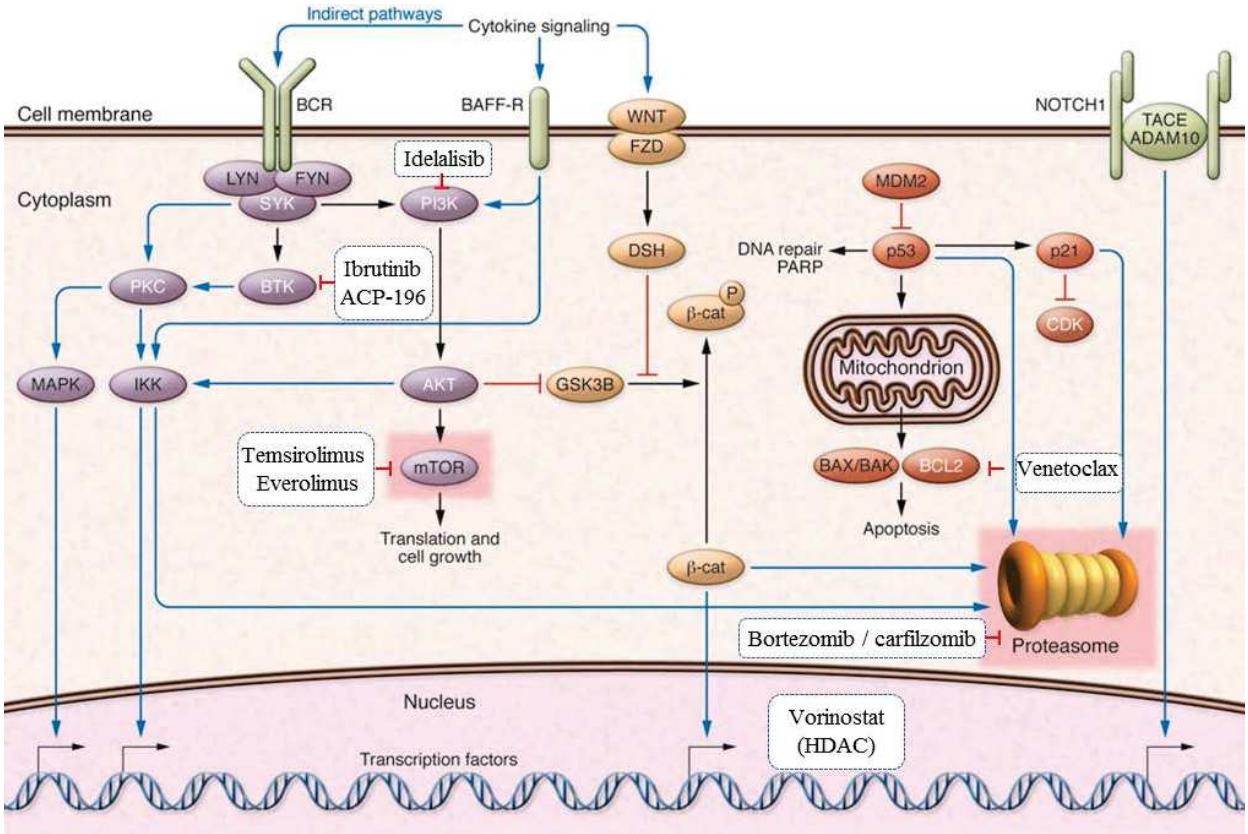

Figure 8. Major aberrant cellular pathways in mantle cell lymphoma targeted by novel mechanism-based treatments

BCR, BAFF-R, mTOR, WNT, and NOTCH1 signaling pathways are constitutively active in MCL, leading to cell survival and cellular growth. Novel therapies that inhibit critical elements of B-cell receptor signaling pathway are shown in white boxes. Temsirolimus, bortezomib, ibrutinib, and lenalidomide (the cereblon-binding agent, not shown in the image) have been approved by the Food and Drug Administration (FDA) for patients with relapsed/refractory disease. Adapted from (Cheah et al., 2016; Jares et al., 2012).

2.4.2. Recurrent gene mutations in MCL

Recently, by using next-generation sequencing (NGS) of whole-exome (WES) or whole-genome (WGS), or RNA-sequencing a total number of 552 MCL primary samples were analyzed to describe the landscape of recurrently mutated genes in MCL by six different studies (Bea et al., 2013; Greiner et al., 2006; Kridel et al., 2012; Meissner et al., 2013; Rahal et al., 2014; Zhang et al., 2014)(Rossi D et al, Blood 2015 126:336). These studies revealed the recurrent gene mutations in MCL which are targeting different cellular functions such as cell cycle control & DNA damage pathways (*ATM*, *CCND1* and *UBR5*), apoptosis & tumor suppression (*TP53*, *BCL2*), developmental signaling pathways (*NOTCH1, BIRC3, BIRC2, TRAF2/3, BTK*) and also epigenetic modifiers of histones (*MLL2/3*, *WHSC1, SMARCA4)* (Figure 9).

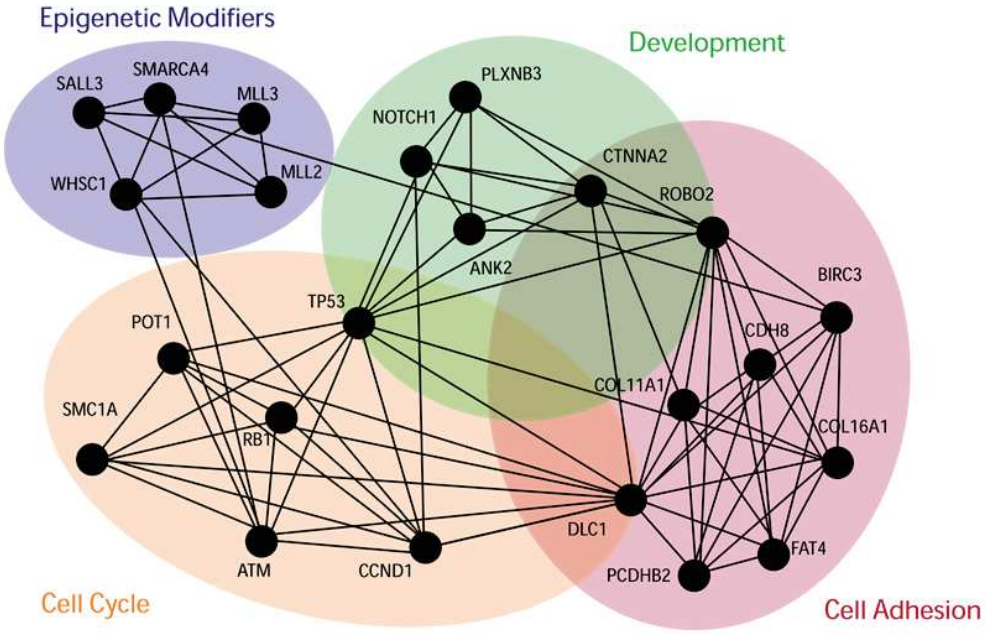

Figure 9. Functional network of mutated genes in MCL. From (Zhang et al., 2014).

These genetic lesions and related impaired pathways could impact the therapeutic strategies and patient outcome. For example, Olaparib and Veliparib, two PARP inhibitors, enhanced cyto-toxicity in MCL cells harboring mutations in both *ATM* and *p53* (Williamson et al., 2012). Mutations in *BIRC3*, *TRAF2*, or *MAP3K14* induce resistance to Ibrutinib and Sotrastaurin, inhibitors of BTK and PKC receptivity, via activation of an alternative NF-κB

pathway which is not dependent on BTK and PKC (Rahal et al., 2014) (Figure 10A). Mutations in PEST domain of NOTCH1, leading to the constitutive activation of the protein, as well as *p53* mutations were shown to be associated with a shorter overall survival of patients (Figure 10 B-C) (Kridel et al., 2012).

A)

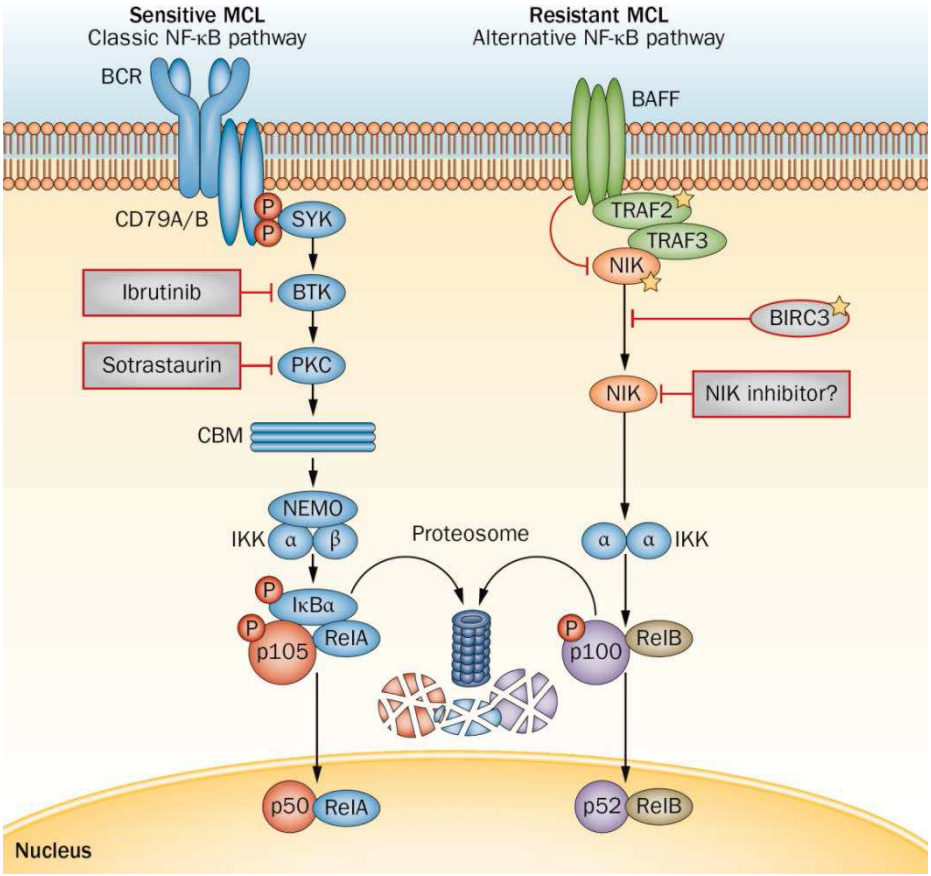

B)

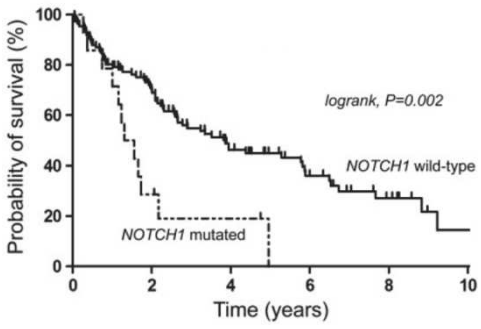

C)

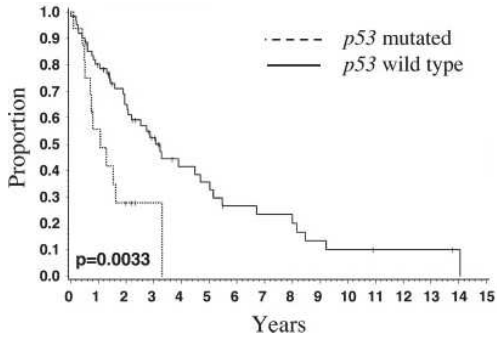

Figure 10. A) Possible mechanism of ibrutinib resistance in MCL as reported by Rahal et al. Survival curves showing the association of (B) NOTCH1, n=18, and (C) TP53, n=82, mutations to the poor prognosis in MCL. Adapted from (Greiner et al., 2006; Intlekofer and Younes, 2014; Kridel et al., 2012)

The MCLs have a distinct mutational profile compared with other B cell lymphomas. In 2014, Zhang et al., (Zhang et al., 2014) proposed an interplay between epigenetic alterations during normal B-cell differentiation and the acquisition of somatic mutations that occur more frequently in either MCLs or Burkitt lymphomas. This study discovered that the frequently mutated regions were associated with open chromatin in their respective B cells of origin, naïve B cells, and germinal center B cells by performing chromatin immunoprecipitation and sequencing (ChIP-seq) analysis of these cells for different histone marks that define chromatin structure.

2.4.3. Epigenetic aberrations in MCL

In addition of genome instability, MCL is also a case of illegitimate tissue-specific gene activation. Most MCL patients, including CYCLIN D1 negative cases, express high levels of the neural transcriptional factor SOX11 (SRY (Sex determining region Y)-box11) which is not expressed in normal lymphoid tissues, progenitors, or normal B-cells. *De novo* expression of *SOX11* has been shown to be mediated by a shift from inactivating (H3K9me2 and H3K27me3) to activating histone modifications (H3K9ac and H3K4me3) in the promoter region of malignant B-cells compared with normal hematopoietic cells (Vegliante et al., 2011).

Vegliante et al., showed that SOX11 promotes tumor growth in a MCL-xenotransplant mouse model and identified target genes and transcriptional programs regulated by SOX11. This study proposed that SOX11 contributes to MCL tumor development by impairing the terminal B-cell differentiation program via direct regulation of *PAX5* gene expression (Vegliante et al., 2013). SOX11 expression represent diagnostic and prognostic values in MCL and high levels of SOX11 have been shown to be associated with more aggressive evolutions (Ek et al., 2008; Mozos et al., 2009).

The recurrent mutations that impact histone modifier coding genes as well as DNA methylome perturbations in MCL are discussed in epigenetic section.

2.5. Treatments

The therapeutic objectives for MCL are focusing on improving the survival and reducing the treatment side effects. Initial therapeutic decisions are made regarding the age and general health state of the patient. First-line treatment for young (<65 years) and fit (Eastern Cooperative Oncology Group performance status ≤1 with preserved end-organ function) patients is intense dose therapies followed by consolidation and maintenance therapy. These therapies including the Nordic MCL2 regimen (induction therapy with Rituximab plus alternating cycles of dose-intense cyclophosphamide/doxorubicin/vincristine/prednisone (maxi-CHOP) and high-dose Cytarabine followed by autologous stem cell transplantation (ASCT). These regimens have been shown to provide durable remission however relapses continue to occur after 10 years (Chihara et al., 2016; Geisler et al., 2008; Romaguera et al., 2005). A French study, within the European Mantle Cell Lymphoma Network, described a sequential use of Rituximab (anti CD20 monoclonal antibody), Cyclophosphamide, Doxorubicin, Vincristine, Prednisone (RCHOP) and Rituximab, Dexamethasone, high-dose Cytarabine, cisplatin (R-DHAP) followed by ASCT as the most efficient intensive therapy (Lefrere et al., 2002). A recent study of 240 MCL patients showed that Rituximab maintenance therapy after transplantation prolonged event-free survival, progression-free survival, and overall survival in young patients (Le Gouill et al., 2017).

For the unfit patients, the conventional chemotherapy is based on R-CHOP, combination of Rituximab and Bendamustine (RB), RB+lenalidomide or VR-CAP. For the patients with relapse from the front-line therapies, Ibrutinib targeted therapy was associated with a high overall response (Wang et al., 2013b). Single-agent Bendamustine is the first chemotherapy-based choice for the second-line therapy in patients that did not receive it previously. Bendamustine is also used in combinations with rituximab, Cytarabine, Bortezomib (proteasome inhibitor), Mitoxantrone, Lenalidomide, and Ibrutinib (Martin et al., 2017).

Chapter 3: General introduction on epigenetics

Various cell types in multicellular organisms contain the same genetic information, represented by the DNA sequence, but are however different in their morphology, function and identity throughout development. In fact the same genome undergoes different spatial and temporal programs of gene activation and repression in each tissue. The fine-tuned regulation of transcriptional program is a multilayer mechanism which is ensured by different actors. Each gene contains several sequences with regulatory function in gene expression within or outside of the gene, including promoters, enhancers and silencers. General and sequence-specific transcription factors (TFs) are crucial determinants for the regulation of gene expression. They activate or repress specific genes through sequence-specific interactions with their promoters. DNA accessibility to the tissue specific TFs and other DNA binding proteins differs in distinct cell types through epigenetic regulation of chromatin structure discussed below. The complex interplay between TFs and epigenetic regulators guaranties the stable cell type specific gene expression pattern and the cell identity.

3.1. General overview on Epigenetics

Epigenetics refers to heritable information which is not directly recorded by the genetic code but contained in various supports including reversible chemical modifications of histones and DNA. The primary function of this non-genetic information is the control of various activities of the genome.

In eukaryotes, DNA is compacted in chromatin macromolecule which is made of repetitive units called nucleosomes. Each nucleosome is made of a 147bp DNA wrapped around histone octamers containing two copies of each histone proteins H2A, H2B, H3 and H4. Chromatin compaction is further facilitated by linker histones and other chromatin architectural cofactors that lead to higher-order chromatin structures.

Histone proteins are subject to a variety of posttranslational modifications (PTMs) such as phosphorylation, acetylation, methylation, and ubiquitination and in different degrees. For

example, lysine residues could be mono-, di- or tri-methylated. These PTMs together with DNA methylation state can act as binding sites for other proteins. These factors underlay the condensation state and the nuclear organization of chromatin depending on the modified residues and the degree of modification. The histone PTMs are mostly studied on the N-terminal extremity of histone proteins that are standing out of the nucleosome core and show dynamic structure. Accessibility of DNA sequences to the transcriptional, repairing and replication machinery is tightly controlled by chromatin compaction levels (Stewart et al., 2005; Zhang et al., 2015).

The enzymes that catalyze these chemical modifications to DNA or histones are called **writer** enzymes, including DNA methyltransferases (DNTMs), histone lysine or arginine methyltransferases (KMTs, PRMTs), histone acetyltransferases (HATs). Chromatin modifications then can be bound by downstream effector proteins or epigenetic **readers**, containing a chromatin reading 'pocket'. These proteins are very important in regulation of gene expression as they could recruit different protein partners such as transcription factors, transcription repressors and transcription elongation factors. Reader proteins recognize specific types and degrees of chromatin modifications, for example chromodomain containing proteins (for example HP1 family, CHD family), and PHD and tudor domain containing proteins bind to methylated residues whereas bromodomain (BRD) containing readers (such as BRD1/2/3/4, BRDT, CREBBP/P300, SMARCA4) target acetylated lysine residues and methyl-CpG-binding domain (MBD) containing proteins (MBD1/2/3/4, MeCP2) are recruited to the methylated DNA regions.

Epigenetic modifications are highly dynamic and reversible and could be removed from DNA or histones by separate **eraser** enzymes such as histone deacetylases (HDACs), histone demethylases (KDMs) and DNA demethylases (Figure 11).

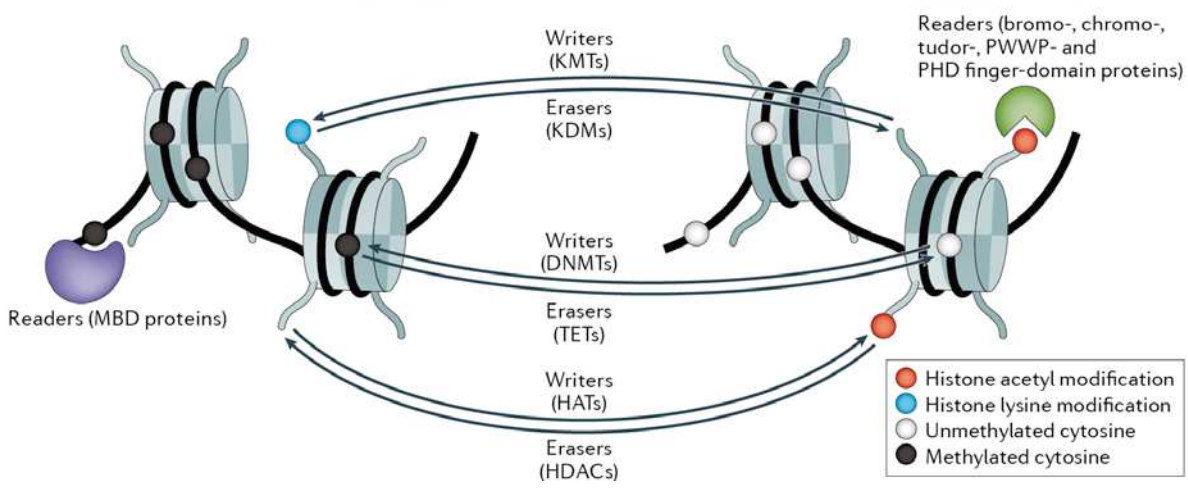

Figure 11. Schematic representation of DNA and histone modifiers and readers. From (Jones et al., 2016).

Chromatin is functionally divided into two categories: **euchromatin** and heterochromatin. Euchromatin presents an open structure with a low DNA density and high rates of transcription>. It is defined as transcriptionally active chromatin. **Heterochromatin** (HC) has a relatively high density of DNA and presents low rates of gene transcription. It is considered therefor as transcriptionally repressed. Each chromatin compartment is characterized with distinct combination of histone PTMs. For example, histone H3 and H4 lysine acetylation (H3Kac and H4Kac) as well as mono- or tri-methylation of lysine 4 on histone H3 (H3K4me1 or H3K4me3) or ubiquitination of lysine 120 on histone H2B (H2BK120ub1) are enriched in transcriptionally active regions within euchromatin. Whereas the most prominent histone featur in heterochromatin is global hypoacetylation in addition to enrichment of histone H3 lysine 9 or 27 trimethylation (H3K9me, H3K27me) or H2A119ub1. Some histone marks are mutually exclusive such as H3K4me3 and H3K9me3 at promoter region whereas some of them could accumulate on the same histone, such as H3K4me1 co-existing with H3K27ac or H3K27me3 in active or poised enhancers respectively (Figure 12).

There are two different forms of repressive chromatin or heterochromatin (HC). **Facultative** heterochromatin refers to regions which retain the potential to interconvert between HC and euchromatin state. Compaction and silencing in facultative HC regions is dynamic during development and represents different patterns at cell type-specific genes (such as homeobox (HOX) transcription factor family) and enhancers in different cell types.

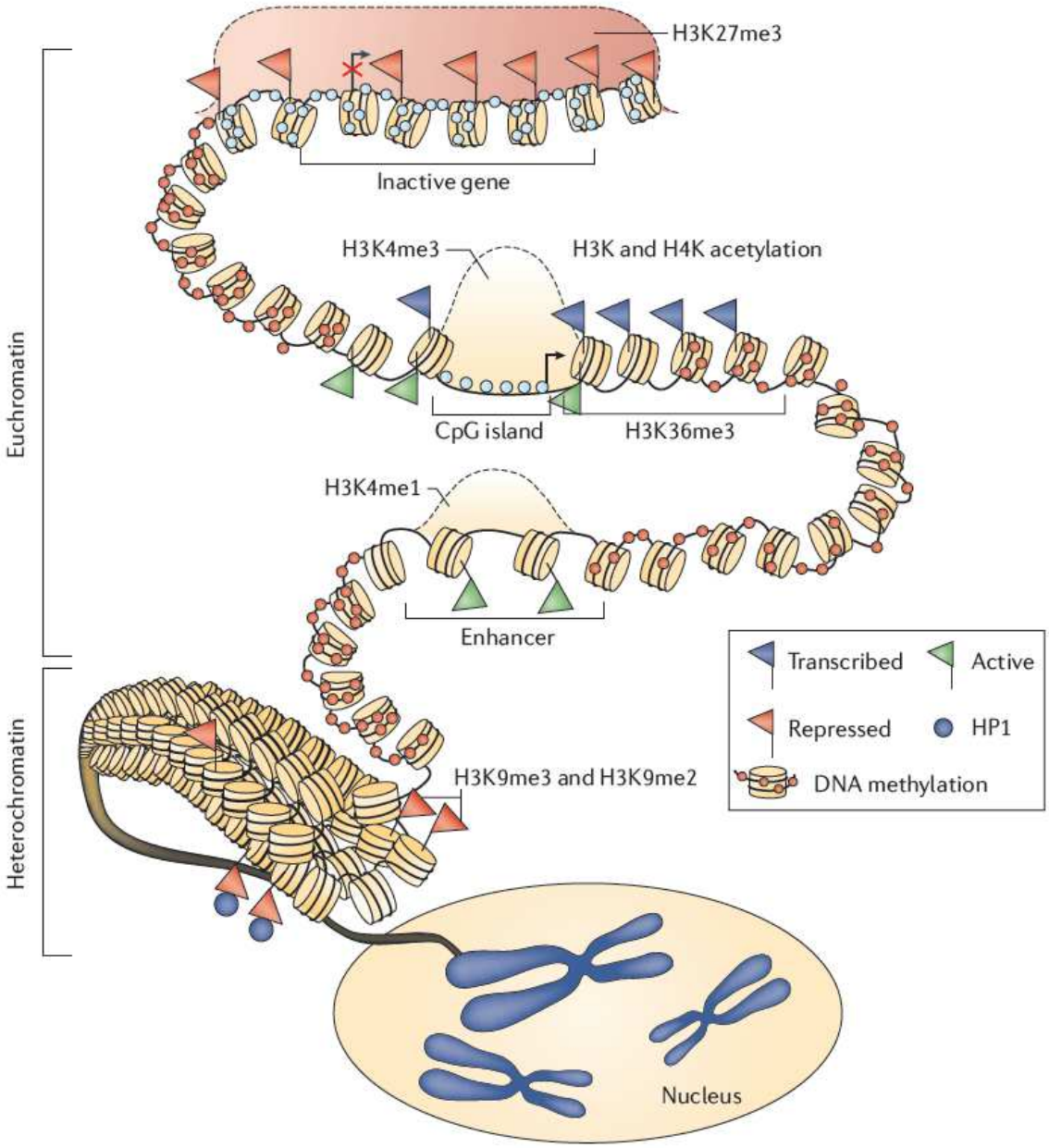

Figure 12. Overall structure of chromatin in human cells. From (Baylin and Jones, 2011).

H3K27me3 is typical histone mark that is enriched in facultative HC regions which is established by catalytic subunit of polycomb repressive complex 1 (PRC1), EZH2 protein (Trojer and Reinberg, 2007). The H3K27me3 repressed regions can still be accessible for binding of general transcription factors and RNA polymerase, however transcription initiation is blocked at the presence of this mark (Breiling et al., 2001).

In the contrary of facultative HC, **constitutive** HC is believed to repress the same genomic regions across developmental lineages. These regions represent a big fraction of mammalian genome and are made of repeat rich sequences, including centromeric satellite repeats,

telomeres and sub telomeric regions, retrotransposons elements and endogenous retroviruses. Silencing and highly compaction of these regions ensure genome stability. The hallmarks of constitutive heterochromatin are **H3K9 di- and trimethylation** which are catalyzed by SET-domain containing family of histone methyltransferases. H3K9me2/3 is then recognized by the chromodomain (CD) containing family of heterochromatin protein 1 (HP1) proteins which have an essential role in forming higher order chromatin structures and heterochromatin spreading via direct interaction and recruitment of more HP1 itself and histone methyltransferases to the chromatin. Our study was focused on H3K9me3 mark which is introduced in the next chapter.

Another layer of epigenetic regulation of gene transcription is the genome spatiotemporal organization within the nucleus. Around one third of human and mouse genomes make molecular contacts and stays associated to nuclear lamina (NL) during interphase. These genomic regions are called **lamina-associated domains** (LADs). LAD chromatins present similar features with heterochromatin. These regions contain a low gene density and the genes that are located in LADs are silent or have very low transcriptional rates. However around 5 to 10% of genes located in LADs can escape the repressive effects of LAD environment and become highly expressed via unknown mechanisms. LADs are within the late replicating regions during S phase of cell cycle and are associated mostly with constitutive HC histone modifications H3K9me2/3 and in some cell types with H3K27me3. NL contact of chromatin is dynamic. As embryonic stem cells (ESC) differentiate, the global intensity levels of LADs increase in a cell type specific manner so the dark-staining heterochromatin at the nuclear periphery shows distinct distribution across differentiated cells (Figure 13). During normal differentiation or cancer development tissue specific genes could change their position relative to NL and the later affects their transcriptional levels as detachment from NL is frequently associated with gene activation and sequestration of genes within the nuclear periphery heterochromatin, far from transcription factory, is accompanied with gene silencing (van Steensel and Belmont, 2017). During early B cell development for example it has been shown that early B cell factor (Ebf1) encoding locus switches its nuclear position. In progenitor cells this locus is trapped in NL and is transcriptionally inactive. This localization is considered to contribute to preserving the multipotency of progenitor cells. After development into the pro-B cell stage, *Ebf1* and other genes (*Foxo1*, *Igk* and *Igl)* repositioned from the repressive to permissive compartment to establish new intra- and interdomain

interactions which are required for B lineage–specific transcription signature (Lin et al., 2012).

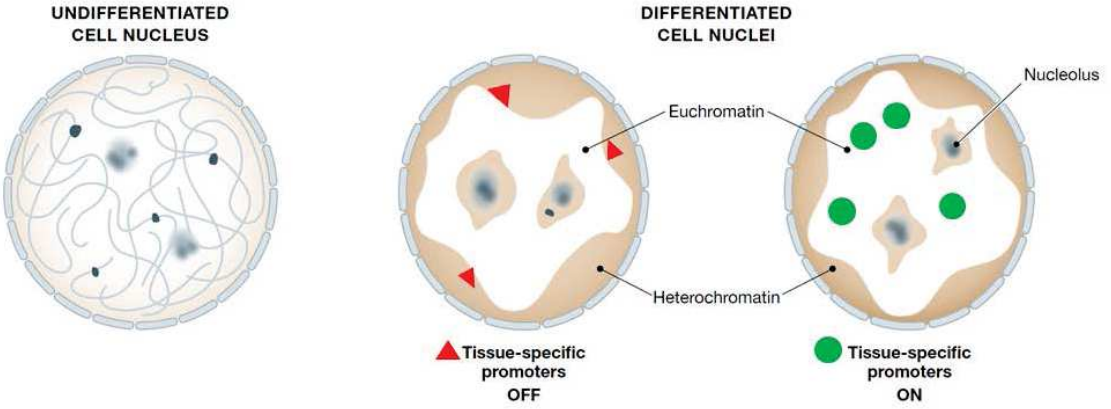

Figure 13. Chromatin distribution changes during cell differentiation. Adapted from (Harr et al., 2016)

3.2. Epigenome dysregulations in hematological malignancies

The epigenetic modifier genes are frequently mutated in cancer leading to dysregulations in nearly every levels of epigenetic machinery and few if any cancers escape mutations in one of the major chromatin regulators. One of the first examples of epigenetic dysregulation in cancer are pediatric cancers which are associated with relatively low mutation rates and simple genome but show recurrent epigenetic defects such as alteration in chromatin remodeler genes (*SMARCB1* loss in pediatric rhabdoid, *ATRX* and *DAXX* mutations in pediatric glioblastoma) or abnormal DNA-methylation profiles (medulloblastoma). Recently, mutations in the isocitrate dehydrogenase genes, *IDH1* and 2 have been described in AML and gliomas. Strikingly, mutant IDH enzymes impair H3K9me3 demethylation, blocking cellular differentiation (Figueroa et al., 2010; Lu et al., 2012).

Mutated gene	Cancer type and mutation frequency
IDH1/2	GBM (88%), WHO grade II/III glioma (71%), AML (23%)
EZH2	FL (7-22%), DLBCL (14-21%), MDS/MPN (6-13%), CMML (11.1%)
DNMT3A	AML (22,1%), MDS (3-8%)
NSD2	Pediatric B-ALL (7.5%)
MLL2	FL (89%), DLBCL (24-32%)
SMARCA4	NSCLC (15-50%)
TET2	MDS (19%), AML (12-24%), CMML (42-46%)
KDM6A	Bladder (20-29%), Breast
CREBBP	NHL (21%), FL (32,6%), relapsed AML (18.3%), DLBCL (29%)

Table 2. Frequently mutated epigenetic regulators in solid and hematological cancers along with mutation frequency by tumor histology. Adapted from (Roy et al., 2014).

Epigenetic dysregulation in hematological malignancies is largely described in different studies. Diffuse large B-cell lymphoma (DLBCL), which is one of the most common non-Hodgkin lymphomas (NHLs), shows frequent inactivating mutations in *MLL2*, nonsynonymous mutations in *CREBBP/EP300* histone acetyltransferase in around 25% of cases as well as in *KDM2B*, histone demethylase and *EZH2* (mostly in GC subtype) (Amin et al., 2017; Morin et al., 2011).

Acute myeloid leukemia (AML) is one of the most common types of adult leukemia. Whole genome sequencing of AML patients revealed recurrent somatic mutations in the genes encoding for different epigenetic regulators involving in DNA methylation (*DNMT3A, TET2, IDH1/2*), histone post-translational modifications (*EZH2, ASXL1, NSD1*) and nuclear organization (cohesin complex family). The majority of AML patients harbor at least one mutation that hits epigenome (Figueroa et al., 2010).

3.2. Epigenetic alterations in Mantle cell lymphoma (MCL)

As previously discussed, MCL is characterized with high levels of genome instability, chromosomal translocations, and increasing number of gene mutations that affect also epigenetic modifier coding genes. Three studies also analyzed genome-wide DNA methylation pattern in MCL and reported DNA methylome alterations in this disease. The findings of these papers are discussed below.

3.2.1. Recurrent mutations of histone modifiers in MCL

- *MLL2* or *KMT2D*, a member of myeloid/lymphoid or mixed-lineage leukemia family encoding for H3K4 methyltransferase, is the most frequent mutated epigenetic regulator in MCL patients with a recurrence of 13.8% (4/29) in Beà S. et al., (Bea et al., 2013) study, 19.6% (11/56) in Zhang J. et al., study (Zhang et al., 2014) and 12% (18/151) in Rossi D. et al., study (Rossi D et al, Blood 2015 126:336). Furthermore the latter study showed that *MLL2* mutation was associated with a shorter progression free survival (2-years PFS 67% vs 81%; p=0.004) and high risk prognostic features when co-occurred with *TP53* mutation or an intermediate risk prognostic exclusive of *TP53*.

- *MLL3* or *KMT2C*, encodes for another member of MLL family, MLL3, which is also a H3K4 methyltransferase. *MLL3* was shown to be mutated in <15% of MCL patients in Zhang J. et al., (Zhang et al., 2014) study.

- *WHSC1* encodes for nuclear SET domain-containing protein2 (NSD2), also called MMSET, with H3K36 methyltransferase activity. This gene has been previously shown to be overexpressed in multiple myeloma (MM) patients harboring t(4;14) translocations (Martinez-Garcia et al., 2011) where it contributes to cell growth and prevents apoptosis. NSD2 is also reported to be mutated in pediatric acute lymphoblastic (Jaffe et al., 2013) and renal carcinoma (Staller, 2010). In mantle cell lymphoma, *WHSC1* was mutated in 10% of cases in Beà S. et al study (Bea et al., 2013), in 7% of Zhang J et al., cohort (N=56) (Zhang et al., 2014) as well as in 13% of Rossi D et al., cohort (N=151) (Rossi D et al, Blood 2015 126:336).

3.2.2. DNA methylation alterations in MCL

Abnormal DNA methylation profiles are widely reported in solid and hematological cancers. Generally cancers are associated with global loss of DNA methylation and local gains in promoter region CpG islands of a selected number of genes. For example, the tumor suppressor gene *CDKN2A* (encoding for INK4A and ARF) is hypermethylated in several tumor types, including MCL (Hutter et al., 2006).

Other single locus studies showed hypermethylation of phosphatase *SHP-18* and Rho–adenosine triphosphatase *PARG-1* genes in MCL (Chim et al., 2004; Ripperger et al., 2007).

In 2010, Leshchenko VV. et al., (Leshchenko et al., 2010) performed the first genome-wide analysis of DNA methylation and gene expression in MCL compared to purified normal naive B cells (NBCs), considered as normal counterparts of MCL cells. This study reported aberrant genomic methylation profiles in MCL primary samples (n=22) compared with naive B cells (n=10) and key protein-coding genes such as histone deacetylase 1 (*HDAC1*) and nuclear factor B 1 (*NFKB1*) transcription factor identified among differentially methylated loci. Also 4 hypermethylated genes *CDKN2B*, *MLF-1*, *PCDH8*, and *HOXD8* and 4 hypomethylated genes *CD37*, *HDAC1*, *NOTCH1*, and *CDK5* showed down and upregulation of their mRNA transcription respectively.

In 2013, Pedro Jares lab performed genome-wide methylation profiling of a larger cohort of primary MCL tumors (n = 132), 6 MCL cell lines and 31 normal lymphoid tissue samples (Enjuanes et al., 2013). They identified 454 hypermethylated (including *CDKN2A*) and 875 hypomethylated genes differentially methylated in at least 10% of primary MCL. Further they showed that WNT-pathway inhibitors are frequent target of *de novo* DNA methylation. They also found a significant correlation between accumulation of hypermethylated genes and MCL clinicopathological parameters: the higher number of hypermethylated loci was associated with higher number of chromosome alterations, higher proliferation signatures and poor prognosis and finally they suggested that hypermethylation of promoter regions has a stronger effect on MCL biological behavior than hypomethylations.

In a recent study, Queirós et al., (Queiros et al., 2016) analyzed epigenome of MCL in the context of the DNA methylome during normal B cell maturation program. This study revealed

two distinct subtypes of MCL in one of which (C1) DNA methylation pattern is more similar to germinal-center-inexperienced B cells (naïve B cells) whereas in the other group (C2) it is similar to germinal-center-experienced B cells (memory B cells) (Figure 14). Although *CYCLIN D1* expression was comparable in both group, C1 group showed more aggressive clinicobiological features including less *IGHV* mutation levels, higher number of copy number alterations, higher levels of *SOX11* expression, nodal presentation and finally a significant worse overall survival.

A subset of regions which were hypomethylated exclusively in C1 group and not in C2, normal naive or memory B cells, were enriched for both H3K27ac and H3K4me1, pointing toward *de novo* active enhancers at these regions. One of these regions overlapped with an enhancer region located 624–653 kb downstream of *SOX11* gene and showed three dimensional association with *SOX11* locus only in the SOX11-expressing C1 MCL cases. SOX11 negative cases and cell lines didn't show hypomethylation of this enhancer region and the looping with *SOX11* locus.

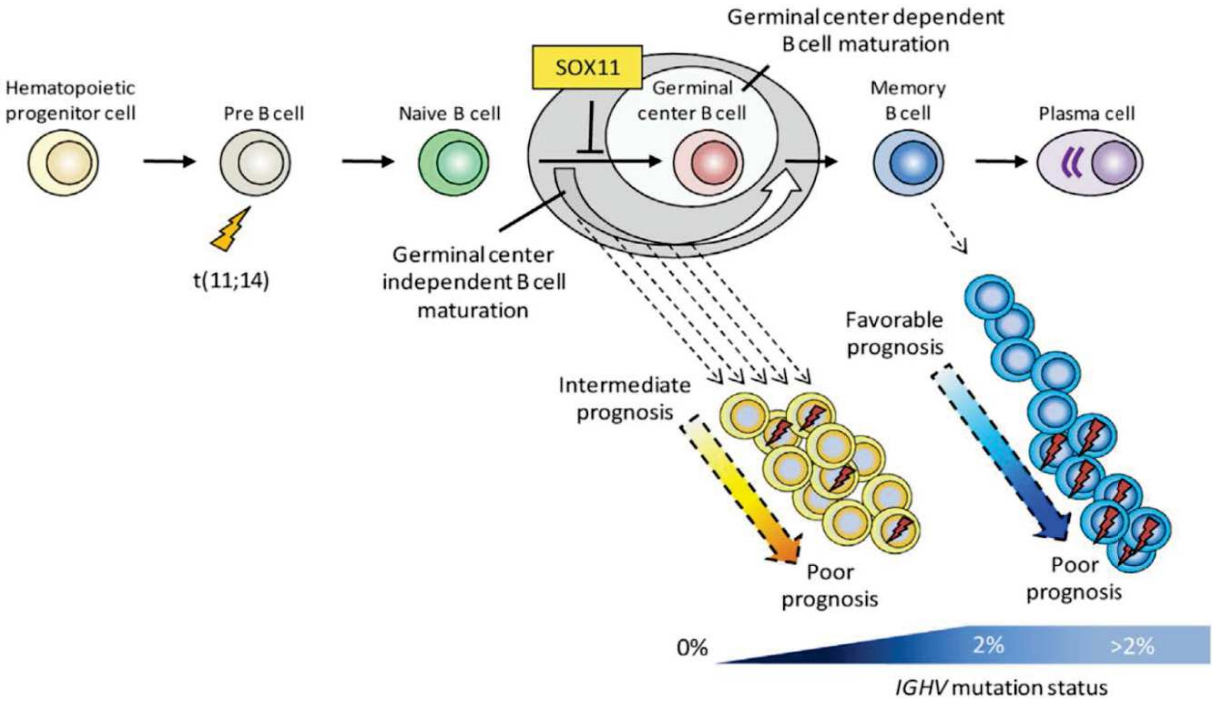

Figure 14. Epigenetic model of MCL pathogenesis proposed by (Queiros et al., 2016).

3.3. Targeting the epigenome in hematological malignancies

Considering the high frequency of epigenome dysregulation in cancer and reversibility of these changes, therapeutic strategies that reverse or inhibit epigenetic defective pathways represent a great interest in cancer therapy. The current methods of targeting epigenetic regulators are mostly based on development of small molecule compounds which prevent enzymatic activity (Figure 15 A), protein interactions (Figure 15 B) or stability of target proteins (Figure 15 C).

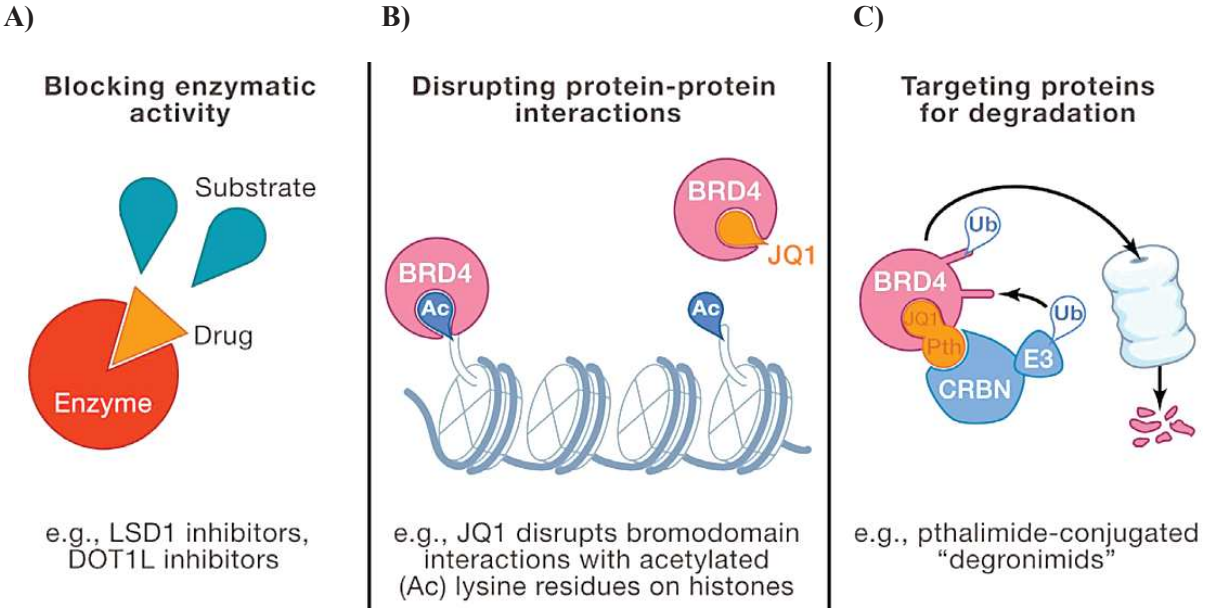

Figure 15. Strategies for Targeting Epigenetic Regulators (A) Inhibiting enzymatic activity with competitive small molecule compounds, (B) disrupting protein- protein interactions, and (C) using phthalimide- conjugated small molecules to redirect difficult-to-target proteins for proteasomal degradation via the cereblon (CRBN) E3 ubiquitin (Ub) ligase complex. From (Cai et al., 2015).

In hematological malignancies histone deacetylase inhibitors (HDACi) (Vorinstat, Romidepsin and Panobinostat) alone or in combination with DNA methyltransferase 1 inhibitors (Decitabine and azacitidine) have proven clinical efficiency in multiple myeloma, cutaneous T cell lymphomas, MDS and AML. Other small molecules that interfere with different chromatin regulators have also shown success in modification of cancer-promoting epigenetic states and cancer-associated gene expression programs *in vitro* and in clinical trials. Table 3 represents a selection of epigenetic therapies in use or under investigation in clinical trials for hematological malignancies.

Protein	Biological Function	Small-Molecule	Cancer Type	Stage of drug development	References
Chromatine writers					
DOT1L	H3K79 methylation	EPZ-5676	AML, ALL	Phase I trial	Daigle et al., 2013
EZH2	H3K27 methylation	GSK2816126	DLBCL	Phase I trial	McCabe et al., 2012b
DNMT1	DNA methylation (maitenance)	azacitidine decitabine	MDS, CMML	FDA approved	Issa & Kantarjian, 2009
Chromatine readers					
BET family	acetyl-lysine binding	OTX015, CPI-0610	AML, MDS, lymphoma, MM	Phase II trial Phase I trial	Filippakopoulos et al., 2010 ; Delmore et al., 2011 ; Zuber et al., 2011
Chromatine erasers					
LSD1	H3K4/K9 demethylation	GSK2879552 tranylcypromine	AML, MDS	Phase I trial	Harris et al., 2012 Mohammad et al., 2015 ; Schenk et al., 2012
HDAC 1/2/3	lysine deacetylation	vorinstat romidepsin panobinostat	cutaneous T cell lymphoma MM	FDA approved	Mann et al., 2007 Khan & La Thangue, 2012

Table 3. Selection of targeted epigenetic therapies in use or under clinical investigation in cancer patients. DOT1L: DOT1 like histone lysine methyltransferase; EZH2: enhancer of zeste 2 polycomb repressive complex 2; BET: Bromodomain and Extra-Terminal motif protein; LSD1: lysine-specific demethylase 1. From (Brien et al., 2016).

Among these treatments, BET inhibition opened a new chapter in 'epigenetic therapy'. These highly selective drugs were designed based on high quality structural and functional data and represent the first molecules that pharmacologically interfere with epigenetic readers (Figure 15 B).

These molecules reversibly bind the bromodomains of BET protein family members (BRD2, BRD3, BRD4, and BRDT), and prevent interaction between BET proteins and the acetylated histones and non-histone proteins. This perturbation abolishes the further recruitment of BET protein partners, including transcription initiation and elongation factors, to the acetylated site (Filippakopoulos and Knapp, 2014). In cancer, BET proteins are involved in regulating expression of key oncogenes and anti-apoptotic proteins making them an important therapeutic target to modulate expression of disease promoting genes. This is due to the preferential binding of BET proteins to super-enhancers which regulate critical oncogenic drivers in many tumor cells (Loven, 201). The oncogenic transcription supported by these

super-enhancers is therefore extremely sensitive to BET inhibition. BET inhibitors have shown a wide preclinical activity in hematological malignancies by impairing the activity of super-enhancers that are associated with key transcription factors implicated in lymphomagenesis, including MYC, BCL6, IRF8, PAX5 (Amorim et al., 2016; Boi et al., 2015; Chapuy et al., 2013)

Chapter 4: H3K9methylation

One of the most abundant and stable histone modifications is methylation of histone H3 at lysine 9 (H3K9) which is associated with repressed regions on chromatin. This histone mark is broadly enriched at pericentromeric heterochromatin, various classes of retrotransposons, imprinted loci and developmental repressed genes (Pasquarella et al., 2016).

4.1. H3K9me writers

Several H3K9-specific histone methyltransferases (HKMTs) have been characterized. They all contain a conserved SET (Su(var)3-9, Enhancer of zest, and Trithorax) domain with catalytic activity (Table 4).

	Alias	Gene location	Protein length	Sub-cellular localization	Substrate H3K9
SUV39H1	KMT1A	ChrXp11	412aa	Chromatin associated	me1
SUV39H2	KMT1B	Chr10p13	410aa	Nuclear & chromatin associated	me1
G9a (EHMT2)	KMT1C	Chr6p21	1210aa	Nuclear & chromatin associated	me0/1
GLP (EHMT1)	KMT1D	Chr9q34	1298aa	Nuclear & chromatin associated	me0/1
SETDB1	KMT1E	Chr1q21	1291aa	Nuclear, chromatin associated & cytoplasmic	Me0/1/2
SETDB2	KMT1D	Chr13q14	719aa	Nuclear	

Table 4. SUV39 subfamily of H3K9 methyltransferases

These KMTs use S adenosylmethionine (SAM) as methyl donor and are able mono-, di- or trimethylate H3K9, none of which change the electronic charge of the amino-acid side chain (Figure 16). Clr4, also called KMT1, is the only H3K9 methyltransferase in fission yeast and is able to catalyze all of three degrees of H3K9 methylation.

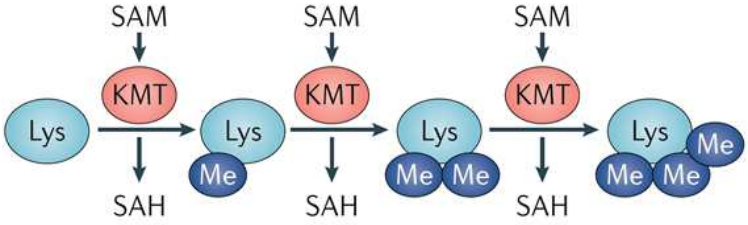

Figure 16. Lysine methylation reaction by KMTs. KMTs mono-, di- or trimethylate histone substrates by a common, putative S^N2 nucleophilic substitution reaction that transfers a methyl group from the common methyl donor *S*-adenosylmethionine (SAM) to the nucleophilic ε-nitrogen of the lysine side chain.

Different H3K9 KMTs cooperate and interact with each other to establish different degrees of H3K9 methylation. For example, Setdb1 has been reported to interact in a complex with HP1 and CAF-1 (Chromatin assembly factor 1) histone chaperon and monomethylate non-nucleosomal H3K9, providing substrate for Suv39h1 during DNA replication (Loyola et al., 2009). It has been also shown that a subset of G9a, GLP, and SETDB1 and SUV39H1 form multimeric complexes and stability of each of them is interdependent (Fritsch et al., 2010).

4.2. H3K9me reader

The major reader of H3K9 methylation is a protein called heterochromatin protein 1 (HP1), which has at least three isoforms in mammalian cells and two in *C. elegans* and *S. pombe*. Human possess three main HP1 paralogs – alpha (α), beta (ß), and gamma (γ) – encoded by the CBX5, CBX1, and CBX3 genes, respectively. All HP1 proteins contain an N-terminal chromodomain that specifically recognizes both H3K9me2 and me3 and a C-terminal chromo-shadow domain that mediates the interaction with other proteins including Dnmt1, Dnmt3a, CAF-1, SUV39H1 and HP1 itself, contributing to heterochromatin compaction and propagation. A spacer domain, called hinge region, is less conserved between different HP1 proteins and induces functional differentiation between them. This region interacts with different types of ligand including RNA and DNA, histone modifying enzymes such as HDACs and the inner centromere protein (INCENP).

PTMs on HP1 proteins modulate their affinity to their ligands. For example, phosphorylation of serine residues in N-terminal region of mouse HP1α increases its affinity to H3K9me3-tail peptide up to fivefold. On the other hand Suv39h1 mediated SUMOylation of mouse HP1α in the hinge region promotes specific interaction between SUMO-HP1α and pericentric RNA transcripts and establishment of constitutive heterochromatin in these regions, even in the absence of Suv39h-dependent H3K9me3 ligand (Canzio et al., 2014; Harr et al., 2016; Maison et al., 2016; Maison et al., 2011).

4.3. H3K9me erasers

Due to a low turn-over rate of the methyl group histone methylation was originally considered as an irreversible and permanent modification which is only removed by histone exchange or by dilution during DNA replication. However in 2004 discovery of the first enzyme with histone demethylation activity, Lys-specific demethylase 1 or LSD1 or KDM1A, revealed that histone lysine methylation is highly dynamic and reversible (Shi et al., 2004). Since that time, expect for H3K79, the histone demethylases (KDMs) for all the major lysine methylation sites are discovered. The Table 5 presents major KDMs responsible for demethylation of H3K9.

Name	synonyms	Substrate
LSD1	KDM1A	H3K9me1/2, H3K4me1/2, H4K20me1/2
JMJD1A/B	KDM3A/B	H3K9me1/2
JMJD2A/B/C/D	KDM4A/B/C/D	H3K9me2/3, H3K36me2/3 (A,C)
JHDM1D	KDM7A	H3K9me1/2
PHF8	KDM7B	H3K9me1/2, H3K27me1/2
PHF2	KDM7C	H3K9me2

Table 5. List of KDMs with demethylase activity on H3K9.

Two major mechanisms of histone lysine demethylation are demonstrated in Figure 17. In oxygenation mechanism Jumonji C (JMJC) domain containing family of demethylases (JHDMs) demethylate mono-, di- and trimethylated substrates dependent on Fe(II) cofactor and α‑ketoglutarate (α-KG). In oxidation mechanism, LSD1 and LSD2 enzymes demethylate mono- and dimethylated substrates dependent on flavin adenine dinucleotide (FAD).

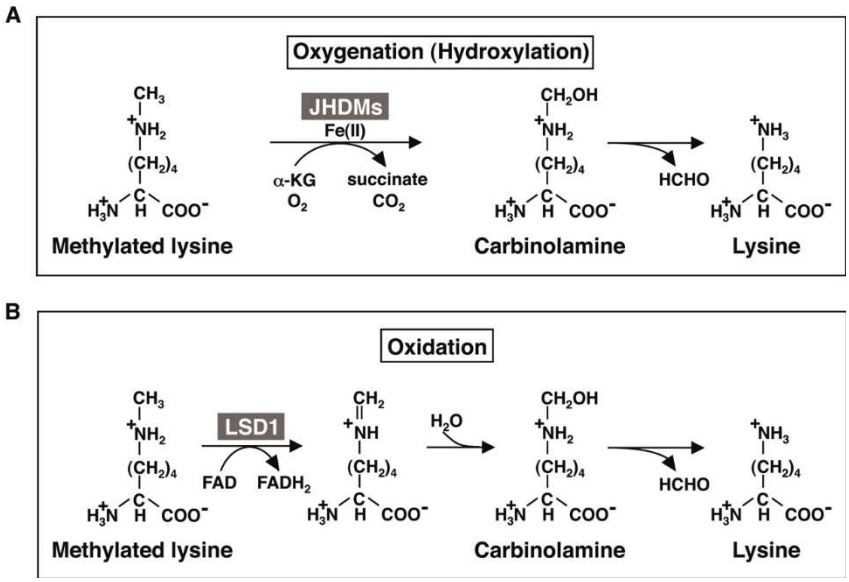

Figure 17. Histone demethylation reactions by (A) Jumonji C (JMJC) domain containing or (B) LSD family of demethylases.

4.4. Cross-talk between H3K9 methylation and DNA methylation

Similar to H3K9 methylation, DNA methylation also serves in long-term silencing of genes and retroelements. DNA methylation was the first epigenetic modification to be identified. DNA methylation is the post-replicative addition of methyl groups to the C5 position of cytosines catalyzed by the family of DNA methyltransferases (Dnmt). DNA methylation occurs almost exclusively in the context of CpG dinucleotides that tend to cluster in regions called CpG islands and constitute about one to two percent of the genome. In general, CpG islands are DNA stretches of more than 200 base pairs in length (0.2-3 kb) characterized by an elevated C/G content. *De novo* DNA methylation is carried out by the DNA methyltransferase enzymes Dnmt3a and Dnmt3b complexed with Dnmt3l, a closely related homologue that lacks methyltransferase activity. The basic DNA methylation pattern that is generated at the time of embryo implantation is maintained throughout development through the action of Dnmt1. Dnmt3l recruits the methyltransferases to DNA by binding to histone H3 in the nucleosome.

DNA methylation is a dynamic modification and can be removed by the ten-eleven translocation (TET) family of Fe(II)-dependent dioxygenases (TET1, TET2 and TET3) (Figure 18).

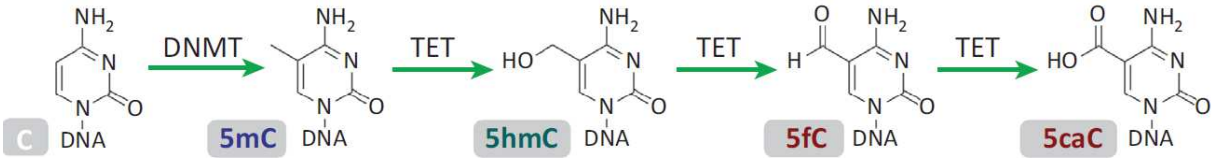

Figure 18. Model pathway of DNA demethylation by TET family.

DNA methylation is associated with numerous biological processes, such as silencing of transposable elements, regulation of gene expression, genomic imprinting, and X-chromosome inactivation.

The regulation of DNA methylation is crucial for normal development. Post-implantation inactivation of pluripotency genes such as Oct3/4 and Nanog is a multi-stage process in which de novo DNA methylation plays an important role. Knockout mutations of any of the three

DNA methyltransferases (Dnmt1, Dnmt3a and Dnmt3b) are lethal (Lei et al., 1996; Okano et al., 1999), demonstrating that aberrant DNA methylation impair normal development.
Genome-scale DNA methylation profiling showed DNA methylation correlates with the absence of H3K4 methylation and presence of H3K9 methylation (Meissner et al., 2008). During facultative heterochromatin formation in ESCs, for example the case of Oct3/4 inactivation, Dnmt3a and Dnmt3b are recruited to the target loci by interaction with G9a H3K9 methyltransferase. Heterochromatinization of pericenromeic satellite repeats is also associated with recruitment of Dnmt3a and Dnmt3b via SUV39H1 and SUV39H2 and methylation of CpG sites within these sequences. Genetic ablation of G9a (Dong et al., 2008; Ikegami et al., 2007) and suv39h (Lehnertz et al., 2003) in mouse ESCs leads to DNA hypomethylation at specific loci in genomic DNA and altered DNA methylation of pericentric satellite repeats, respectively. However, deletion of Dnmt1 or Dnmt3a and Dnmt3b had no effect on H3K9me3 of pericentromeric heterochromatin in mice (Lehnertz et al., 2003). On the other hand, an existing methylated DNA site also directs further histone methylation. The family of the methyl-CpG binding proteins (MBPs) binds to methylated DNA and recruits protein complexes that contain HDACs and histone methyltransferases, including H3K9 methyltransferases. MBD1 was shown to recruit SETDB1 to the chromatin assembly complex CAF-1, facilitating SETDB1- mediated methylation of H3K9 on newly deposited nucleosomes (Epsztejn-Litman et al., 2008; Feldman et al., 2006; Fuks et al., 2003; Sarraf and Stancheva, 2004).

In tumor cells, the DNA methylation pattern is altered, resulting in global hypomethylation of the genome and hypermethylation at CpG sites of tumor-suppressor genes (Esteller, 2008).
(Hamidi et al., 2015) Dnmt1 is frequently mutated in neurodegenerative diseases. Dnmt3a is frequently mutated in hematologic malignancies including 12-30% of AML patients in which it is associated with lower overall survival, and concurrent mutations in FLT3, NPM1 and IDH1/2. And to a lesser degree with other malignancies, including myelodysplastic syndrome (MDS), myeloproliferative neoplasms (MPN), T-cell acute lymphoblastic leukemia (T-ALL) and angioimmunoblastic T-cell lymphoma (AITL). TET2 is also frequently mutated somatically in both myeloid and lymphoid malignancies. These mutations cause impairment of enzymatic activity of the TET2 dioxygenase, resulting in the failure of 5-mC to 5-hmC conversion, and eventually failure of demethylation (Chiba, 2017; Hyun et al., 2017; Torres and Fujimori, 2015).

4.5. H3K9me3

During my thesis we focused on trimethylation of histone H3 lysine 9 (H3K9me3) and two major enzymes responsible for establishment of this mark in somatic cells: SUV39H1 and SETDB1 (Table 5). H3K9me3 is implicated in different processes including genome stability, cell differentiation and reprograming that will be further described below.

4.5.1. Role of H3K9me3 in cell differentiation

H3K9me3 was believed for a long time to exist only in gene poor constitutive HC regions, but genome wide mapping studies revealed the involvement of this mark also in regulation of facultative HC suppression of gene transcription and restriction of differentiation potential during development (Nestorov et al., 2013). H3K9me3 was found at the promoter regions of s-phase genes (Nielsen et al., 2001), tissue specific genes (Ait-Si-Ali et al., 2004; Allan et al., 2012; Mal, 2006) and p53 target genes (Mungamuri et al., 2016) dependent or independent of further HP1 binding (Snowden et al., 2002).

The subnuclear distribution of H3K9me3 also changes as cells differentiate and modulates peripheral positioning and silencing of cell type specific genes at LADs (van Steensel and Belmont, 2017).
For example, differentiation of hematopoietic stem cells (HSCs) to mature hematopoietic cells was shown to be associated with global increase in heterochromatin and localization of H3K9me3 enriched heterochromatin to the nuclear periphery without changes in global levels of this mark (Ugarte et al., 2015). H3K9 methylation perturbation further delayed HSC efficient differentiation in vitro due to impaired silencing of some, but not all, genes associated with differentiation.

It is proposed that in cancer, loss of H3K9me2/3 is implicated in detachment from NL and can induce enhancer–promoter communication within and between topologically associated domains (TADs), enabling the clustering of oncogenic super-enhancers leading to the expression of oncogenic pathway members (Figure 19).

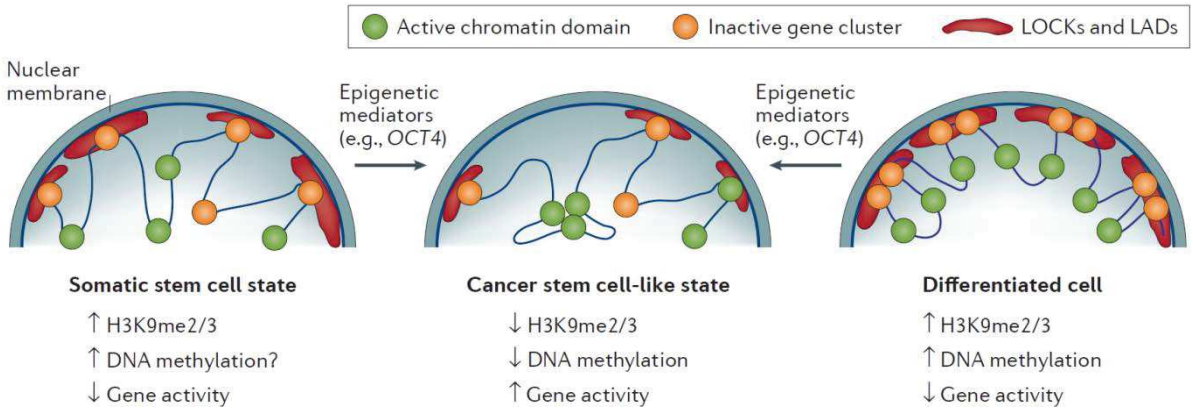

Figure 19. Change in cell state towards cancer stem cell states induced by reprogramming of the 3D epigenome.

Large organized chromatin K9 modifications (LOCKs) (red cloud) overlapping with lamina-associated domains (LADs) are hypothesized to be largely absent in somatic stem cells (left panel) to ensure epigenetic flexibility associated with the multipotent state. The coordination of cell-type-specific repressed states (right panel) within the LOCKs/LADs is facilitated by epigenetic modifiers establishing multiple layers of epigenetic modifications, such as H3K9me2, H3K9me3, and DNA methylation. The localization of LOCKs/LADs to the lamina leads to the separation of active and inactive domains to reduce transcriptional noise and to provide barriers for dedifferentiation. Conversely, the unscheduled activation of epigenetic mediators leads to the erosion of LADs/LOCKs and the emergence of hypomethylated blocks during the neoplastic process. This, in turn, induces phenotypic heterogeneity by increasing the variability in expression and the probability of switches between the diverse cellular states within the tumour. A loss of LOCKs is postulated, moreover, to interfere with the constraints of enhancer–promoter communication within and between topologically associated domains (TADs), enabling the clustering of oncogenic super-enhancers and expression domains (green circles) to coordinate the expression of oncogenic pathway members (centre panel). From (Feinberg et al., 2016).

4.5.2. Role of H3K9me3 in cell fate and reprograming

Differentiation of embryonic stem cell (ESC) to committed somatic cells is finely regulated by remodeling of chromatin structure to ensure proper regulation of gene expression leading to gradual loosening of pluripotency and self-renewal capacity and acquisition and maintenance of tissue specific cell identity, which is required for efficient physiological function of the cell. Disruption of cell identity is today known to be associated with development of many diseases, including cancer. This indicates the pivotal role of regulatory pathways that safeguard the somatic state from erasure of the identity and reversion to pluripotent state or transdifferentaition to another cell type, called reprogramming.

Reprogramming of adult somatic cells to pluripotent stem cells can be induced by different techniques:

- **Somatic nuclear transfer** (SNT): transfer of a terminally differentiated somatic cell nuclei to enucleated oocyte (Gurdon, 1962).
- **Cell fusion**
- **Induced pluripotent stem cell** (iPS) by ectopic expression of reprogramming transcription factors Oct4, Klf4, Sox2, and c-Myc (OKSM) (Takahashi et al., 2007).

Reprograming process, whether in NCT or iPS, is very slow an inefficient and a complete process happen only in a small fraction of cells (less than 0.1%).
H3K9me3 marked heterochromatin is known as the major epigenetic barrier to a successful reprogramming in both SNT and iPS systems, probably by distinct mechanisms (Chen et al., 2013; Matoba et al., 2014; Onder et al., 2012; Soufi et al., 2012). Focal and global chromatin structure also changes during reprograming to modulate TF binding and activity.

Somatic Cell Nuclear Transfer (SNT): H3K9me3 impedes SNT induced reprogramming. The reprogramming resistant regions (RRRs) are shown to be selectively decorated by H3K9me3 during SNT. The genes that are located within these regions are active in normal two-cell mouse embryos but repressed in embryos derived by SNT. Erasure of H3K9me3 by exogenous expression of specific demethylase Kdm4d, or downregulation of Suv39h1/2 methyltransferases increased the expression of the RRRs genes and improved in the developmental potential of the SCNT-derived embryos (Matoba et al., 2014).

iPS reprogramming: the regions that are refractory to OKSM binding are dominantly marked by H3K9me3 in differentiated fibroblasts whereas the same regions are depleted for H3K9me3 and are accessible for these transcription factors in ES cells. These regions are called differentially bound regions or **DBR**s (Soufi et al., 2012). H3K9me3 protect the transcriptional depression of essential pluripotency genes within the DBRs, such as NANOG and SOX2. The reactivation of these genes is restricted to fully reprogramed cells. Consistently, knockdown of the major H3K9me3 methyltransferases SUV39H1/H2 (Soufi et al., 2012), or SUV39H1 alone (Onder et al., 2012), decreased H3K9me3 levels and increased significantly human iPS colony formation. Also, knockdown of Setdb1 was shown to be sufficient to convert pre-iPSCs into iPSCs in mice fibroblasts (Chen et al., 2013).
The histone chaperone CAF-1 (chromatin assembly factor complex) has recently identified as a potent barrier to iPS cellular reprogramming. CAF-1 loss leads to a more accessible chromatin structure and binding of SOX2 to enhancer elements. CAF- 1 depletion also leads

to the dilution of H3K9me3 across reprogramming resistant regions (RRRs), but not elsewhere, and accelerates both iPS cell formation and direct lineage conversion (Cheloufi et al., 2015).

One cell type can also convert to another directly, without the need to first dedifferentiate to a pluripotent state (transdifferentiation or lineage reprogramming), by ectopic expression of lineage-specific transcription factors. Known examples are direct conversion of MEFs into induced neurons by ASCL1 (Chanda et al., 2014), fibroblast transdifferentiation to myoblast by overexpression of *MyoD* and rapid and efficient reprogramming of differentiated B cells into macrophages under enforced expression of C/EBPα and ß (Bussmann et al., 2009; Xie et al., 2004).

Oncogenic transformation shares similar mechanisms with reprograming. Each of key reprograming TFs has established roles in initiating human malignancies and chromatin regulators of reprograming frequently undergo loss or gain of function mutations or are fused to other oncogenic proteins.

4.5.3. Role of H3K9me3 in genome stability

In mammals coding sequences represent only a small fraction of the genome, less than 5% in human, whereas repeat sequences account for 40-60% of genome (Lander et al., 2001). These regions, including tandem-repeat satellites near centromeres and telomeres, retrotransposons, and endogenous retroviruses (ERVs), are considered as a threat for genome integrity as they have recombination and self-duplication capacities. Thus early during embryogenesis these sequences are packed in condensed constitutive heterochromatin, enriched for di- and trimethylated H3K9, which keeps them permanently inaccessible and transcriptionally repressed in all cell types afterward.

The Suv39h1 and Suv39h2 are major enzymes responsible for H3K9me3 deposition at pericentric heterochromatin and silencing of major satellite repeats in these regions (Bulut-Karslioglu et al., 2014). Suv39h1/2 dependent H3K9me3 chromatin also specifically represses intact LINE elements in the ESC epigenome, which is replaced by DNA methylation in more differentiated committed cells. Setdb1 seems to be the primary enzyme to ensure

transcriptional silencing of intact ERV elements (Karimi et al., 2011) and Suv39h1/2 expand H3K9me3 to neighboring regions.

Reduced methyltransferase activity of SUV39H1 induced heterochromatin relaxation followed by increased satellite repeat transcription and caused genome instability reflected by increased micrococal nuclease sensitivity, micronuclei formation and chromosome defects (Wang et al., 2013a).

Suv39h1 and Suv39h2 are also involved in regulation of telomere length (Garcia-Cao et al., 2004; Petti et al., 2015) and prevention of chromosome end-to-end fusions (Porro et al., 2014) in mammalian cells. Telomeres of Suv39h1/2 double null ESCs and MEFs are depleted for di- and trimethylated H3K9 and are abnormally longer compared to wild types (Garcia-Cao et al., 2004). Also primary cells derived from suv39h1 overexpressing mice showed higher levels of H3K9me3 at telomeric regions associated with shortening of telomere length (Petti et al., 2015).

4.6. Introduction of two major H3K9me3 methyltransferases

4.6.1. SUV39H1 (suppressor of variegation 3-9 homolog 1)

SUV39H1 gene, also kwon as *KMT1A*, is located on chromosome Xp11 and encodes the histone-lysine N-methyltransferase SUV39H1 protein of 412aa (~48KD). SUV39H1 contains two functionally distinct domains, the N-terminal chromodomain (CD) and the C-terminal SET domain, flanked by two cysteine-rich regions. This CD and SET domain combination is also preserved in *Schizosaccharyomyces pombe* silencing factor clr4 and the *Drosophila* suppressor of variegation 3-9 enzyme (Su(var)3-9) (Figure 20) (Aagaard et al., 1999).

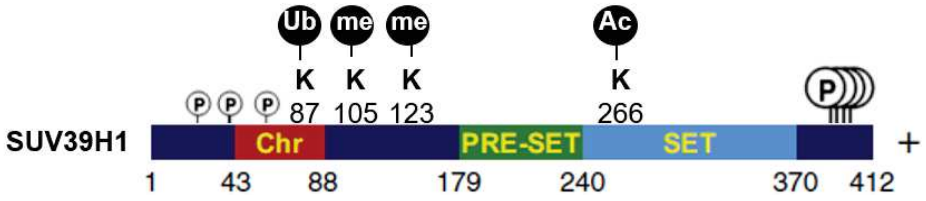

Figure 20. Schematic presentation of human SUV39H1 protein domains and known posttranslational modification sites.

4.6.1.1. SUV39H1 subcellular localization and function

SUV39H1 selectively di- and trimethylates lysine9 residue on histone H3, using monomethylated H3K9 as substrate. *In vitro* experiments with short internal deletion containing mutants showed that the $_{320}$H$^{\phi\phi}$NHSC$_{326}$ motif in the SET domain is an important catalytic site and the cysteine-rich regions have a significant contribution on methyltransferase activity of the SUV39H1 (Rea et al., 2000). Methylation of H3K9 by SUV39H1 creates high affinity binding sites for chromodomain of HP1 proteins which in turn contributes to propagation of constitutive heterochromatin at pericentric, telomeric and sub-telomeric repeats (Lachner et al., 2001).

SUV39H1 is not only involved in heterochromatin silencing. It is also implicated in *de novo* euchromatin gene silencing of s-phase genes (Nielsen et al., 2001), tissue specific genes (Ait-

Si-Ali et al., 2004; Allan et al., 2012; Mal, 2006) and p53 target genes (Mungamuri et al., 2016) dependent or independent of further HP1 binding (Snowden et al., 2002).

SUV39H1 protein has a dominantly nuclear localization and shows a dynamic chromatin association which is regulated during the cell cycle via PTMs of SUV39H1. During interphase, SUV39H1 is enriched at heterochromatic foci, overlapping with HP1ß protein whereas it is mostly accumulated at the outer region of centromeres during prometaphase and dissociates from centromeric positions at the meta- to anaphase transition. This transitional accumulation at centromeric regions is associated and regulated by phosphorylation of the SUV39H1 mostly at serine and, to a lesser degree, at threonine residues during mitosis (Aagaard et al., 1999; Aagaard et al., 2000).

4.6.1.2. SUV39H1 posttranslational modifications

As represented in Figure 20, SUV39H1 is subjected to a series of posttranslational modifications which modulate its activity, localization and stability.

- Localization

  As mentioned above, the phosphorylation state of SUV39H1 changes during different phases of cell cycle and this is associated with changes in sub-nuclear localization of SUV39H1. During interphase, SUV39H1 is non-phosphorylated and shows a regular enrichment at heterochromatin foci. In prometaphase, SUV39H1 is phosphorylated at the C-terminal tail, the SET domain, and also, to a lesser extent, the chromo domain and is mostly localized to the centromere regions (Aagaard et al., 1999; Aagaard et al., 2000).

- Methyltransferase activity

  The enzymatic activity of SUV39H1 is negatively regulated by acetylation of lysine 266 residue within the SET domain, and deacetylation of this residue selectively by Sirtuin 1 (SIRT1) abolishes this inhibition (Vaquero et al., 2007). Methylation of SUV39H1 at lysine 105 and 123 by SET domain-containing protein 7 (SET7/9) reduces greatly methyltransferase activity of the enzyme without affecting subcellular localization or protein levels (Wang et al., 2013a).

- Protein stability

Polyubiquitination of Lysine 87 in the Suv39h1 chromodomain by MDM2 E3-ubiquitin ligase induces proteasomal degradation of Suv39h1. Under stress conditions which threaten genome stability, Suv39h1 protein is protected from MDM2-mediated degradation by SirT1 to ensure genome stability (Bosch-Presegue et al., 2011). HP1α also protects Suv39h1 from ubiquitination with the same mechanism (Raurell-Vila et al., 2017). It has been shown that USP7 (ubiquitin-specific peptidase 7) form a complex with MDM2 and SUV39H1 to impede SUV39H1 ubiquitination and proteasomal degradation (Mungamuri et al., 2016).

4.6.1.3. SUV39H1 recruitment to the chromatin

SUV39H1 is directed to the target chromatin regions by different means that are discussed below.

- Transcription factor based

Association with Rb protein in complex with E2F1 transcription factor, leads SUV39H1 to the euchromatic loci of E2F1 targets (Nielsen et al., 2001). SUV39H1 is also shown to interact with RUNX1 (AML1) and participate in gene silencing in murine erythroleukemia cells (Chakraborty et al., 2003; Reed-Inderbitzin et al., 2006). SUV39H1 has been shown to interact with the transcription factor Evi1 (ecotropic viral integration site 1), aberrantly expressed in acute myeloid leukemia (AML) and myelodysplastic syndrome (MDS), and enhance Evi1 transcriptional repression (Spensberger and Delwel, 2008).

Suv39h1 recruitment at and silencing of major satellite in mice is ensured via interaction with Pax3 and Pax5 transcription factors to these regions. Indeed major satellite repeats in mice contain several binding sites for Pax and other transcription factors in intergenic regions (Bulut-Karslioglu et al., 2012).

- Non-coding RNAs

SUV39H1 can be recruited to heterochromatic regions via recognition of preexisting H3K9me3 by its chromodomain and spreads heterochromatin afterward. Recently three independent studies discovered a new property of both mice and human SUV39H1 chromodomain which is proposed to mobilize SUV39H1 to H3K9me3-free, naive

chromosomal regions to silent heterochromatin. Indeed transcriptional activity in heterochromatin regions is not totally stopped. Non-coding RNAs transcribed from human (Johnson et al., 2017) and mice (Shirai et al., 2017; Velazquez Camacho et al., 2017) pericentric satellite repeats stay associated in cis with their transcription site. SUV39H1 chromodomain is able to recognize directly these chromatin associated RNA and this interaction recruits and stabilizes SUV39H1 at constitutive heterochromatin.

Long non-coding RNAs (lncRNA) are also able to recruit SUV39H1 for euchromatic silencing, similarly to what has been largely described for recruitment of PRC2 to inactive X by XIST or to HOX locus by HOTAIR non-coding RANs. Oct4P4lncRNA, encoded by X-linked Oct4 pseudogene, have been shown to form a complex with Suv39h1 and induce H3K9 trimethylation at the ancestral *Oct4* gene (chr17) promoter leading to gene silencing and reduced self-renewal features in mESC. RNAi-mediated knockdown of Suv39h1 abolished *Oct4* silencing at mRNA and protein level in mESCs, providing first evidence that Suv39h1 controls *Oct4* expression in these cells (Scarola et al., 2015).

4.6.1.4. Role of SUV39H1 different cellular functions

- Control of cell proliferation

Transcriptional repression of S-phase genes in G0/G1 by the retinoblasma protein (Rb) is crucial for the proper control of cell proliferation. SUV39H1 is recruited to the promoter of these genes, such as *cyclin E* and *cyclin D*, via Rb protein and contributes to the gene silencing by promoting H3K9me3 (Nielsen et al., 2001; Vandel et al., 2001). Consistent with this, depletion of SUV39H1 in differentiating myoblasts induced upregulation of both cyclin genes (Ait-Si-Ali et al., 2004) and SUV39H1 overexpressing primary erythroblasts showed cell cycle deregulation and immortalization of these cells *ex vivo* (Czvitkovich et al., 2001).

- Cellular senescence

Permanent arrest of cell division, called cellular senescence, and apoptosis are considered as tumor suppressor mechanisms which protect organism from development of malignant tumors at very early stages. It has been shown that activation of mitogenic oncogenes, such as RAS and BRAF, induce cellular senescence which is characterized by accumulation of heterochromatic foci called senescence associated heterochromatin foci (SAHF). This heterochromatin induction is proposed to suppress transcription of proliferation-promoting

genes in cooperation with Rb protein. Primary Suv39h1 -/- splenocytes, in contrary to their wild type counterparts, failed to exhibit senescence phenotype of increased H3K9me3 and SAHF-like construct formation under oncogenic *Ras* expression *in vitro*. Also Eμ-*N-Ras* transgenic mice harboring hetero- or homozygous deletion of *suv39h1* locus developed invasive T-cell lymphoma very rapidly whereas suv39h1 wild type Eμ-N-Ras transgenic animals developed non-lymphoid neoplasia significantly later. This indicates the important role of SUV39H1 in control of RAS/BRAF mitogenic induced senescence as an early tumor-suppressive barrier (Braig et al., 2005). Suppression of MYC-driven tumor development, such as B-cell lymphoma, was kwon to be more relied on cellular apoptosis. Schmitt CA and colleagues showed a crucial role for suv39h1 to limit lymphomagenesis in Eμ-*myc* transgenic mice by ensuring cellular senescence initiated by tumor/host immune cell interactions (Reimann et al., 2010). Successful senescence induction of anticancer agents, called therapy-induced senescence (TIS), also has been shown to be highly dependent on Suv39h1 presence in Eμ-*myc* transgenic mice (Dorr et al., 2013).

- Cell differentiation:

SUV39H1 has been shown to be implicated in differentiation of muscle cells (Ait-Si-Ali et al., 2004; Mal, 2006), T helper 2 cell (Th2) lineage commitment (Allan et al., 2012) and during oligodendrocyte differentiation in brain (Liu et al., 2015).

4.6.1.5. Role of SUV39H1 in normal development

- Embryogenesis

The vast role of SUV39H1 in development was first showed in 2001 where overexpression of human SUV39H1 in transgenic mice induced growth delay especially within 2 months after birth, skeletal abnormalities and cell cycle defect in erythroblasts leading to impaired transgenic erythroblasts differentiation (Czvitkovich et al., 2001).

Another mammalian H3K9 methyltransferase is SUV39H2 (KMT1A), encoded by human (chr10p13) or mice (chr2) *SUV39H2* gene. Suv39h1 and Suv39h2 are expressed at similar levels during embryogenesis, but suv39h2 expression is downregulated in most adult tissues and the protein is detectable only in testis (O'Carroll et al., 2000).

Although deficiency for either Suv39h1 or Suv39h2 is not lethal for mice embryo, the majority (~70%) of suv39h double null (dn) embryos are nonviable after E12.5 (Peters et al., 2001). The few viable suv39h dn mice are growth retarded an infertile, show high genome instability due to chromosomal missegregation in somatic and germ cells and are severely depleted of H3K9me3 staining in immunohistochemistry (IHC) sections. Around 33% of them developed spontaneous B-cell lymphoma, while 28% of suv39h1 heterozygous or null mice and only less than 5% of suv39h2 (-/-) or (-/+) mice showed tumor formation.

- Hematopoiesis

Heterochromatin regulation via SUV39H1 plays an important role in human hematopoietic stem cell (HSC) aging and B lymphopoiesis. Djeghloul et al (Djeghloul et al., 2016) recently demonstrated that expression of SUV39H1 and consequently global levels of H3K9me3 are reduced in HSCs during aging and this is associated with the reduced capacity of HSCs to generate B lymphocytes in the elderly. They showed that SUV39H1 is a target of microRNA miR-125b, a known regulator of HSC function, and downregulation of SUV39H1 in human HSC is due to increased expression of miR-125b with age.

4.6.1.6. Role of SUV39H1 in Cancer

SUV39H1 has an important role in protecting genome stability, silencing of proliferation genes, control of differentiation and impeding cell reprogramming. Suv39h1 loss increased spontaneous or oncogene induced tumorigenesis in experimental models (Braig et al., 2005; Peters et al., 2001) and deregulation of its expression or function has been reported in several cancers.

- Blood cancers:

The role of SUV39H1 in hematopoietic malignancies is more studied in leukemia, including acute myeloid leukemia (AML) and myelodysplastic syndrome (MDS). As discussed above, SUV39H1 interacts with several DNA-binding proteins involved in leukemogenesis, such as AML1 (Runx1) (Chakraborty et al., 2003) and Evi1 (Cattaneo and Nucifora, 2008; Spensberger and Delwel, 2008) and promotes the silencing of their target tumor suppressor genes, such as *p16* and *E-Cadherin* suppression in MDS and AML. Inhibition of SUV39H1 activity (by chaetocin treatment) or expression (shRNA targeting) alone or in combination

with other drugs showed therapeutic interests in AML (Chaib et al., 2012; Lakshmikuttyamma et al., 2010).

In the contrary, Muller-Tidow et al., showed a close association of H3K9me3 patterns with AML patients' event free survival where higher levels of H3K9me3 reflected better prognosis prediction independent from karyotype, age, and NPM1/FLT3 mutations (Muller-Tidow et al., 2010). Also, in leukemias with rearrangement of the mixed-lineage leukemia gene (MLL-r leukemias) suv39h1 mediated H3K9 methylation has been shown to be involved in silencing of leukemic genes, *Hoxa7* and *Meis1*, in mice *(Chen et al., 2015)*.

In the murine Eμ-myc model of aggressive B cell lymphoma, Suv39h1/H3K9me3 has been shown to play an important role in limiting lymphogenesis by induction TGF-ß mediated cellular senescence. Human diffuse large B cell lymphoma (DLBCL), in which MYC is frequently activated and TGF-ß1 signaling is reported prognostically favorable, showed similar features of the murine model including association of low Ki67 stained subgroup with higher levels of H3K9me3, apoptosis and TGF-ß signaling activation (Reimann et al., 2010).

- Solid cancers:

Degradation of SUV39H1 by Pin1 protein peptidyl-prolyl cis/trans isomerase in human breast cancer tissues has been shown to promote tumorigenesis and overexpression of SUV39H1 in human and mice cell line models reduced the colony formation *in vitro* and tumor growth *in vivo* respectively (Khanal et al., 2013).

However another study showed high SUV39H1 protein levels in basal like breast cancer (BLBC), an aggressive subtype of breast cancer which is associated with metastasis and poor outcome. Dong et al (Dong et al., 2013) showed that SUV39H1 in association with Snail protein, a zinc-finger transcriptional repressor, contributes to establishment of H3K9me3 and DNA methylation at E-Cadherin promoter and downregulation of this gene in BLBC. E-Cadherin downregulation is a hallmark of epithelial mesenchymal transition (EMT) which is a characteristic of embryonic development, tissue remodeling and metastasis.

SUV39H1 downregulation, using both gain-of-function and loss-of-function and rescue systems with CRISPR-Cas9 mediated knockout (KO) and re-expression of SUV39H1, has been shown to reduce migration of human prostate cancer cell lines (Yu et al., 2017).

Above findings suggest that although SUV39H1 have a predominantly tumor-suppressor activity it can however participate in silencing of other tumor suppressor genes and inducing metastasis dependent of the cancer cell context and available partners.

4.6.2. SETDB1 (SET domain bifurcated 1)

SETDB1, located on chromosome 1q21, encodes for the histone-lysine N-methyltransferase protein SETDB1, also called ERG-associated protein with a SET domain (ESET) and KMT1E.

The SETDB1 protein (1291 aa, ~143KD) contains two major functional domains: the N-terminal, containing two tudor domains which bind to both methylated Arg and, and the C-terminal contains the pre-SET, SET and post-SET domains, which are all required to catalyze methylation of H3-K9 (Figure 21). The evolutionarily conserved SET domain homology of SETDB1 is interrupted by a large 347-aa insertion conserved across different organisms (Schultz et al., 2002). Although mutation of conserved amino acid residues in the catalytic domain, including the pre-SET, SET, and post-SET domains, significantly impairs the enzymatic activity of SETDB1, the function of the interposed sequence is not well known. Recently Lidong Sun et al., demonstrated that mono-ubiquitination of lysine-867, located in the insertion domain, is essential for SETDB1 enzymatic activity and function (Sun and Fang, 2016).

SETDB1 protein also contains a putative CpG DNA methyl binding domain of the MeCP2 family (MDB) which is thought to mediate to methyl-CpG binding and protein-protein interactions. A point mutation (R643V) in the MBD homology had no effect on this enzymatic activity (Schultz et al., 2002).

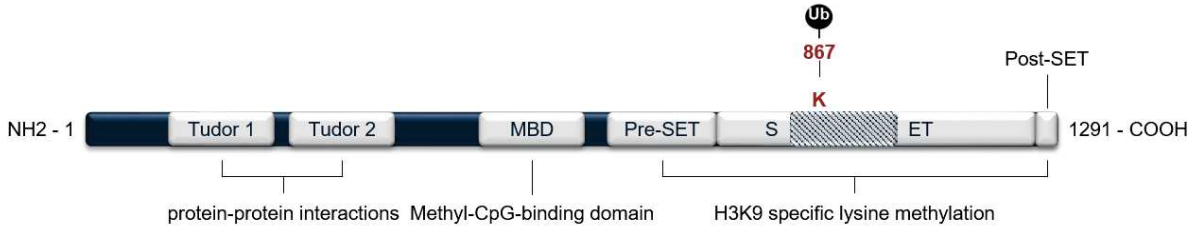

Figure 21. Schematic presentation of human SETDB1 protein domains and known posttranslational modification sites.

4.6.2.1. SETDB1 subcellular localization and function

K9-specific histone H3 methyltransferase activity of SETDB1 was first identified in association with KAP-1 protein (KRAB-associated protein-1, also called TRIM28), the corepressor partner of KRAB domain zinc-finger proteins (KRAB-ZFP) (Schultz et al., 2002). In this study SETDB1 was shown to localize predominantly in euchromatic regions of interphase nuclei overlapping with HP1 staining in non-pericentromeric regions of chromatin. SETDB1 is recruited to the KRAB-ZFPs complex via SUMOylated-bromodomain part of the KAP-1 protein and contributes to HP1-mediated silencing of euchromatic genes by KRAB-ZFPs complex (Figure 22) (Dodge et al., 2004; Schultz et al., 2002).

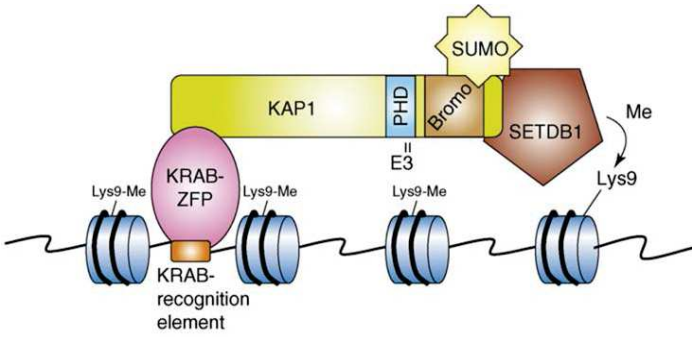

Figure 22. Schematic presentation of SETDB1 recruitment to the target genes after interaction with KAP1 SUMO-bromodomain. Adapted from (Peng and Wysocka, 2008).

SETDB1 has been reported to be both nuclear and cytoplasmic (Beyer et al., 2016; Loyola et al., 2006; Tachibana et al., 2015). This is in line with the existence of two predicted nuclear export signals (NESs) and two nuclear localization signals (NLSs) in its amino terminal domain. These motifs are also found in mouse Setdb11 at the preserved positions (Cho et al., 2013). However, the regulation and function of SETDB1 subcellular localization remain largely unknown. Recently, Beyer *et al.,* showed that Setdb1 is homogeneously distributed between the cytoplasm and the nucleus in majority (77%) of proliferating C2C12 myoblasts whereas it was dominantly cytoplasmic in 75% of differentiating C2C12 myoblasts. Setdb1 relocation to cytoplasm was dependent on canonical Wnt signaling in these cells and was concomitant to release of Setdb1 from selected target genes upon myoblast terminal differentiation. These results suggest subcellular relocalisation of Setdb1 as a novel mechanism regulating Setdb1 functions in myogenesis (Beyer et al., 2016).

4.6.2.2. SETDB1 recruitment to the chromatin

Recruitment of SETDB1 at the target regions is achieved thanks to interacting with its DNA binding partners, such as certain Zinc finger proteins, like ZNF274 (Frietze et al., 2010), and some transcription factors, such as POU5F1 (Yuan et al., 2009) and KAP1 (Trim28). Consistent with this, deletion of KAP1, which recruits SETDB1 to proviral loci, leads to loss of histone 3 lysine 9 trimethylation (H3K9me3) specially at intracisternal A particle (IAP) endogenous retroviruses and ectopic activation of these regions in early embryogenesis (Rowe et al., 2010).

SETDB1 function can also be modulated by its partners. SETDB1 can catalyze both di- and trimethylation of H3K9 in euchromatic regions. H3K9 trimethylation activity of SETDB1 is related to the human homolog of murine ATFa-associated modulator (hAM) cofactor which promotes H3K9me3 rather than H3K9me2 and enhances transcriptional repression by SETDB1 on a chromatin template once associated to SETDB1 (Wang et al., 2003).

4.6.2.3. Role of SETBD1 in normal development

SETDB1 controls H3K9me3 outside of pericentric heterochromatin and plays crucial roles in development.
Setdb1 is essential for early development and homozygous mutations of setdb1 leads to embryonic lethality at pre-implantation stage (Dodge et al., 2004). It has also shown to be important in the control of stem cell maintenance by repression of developmental regulator genes (Bilodeau et al., 2009) and class I and II endogenous retroviruses in mESCs (Karimi et al., 2011).

- B-cell development:

Setdb1 is constitutively expressed and is necessary during B cell development. Loss of setdb1 in pro-B stage only modestly reduces global H3K9me3 levels (Collins et al., 2015) but abolishes completely B-cell development by de-repression of retrotransposons transcription, notably endogenous murine leukemia virus (MLV) elements. Forced MLV expression is associated with unfolded protein response (UPR) followed by apoptosis of pro-B cells, confirming prosurvival function of Setdb1 at early stages of B development (Pasquarella et

al., 2016). Setdb1 is the first H3K9 histone methyltransferase to be identified as an essential regulator of hematopoietic stem and progenitor cells (HSPCs). In contrary to pro-B cells, in HSPCs Setdb1 is dispensable for the silencing of ERVs and restricts preferentially non-hematopoietic gene expression, the ectopic expression of which compromises the function of HSPCs. Activation of glycolysis antagonizing pathways upon Setdb1 depletion seems to be detrimental to HSPCs. Similar to HSPCs, HSCs are also depleted in the absence of Setdb1 potentially as a result of increased reactive oxygen species levels (Koide et al., 2016).

- Neurogenesis:

SETDB1 plays crucial roles in brain development. It is highly expressed in neural progenitor cells (NPCs) and represses non-neural genes and retrotransposons in these cells. Its expression is downregulated over time and is at the lowest levels during the neuron-to-astrocyte fate switch. Setdb1 ablation impairs neurogenesis (Tan et al., 2012).

- Bone development:

ESET has been showed to have a critical role in differentiation of mesenchymal stem cells into osteoblasts and postnatal bone development in mice. Specific knockout of Eset in mesenchymal cells was associated to deregulation of Runx2 and Indian hedgehog (Ihh) genes, which are master regulators of both osteoblast and chondrocyte differentiation, and severely impaired osteoblast differentiation in mutant mice (Lawson et al., 2013).

4.6.2.4. Role of SETDB1 in cancer and drug resistance

SETDB1 deregulated expression, mostly due to the focal amplification of the gene, also has been reported to be associated to different types of cancers and non-cancer diseases.

- Melanoma:

SETDB1 has been shown to be focally amplified in a broad range of malignancies including melanoma cell lines and samples as well as in non-small-cell lung cancer, small-cell lung cancer, ovarian cancer, hepatocellular carcinoma and breast cancer tissues.

In melanoma, SETDB1 overexpression significantly accelerated melanoma onset in zebrafish model and was associated to a more aggressive phenotype. Also, high levels of SETDB1 protein were observed in 70% of malignant melanomas (n=91) whereas it is present in 15% of

benign naive melanomas (n=20) and only 5% of normal melanocytes (n=20) (Ceol et al., 2011).

- Lung cancer:

The copy-number gain for *SETDB1* in lung cancer is associated with overexpression of the transcript and protein levels and has the oncogenic role of increasing cell growth *in vitro* and in primary tumors. It was proposed to be as a result of stimulated activity of the WNT-β catenin pathway by SETDB1 and consequent increased levels of c-MYC and Cyclin D1 in non-small cell lung cancer (Sun et al., 2015). Interestingly, lung cancer cells carrying a *SETDB1* gene amplification are also more sensitive to the anti-proliferative action mediated by mithramycin treatment. This raises the possibility of exploring new targeted therapies for the subset of lung tumor patients harboring the SETDB1 gene amplification event (Rodriguez-Paredes et al., 2014).

- Hepatocellular carcinoma (HCC):

In hepatocellular carcinoma, *SETDB1* moderate copy number gain and overexpression is associated with GOF TP53 mutations including R249S. GOF but not wild-type p53 status renders cell growth dependent on SETDB1 and downregulation of SETDB1 in HCC cell lines bearing the R249S mutation suppresses cell growth *in vitro* and *in vivo (Fei et al., 2015)*.

- Breast cancer:

SETDB1 is often amplified in primary breast tumors, and its depletion confers to breast cancer cells growth disadvantage. Regina et al., showed that SETDB1 is a binding partner of p63, which contributes to the self-renewal potential of breast cancer stem cells. P63 protein stability increases upon interaction with SETDB1 and represses the genes whose expression is positively correlated to survival of breast cancer patients. This study suggests a diagnostic and prognostic potential for p63 and SETDB1 expression in breast cancer (Regina et al., 2016).

- Blood cancers:

CRISPR/Cas9 genetic screening in AML cell lines revealed that *SETDB1* is a critical regulator of AML cell survival by suppressing innate immunity response. This study showed that SETDB1 loss of function leads to rapid de-repression of transposable elements (TEs), including ERVs, satellite repeats, and LINEs. Expression of these elements increased the

dsRNA content of the cancer cells, resulting to activation of the cytosolic RNA–sensing pathway and IFN-induced apoptosis (Cuellar et al., 2017).

Chromosome 1q aberrations are very frequent in B cell non-Hodgkins lymphoma (NHL) and multiple myeloma (MM) (Fournier et al., 2007). This region is target of different cytogenetic abnormalities such as balanced translocations, amplifications, and jumping translocations leading to copy number gain of the genes located on this locus. However, the role of SETDB1 in these malignancies remains uncharacterized.

- Drug resistance:

SETDB1 expression is induced also upon lethal chemotherapeutic drug exposure in solid tumors. Classon and colleagues recently showed that mRNA levels of SETDB1 are elevated in drug-tolerant cancer cell subpopulations, which harbor the potential of inducing disease relapse. The chromatin structure of these cells exhibited a repressed state, characterized by global decrease of H3K acetylation and increased SETDB1-mediated H3K9me3 over long interspersed repeat element 1 (LINE-1). Reduced expression of SETDB1 via knockdown and knockout approaches abolished establishment of drug-tolerant state. Perturbing H3K9me3 heterochromatin formation by using HDAC inhibitors resulted in re-expression of LINE-1. The authors proposed H3K9me3-mediated repression of this transposable element as a mechanism for transient survival of cancer cells from lethal drug exposure (Guler et al., 2017).

Taken together the above findings suggest that upregulation of SETDB1 is predominantly an oncogenic event in human cancers and targeting this enzyme provides considerable impacts on cancer cell survival by distinct mechanisms.

4.6.2.5. SETDB1 in other diseases

- Huntington disease:

In 2006 Ryu and colleagues showed an elevated expression of SETDB1 protein concomitant with higher levels of H3K9me3 in Huntington disease (HD) patients and in transgenic HD mice. This study showed that blocking of transcription activators of SETDB1 promoter in neural cells, specificity protein 1 (Sp1) and specificity protein 3 (Sp3), by the anti-tumoral antibiotic mithramycin reduces SETDB1 expression and H3K9me3 levels. This was

associated with better behavioral and neuropathological phenotype and survival in the HD mice (Ryu et al., 2006).

- Schizophrenia:

SETDB1 mRNA level is elevated in lymphocytes and in postmortem parietal cortex samples obtained from patients, associated with higher levels of SETDB1 mRNA levels of H3K9me3, longer illness duration, and with family history of schizophrenia (Chase et al., 2013).

- Autism:

Autistic patients carry potentially detrimental alterations in MBD6 and SETDB1. Autism spectrum disorders (ASD) have been showed to be associated with a nonsynonymous deletion Pro1067del in *SETDB1* gene, which correspond to the SET domain region of the protein (Cukier et al., 2012).

Scientific arguments

Mantle cell lymphoma (MCL), accounts for approximately 5–10% of B-cell lymphomas with an annual incidence of 0.45/100,000 persons in Europe. Despite progress in treatment over the last two decades, MCL remains incurable. In a national epidemiological the median overall survival (OS) of French MCL patients is only 40 months (Leux C et al, Ann Hematol. 2014). High dose immune chemotherapy with or without consolidation by autologous-stem cell transplantation (ASCT), followed or not by maintenance therapy with anti-CD20 monoclonal antibodies such as Rituximab is showing benefit in younger MCL patients. For older patients Rituximab associated to chemotherapy followed or not by Rituximab maintenance is emerging as standard of care. With these regimens more than 80% of patients reach complete remission at end of therapy but many, if not all patients, will experience iterative relapses and response duration steadily decreases from one salvage therapy to the next.

MCL is characterized by a high degree of genomic instability, including losses, gains, amplifications or deletion of numerous chromosomal regions. About 90% of MCL patients present the t(11;14)(q13;q32) translocation that leads to illegitimate overexpression of the cell cycle regulator Cyclin D1 (CCND1). It is of note that CCND1 expression is normally restricted to non- haematopoietic tissues. More recent genomic studies have identified a number of recurrently mutated genes; in order of descending frequency these include ATM, CCND1, UBR5, TP53, BIRC3, NOTCH1/2 and TRAF2 (Kridel R, Blood. 2012; Meissner B et al,; Blood. 2013; Bea S et al, Proc Natl Acad Sci U S A. 2013; Rahal R et al, Nat Med. 2014; Zhang J et al, Blood. 2014). However, no clear oncogenic driver has been identified yet and studies investigating clonal evolution on therapy are lacking.

Epigenetic deregulation also appears to play a role in MCL pathogenesis. This is supported by the discovery of mutations in genes encoding epigenetic modifiers such as WHSC1, MLL2, and MEF2B, in a subgroup of MCL patients (Bea S et al, Proc Natl Acad Sci U S A. 2013). Likewise, unscheduled activity of transcriptional regulators such as SOX11 is implicated in differentiation arrest in MCL B cells, irrespective of the mutational landscape (Vegliante MC et al, Blood. 2013). The clinical relevance of the latter findings is not currently known but indications are that epigenetic therapy will be beneficial in MCL. Finally, MCL cells are antigen-experienced cells and clinical and laboratory observations indicate a key role for the tumour microenvironment and B-cell receptor engagement in MCL pathogenesis.

Based on these observations we have proposed that MCL bears hallmarks of disordered lineage and differentiation stage-specific gene expression programs. We hypothesized that heterochromatin alterations / plasticity might be responsible for this. We have previously shown that aberrant topological organisation of constitutive heterochromatin compartments can drive gene silencing, including of candidate tumour suppressors, by a 'heterochromatin spreading or invasion' process that show parallels with 'position effect' described in species such as Drosophila and yeast (Fournier et al, EMBO Mol Med, 2010). Likewise, we have shown that in aggressive lymphoid cancers, 'Loosening' of heterochromatin compaction can lead to unscheduled activation of tissue specific genes, including male germ line genes, which can have potent tumour promoting properties (Emadali et al, EMBO Mol Med, 2013).

In this work we set out to assess the heterochromatin mark H3K9me3 integrity in MCL. H3K9me3 modification has been most often studied in the context of constitutive heterochromatin in repetitive regions and genome stability but it has been shown that this epigenetic mark is also involved in regulation of tissue-specific gene expression and is a key guardian of lineage identity in somatic cells (Cheloufi S et al, Nature. 2015). Two major enzymes responsible for catalysis of this mark, SUV39H1 and SETDB1, represent therapeutic interests as they are implicated in different types of cancer with a dominant tumour-suppressor and oncogene contributions respectively. We reasoned that exploring this mark could lead to new insights to disease mechanisms in MCL. We also hypothesized that these disease mechanisms could lead to the discovery of new treatment strategies in this aggressive lymphoma subtype.

By diverse approaches we showed that the MCL can be divided into two biological entities based on H3K9me3 profiles ('low' versus 'high') which are associated with differential expression of key cancer signatures relating to embryonic/hematopoietic stem cell function and B cell differentiation programs. Low H3K9me3 was linked to lowered expression/ activity of the two major histone methyltransferases SUV39H1 and SETDB1, without association to mutations in these epigenetic modifiers. Knockdown of SUV39H1 accelerated tumour growth in MCL xenografts, supporting a tumour-suppressor role for this enzyme in MCL. Whereas SETDB1 depletion induced G1/S arrest coincident to reprogramming to a pre-B cell phenotype.

These findings indicate a previously-unsuspected and complex role for H3K9me3 in MCL pathogenesis, through amplification of defined oncogenic signalling pathways and in

tumour suppression. Taken together it is predicted that this investigation will generate novel biomarkers – including H3K9me3 itself – and therapeutic strategies focused on blockade or correction of H3K9me3 chromatin signalling in MCL.

Results

H3K9 trimethylation controls oncogenic signaling and the malignant state in mantle cell lymphoma.

Azadeh Hajmirza[1], Anouk Emadali[1], Samuel Duley[1], Sarah Bertrand[1], Els Verhoeyen[2], Sieme Hamaidia[1], Patricia Betton-Fraise[1], Barbara Burroni[3], Antoine Martin[4], Thierry Bonnefoix[1], Rémy Gressin[1], Saadi Khochbin[1], Steven Le Gouill[5], Mary Callanan[1,6]

Affiliations :

[1]INSERM U1209, CNRS UMR 5309, Faculté de Médecine, Université Grenoble Alpes, Institut pour l'avancée des Biosciences, Grenoble, France

[2]INSERM U1065, Centre Méditerranéen de Médecine Moléculaire, Nice, France

[3]Service de pathologie, hôpital Cochin, AP-HP , 75014 Paris, France

[4]Department of Pathology, Avicenne Hospital, Bobigny, France University of Paris 13, Bobigny, France

[5]Centre de Recherche en Cancérologie Nantes-Angers, INSERM, Centre National de la Recherche Scientifique (CNRS), Université de Nantes, Nantes, France

[6]Centre d'innovation en génétique et épigénétique des cancers, CHU François Mitterand, Dijon, France

Correspondance :

mary.callanan@univ-grenoble-alpes.fr

Abstract

Mantle cell lymphoma (MCL) is an aggressive lymphoid cancer characterised by iterative clinical relapses and short survival. MCL displays complex genetics and hallmarks of misregulated expression of lineage specific genes. We have hypothesized that the latter might result from corruption of H3 lysine 9 trimethylation signalling a key pathway for suppression of lineage inappropriate programmes in somatic cells. By screening for H3K9me3 levels across a cohort of 120 MCL cases, we found global reductions of H3K9me3 in 1/3 of cases. This was linked to a dramatically altered H3K9me3 landscape defining two 'epigenetic subtypes' of MCL defined by distinct gene expression programs. Mechanistically, this could be linked to differential regulation of SUV39H1 and SETDB1 histone methyl transferase expression / activity respectively and activation of key cancer signatures relating to hypoxic signalling, embryonic/hematopoietic stem cell function, and B cell differentiation. In keeping with the pathological relevance of these findings, knockdown of SUV39H1 accelerated tumour growth in MCL xenografts while SETDB1 depletion induced G1/S arrest coincident to reprogramming to a pre-B cell-like phenotype. Taken together this identifies convergence of H3K9me3 signalling pathways to essential targets for MCL disease initiation and progression.

Introduction

Mantle cell lymphoma (MCL) accounts for 5–10% of all lymphomas (annual incidence is 0.45/100,000 persons). MCL remains incurable with a median overall survival (OS) in French MCL patients of only 40 months, despite intensive chemotherapy (Leux et al., 2014). Induction immuno-chemotherapy including high-dose cytarabine followed by autologous stem cell transplantation and maintenance therapy is recommended for young patients(Hermine et al., 2016; Le Gouill et al., 2017) while elderly patients should be treated with 8 courses of R-CHOP followed by rituximab maintenance(Kluin-Nelemans et al., 2012). Although more than 80% of patients reach complete remission at the end of therapy, all patients eventually experience iterative relapses and response duration decreases from one salvage therapy to the next. At relapse, drugs such as ibrutinib, lenalidomide, velcade, temsirolimus alone or in combination with other chemotherapies are proposed, and allogeneic stem cell transplantation for young fit patients may be the only curative treatment.

The MIPI score and its biological variant (bio-MIPI) are the most widely used prognostic scoring systems. Both classify patients according to clinical (age and disease stage) and biological

(lymphocyte count, LDH level, percentage of KI67 positive cells) parameters (Bottcher et al., 2008). However, these scores have major limitations in clinical practice and were not designed to decide treatment strategy.

More than 90% of MCL present the t(11;14)(q13;q32) translocation that leads to overexpression of the cell cycle regulator Cyclin D1 (*CCND1*). Genomic studies have identified a number of recurrently mutated genes (*ATM, CCND1, UBR5, TP53, BIRC3, NOTCH1/2 and TRAF2)*(Bea et al., 2013; Kridel et al., 2012; Meissner et al., 2013; Rahal et al., 2014; Zhang et al., 2014). However, no clear cut oncogenic driver has been identified and studies investigating clonal evolution on therapy are lacking. Epigenetic deregulation also appears to play a role in MCL disease pathogenesis (Queiros et al., 2016). This is supported by the discovery of mutations / altered activity of genes encoding epigenetic regulators (WHSC1, MLL2, MEF2B and SOX11) (Bea et al., 2013) and evidence that DNA methylation is globally perturbed (Queiros et al., 2016). The clinical relevance of the latter findings is not currently known but indications are that epigenetic therapy will be beneficial in MCL.

Finally, MCL cells are antigen-experienced cells and laboratory observations indicate a key role for the tumour microenvironment and B-cell receptor engagement in disease pathogenesis.

MCL bears hallmarks of disordered lineage and differentiation stage-specific gene expression programmes. Based on our hypothesis that epigenetic reprogramming is an integral component of malignant transformation and clonal evolution in lymphoid cancers(Emadali et al., 2013; Fournier et al., 2010), we have investigated the integrity of the histone mark, H3K9me3 (trimethylation of histone H3 lysine 9) - a major regulator of lineage identity in somatic cells - in MCL(Cheloufi et al., 2015; Sridharan et al., 2013). Remarkably we find that MCL can be subdivided into 2 epigenetic subtypes according to H3K9me3 landscapes that further associate to distinct gene expression programs.

Materials and methods

MCL patient samples

MCL patients were recruited retrospectively between 1997 and 2016 through the Grenoble University Hospital lymphoma bank or were selected for analysis from the LYSA tumour bank for the RiBVD phase II trial, coordinated by the French Lymphoma Study Association (LYSA). Following review of

clinical and biological criteria for MCL diagnosis, and on the basis of available histologic data, DNA and RNA samples and access to clinical and cytogenetic data, 30 patients were enrolled in the initial MCL gene panel testing phase (Supplemental Table 1).

MCL cell lines

The human MCL-derived cell lines (HBL-2, Jeko-1, JVM-2, Maver-1, Mino and Rec-1) were grown in RPMI 1640 and 25mM HEPES (Gibco), supplemented with 2mM L-glutamine (Gibco) and 100µg/ml Penicillin/Streptomycin solutions (Gibco) and 10% (HBL-2, JVM-2 and Rec-1) or 20% (Jeko-1, Maver-1, Mino) of fetal bovine serum (FBS) (Biowest). HBL-2 was also supplemented with 1mM sodium pyruvate (Gibco), non-essential amino acids (Gibco) and vitamins (Gibco). Granta-519 cells were grown in DMEM and 25mM HEPES (Gibco), supplemented with 10% FBS (Biowest), 4.5g/L glucose (Gibco) and 100µg/ml Penicillin/Streptomycin solutions (Gibco).

RT-qPCR, gene expression profiling, and Sanger sequencing

Total RNA was obtained from whole cells using the Trizol reagent (Invitrogen Life Technologies). The quality was controlled by using the Agilent Bioanalyzer system and quantity was evaluated by Nanodrop.

For RT-qPCR analysis, RNAs were reverse transcribed by using the SuperScript® III First-Strand Synthesis SuperMix (Invitrogen) and subjected to quantitative PCR by using SYBR® Green PCR master mix (Applied Biosystems) and primers shown in Supplemental Table 2, according to manufacturers' instructions. The *ABL* gene was used as a control for normalization of gene expression data. qPCR was performed on a MX3000P machine (Stratagene).

Affymetrix microarrays were processed in the Microarray Core Facility of the Institute of Research on Biotherapy, CHRU-INSERM-UM1 Montpellier (http://irb.chu-montpellier.fr/). Biotinylated cRNA was amplified with double in vitro transcription and hybridized to the Affymetrix HG U133 set microarrays, according to the manufacturer's instructions (Affymetrix, Santa Clara, CA, USA). Fluorescence intensities were quantified and analyzed using the GCOS 1.2 software (Affymetrix). GEP data normalization and gene set enrichment analysis (GSEA) were performed as described previously (Emadali et al., 2016).

Sanger sequencing of the *SUV39H1* locus was performed on seven MCL cell lines by standard methods using primers shown in table S3 and PCR conditions, as described (Kridel et al., 2012). Purified PCR products were directly sequenced in both directions, using BigDye Terminator Mix (Applied Biosystems), on the Applied Biosystems 3130xl Genetic Analyzer. Data were analyzed with the SeqScanner software version 1.0.

Immunohistochemistry and western blotting

To evaluate H3K9me3, HP1α, and CYCLIN D1 levels, IHC was performed on formalin-fixed paraffin-embedded tissue. Used antibody dilutions, the incubation time, antigen retrieval methods, and detection kits are indicated supplemental Table 4. The H-score method was used for evaluation of the immunostaining, by multiplying the intensity of the staining (0: no staining, 1: weak, 2: moderate and 3: strong staining) with the percentage of the tumor stained. The minimum score was 0 and the maximum was 300. H-score > or = to 100 was evaluated as high and H-score < 100 as low H3K9me3.

For western blot, whole cell lysates, obtained by sonication of cell pellets in Laemmli buffer, were resolved by SDS-PAGE and transferred onto nitrocellulose membranes. After treatment with blocking solution (1X PBS, 8% skimmed milk, 0.1% Tween 20), membranes were incubated with primary antibody (Supplemental Table 3) in PBS 3% skimmed milk 0.1% Tween 20, then washed three times for 10 minutes and incubated with anti-rabbit or mouse IgG-HRP secondary antibodies (Thermo Fisher Scientific) before revelation in ECL SuperSignal West Pico Chemiluminescent Substrate (Thermo Fisher Scientific). Images were captured using autoradiography films.

Gene silencing

Non-targeting (control; Ctrl), SUV39H1-targeting, and SETDB1-targeting short hairpin RNA (shRNA) sequences were designed using the DSIR algorithm (http://biodev.cea.fr/DSIR/DSIR.html) (Vert et al., 2006). Hairpin sequences are provided in supplemental Table 5. Short hairpin sequences were cloned into the pLKO-1 lentiviral vector (Addgene) and packaged, as described previously (Levy et al., 2010). Cell lines stably expressing shCtrl, shSUV39H1, and shSETDB1 were established under puromycin selection.

Drugs treatments, and cell viability

For drug treaments, $5x10^5$ cells per milliliter were treated for the desired time and drug concentration. All compounds were purchased from Sigma. Cell viability was evaluated by AnnexinV-FITC/PI (propodium iodide) double staining (Beckman Coulter) or PI staining followed flow cytometry analysis (LSIIR, BD). Specific cell death was calculated as (% of drug-induced cell death - % control cell death)/(1- % control cell death), as described (Lajmanovich et al., 2009).

Phenotypic labeling for Flow cytometry

Cells were labeled with human anti-CD19 (Biolegend-Ozyme, IgG1k, mouse FITC - 302205), anti-CD20 (Biolegend-Ozyme, IgG2bk, mouse FITC -302303), anti-CD40 (Biolegend-Ozyme, IgG1k, mouse APC -313008) and anti-IgM (Biolegend-Ozyme, IgG1k, mouse PE –MHM-88) antibodies for flow cytometry analysis (LSR II, BD, Diva software).

Cell cycle analysis and PKH26 labeling

For cell cycle analysis, cells (10^6 cells) were washed, resuspended in 1X PBS buffer and fixed in ice cold 70% ethanol, by dropwise additional while vortexing. Cells were fixed overnight at 4°C, then washed and rehydrated in 1X PBS for at least 4 hours at 4°C. RNA was degraded by adding 10 µg RNAase and DNA was stained with 10 µg propidium iodide. After 30 minutes incubation, samples were analyzed on FACS. Cell cycle analysis was performed using Modfit analysis software. PKH26 cell proliferation assays were performed according to the manufacturer's instructions (SIGMA, MINI26-1KT). After labeling, cells were re-suspended in cell culture medium and FACS analysis was performed at 0, 24, 48 and 72 hour time points, after labeling. Proliferation index calculation was performed using Modfit analysis software.

Xenotransplantation assays

All animal experiments were conducted in agreement with the Principles of Laboratory Animal Care (National Institutes of Health publication no. 86-23, revised 1985) and approved by the regional ethics committee (ComEth-CEEA12, n°180). For xenotransplants, $5x10^6$ Jeko-1 cells (shCtrl, and shSUV39H1) were injected subcutaneously into the flanks of 6 to 8 week-old female SCID mice

(Charles River). For follow-up of tumor engraftment and growth, tumor volume was measured every 2 to 3 days with a caliper and calculated using the formula breadth^2 x Length x 0.52.

3D-preserved nuclei preparation

Sixteen hours prior to harvesting and preparation of 3D preserved cell nuclei for immunofluorescence (IF), cells were diluted to a concentration of 0.5 million per ml in RPMI medium. Briefly, lymphocytes were harvested and resuspended to a concentration of 2.5 x10^6 / 2ml of nuclei buffer (5mM Hepes, 50mM KCL, 10mM MgSO4, 0.05% Tween 20 pH8) with 30µl of RNase (10mg/ml). Lymphocytes were then permeabilised by addition of 50µl of Triton X-100 (10% v/v) for 10 minutes at 4°C, incubated for 30 minutes at 37°C and fixed in paraformaldehyde (PFA 4%, 1X PBS), under agitation. The reaction was stopped by addition of 30 ml of Tris-HCl 100mM, pH 7.0. The released nuclei were washed 3 times in 1X PBS Nuclei (50,000), and cyto-centrifuged onto vectabond-treated glass slides.

Immuno-fluorescence in 3D-preserved cell nuclei

Cell nuclei on vectabond slides were permeabilised in 1X PBS / 0.5% Triton X-100 / 0.5% saponin buffer for 5 minutes at room temperature, then washed in 1X PBS and blocked in PBS 1X / 5% non-fat skimmed milk for 30 minutes at 37°C in a moist chamber. Slides were then incubated with rabbit anti-H3K9me3 (Upstate, 07-523, 1/200ème) and mouse anti-HP1α (Euromedex MAB 3584, 1/500ème) in 1X PBS / 1% non-fat skimmed milk for 1h at 37°C in a moist chamber. After 3 washes of 5 minutes each in 1X PBS / 0.1% Tween 20, secondary antibodies (Alexa Fluor488 conjugated anti-rabbit IgG – Invitrogen A-1134 and Alexa Fluor546-conjugated goat anti-mouse IgG – Invitrogen A-11030) were applied and incubated for 30 minutes, under the same conditions. After 3 x 5 minute washing steps in 1X PBS / 0.1% Tween 20, followed by 5 minute wash in 1X PBS, slides were briefly air dried and mounted in vectashield antifade and DAPI solution (SIGMA F6057).

Microscopy, image recovery and analyses

All 3D imaging was performed with an Optogenetic BiFocal Rapid microscope using a spinning disk equipped with 405, 488 and 546 nm laser excitation, with electrom multiplying (Em) gain of 200 and respectively with laser intensity and exposure times as follows : 70% (200 millisecond), 50% (200 milliseconds) and 30% (50 milliseconds). For each nucleus, images were captured in 3D with 35 z stacks of 0.3µm depth for a 10.2µm total depth. All images were obtained with the same threshold parameters for each fluorescence channel. All data were collected with Icy software with the same

protocol. H3K9me3 marks were obtained with the wavelet spot detector block and DAPI was obtained with HK-means correction.

H3K9me3 ChIp-seq chromatin assay

Nuclei were isolated from 10^7 cells using 1ml of cell lysis buffer (15 mM Tris ph 7.5, 15 mM NaCl, 15 mM KCl, 150 mM Sucrose, 0.2 mM Spermin, 0.65 mM Spermidin, 1mM DTT, 1X cOmplete™ Protease Inhibitor Cocktail (Roche), 5 mM NaF, 2 mM Na_3SO_4, 50 ng/ml TSA, 0.4% NP40) for 5 min and washed in MNase buffer (10 mM Tris ph 7.8, 10 mM KCl, $CaCl_2$ 1 mM, 1X cOmplete™ Protease Inhibitor Cocktail (Roche), 5 mM NaF, 2 mM Na_3SO_4, 50 ng/ml TSA). Chromatin was prepared using micrococcal nuclease digestion (Nuclease S7, Roche - 5U for 100µg DNA, 9 min at 37°C). Immunoprecipitations were performed on 50 µg chromatin fragments using 10 µg of anti-H3K9me3 (Abcam ab8898) or control IgG antibodies (Millipore 12-370) overnight at 4°C. 50 µl Protein A/G dynabeads (Invitrogen) were added for one additional hour. Beads complexes were washed three times in LSDB buffer (50 mM HEPES pH7.4, 350 mM KCl, 3 mM $MgCl_2$, 20% Glycerol, 1X cOmplete™ Protease Inhibitor Cocktail (Roche), 5 mM NaF, 2 mM Na_3SO_4, 50 ng/ml TSA). Complexes were then eluted for 20 min in elution buffer (10 mM Tris HCl pH 8.5, 1 mM EDTA, 1% SDS), treated with RNase A and proteinase K. DNA was isolated using phenol/chloroform extraction followed by ethanol precipitation, purified using Agencourt AMPure XP (Beckman Coulter) and yield quantified using Qubit fluorometer. Sequencing was performed by the IGBMC Microarray and Sequencing platform, a member of the 'France Génomique' consortium (ANR-10-INBS-0009). Briefly, ChIp seq libraries were constructed from 10 ng of input of immunoprecipitated DNA using the MicroPlex Library Preparation™ (Diagenode). Libraries were then purified, quantified and quality controlled by capillary electrophoresis (Bioanalyzer, Agilent) and submitted for paired-end 50 bp Illumina HiSeq 4000 sequencing.

H3K9me3 ChIp-seq bioinformatic analyses

ChIP-seq data were first check for quality sing metrics generated by FastQC (v0.11.5). Sequence reads were mapped to hg19 reference genome using Bowtie (v1.0.0) (Langmead et al., 2009) (with the following parameters -m 1 --strata --best -y -S -l 40 -p 2). Peak calling was performed for individual replicates using SICER (v1.1, window size=200, gap size=800, FDR= 0.01) (Zang et al., 2009).

Consensus peaks between replicates and differential peak lists between conditions (cut-off: FC>1.5, FDR<10^5) were identified using BedTools Intersect Intervals (Quinlan and Hall, 2010). Gene-centric annotation was performed using ChIpSeeker (Yu et al., 2015). Motif-based sequence analyses have been performed using MEME-ChIP (Machanick and Bailey, 2011). Graphical outputs were generated using DeepTools (Ramirez et al., 2016).

Results

MCL displays an altered H3K9me3 landscape characterized by discrete lineage and cell state-specific gene expression programs

To investigate the role of H3K9me3-dependent lineage integrity pathways in MCL pathogenesis, we screened H3K9me3 levels by immunohistochemistry in a series of 30 primary MCL cases that were recruited at our centre (Table S1). Remarkably, this revealed global alterations of H3K9me3 levels in a subset of MCL cases (1/3 of cases), indicative of major reprogramming of the heterochromatin landscape in MCL (Figure 1A). This did not appear to be associated to proliferation rates (as judged by Ki67 staining) or to histological subtypes with altered chromatin morphology (blastoid pleomorphic MCL) (not shown, in preparation). We next screened a series of 6 MCL cell lines for their H3K9me3 levels. Consistent with observations in patient biopsies, 2 of the 6 cell lines (HBL and Maver-1) showed marked depletion of H3K9me3 levels compared to the 4 other MCL lines (Figure 1B), thus further reinforcing the notion that H3K9me3 signaling is misregulated in MCL, in a cell intrinsic manner. Importantly, this did not seem to be the consequence of global alterations in histone methylation since histone H3 lysine 27 methylation did not show perturbations, at least under these assay conditions. More detailed analysis by immunofluorescence confocal microscopy in 3D-preserved nuclei revealed that H3K9me3 depletion in MCL cells was associated to partial collapse of H3K9me3 heterochromatic foci (HBL and Maver-1) and/or redistribution of H3K9me3 foci away from the nuclear periphery (Maver-1 cells) in ‘H3K9me3 low’ compared to ‘H3K9me3 high’ MCL cells (Figure 1C and D, Supplemental Figure S1A).

In view of the potentially pleiotropic effects of the above on gene expression programs, the next step was to determine the influence of this altered H3K9me3 landscape on gene expression in MCL (Figure 1E). For this, gene expression profiling followed by gene set enrichment analysis (GSEA)

of tumour biopsies from 28 MCL cases classed as either high (H-score > or = to 100) or H3K9me3 low (H-score < 100) were performed. Remarkably, this revealed enrichment of embryonic stem cell programs in H3K9me3 high compared to low MCL tumours, a feature also seen in MCL cell lines according to H3K9me3 levels. Conversely, 'H3K9me3 low' MCL tumours and cell lines showed gene expression programs that were more characteristic of germinal centre B cells, notably signatures related to CD40, including BCL2 family members and immune signalling via PD1 and TLR pathways (Figure 1E). Furthermore, 'H3K9me3 high' MCL tumours and cell lines showed enrichment for multiple non-B cell lineage programs, including numerous signatures related to hormone-dependent cancers, including breast and prostate cancers. In aggregate, this indicates that altered H3K9me3 landscapes are associated to global reprogramming of the expression of key cell identity and cell signalling programs of relevance to MCL pathogenesis.

H3K9me3 epigenome programming in MCL

We next wished to map the locations of H3K9me3 reprogramming across MCL 'H3K9me3 low' versus 'high' MCL genomes. To this end, we comprehensively mapped the epigenomic landscape of two representative 'H3K9me3 high' (Jeko-1 and Rec-1 cells) versus 'low' MCL lines (Maver-1 and HBL cells) by ChIP-seq (chromatin immunoprecipation [ChIP] combined with high-throughput sequencing) (Figure 2A). Differential analyses of H3K9me3 peaks revealed two classes of peaks ; narrow peaks localised to a restricted number of gene promoter and intergenic regions that were depleted for H3K9me3 in 'low' versus 'high' H3K9me3 MCL cells (357 peaks), together with a large number of very broad peaks - some of which may correspond to differentially reprogrammed 'large organized chromatin histone H3 lysine 9 (H3K9)-modified' (LOCK) heterochromatin regions - that were consistently gained in the MCL 'H3K9me3 low' compared to 'high' MCL cell line genomes (29828 peaks ranging in size from 10 to more than 100kb). Of note, fold changes for H3K9me3 enrichment across the broad compared to narrow H3K9me3 peaks were consistently lower (Figure 2A and B).

Peak annotation by the Panther algorithm was performed on the genes associated to the narrow ChIP-seq peaks that showed H3K9me3 loss in the H3K9me3 'low' versus 'high' MCL cell lines. This revealed differential enrichment for key biological processes of relevance to MCL pathogenesis and that broadly corresponded to functions that were identified by GSEA in the same cells. These

included enrichment for kinase signaling pathways characteristic of activated germinal center B cells and covalent chromatin modification (Figure 2C and D).

Diminished SUV39H1 expression is linked to global changes in H3K9me3 and to engagement of hypoxia and MYC signaling gene expression programs in MCL

To investigate further the underlying cellular mechanisms responsible for differential H3K9me3 epigenome programming in MCL, we first focused on the role of SUV39H1, a well-established H3K9me3 methyltransferase that has been linked to lymphomagenesis in humans and mice (Braig et al., 2005; Rui et al., 2010). Remarkably, despite abundant SUV39H1 transcript levels, SUV39H1 protein was substantially lower in 'H3K9me3 low' MCL compared to 'high' cells (Figure 1B and Supplemental Figure S2A). DNA sequencing established that this was not related to gene mutations. Rather, reduced SUV39H1 expression could be attributed to decreased half-life due to targeting for proteasomal degradation, probably via an MDM2/USP7 pathway (supplemental Figure 2B and C). Consistent with differing mechanisms of post-translational control of protein stability for SUV39H1 compared to SETDB1, a second major H3K9 methylase, SETDB1 levels were unchanged across H3K9me3 high versus low MCL cells (Figure 1B). This is consistent with different mechanisms for stabilization of SUV39H1 compared to SETDB1 (Timms et al., 2016). ChIP-seq for H3K9me3, and gene expression profiling followed by GSEA, were then performed in Jeko-1 cells (H3K9me3 'high' MCL) that had been treated by short hairpins against SUV39H1 versus controls, in order to establish its relative contribution to the H3K9me3 landscape in MCL (Figure 3B, and supplemental Figure 1). These experiments established that SUV39H1 modulates a significant proportion of H3K9me3 ChIP-seq peaks in MCL of which many related to MCL-relevant genes (Figure 3B and data not shown). Consistent with a role in reprograming to 'primed' chromatin, rather than a direct role in activation of gene expression in MCL, only a very restricted number of SUV39H1-dependant reprogrammed H3K9me3 domains could be correlated to gene de-repression. Gene expression profiling, followed by GSEA, identified profound changes in gene expression programs of importance for MCL biology including HIF1A hypoxic response, MYC signaling and proliferation signatures (Figure 3C). No obvious changes in cellular proliferation of SUV39H1 cells could be seen *in vitro* (normoxia). However, a xenotransplantation assay revealed a clear cut role for SUV39H1 suppression in accelerated tumour grow in vivo, indicative of a tumour suppressor function for SUV39H1 in MCL (Figure 3E and F).

SETDB1 controls and oncogenic network of H3K9me3 domains that control stem and MCL identity programs

Since both 'H3K9me3 high' and 'low' MCL cells displayed significant localisation of H3K9me3 at euchromatin sites, we reasoned that MCL cells might display a dependency on SETDB1 activity for maintenance of oncogenic phenotypes (SETDB1 plays a key role in euchromatic H3K9me3). In particular, we were keen to investigate this question in relation to stem cell function signatures which were shown to be enriched in 'H3K9me3 high' MCL compared to 'H3K9me3 low' MCL. We thus investigated the role of the SETDB1 histone methylase in H3K9me3 epigenome landscapes in MCL. Here, we again used Jeko-1 MCL cells as a study model. Short hairpin RNA knockdown against SETDB1 in these cells, coupled to H3K9me3 ChIP-seq, gene expression profiling / GSEA was performed, as for SUV39H1. Remarkably this revealed modulation of 1000s of H3K9me3 domains many of which overlap with the H3K9me3 'regulome' of SUV39H1 and with those peaks identified in the differential analysis of H3K9me3 epigenome in the 'high' versus 'low' H3K9me3 MCL lines (Figure 4B). Global levels of H3K9me3 did not appear to show major modulation, although heterochromatic foci collapse was observed, suggestive of re-deployment of H3K9 methylase activity to non-foci (possibly euchromatic) sites (Figure 4A and supplemental Figure 1B,C and D).

Consistent with this, GEP / GSEA reveal major reprogramming of gene expression signatures, including enrichment for G1/S arrest, and loss of BCR and B lymphoid stem signatures, in keeping with previous reports showing a key role for SETDB1 in maintaining stem cell properties in the HSC (Figure 4C). Supporting, the functional relevance of these findings, SETDB1 Jeko-1 knockdown cells showed G1/S arrest and evidence of 'de-differentiation' to a more immature B cell state (Figure 4D and E). The latter was characterised by reduced expression of mature B cell differentiation (CD19, CD20, IgM) and activation / memory cell surface markers (CD27). Importantly this 'de-differentiation' phenotype was not observed in SUV39H1 knockdown Jeko-1 cells, and seemed to rely on signalling networks distinct from those operated by SUV39H1 (supplemental figure 3). Taken together, this identifies SETDB1 as a major regulator of MCL identity and cell survival.

In keeping with our starting hypothesis concerning SETDB1, 'H3K9me3 low' MCL cells showed similar dependence phenotypes on SETDB1 activity compared to Jeko-1 cells (data not shown).

Clinical significance of H3K9me3 epigenome landscapes in MCL

In view of our findings linking H3K9me3 depletion to a SUV39H1-regulated tumour suppressor pathway in MCL ('H3K9me3 / SUV39H1 low' MCL), we next wished to establish how this related to mutational landscapes in MCL. For this, we performed targeted deep sequencing across 44 genes that are recurrently mutated in MCL, in both our MCL lines and our primary MCL cases. Interestingly, ATM mutations appear to be more frequent in 'H3K9me3 high' MCL compared to 'H3K9me3 low' MCL. In patient samples but not MCL lines, TP53 mutation was present in the 'H3K9me3 high' MCL cases but absent from the 'H3K9me3 low' cases, although numbers of TP53 mutant cases are low (3 patients) (Figure 5A). We next evaluated the potential role of H3K9me3 profiles in MCL disease progression by performing overall survival analysis in the initial MCL cohort (n=30). This analysis showed a tendency toward poorer prognosis in the MCL group with low levels of H3K9me3 (Figure 5B). The same analysis is now ongoing for a larger cohort (n=90) in order to confirm this result and enhance the statistic calculations (LYMA phase III trial).

Discussion

In this work, we have succeeded in identifying two new 'epigenetic' subtypes of MCL that according to their biological characteristics should offer new opportunities for precision medicine in MCL. These epigenetic subtypes are underpinned by stable and probably clonally propagated H3K9Me3 reprogramming events that affect gene, enhancer and chromatin topology-mediated regulation of gene activity, early in MCL pathogenesis.

The first MCL subtype is characterised by high H3K9me3 and stem / epithelial gene expression signatures. The second MCL subtype is characterised by H3K9me3 depletion, associated to decreased SUV39H1 activity and with gene expression programs more characteristic of germinal centre lymphoma. This raises the possibility that tailoring targeted therapies to our newly identified MCL 'epi-subtypes' may benefit patients. Indeed, new drugs that target BCR signaling, Bcl-2 family proteins, the mTOR, PI3K or NFKB pathways are under investigation in phase I/II/III clinical trials in MCL. These drugs are showing promise but treatment resistance is problematic. For example, ibrutinib a first-in-class BTK inhibitor approved for clinical use in relapse/refractory patients, induces response rates of 70% but 30% of patients are refractory to therapy and median duration of response is 16 months (Wang et al., 2013b). Point mutations in BTK have been described in a subset of MCL patients

with acquired resistance to Ibrutinib (Chiron et al., 2014) while activation of the alternative NF-κB pathway may be linked to *de novo* ibrutinib resistance (Rahal et al., 2014). Targeted therapies may also be responsible for clonal selection that can ultimately jeopardize patient outcome, suggestive that directing therapy to a single target is probably not the solution to cure patients (Martin et al., 2016). It is tempting to propose that H3K9me3 reprograming in the MCL epigenome could account for the prowess of MCL B cells to rapidly and stably mount adaptive / immune / treatment escape strategies, including at the residual disease level. Therapeutic intervention to halt or correct the consequences of this reprogramming / epigenetic plasticity is likely to be of benefit to patients. Two pathways that feed to H3K9me3 maintenance in the MCL epigenome are of importance. The first is a tumour suppressor pathway driven by SUV39H1. The second centres on SETDB1 which is a new candidate oncogene in MCL.

In summary, our work points to use of chromatin active agents, in particular directed to resetting cell identity programs mediated by H3K9me3 signalling, as an attractive therapeutic option in MCL. Our work indicates that treatment strategies aimed at this target will need to focus on both remission induction and on maintenance strategies (MCL stem cell properties).

Bibliography

1. Leux C, Maynadie M, Troussard X, et al. Mantle cell lymphoma epidemiology: a population-based study in France. *Ann Hematol*. 2014;93(8):1327-1333.
2. Hermine O, Hoster E, Walewski J, et al. Addition of high-dose cytarabine to immunochemotherapy before autologous stem-cell transplantation in patients aged 65 years or younger with mantle cell lymphoma (MCL Younger): a randomised, open-label, phase 3 trial of the European Mantle Cell Lymphoma Network. *Lancet*. 2016;388(10044):565-575.
3. Le Gouill S, Thieblemont C, Oberic L, et al. Rituximab after Autologous Stem-Cell Transplantation in Mantle-Cell Lymphoma. *N Engl J Med*. 2017;377(13):1250-1260.
4. Kluin-Nelemans HC, Hoster E, Hermine O, et al. Treatment of older patients with mantle-cell lymphoma. *N Engl J Med*. 2012;367(6):520-531.
5. Bottcher S, Ritgen M, Buske S, et al. Minimal residual disease detection in mantle cell lymphoma: methods and significance of four-color flow cytometry compared to consensus IGH-polymerase chain reaction at initial staging and for follow-up examinations. *Haematologica*. 2008;93(4):551-559.
6. Bea S, Valdes-Mas R, Navarro A, et al. Landscape of somatic mutations and clonal evolution in mantle cell lymphoma. *Proc Natl Acad Sci U S A*. 2013;110(45):18250-18255.
7. Kridel R, Meissner B, Rogic S, et al. Whole transcriptome sequencing reveals recurrent NOTCH1 mutations in mantle cell lymphoma. *Blood*. 2012;119(9):1963-1971.
8. Meissner B, Kridel R, Lim RS, et al. The E3 ubiquitin ligase UBR5 is recurrently mutated in mantle cell lymphoma. *Blood*. 2013;121(16):3161-3164.
9. Rahal R, Frick M, Romero R, et al. Pharmacological and genomic profiling identifies NF-kappaB-targeted treatment strategies for mantle cell lymphoma. *Nat Med*. 2014;20(1):87-92.

10. Zhang J, Jima D, Moffitt AB, et al. The genomic landscape of mantle cell lymphoma is related to the epigenetically determined chromatin state of normal B cells. *Blood*. 2014;123(19):2988-2996.
11. Queiros AC, Beekman R, Vilarrasa-Blasi R, et al. Decoding the DNA Methylome of Mantle Cell Lymphoma in the Light of the Entire B Cell Lineage. *Cancer Cell*. 2016;30(5):806-821.
12. Emadali A, Rousseaux S, Bruder-Costa J, et al. Identification of a novel BET bromodomain inhibitor-sensitive, gene regulatory circuit that controls Rituximab response and tumour growth in aggressive lymphoid cancers. *EMBO Mol Med*. 2013;5(8):1180-1195.
13. Fournier A, McLeer-Florin A, Lefebvre C, et al. 1q12 chromosome translocations form aberrant heterochromatic foci associated with changes in nuclear architecture and gene expression in B cell lymphoma. *EMBO Mol Med*. 2010;2(5):159-171.
14. Cheloufi S, Elling U, Hopfgartner B, et al. The histone chaperone CAF-1 safeguards somatic cell identity. *Nature*. 2015;528(7581):218-224.
15. Sridharan R, Gonzales-Cope M, Chronis C, et al. Proteomic and genomic approaches reveal critical functions of H3K9 methylation and heterochromatin protein-1gamma in reprogramming to pluripotency. *Nat Cell Biol*. 2013;15(7):872-882.
16. Braig M, Lee S, Loddenkemper C, et al. Oncogene-induced senescence as an initial barrier in lymphoma development. *Nature*. 2005;436(7051):660-665.
17. Rui L, Emre NC, Kruhlak MJ, et al. Cooperative epigenetic modulation by cancer amplicon genes. *Cancer Cell*. 2010;18(6):590-605.
18. Timms RT, Tchasovnikarova IA, Antrobus R, Dougan G, Lehner PJ. ATF7IP-Mediated Stabilization of the Histone Methyltransferase SETDB1 Is Essential for Heterochromatin Formation by the HUSH Complex. *Cell Rep*. 2016;17(3):653-659.
19. Wang ML, Rule S, Martin P, et al. Targeting BTK with ibrutinib in relapsed or refractory mantle-cell lymphoma. *N Engl J Med*. 2013;369(6):507-516.
20. Chiron D, Di Liberto M, Martin P, et al. Cell-cycle reprogramming for PI3K inhibition overrides a relapse-specific C481S BTK mutation revealed by longitudinal functional genomics in mantle cell lymphoma. *Cancer Discov*. 2014;4(9):1022-1035.
21. Martin P, Maddocks K, Leonard JP, et al. Postibrutinib outcomes in patients with mantle cell lymphoma. *Blood*. 2016;127(12):1559-1563.

Figure legends

Figure 1: MCL is characterized by an altered H3K9me3 landscape associated with altered expression of stem cell and B cell differentiation signatures

(A) Examples of immunohistochemistry staining of H3K9me3. 2/3 of cases showed intense labeling for H3K9me3 (represented in example case 1-H), whereas 1/3 of samples showed loss of staining by anti-H3K9me3 antibody (represented in example case 2-L). Cyclin D1 expression in shown in both cases. (B) Whole cell lysate were used to point H3K9me3 profiles and SUV39H1, SETDB1 and CCND1 expression levels in MCL cell lines by westernblot. (C) Immunofluorescent staining of H3K9me3 (green) in two high (Jeko-1,Rec-1) and two low (HBL, Maver-1) MCL cell lines. Nuclei staining were performed by using DAPI. (D) Number of H3K9me3 foci per nuclei (n>100). (E) Heatmap representation of the differentially expressed genes among low H3K9me3 patients (left panel) and low MCL cell lines (right panel) compared with high H3K9me3 patients and cell lines respectively. GSEA plots show gene regulatory circuits that are differentially expressed between high versus low H3K9me3 subtypes.

Figure 2: Genome wide mapping of H3K9me3 in MCL cell lines

(A) Heatmaps illustrate the regions loosing (left panel) or gaining (right panel) H3K9me3 ChIP-seq signal in low MCL cell lines compared to high cell lines. (B) Schematic presentation of H3K9me3 lost narrow and gained broad peak features in MCL low cell lines, HBL and Maver-1. (C) Genomic distribution of H3K9me3 lost and gained peaks in 'low' cell lines (left) and Panther GO analysis showing top enriched biological process associated with identified genes for each group (right).

Figure 3: SUV39H1-related loose of H3K9me3 in MCL accelerates tumor growth *in vivo*

(A) SUV39H1 knockdown was validated by western blot using anti-SUV39H1 antibody in Jeko-1 cells transduced with control (shCtrl) or SUV39H1-targeting short hairpin (shSUV39H1). (B) The heatmap (left) shows the regions loosing H3K9me3 enrichment after SUV39H1 knockdown in Jeko-1 cell line compared to the control cells and the graph (right) presents genomic annotation of these regions. (C) Heatmap represents differentially expressed genes in Ctrl versus SUV39H1 knockdown cells (n=4 for each group) (left), GSEA plots were obtained by comparing gene expression profiles of SUV39H1 depleted versus Ctrl cells (right). (D) Tumor growth kinetics measured in SCID mice engrafted with

shCtrl (n=10) or shSUV39H1-transduced (n=10) Jeko-1 cells at the indicated days after tumor engraftment. (D) Representative images of collected tumor tissues for two mice groups at day 22.

Figure 4: SETDB1-related alteration of H3K9me3 impacts MCL cell differentiation and cell proliferation

(A) SETDB1 knockdown validation in Jeko-1 cells by westernblot. (B) The heatmap and genomic distribution of regions loosing H3K9me3 after SETDB1 knockdown compared with controls. (C) Heatmap at the left shows differential gene expression profiles between cells transduced with shSETDB1 (n=4) compared with shCtrl (n=4) cells and the GSEA plots at the right show the enriched functional signatures for each group. (D) Representative histograms showing PI staining in SETDB1 depleted or Ctrl cells reflecting the percentage of cells in each phase of cell cycle (E) FACS analysis of indicated cell surface markers in SETDB1 depleted versus Ctrl cells.

Figure 5: H3K9me3 profile according to mutation landscape and impact on survival in MCL

(A) Heatmap depicting the somatic mutation pattern in 5 MCL cell lines and 18 MCL patients (diagnosis samples) with high or low levels of H3K9me3, as indicated. Each row represents a gene and each column represents a primary tumour sample /cell line. (B) Kaplan–Meier cumulative survival curves depicting overall survival in MCL according to H3K9me3 levels, p values from log-rank test.

Figure S1: H3K9me3 foci quantification and subnuclear distribution in MCL cells

(A) Histogram shows the frequency of H3K9me3 foci at the indicated distances from nuclear edge. More than 100 nuclei were analyzed for each cell line. (B) Immunofluorescent staining of H3K9me3 and (C) quantification of H3K9me3 foci in Jeko-1 cells transduced with shCtrl, shSEUV39H1 or shSETDB1 expressing vectors. (D) Sub-nuclear distribution of H3K9me3 foci regarding to the nulear edge in the indicated cells.

Figure S2: Loss of SUV39H1 proteins level in 'low' MCL cell lines is related to a shorter protein half-life

(A) Affymetrix values for mRNA levels (top) and western blot showing protein levels (bottom) of SUV39H1 in MCL cell lines. (B) and (C) show SUV39H1 protein levels after cyclohexemide or HBX41108±MG132 treatment in indicated cell lines respectively. (D) Proposed model for SUV39H1 protein degradation/stabilization pathway in 'low' MCL cell lines.

Figure S3: SUV39H1 knockdown doesn't affect MCL phenotype *in vitro*

(A) Histograms showing intensity of indicated cell surface markers in SUV39H1 knockdown and Ctrl cells.

Figures

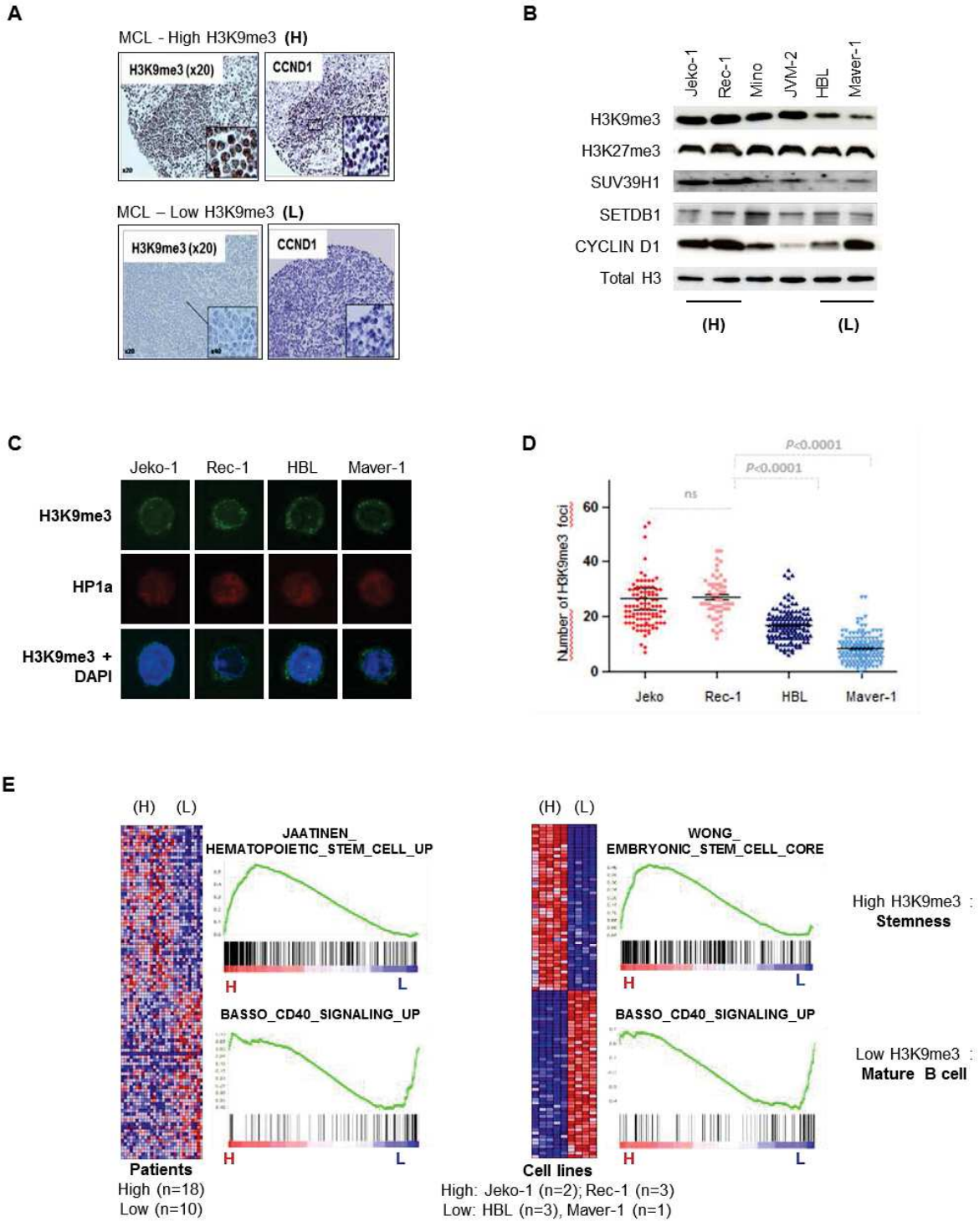

Figure 1

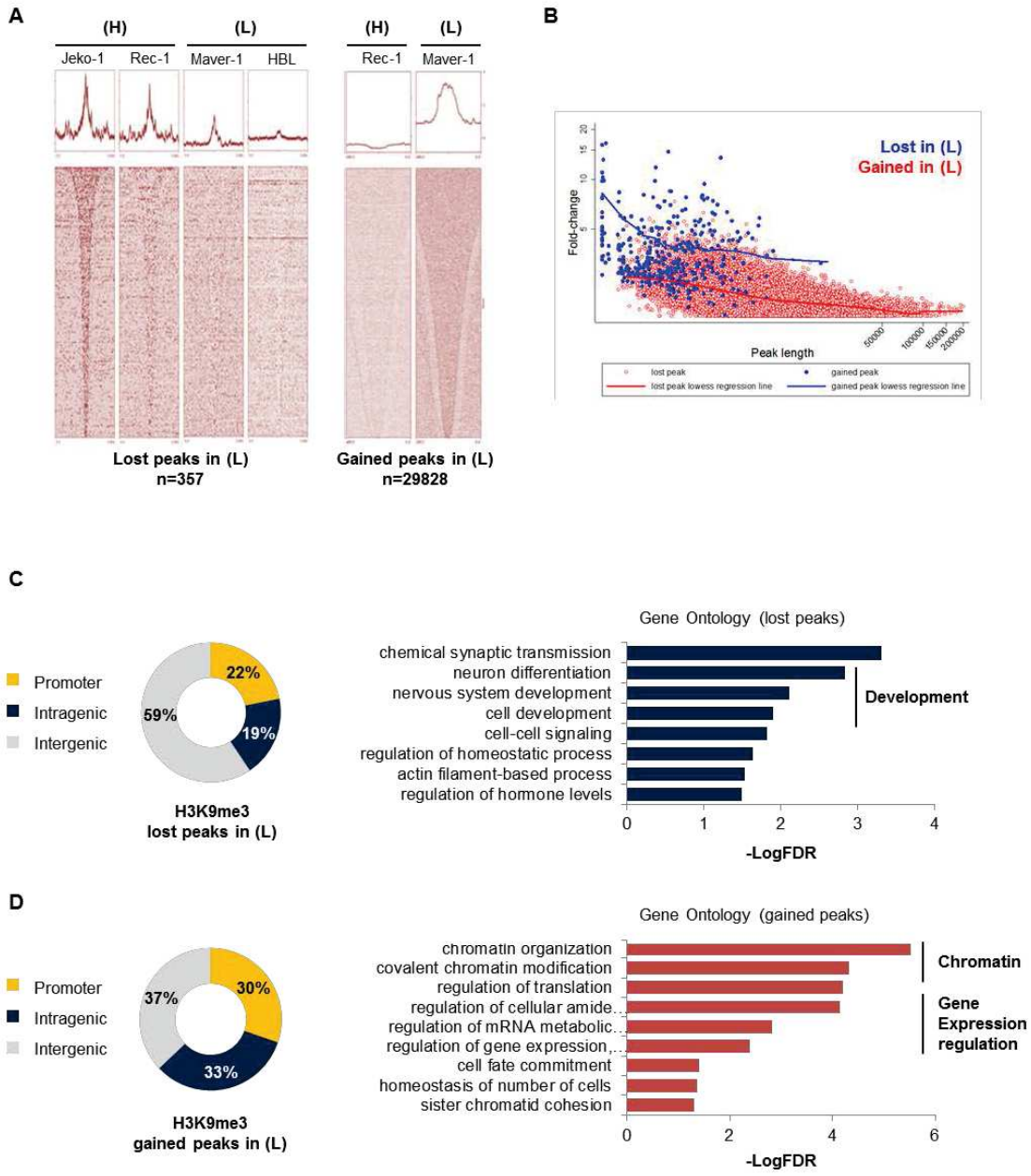
A
(H)
(L)
Jeko-1
Rec-1
Maver-1
HBL
Lost peaks in (L)
n=357
(H)
(L)
Rec-1
Maver-1
Gained peaks in (L)
n=29828
B
Lost in (L)
Gained in (L)
Fold-change
Peak length
lost peak
gained peak
lost peak lowess regression line
gained peak lowess regression line
C
Promoter
Intragenic
Intergenic
22%
19%
59%
H3K9me3
lost peaks in (L)
Gene Ontology (lost peaks)
chemical synaptic transmission
neuron differentiation
nervous system development
cell development
cell-cell signaling
regulation of homeostatic process
actin filament-based process
regulation of hormone levels
Development
-LogFDR
D
Promoter
Intragenic
Intergenic
30%
33%
37%
H3K9me3
gained peaks in (L)
Gene Ontology (gained peaks)
chromatin organization
covalent chromatin modification
regulation of translation
regulation of cellular amide...
regulation of mRNA metabolic...
regulation of gene expression,...
cell fate commitment
homeostasis of number of cells
sister chromatid cohesion
Chromatin
Gene Expression regulation
-LogFDR

Figure 2

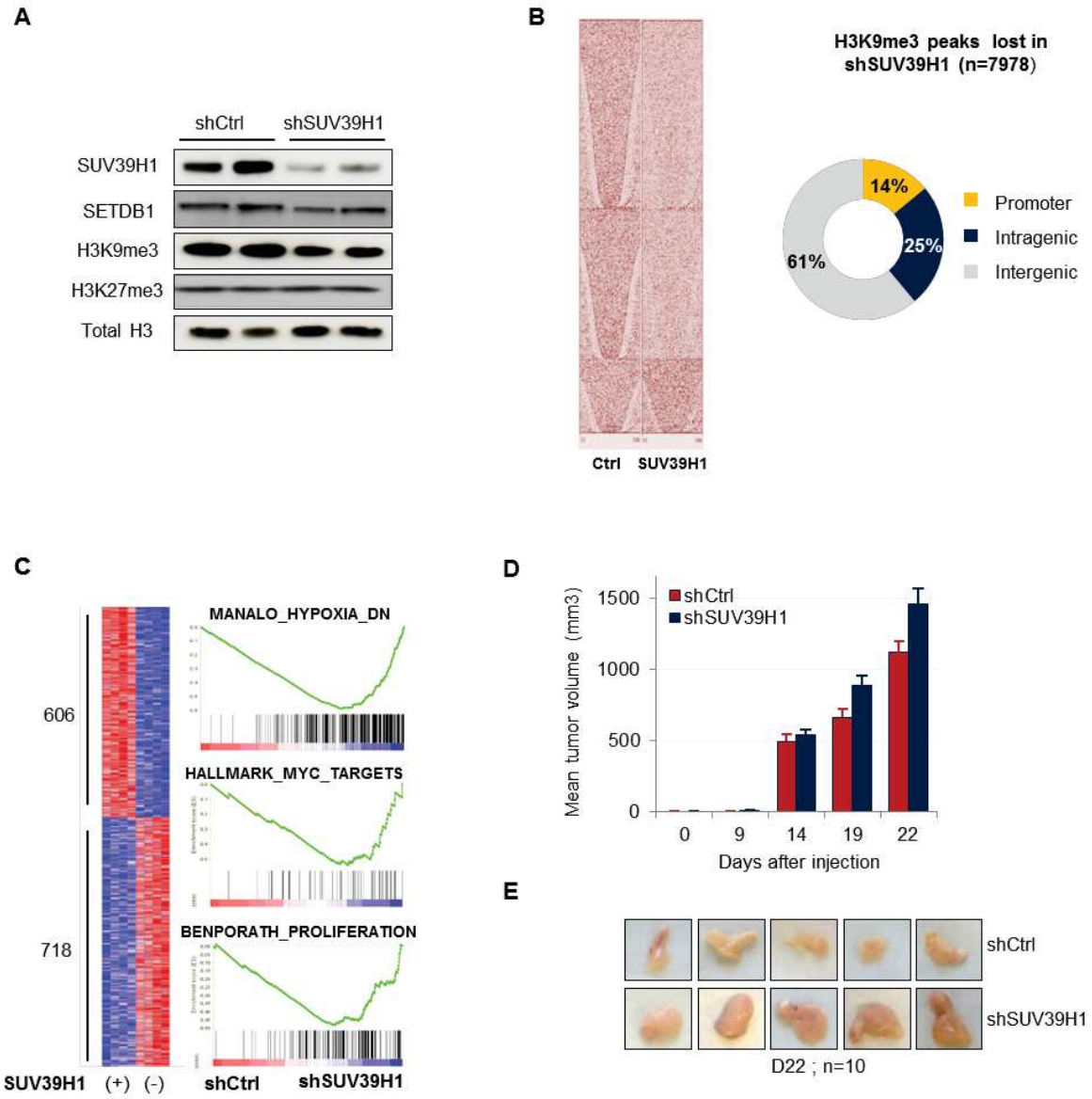
A
shCtrl
shSUV39H1
SUV39H1
SETDB1
H3K9me3
H3K27me3
Total H3
B
H3K9me3 peaks lost in shSUV39H1 (n=7978)
14%
25%
61%
Promoter
Intragenic
Intergenic
Ctrl
SUV39H1
C
606
718
MANALO_HYPOXIA_DN
HALLMARK_MYC_TARGETS
BENPORATH_PROLIFERATION
SUV39H1 (+) (-)
shCtrl
shSUV39H1
D
shCtrl
shSUV39H1
Mean tumor volume (mm3)
1500
1000
500
0
0
9
14
19
22
Days after injection
E
shCtrl
shSUV39H1
D22 ; n=10

Figure 3

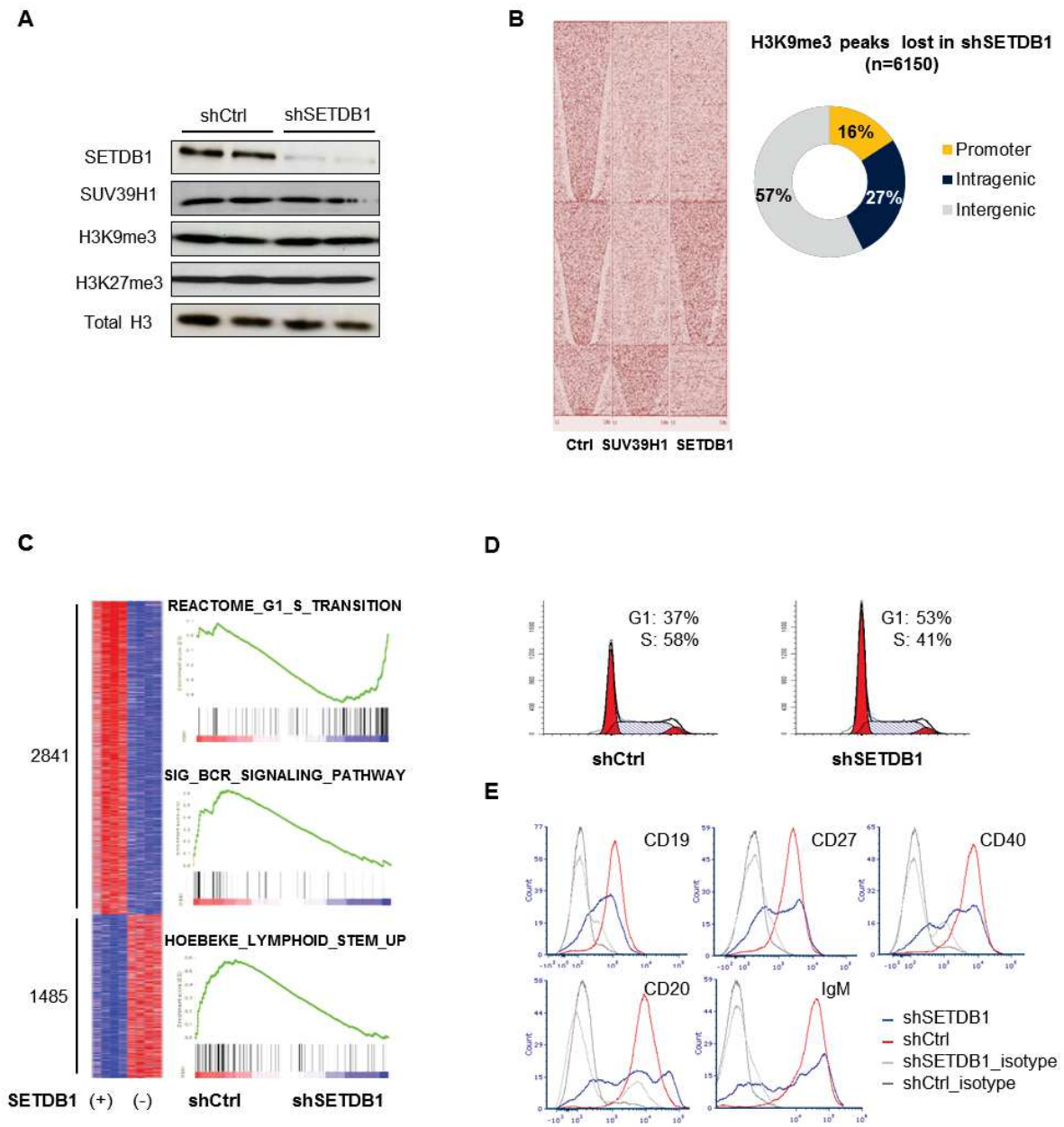
A
shCtrl
shSETDB1
SETDB1
SUV39H1
H3K9me3
H3K27me3
Total H3
B
H3K9me3 peaks lost in shSETDB1
(n=6150)
16%
27%
57%
Promoter
Intragenic
Intergenic
Ctrl SUV39H1 SETDB1
C
REACTOME_G1_S_TRANSITION
SIG_BCR_SIGNALING_PATHWAY
HOEBEKE_LYMPHOID_STEM_UP
2841
1485
SETDB1 (+) (-)
shCtrl
shSETDB1
D
G1: 37%
S: 58%
G1: 53%
S: 41%
shCtrl
shSETDB1
E
CD19
CD27
CD40
CD20
IgM
shSETDB1
shCtrl
shSETDB1_isotype
shCtrl_isotype

Figure 4

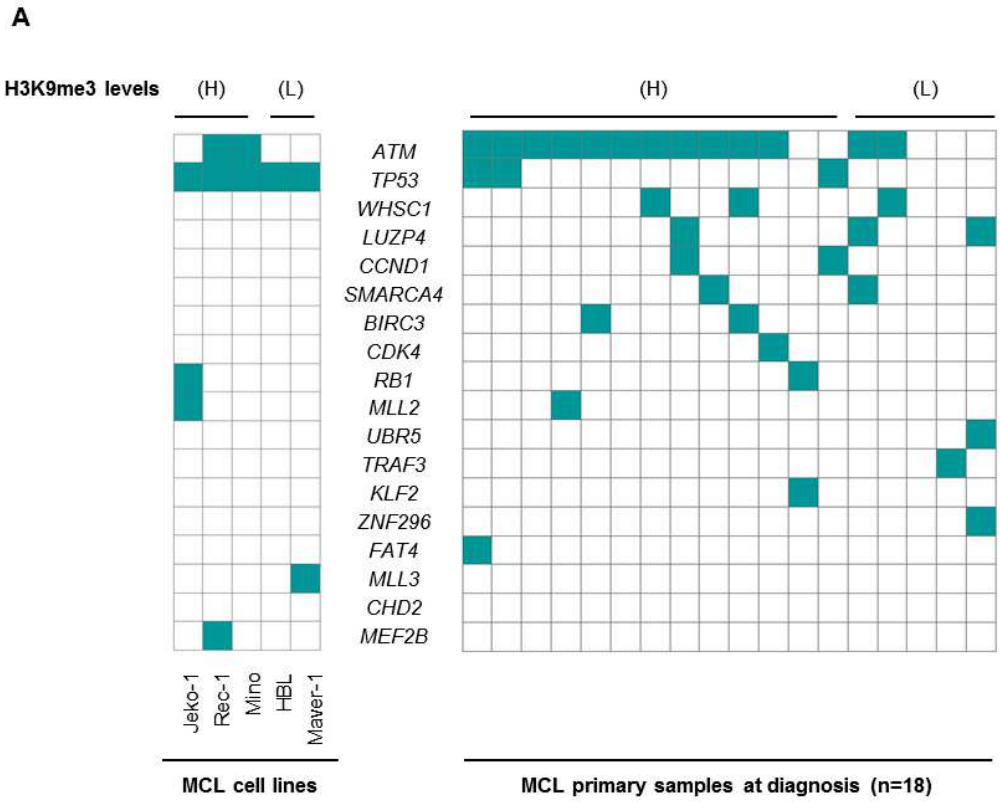
A
H3K9me3 levels
(H)
(L)
(H)
(L)
ATM
TP53
WHSC1
LUZP4
CCND1
SMARCA4
BIRC3
CDK4
RB1
MLL2
UBR5
TRAF3
KLF2
ZNF296
FAT4
MLL3
CHD2
MEF2B
Jeko-1
Rec-1
Mino
HBL
Maver-1
MCL cell lines
MCL primary samples at diagnosis (n=18)

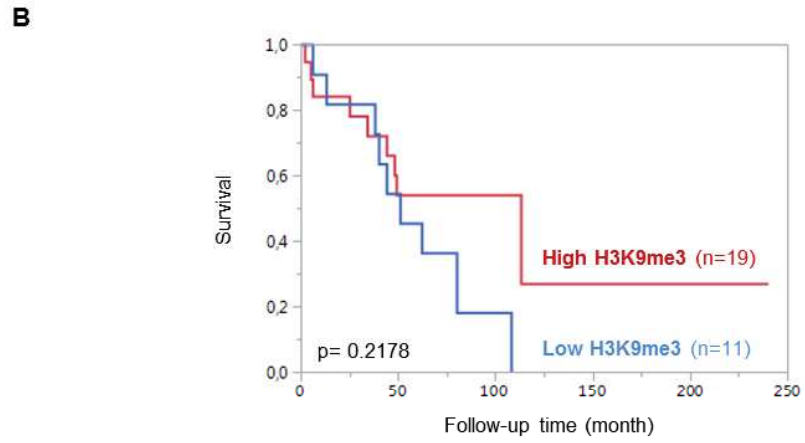
B
Survival
1,0
0,8
0,6
0,4
0,2
0,0
High H3K9me3 (n=19)
Low H3K9me3 (n=11)
p= 0.2178
0
50
100
150
200
250
Follow-up time (month)

Figure 5

Supplemental information

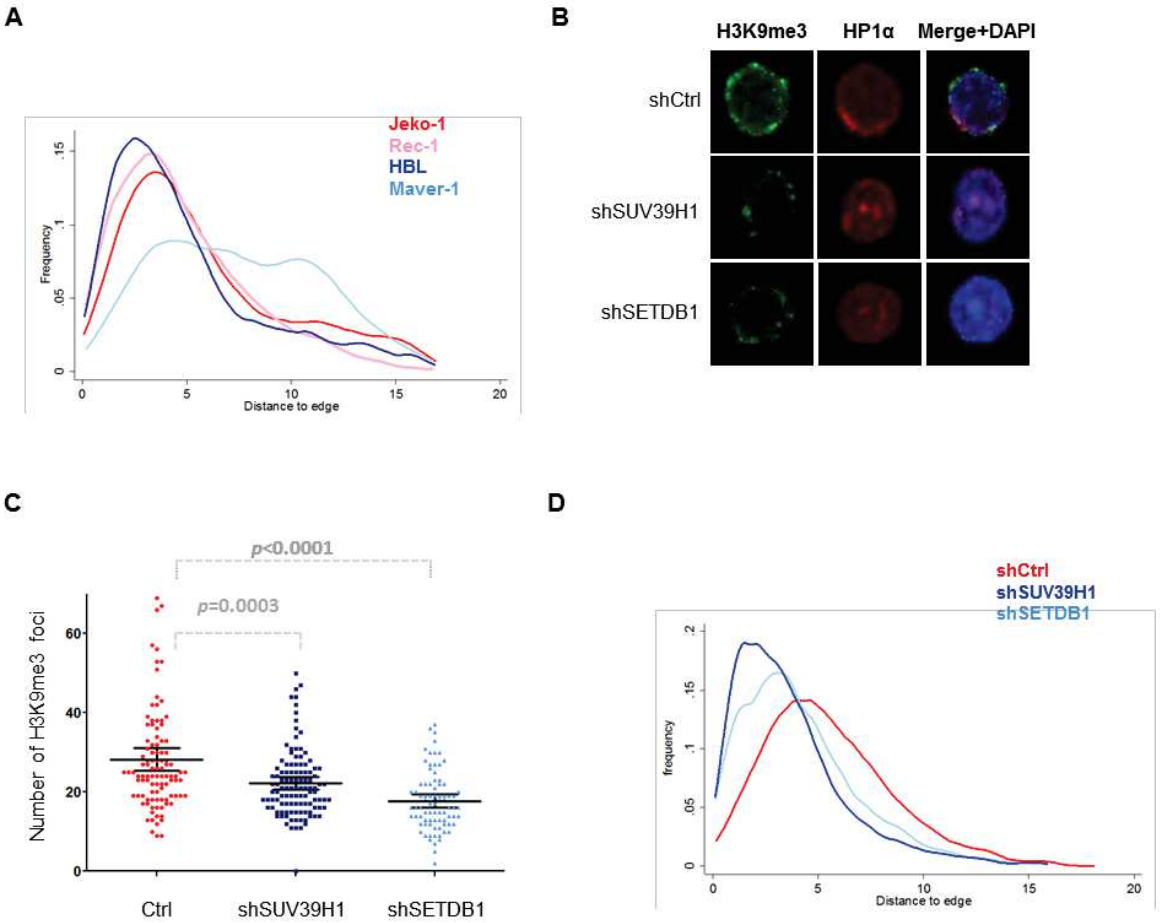

Supplemental Figure 1

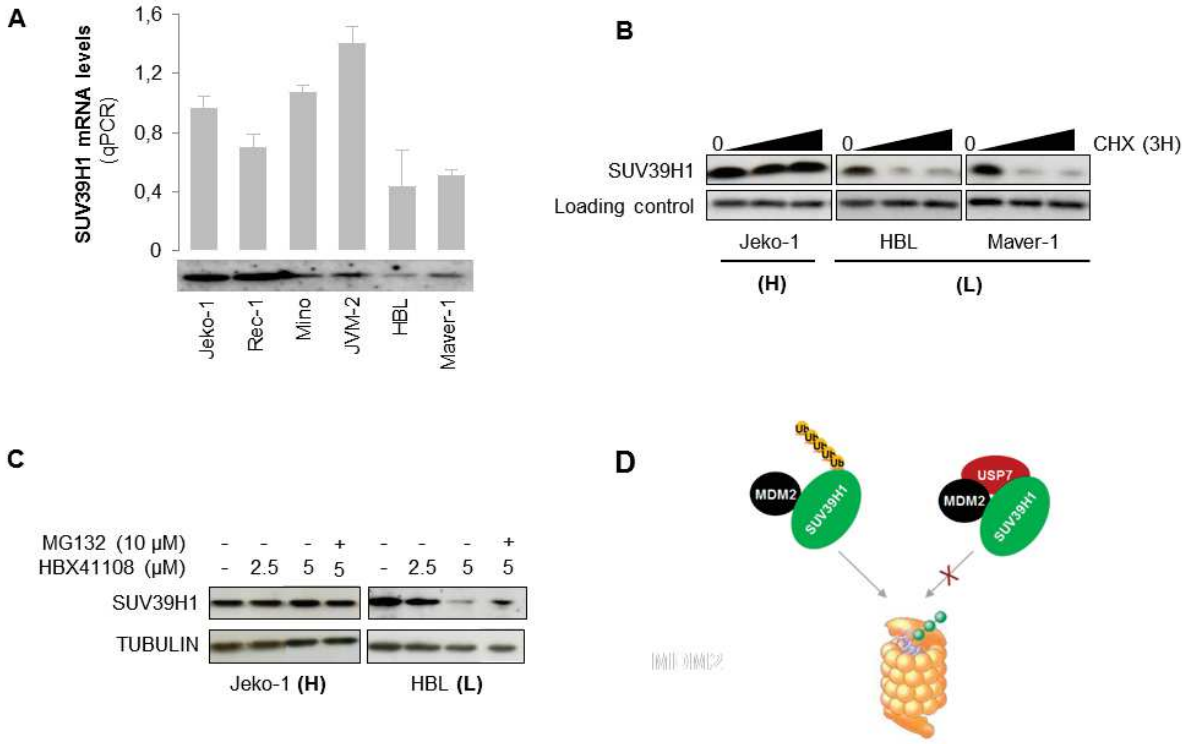

Supplemental Figure 2

A

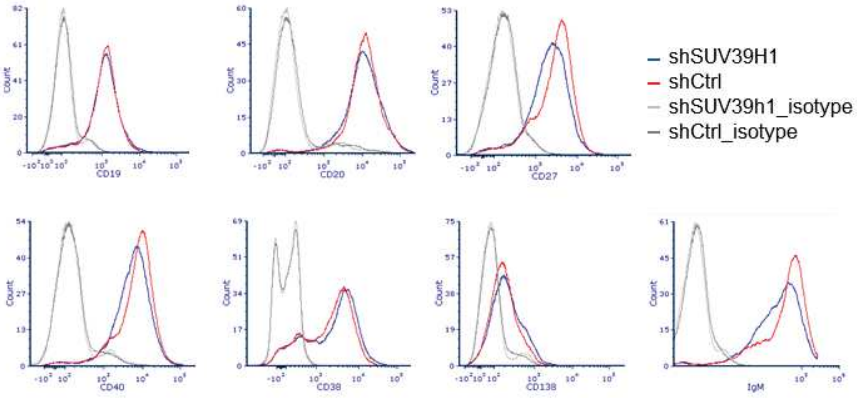

Supplemental Figure 3

Table S1: MCL patient clinical data

UPN	Name	Diag/ Relapse	Sample source	MIPI score	IPI	Caryotype	Forme	H3K9me3 score
1	MAR An	Diag	LN			47,XY,+3<1>/46,XY<8>	Classical	0
2	VIN Co	Relapse	LN	4	3	47,XX,del(4)(q3?3),6,t(11;14)(q13;q32),+der(11)t(3;11)(q12;q11),add(15)(q25),+mar<10>	Blastoid	0
3	VON Er	Diag	spleen	2	2	43,?X,Y,del(1)(q?31),add(2)(q37),-7,8,9, add(9)(p13), ?der(11)t(11;14)(q13;q32),-13, add(14)(q32),-18,?22,+mars,inc[3]	Blastoid	0
4	BAC Re	Diag	LN	3	2	Normal	Classical	0
5	FRA Mi	Diag	LN	3	2	46,XY,del(1)(q41),add(4)(q32),del(7)(q31,add(8)(q24),del(9)(q22q31),t(11;14)(q13;q32),add(16)(q2?2)add(17)(p11),add(19)(q1?3)<6>	Classical	0
6	GOL Mi	Diag	LN				Classical	0
7	LAM Ro	Treated	LN				Blastoid	10
8	ALO Je	Diag	spleen	3	3	44,XY?,2,add(3(q2?1),del(3)(q2?7),add(4)(p16),add(9)(q2?2),-11,-12,-13,-14,+3mar,inc<7>/46,XY<4>	CCND2+	50
9	MOR Je	Relapse	LN	2	1	46,XY,del(1)(p22p32),-10,t(11;14)(q13;q32),?13,-17, add(19)(p13),mars,var<9>/46,XY<3>	Classical	50
10	CHA Ma		spleen				Classical	80
11	VIN Co	Diag	spleen	4	3		Blastoid	90
12	BRO Da	Relapse	LN	3	Low	45,XY,del(1)(q31),add(4)(p16),-8,-10,der(?), t(11;14)(q13;q32),-13x2,-15,inc<5>/46,XY<2>	Classical	100
13	VIL Au	Diag	LN			45,XY,del(1)(p13q31),der(6),-7,t(11;14)(q13;q32),-13,-15,-22,+mar<6>/45,idem,add(4)(q3?5),inc<2>	Classical	100
14	BON Fr	Diag	spleen	2	3	45,XY,der(1)t(1;3)(p36;q21),del(1)(p12p31),add(3)(q12),add(3)(q21),der(6)t(3;6)(q21;q24),add(8)(q24),t(11;14)(q13;q32),del(11)(q14q25),dic(12;15)(p11;p11),13,del(13)(q14q22), +M1<9>	Classical	100
15	NAC Ab		LN			46,XY,add(1)(q23),t(11;14)(q13;q32),-13,-15,-22, +3mars <4>/47,idem,+X <2>/46,XY <1>	Classical	160
16	BER Ra	Diag	LN		Low int (2)	46, XY,del(1)(p21p13),der(3), -9, t(11;14)(q13;q32), -11,del(13q),+2 mar <9>	Classical	200
17	GUI Yv	Relapse	LN	3	Int	46,X,t(X;1)(q2,1;p13),t(11;14)(q13;q32),del(15q)<1>/46,idem,der(3q),variations+++<3>/46,XX<16>	Classical	200
18	LAM Ro	Treated	spleen			4243,X,?Y,add(1)(q?25),add(2)(p12),add(2)(q13),i(8)(q10),-9,-10,t(11;14)(q13;q32),add(11)(q25),-13,-17,-21,-22, +mars, inc<3>/46,XY<7>	Blastoid	200
19	GIR Je		LN	3	2	77,XXY,add(3)(p12),add(6)(p2?5),-8, 9, del(9)(q21q32),?t(11;14)(q13;q32),-16,-17,?18,-19,-21,+mars,inc[6]	Pleiomorphic	200
20	BOC Ja	Diag	LN	3	2	86-88,XXYY,add(1)(q21),add(1)(q23), add(1)(p13),der(1) add(1)(p21)add(1)(q43) ,del(4)(p13p16)x2,der(4)t(4;9)(p12;q22)x2,del(5)(q23q34),add(6)(p22),add(7)(q3?1)x2,add(9)(p21)x2,t(11;14)(q13;q32),der(11)t(11;14)(q13;q32),12,add(12)(p12),add(14)(q32),-15,-15,add(17)(p11),-18,-18,add(19)(q13)x2,+M1,+M2,inc<cp11>/46,XY<3>	Blastoid	200
21	CHA Ma	Diag	LN	4	4	45,Xdel(X)(q21;q25),der(1),add(4)(p15),add(4)(q2?5),?9,t(11;14)(q13;q32) add(11)(q22),-12,21, +mar<7>/45,idem,add(3)(p2?1), ?6,add(9)(p12),mars,var<4>/46,XX<3>	Classical	300
22	FRE Jo	Diag	LN	2	2	46,XY,t(11;14)(q13;q32),-13,+mar<2>/46,XY<2>	Classical	300
23	MEU Da	Diag	LN	6	High	46,XX,del(1)(p21p31),del(9)(p21p23),t(11;14)(q13;q32)<5>/46,idem,add(11)(q12)<2>	Blastoid	300
24	ARG Pa	Diag	LN	3	3	46,XY,add(5)(q35),t(11;14)(q13;q32)<4>/92,idemx2<4>/46,XY,add(4)(p1?4)<2>/46,XY<1>	Pleiomorphic	300
25	GIV Ma	Diag	spleen	4	4	39,X,-Y, 4,der(4)ins(4;?)(q12;?),del(8)(p12), add(8)(q24),-9,10, t(11;14)(q13;q32), add(12)(p12),-13,-13,-16,18,add(21)(q22), +M1,+M2, inc[5]/78, idemx2[3]	Pleiomorphic	300
26	JOU An	Diag	LN	4	3		Classical	300
27	CHA Ph	Treated	spleen			46,XY,t(11;14)(q13;q32)[18]/46,XY[2]	Classical	300
28	CON Sy	Diag	LN	3	2	45,XY,t(5;11)(q33;q13),der(11)t(11;14)(q13;q32),-13,-13,der(14)t(11;14)(q13;q32)del(11)(q21),-15,-18,+mars,inc[6]/46,XY[1]	Classical	300
29	BIR Ca	Diag	LN	3	2	46,XY,del(1)(p13p22),del(6)(q16q26),t(11;14)(q13;q32),del(11)(q14q24),+12,der(12;14)(q10;q10),13,add(13)(q34),add(16)(q23),add(21)(q22),mars[cp17]/46,XY[3]	Classical	300
30	VIN Ma	Relapse	LN	3	3		Classical	300

Table S2: Primer pairs used for sequencing (5' tagged with M13 sequences) or RT-Q-PCR analysis.

Sanger sequencing primers	Forward (5'-3')	Reverse (5'-3')
SUV39H1 pair-1	TGTAAAACGACGGCCAG**TCTCTTCTCGCGAGGCCGG**	CAGGAAACAGCTATGACA**ACCTGGTTGAGGGTGATGC**
SUV39H1 pair-2	TGTAAAACGACGGCCAG**TCTGGGACGCATCACTGTAG**	CAGGAAACAGCTATGACA**ACGTCCTCCACGTAGTCCAG**
SUV39H1 pair-3	TGTAAAACGACGGCCAG**CCAGATCTACGACCGTCAGG**	CAGGAAACAGCTATGACA**AGTGGGGGAGGTGCATGTAG**
RT-Q-PCR primers	**Forward (5'-3')**	**Reverse (5'-3')**
ABL (all variants)	TGGAGATAACACTCTAAGCATAACTAAAGGT	GATGTAGTTGCTTGGGACCCA
SUV39H1	GGCAACATCTCCCACTTTGT	CAATACGGACCCGCTTCTTA
SETDB1	TGCTGGCATTGTAGCTGAGAC	CCGGCAAATGGGATACAGTT

Table S3: Antibodies used for western bloting, immunofluorescence and ChIP experiments

Primary antibodies	Reference	Type
H3K9me3	Millipore (Upstate 07-523)	Polyclonal
H3K27me3	Millipore (Upstate 07-449)	Polyclonal
H3K9ac	Millipore (Upstate 07-352)	Polyclonal
Pan H3	Millipore (Upstate 04-928)	Monoclonal
HP1α	Euromedex (2HP-2G9-AS)	Monoclonal
TUBULIN α	Sigma (T5168)	Monoclonal
SUV39H1	Millipore (Upstate 07-550)	Polyclonal
SETDB1	Abcam (ab 107225)	Monoclonal
c-MYC	Santa Cruz (9E10 – sc40)	Monoclonal
CYCLIN D1	Santa Cruz (M-20 – sc718)	Polyclonal
SOX11	Santa Cruz (H-290 - sc-20096)	Polyclonal
Secondary antibodies	**Reference**	**Type**
Rabbit anti-Mouse HRP	Dako (P0260)	Polyclonal
Pig anti-Rabbit HRP	Dako (P0399)	Polyclonal
Rabbit anti-Goat HRP	Dako (P0449)	Polyclonal

Table S3: Antibodies and methods used for IHC staining

Antibody	Reference	Dilution	Antigen retrieval	Protocol	Detection Kit
H3K9me3	Abcam (ab8898)	1/800,60min	BM, 60min, Citrate pH 6	Discorvery n°513	iVIEW DAB
HP1 alpha	Euromedex (2HP-2G-AS)	1/100, 60min	BM, 60min, Citrate pH 6	Discorvery n°519	iVIEW DAB
CYCLIN D1	Neomarkers (RM-9104-S)	1/50, 60min	CC1, 60 min, +Amplification	Benchmark n°141	ultraVIEW DAB

Table S5: Short hairpin sequences

Hairpin name	Sequence
shCtrl	CATGTCATGTGTCACATCTCTT
shSUV39H1 I	Chosen from (Ait-Si-Ali et al., 2004)
shSUV39H1 II	CGGTGTACAACGTCTTCATAGAA
shSETDB1 a	GATGGATTGTGTACAGCAACG
shSETDB1 b	GGAGAAGATGGATTGTGTACA

Discussion and perspectives

Although the genetics of MCL has been intensively studied, bona fide oncogenic driver and malignant reprogramming events have not as yet been identified in MCL. Indications are that epigenetic processes are of importance in disease biology, but studies remain scarce. In the present work, we have investigated the integrity of the H3K9me3 histone 'mark' in MCL. This mark was chosen as it plays a guardian of lineage identity in somatic tissues, acts as barrier to reprogramming, and at least in experimental models of RAS-driven lymphomagenesis acts as a tumour suppressor. By using a simple immunohistochemical assay combined to ChIP-seq and functional assays we find that MCL can be divided into two biological entities, based on H3K9me3 profiles. Each MCL 'epi-subtype' presents novel gene expression profiles of potential for the derivation of new biomarkers and therapeutic strategies in MCL.

H3K9me3-related transcriptional programmes in MCL: oncogene and tumour suppressor pathways.

Differentially expressed genes between the groups with 'high' or 'low' levels of H3K9me3 are implicated in B-cell differentiation signaling and embryonic/hematopoietic stem cell properties. Gene set enrichment analysis also showed enrichment for multiple non-B cell lineage programs in 'H3K9me3 high' MCL samples while 'H3K9me3 low' group showed enrichment for germinal center B cell signatures, notably CD40 signature. The above findings are in line with previous studies that associate H3K9me3 with regulation of tissue-specific gene expression via regulation of chromatin accessibility at promoter (Ait-Si-Ali et al., 2004; Allan et al., 2012; Mal, 2006) and/or lineage-specific distal elements (Figure 23) (Ugarte et al., 2015) (Jiang et al., 2017).

ChIP-seq analysis permitted us to identify the genome regions with differential occupancy of H3K9me3 in 'high' versus 'low' MCL cell lines. Only 22% of the regions with lower H3K9me3 enrichment in 'low' cell lines correspond to promoter regions. This percentage was even lower in our knockdown models for SUV39H1 and SETDB1, suggestive that H3K9me3 regulates a unique set of genes in the MCL genome. Promoter annotation of this 'direct regulation' gene list will elucidate how this is occurring. A major focus will also be annotation of the numerous intergenic regions with differential enrichment for H3K9me3, in order to identify the affected long-range regulatory elements and their corresponding genes.

Specifically, we are performing motif binding analysis in our ChIP-seq data to check for enrichment for specific class of transcription factor binding sites within the differentially – bound H3K9me3 domains. In the longer term, functional assays could be performed to specifically address the functions of any novel TFs in MCL, by using genome editing approaches (Crispr-Cas9), combined to appropriate cellular and molecular assays.

For genes that are aberrantly silenced in MCL via H3K9me3, based on our cellular assays, we suspect a key role for SETDB1. We further speculate that SETDB1 is implicated in differentiation arrest, at least in high 'H3K9me3' MCL and that this may operate through long range mechanisms, as seen in neuronal tissues (see Figure 23). A key task in this respect is thus integration of our ChIP-seq with our gene expression data in MCL.

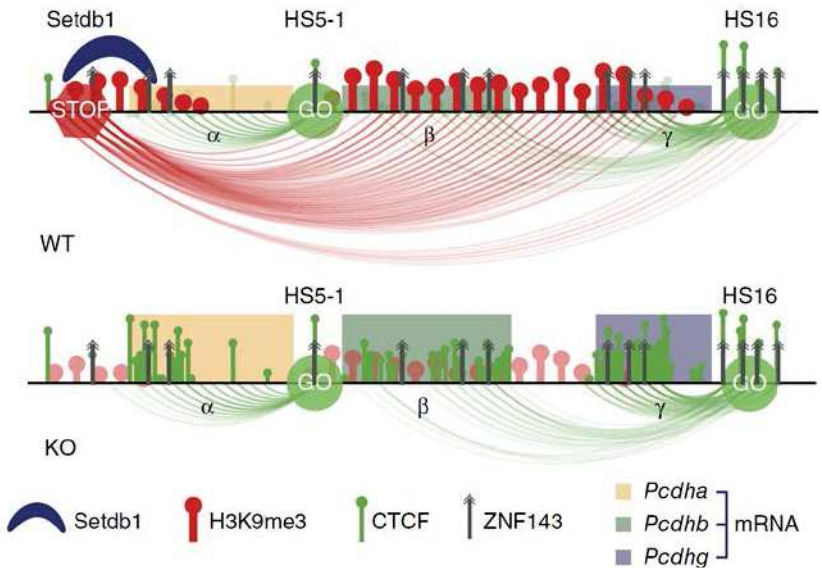

Figure 23. Jiang et al., propose a model in which SETDB1-related H3K9me3 regulates long-range repressive loopings at the clustered protocadherin locus (cPcdh) in neurons. Their study showed that Setdb1 shields neuronal genome from uncontrolled CTCF docking and ablation of Setdb1 triggers collapse of vulnerable TADs. Loss of repressive long-range contacts in KO model shifts the balance toward facilitative shorter-range promoter–enhancer loopings and affects the gene expression.

Also we are currently performing motif binding analysis to determine, if any, enrichment for specific class of TF biding sites within the differentially enriched regions. This information

could provide new insights into identification of favorable gene expression program in MCL, which could be leveraged by induction or inhibition of the related TF(s).

For genes that are aberrantly silenced in MCL via H3K9me3, based on our cellular assays, we suspect a key role for SETDB1. We further speculate that SETDB1 is implicated in differentiation arrest, at least in high 'H3K9me3' MCL and that this may operate through long range mechanisms, as seen in neuronal tissues (see Figure 23). A key task in this respect is is thus integration of our ChIP-seq with our gene expression data in MCL.

H3K9me3 is also well known for its role in silencing of non-coding genome including repetitive sequences, such as transposable elements (TEs). Our preliminary investigations showed upregulation of endogenous retrovirus genes (ERVs) both in patients and cell lines with 'low' levels of H3K9me3. Ectopic expression of TEs has been shown to impact different properties of cancer cells:
(Cuellar et al., 2017) showed that increased expression of ERVs is detrimental for viability of AML cells by activation of the cytosolic dsRNA–sensing pathway leading to IFN-mediated apoptosis. Transcription of retrotransposons leads to the production of retroviral proteins such as retroviral glycosylated envelope (Env). High content of these proteins could trigger the unfolded protein response pathway leading to apoptosis. It has been reported that activation of this pathway in pro-B cells, due to the loss of setdb1-related H3K9me3 in a locus specific manner, abolishes B-cell development (Pasquarella et al., 2016). However whether the mechanism by which SETDB1 represses the retrotransposons in cancer cells involves, totally or partially, the same components that are required for ERV silencing early in development remains unknown. We and others have shown that aberrant nuclear organisation and / or expression of repeat elements is a characteristic of lymphoma and solid tumours (Fournier et al., 2010 and Hall et al., 2017).

Several studies recently demonstrated that TE re-activation can be exploited for development of new therapeutic strategies. Induction of ERV-related interferon response by epi-drugs showed a robust synergic effect with immune checkpoint blockade therapies in preclinical settings for non-small cell lung cancer (NSCLC) and melanoma (Wrangle et al., 2013) (Chiappinelli et al., 2015).

Drug-tolerant sub-populations (DTPs) in solid cancers also have been shown to use H3K9me3-mediated repression of LINE transposable elements as a mechanism for transient survival from lethal drug exposure (Guler et al., 2017). Disruption of repressive chromatin at these regions by knocking down/out SETDB1 induced cell death in DTPs in response of lethal dose of kinase inhibitors.

The above findings highlight the importance of H3K9me3-regulated 'non-coding' genome in controlling viability, differentiation, and therapeutic responses of cancer cells. Our data showed that upregulation of ERVs in 'low' patients and cell lines was associated to enrichment for several interferon response signatures in these groups (data not shown). Also, in line with the major role of SETDB1 in repression of these regions, we observed the same results in SETDB1 knockdown cells. However, further investigations are required to characterize more specifically altered elements and determine their impact on MCL pathology.

Clinical significance of H3K9me3 alterations in MCL

H3K9me3-induced senescence is not only a barrier to malignant transformation during early oncogene signaling (Braig et al., 2005), but is also involved in limiting disease progression and improving the response to anti-cancer treatments as it has been already shown in AML, DLBCL and experimental models for B-cell lymphoma ((Dorr et al., 2013). Our xenograft model shows that global loss H3K9me3 upon SUV39H1 knockdown accelerates MCL tumor growth in mice. In line with this, preliminary survival analysis performed on a cohort 30 MCL patients showed a tendency for poorer survival in the 'low' group. This result is being confirmed by screening an additional MCL cohort (LYSA cohort, n=90), but already suggest that a global loss of H3K9me3 at diagnosis could be predictor of an inferior survival in MCL (Le Gouill et al., 2017).

Contrary to SUV39H1, our results suggest an oncogene role for SETDB1-mediated H3K9me3 in MCL. This is in line with previous studies that also showed positive correlation between upregulation of SETDB1 and aggressive course/drug-resistance in different types of cancer including melanoma, lung, ovarian, and breast cancers (Ceol et al., 2011). However the role of SETDB1 in MCL tumor growth remains to be confirmed *in vivo*.

Further investigations are required to determine the respective role of SUV39H1- and SETDB1-mediated H3K9me3 in efficiency of response to the MCL current treatments. These findings together with evaluation of SUV39H1 and SETDB1 protein levels in patient samples might affect the choice of therapeutic approach for each sub-group.

SUV39H1 stability

Consistent with our results that suggest a tumor-suppressor role for SUV39H1 in MCL, understanding the posttranslational pathways that control the protein stability might introduce clinical benefits. Our preliminary data suggest that SUV39H1 protein levels depend on USP7 (Ubiquitin-specific-processing protease 7) activity in 'low' cell lines. Treatment of these cell lines with USP7 inhibitor reduced global levels of SUV39H1 in three hours. Further experiments with a longer time of treatment are required to show whether this reduction is associated with changes is global levels of H3K9me3 in treated cells. Also this dependency needs to be validated in USP7 overexpressing cells.

USP7-dependent protection of SUV39H1 from degradation has been shown to rely on MDM2 protein and formation of a triplex between these proteins, independent of p53 presence. In the absence of MDM2, up- or downregulation of USP7 did not affect SUV39H1 protein levels (Mungamuri et al., 2016). This finding might explain the insensitivity of SUV39H1 levels to USP7 inhibition in 'high' MCL cell lines. To further investigate this we need to perform MDM2 protein screening and sub-cellular distribution across our MCL cell lines. These findings might provide hints on SUV39H1 stabilization pathways in 'high' and 'low' cell lines.

SETDB1 targeting in MCL

SETDB1 protein levels seem unchanged across 'high' and 'low' MCL cell lines and knock-down of this enzyme did not affect the global levels of H3K9me3. However strikingly, ChIP-seq analysis revealed a comparable number of H3K9me3-depleted regions in SUV39H1 and SETDB1 knockdown cells, of which a large number are in common. Also SETDB1 knockdown induced greater gene expression changes than SUV39H1 knockdown, both in

term of number and fold change ratios. Finally, consistent with the enriched signatures in GSEA analysis, SETDB1 depletion induced cell cycle arrest coincident to reprogramming of the cells to a pre-B cell phenotype.

These results raise the interest of targeting SETDB1, or the partners that are required for its presence and functional activity at chromatin. To our knowledge, highly specific inhibitors for SETDB1 have not been described yet; nonetheless, downregulation of SETDB1 expression by using nonspecific inhibitors such as Mithramycin showed positive effects in SETDB1 overexpressing lung cancer cells. Mithramycin is a DNA-binding antibiotic with FDA approved antitumor activity. This molecule prevents recruitment of Sp-family of transcriptional activators at the promoter region of the target genes including SETDB1.

ATF7IP, also known as hAM or MCAF1, is a SETDB1-interacting partner which has been shown to protect SETDB1 from proteasomal degradation in the nucleus. Absence of this protein does not affect the global levels of SETDB1 but decreases massively the nucleus content of SETDB1. Therefor ATF7IP targeting could introduce an alternative strategy to inhibit SETDB1 activity (Timms et al., 2016).
Constitutive monoubiquitination of SETDB1 at lysine-867, by UBE2E family of E2 enzymes, has been shown to increase enzymatic activity SETDB1 (Sun and Fang, 2016). Thus targeting E2 enzymes might present a relevant approach in controlling SETDB1 activity.

Taken together, our findings indicate that interrogating H3K9me3 signaling in MCL supplies our understanding of pathogenesis mechanisms in this disease. We showed that MCL is divided into two distinct epigenetic MCL subtypes that seem to be independent of other clinical classifiers, but is associated with divergent clinical course of the disease. Genome wide mapping of H3K9me3 within MCL cell lines showed that this mark is altered at cell fate commitment and cell proliferation controlling genes. By targeting two major enzymes that are responsible for establishment of H3K9me3 we propose novel oncogene and tumor suppressor networks in MCL directed by SETDB1 and SUV39H1 respectively. Targeting SETDB1 was also associated with a significant switch in cell differentiation program of MCL cells. Our findings suggest a high therapeutic potential for targeting H3K9me3-mediated signaling networks in MCL.

Bibliography

Aagaard, L., Laible, G., Selenko, P., Schmid, M., Dorn, R., Schotta, G., Kuhfittig, S., Wolf, A., Lebersorger, A., Singh, P.B.*, et al.* (1999). Functional mammalian homologues of the Drosophila PEV-modifier Su(var)3-9 encode centromere-associated proteins which complex with the heterochromatin component M31. The EMBO journal *18*, 1923-1938.

Aagaard, L., Schmid, M., Warburton, P., and Jenuwein, T. (2000). Mitotic phosphorylation of SUV39H1, a novel component of active centromeres, coincides with transient accumulation at mammalian centromeres. Journal of cell science *113 (Pt 5)*, 817-829.

Ait-Si-Ali, S., Guasconi, V., Fritsch, L., Yahi, H., Sekhri, R., Naguibneva, I., Robin, P., Cabon, F., Polesskaya, A., and Harel-Bellan, A. (2004). A Suv39h-dependent mechanism for silencing S-phase genes in differentiating but not in cycling cells. The EMBO journal *23*, 605-615.

Allan, R.S., Zueva, E., Cammas, F., Schreiber, H.A., Masson, V., Belz, G.T., Roche, D., Maison, C., Quivy, J.P., Almouzni, G.*, et al.* (2012). An epigenetic silencing pathway controlling T helper 2 cell lineage commitment. Nature *487*, 249-253.

Amin, A.D., Peters, T.L., Li, L., Rajan, S.S., Choudhari, R., Puvvada, S.D., and Schatz, J.H. (2017). Diffuse large B-cell lymphoma: can genomics improve treatment options for a curable cancer? Cold Spring Harbor molecular case studies *3*, a001719.

Amorim, S., Stathis, A., Gleeson, M., Iyengar, S., Magarotto, V., Leleu, X., Morschhauser, F., Karlin, L., Broussais, F., Rezai, K.*, et al.* (2016). Bromodomain inhibitor OTX015 in patients with lymphoma or multiple myeloma: a dose-escalation, open-label, pharmacokinetic, phase 1 study. The Lancet Haematology *3*, e196-204.

Baylin, S.B., and Jones, P.A. (2011). A decade of exploring the cancer epigenome - biological and translational implications. Nature reviews Cancer *11*, 726-734.

Bea, S., and Amador, V. (2017). Role of SOX11 and Genetic Events Cooperating with Cyclin D1 in Mantle Cell Lymphoma. Current oncology reports *19*, 43.

Bea, S., Ribas, M., Hernandez, J.M., Bosch, F., Pinyol, M., Hernandez, L., Garcia, J.L., Flores, T., Gonzalez, M., Lopez-Guillermo, A.*, et al.* (1999). Increased number of chromosomal imbalances and high-level DNA amplifications in mantle cell lymphoma are associated with blastoid variants. Blood *93*, 4365-4374.

Bea, S., Valdes-Mas, R., Navarro, A., Salaverria, I., Martin-Garcia, D., Jares, P., Gine, E., Pinyol, M., Royo, C., Nadeu, F.*, et al.* (2013). Landscape of somatic mutations and clonal evolution in mantle

cell lymphoma. Proceedings of the National Academy of Sciences of the United States of America *110*, 18250-18255.

Beguelin, W., Teater, M., Gearhart, M.D., Calvo Fernandez, M.T., Goldstein, R.L., Cardenas, M.G., Hatzi, K., Rosen, M., Shen, H., Corcoran, C.M.*, et al.* (2016). EZH2 and BCL6 Cooperate to Assemble CBX8-BCOR Complex to Repress Bivalent Promoters, Mediate Germinal Center Formation and Lymphomagenesis. Cancer cell *30*, 197-213.

Beyer, S., Pontis, J., Schirwis, E., Battisti, V., Rudolf, A., Le Grand, F., and Ait-Si-Ali, S. (2016). Canonical Wnt signalling regulates nuclear export of Setdb1 during skeletal muscle terminal differentiation. Cell discovery *2*, 16037.

Bienvenu, F., Jirawatnotai, S., Elias, J.E., Meyer, C.A., Mizeracka, K., Marson, A., Frampton, G.M., Cole, M.F., Odom, D.T., Odajima, J.*, et al.* (2010). Transcriptional role of cyclin D1 in development revealed by a genetic-proteomic screen. Nature *463*, 374-378.

Bilodeau, S., Kagey, M.H., Frampton, G.M., Rahl, P.B., and Young, R.A. (2009). SetDB1 contributes to repression of genes encoding developmental regulators and maintenance of ES cell state. Genes & development *23*, 2484-2489.

Boi, M., Gaudio, E., Bonetti, P., Kwee, I., Bernasconi, E., Tarantelli, C., Rinaldi, A., Testoni, M., Cascione, L., Ponzoni, M.*, et al.* (2015). The BET Bromodomain Inhibitor OTX015 Affects Pathogenetic Pathways in Preclinical B-cell Tumor Models and Synergizes with Targeted Drugs. Clinical cancer research : an official journal of the American Association for Cancer Research *21*, 1628-1638.

Bosch-Presegue, L., Raurell-Vila, H., Marazuela-Duque, A., Kane-Goldsmith, N., Valle, A., Oliver, J., Serrano, L., and Vaquero, A. (2011). Stabilization of Suv39H1 by SirT1 is part of oxidative stress response and ensures genome protection. Molecular cell *42*, 210-223.

Bottcher, S., Ritgen, M., Buske, S., Gesk, S., Klapper, W., Hoster, E., Hiddemann, W., Unterhalt, M., Dreyling, M., Siebert, R.*, et al.* (2008). Minimal residual disease detection in mantle cell lymphoma: methods and significance of four-color flow cytometry compared to consensus IGH-polymerase chain reaction at initial staging and for follow-up examinations. Haematologica *93*, 551-559.

Braig, M., Lee, S., Loddenkemper, C., Rudolph, C., Peters, A.H., Schlegelberger, B., Stein, H., Dorken, B., Jenuwein, T., and Schmitt, C.A. (2005). Oncogene-induced senescence as an initial barrier in lymphoma development. Nature *436*, 660-665.

Breiling, A., Turner, B.M., Bianchi, M.E., and Orlando, V. (2001). General transcription factors bind promoters repressed by Polycomb group proteins. Nature *412*, 651-655.

Brien, G.L., Valerio, D.G., and Armstrong, S.A. (2016). Exploiting the Epigenome to Control Cancer-Promoting Gene-Expression Programs. Cancer cell *29*, 464-476.

Broske, A.M., Vockentanz, L., Kharazi, S., Huska, M.R., Mancini, E., Scheller, M., Kuhl, C., Enns, A., Prinz, M., Jaenisch, R.*, et al.* (2009). DNA methylation protects hematopoietic stem cell multipotency from myeloerythroid restriction. Nature genetics *41*, 1207-1215.

Bulut-Karslioglu, A., De La Rosa-Velazquez, I.A., Ramirez, F., Barenboim, M., Onishi-Seebacher, M., Arand, J., Galan, C., Winter, G.E., Engist, B., Gerle, B.*, et al.* (2014). Suv39h-dependent H3K9me3 marks intact retrotransposons and silences LINE elements in mouse embryonic stem cells. Molecular cell *55*, 277-290.

Bulut-Karslioglu, A., Perrera, V., Scaranaro, M., de la Rosa-Velazquez, I.A., van de Nobelen, S., Shukeir, N., Popow, J., Gerle, B., Opravil, S., Pagani, M.*, et al.* (2012). A transcription factor-based mechanism for mouse heterochromatin formation. Nature structural & molecular biology *19*, 1023-1030.

Bussmann, L.H., Schubert, A., Vu Manh, T.P., De Andres, L., Desbordes, S.C., Parra, M., Zimmermann, T., Rapino, F., Rodriguez-Ubreva, J., Ballestar, E.*, et al.* (2009). A robust and highly efficient immune cell reprogramming system. Cell stem cell *5*, 554-566.

Cai, S.F., Chen, C.W., and Armstrong, S.A. (2015). Drugging Chromatin in Cancer: Recent Advances and Novel Approaches. Molecular cell *60*, 561-570.

Canzio, D., Larson, A., and Narlikar, G.J. (2014). Mechanisms of functional promiscuity by HP1 proteins. Trends in cell biology *24*, 377-386.

Cattaneo, F., and Nucifora, G. (2008). EVI1 recruits the histone methyltransferase SUV39H1 for transcription repression. Journal of cellular biochemistry *105*, 344-352.

Ceol, C.J., Houvras, Y., Jane-Valbuena, J., Bilodeau, S., Orlando, D.A., Battisti, V., Fritsch, L., Lin, W.M., Hollmann, T.J., Ferre, F.*, et al.* (2011). The histone methyltransferase SETDB1 is recurrently amplified in melanoma and accelerates its onset. Nature *471*, 513-517.

Chaib, H., Nebbioso, A., Prebet, T., Castellano, R., Garbit, S., Restouin, A., Vey, N., Altucci, L., and Collette, Y. (2012). Anti-leukemia activity of chaetocin via death receptor-dependent apoptosis and dual modulation of the histone methyl-transferase SUV39H1. Leukemia *26*, 662-674.

Chakraborty, S., Sinha, K.K., Senyuk, V., and Nucifora, G. (2003). SUV39H1 interacts with AML1 and abrogates AML1 transactivity. AML1 is methylated in vivo. Oncogene *22*, 5229-5237.

Chanda, S., Ang, C.E., Davila, J., Pak, C., Mall, M., Lee, Q.Y., Ahlenius, H., Jung, S.W., Sudhof, T.C., and Wernig, M. (2014). Generation of induced neuronal cells by the single reprogramming factor ASCL1. Stem cell reports *3*, 282-296.

Chapuy, B., McKeown, M.R., Lin, C.Y., Monti, S., Roemer, M.G., Qi, J., Rahl, P.B., Sun, H.H., Yeda, K.T., Doench, J.G.*, et al.* (2013). Discovery and characterization of super-enhancer-associated dependencies in diffuse large B cell lymphoma. Cancer cell *24*, 777-790.

Chase, K.A., Gavin, D.P., Guidotti, A., and Sharma, R.P. (2013). Histone methylation at H3K9: evidence for a restrictive epigenome in schizophrenia. Schizophrenia research *149*, 15-20.

Cheah, C.Y., Seymour, J.F., and Wang, M.L. (2016). Mantle Cell Lymphoma. Journal of clinical oncology : official journal of the American Society of Clinical Oncology *34*, 1256-1269.

Cheloufi, S., Elling, U., Hopfgartner, B., Jung, Y.L., Murn, J., Ninova, M., Hubmann, M., Badeaux, A.I., Euong Ang, C., Tenen, D.*, et al.* (2015). The histone chaperone CAF-1 safeguards somatic cell identity. Nature *528*, 218-224.

Chen, C.W., Koche, R.P., Sinha, A.U., Deshpande, A.J., Zhu, N., Eng, R., Doench, J.G., Xu, H., Chu, S.H., Qi, J.*, et al.* (2015). DOT1L inhibits SIRT1-mediated epigenetic silencing to maintain leukemic gene expression in MLL-rearranged leukemia. Nature medicine *21*, 335-343.

Chen, J., Liu, H., Liu, J., Qi, J., Wei, B., Yang, J., Liang, H., Chen, Y., Chen, J., Wu, Y.*, et al.* (2013). H3K9 methylation is a barrier during somatic cell reprogramming into iPSCs. Nature genetics *45*, 34-42.

Chiappinelli, K.B., Strissel, P.L., Desrichard, A., Li, H., Henke, C., Akman, B., Hein, A., Rote, N.S., Cope, L.M., Snyder, A.*, et al.* (2015). Inhibiting DNA Methylation Causes an Interferon Response in Cancer via dsRNA Including Endogenous Retroviruses. Cell *162*, 974-986.

Chiba, S. (2017). Dysregulation of TET2 in hematologic malignancies. International journal of hematology *105*, 17-22.

Chihara, D., Cheah, C.Y., Westin, J.R., Fayad, L.E., Rodriguez, M.A., Hagemeister, F.B., Pro, B., McLaughlin, P., Younes, A., Samaniego, F.*, et al.* (2016). Rituximab plus hyper-CVAD alternating with MTX/Ara-C in patients with newly diagnosed mantle cell lymphoma: 15-year follow-up of a phase II study from the MD Anderson Cancer Center. British journal of haematology *172*, 80-88.

Chim, C.S., Wong, K.Y., Loong, F., and Srivastava, G. (2004). SOCS1 and SHP1 hypermethylation in mantle cell lymphoma and follicular lymphoma: implications for epigenetic activation of the Jak/STAT pathway. Leukemia *18*, 356-358.

Chiron, D., Di Liberto, M., Martin, P., Huang, X., Sharman, J., Blecua, P., Mathew, S., Vijay, P., Eng, K., Ali, S.*, et al.* (2014). Cell-cycle reprogramming for PI3K inhibition overrides a relapse-specific C481S BTK mutation revealed by longitudinal functional genomics in mantle cell lymphoma. Cancer discovery *4*, 1022-1035.

Cho, S., Park, J.S., and Kang, Y.K. (2013). Regulated nuclear entry of over-expressed Setdb1. Genes to cells : devoted to molecular & cellular mechanisms *18*, 694-703.

Collins, P.L., Kyle, K.E., Egawa, T., Shinkai, Y., and Oltz, E.M. (2015). The histone methyltransferase SETDB1 represses endogenous and exogenous retroviruses in B lymphocytes. Proceedings of the National Academy of Sciences of the United States of America *112*, 8367-8372.

Cooper, M.D. (2015). The early history of B cells. Nature reviews Immunology *15*, 191-197.

Cuellar, T.L., Herzner, A.M., Zhang, X., Goyal, Y., Watanabe, C., Friedman, B.A., Janakiraman, V., Durinck, S., Stinson, J., Arnott, D.*, et al.* (2017). ---Silencing of retrotransposons by SETDB1 inhibits the interferon response in acute myeloid leukemia. The Journal of cell biology *216*, 3535-3549.

Cukier, H.N., Lee, J.M., Ma, D., Young, J.I., Mayo, V., Butler, B.L., Ramsook, S.S., Rantus, J.A., Abrams, A.J., Whitehead, P.L.*, et al.* (2012). The expanding role of MBD genes in autism: identification of a MECP2 duplication and novel alterations in MBD5, MBD6, and SETDB1. Autism research : official journal of the International Society for Autism Research *5*, 385-397.

Czvitkovich, S., Sauer, S., Peters, A.H., Deiner, E., Wolf, A., Laible, G., Opravil, S., Beug, H., and Jenuwein, T. (2001). Over-expression of the SUV39H1 histone methyltransferase induces altered proliferation and differentiation in transgenic mice. Mechanisms of development *107*, 141-153.

Djeghloul, D., Kuranda, K., Kuzniak, I., Barbieri, D., Naguibneva, I., Choisy, C., Bories, J.C., Dosquet, C., Pla, M., Vanneaux, V.*, et al.* (2016). Age-Associated Decrease of the Histone Methyltransferase SUV39H1 in HSC Perturbs Heterochromatin and B Lymphoid Differentiation. Stem cell reports *6*, 970-984.

Dodge, J.E., Kang, Y.K., Beppu, H., Lei, H., and Li, E. (2004). Histone H3-K9 methyltransferase ESET is essential for early development. Molecular and cellular biology *24*, 2478-2486.

Dong, C., Wu, Y., Wang, Y., Wang, C., Kang, T., Rychahou, P.G., Chi, Y.I., Evers, B.M., and Zhou, B.P. (2013). Interaction with Suv39H1 is critical for Snail-mediated E-cadherin repression in breast cancer. Oncogene *32*, 1351-1362.

Dong, K.B., Maksakova, I.A., Mohn, F., Leung, D., Appanah, R., Lee, S., Yang, H.W., Lam, L.L., Mager, D.L., Schubeler, D.*, et al.* (2008). DNA methylation in ES cells requires the lysine methyltransferase G9a but not its catalytic activity. The EMBO journal *27*, 2691-2701.

Dorr, J.R., Yu, Y., Milanovic, M., Beuster, G., Zasada, C., Dabritz, J.H., Lisec, J., Lenze, D., Gerhardt, A., Schleicher, K.*, et al.* (2013). Synthetic lethal metabolic targeting of cellular senescence in cancer therapy. Nature *501*, 421-425.

Ek, S., Dictor, M., Jerkeman, M., Jirstrom, K., and Borrebaeck, C.A. (2008). Nuclear expression of the non B-cell lineage Sox11 transcription factor identifies mantle cell lymphoma. Blood *111*, 800-805.

Emadali, A., Hoghoughi, N., Duley, S., Hajmirza, A., Verhoeyen, E., Cosset, F.L., Bertrand, P., Roumier, C., Roggy, A., Suchaud-Martin, C.*, et al.* (2016). Haploinsufficiency for NR3C1, the gene encoding the glucocorticoid receptor, in blastic plasmacytoid dendritic cell neoplasms. Blood *127*, 3040-3053.

Emadali, A., Rousseaux, S., Bruder-Costa, J., Rome, C., Duley, S., Hamaidia, S., Betton, P., Debernardi, A., Leroux, D., Bernay, B.*, et al.* (2013). Identification of a novel BET bromodomain inhibitor-sensitive, gene regulatory circuit that controls Rituximab response and tumour growth in aggressive lymphoid cancers. EMBO molecular medicine *5*, 1180-1195.

Enjuanes, A., Albero, R., Clot, G., Navarro, A., Bea, S., Pinyol, M., Martin-Subero, J.I., Klapper, W., Staudt, L.M., Jaffe, E.S.*, et al.* (2013). Genome-wide methylation analyses identify a subset of mantle cell lymphoma with a high number of methylated CpGs and aggressive clinicopathological features. International journal of cancer *133*, 2852-2863.

Epsztejn-Litman, S., Feldman, N., Abu-Remaileh, M., Shufaro, Y., Gerson, A., Ueda, J., Deplus, R., Fuks, F., Shinkai, Y., Cedar, H.*, et al.* (2008). De novo DNA methylation promoted by G9a prevents reprogramming of embryonically silenced genes. Nature structural & molecular biology *15*, 1176-1183.

Fei, Q., Shang, K., Zhang, J., Chuai, S., Kong, D., Zhou, T., Fu, S., Liang, Y., Li, C., Chen, Z.*, et al.* (2015). Histone methyltransferase SETDB1 regulates liver cancer cell growth through methylation of p53. Nature communications *6*, 8651.

Feinberg, A.P., Koldobskiy, M.A., and Gondor, A. (2016). Epigenetic modulators, modifiers and mediators in cancer aetiology and progression. Nature reviews Genetics *17*, 284-299.

Feldman, N., Gerson, A., Fang, J., Li, E., Zhang, Y., Shinkai, Y., Cedar, H., and Bergman, Y. (2006). G9a-mediated irreversible epigenetic inactivation of Oct-3/4 during early embryogenesis. Nature cell biology *8*, 188-194.

Figueroa, M.E., Abdel-Wahab, O., Lu, C., Ward, P.S., Patel, J., Shih, A., Li, Y., Bhagwat, N., Vasanthakumar, A., Fernandez, H.F.*, et al.* (2010). Leukemic IDH1 and IDH2 mutations result in a hypermethylation phenotype, disrupt TET2 function, and impair hematopoietic differentiation. Cancer cell *18*, 553-567.

Filippakopoulos, P., and Knapp, S. (2014). Targeting bromodomains: epigenetic readers of lysine acetylation. Nature reviews Drug discovery *13*, 337-356.

Fournier, A., Florin, A., Lefebvre, C., Solly, F., Leroux, D., and Callanan, M.B. (2007). Genetics and epigenetics of 1q rearrangements in hematological malignancies. Cytogenetic and genome research *118*, 320-327.

Fournier, A., McLeer-Florin, A., Lefebvre, C., Duley, S., Barki, L., Ribeyron, J., Alboukadel, K., Hamaidia, S., Granjon, A., Gressin, R.*, et al.* (2010). 1q12 chromosome translocations form aberrant heterochromatic foci associated with changes in nuclear architecture and gene expression in B cell lymphoma. EMBO molecular medicine *2*, 159-171.

Frietze, S., O'Geen, H., Blahnik, K.R., Jin, V.X., and Farnham, P.J. (2010). ZNF274 recruits the histone methyltransferase SETDB1 to the 3' ends of ZNF genes. PloS one *5*, e15082.

Fritsch, L., Robin, P., Mathieu, J.R., Souidi, M., Hinaux, H., Rougeulle, C., Harel-Bellan, A., Ameyar-Zazoua, M., and Ait-Si-Ali, S. (2010). A subset of the histone H3 lysine 9 methyltransferases Suv39h1, G9a, GLP, and SETDB1 participate in a multimeric complex. Molecular cell *37*, 46-56.

Fu, M., Wang, C., Li, Z., Sakamaki, T., and Pestell, R.G. (2004). Minireview: Cyclin D1: normal and abnormal functions. Endocrinology *145*, 5439-5447.

Fuks, F., Hurd, P.J., Deplus, R., and Kouzarides, T. (2003). The DNA methyltransferases associate with HP1 and the SUV39H1 histone methyltransferase. Nucleic acids research *31*, 2305-2312.

Garcia-Cao, M., O'Sullivan, R., Peters, A.H., Jenuwein, T., and Blasco, M.A. (2004). Epigenetic regulation of telomere length in mammalian cells by the Suv39h1 and Suv39h2 histone methyltransferases. Nature genetics *36*, 94-99.

Geisler, C.H., Kolstad, A., Laurell, A., Andersen, N.S., Pedersen, L.B., Jerkeman, M., Eriksson, M., Nordstrom, M., Kimby, E., Boesen, A.M., *et al.* (2008). Long-term progression-free survival of mantle cell lymphoma after intensive front-line immunochemotherapy with in vivo-purged stem cell rescue: a nonrandomized phase 2 multicenter study by the Nordic Lymphoma Group. Blood *112*, 2687-2693.

Gobbi, P.G., Ferreri, A.J., Ponzoni, M., and Levis, A. (2013). Hodgkin lymphoma. Critical reviews in oncology/hematology *85*, 216-237.

Greiner, T.C., Dasgupta, C., Ho, V.V., Weisenburger, D.D., Smith, L.M., Lynch, J.C., Vose, J.M., Fu, K., Armitage, J.O., Braziel, R.M., *et al.* (2006). Mutation and genomic deletion status of ataxia telangiectasia mutated (ATM) and p53 confer specific gene expression profiles in mantle cell lymphoma. Proceedings of the National Academy of Sciences of the United States of America *103*, 2352-2357.

Guler, G.D., Tindell, C.A., Pitti, R., Wilson, C., Nichols, K., KaiWai Cheung, T., Kim, H.J., Wongchenko, M., Yan, Y., Haley, B., *et al.* (2017). Repression of Stress-Induced LINE-1 Expression Protects Cancer Cell Subpopulations from Lethal Drug Exposure. Cancer cell *32*, 221-237.e213.

Gurdon, J.B. (1962). The developmental capacity of nuclei taken from intestinal epithelium cells of feeding tadpoles. Journal of embryology and experimental morphology *10*, 622-640.

Hamidi, T., Singh, A.K., and Chen, T. (2015). Genetic alterations of DNA methylation machinery in human diseases. Epigenomics *7*, 247-265.

Harr, J.C., Gonzalez-Sandoval, A., and Gasser, S.M. (2016). Histones and histone modifications in perinuclear chromatin anchoring: from yeast to man. EMBO reports *17*, 139-155.

Hermine, O., Hoster, E., Walewski, J., Bosly, A., Stilgenbauer, S., Thieblemont, C., Szymczyk, M., Bouabdallah, R., Kneba, M., Hallek, M., *et al.* (2016). Addition of high-dose cytarabine to immunochemotherapy before autologous stem-cell transplantation in patients aged 65 years or younger with mantle cell lymphoma (MCL Younger): a randomised, open-label, phase 3 trial of the European Mantle Cell Lymphoma Network. Lancet *388*, 565-575.

Hutter, G., Scheubner, M., Zimmermann, Y., Kalla, J., Katzenberger, T., Hubler, K., Roth, S., Hiddemann, W., Ott, G., and Dreyling, M. (2006). Differential effect of epigenetic alterations and genomic deletions of CDK inhibitors [p16(INK4a), p15(INK4b), p14(ARF)] in mantle cell lymphoma. Genes, chromosomes & cancer *45*, 203-210.

Hyun, K., Jeon, J., Park, K., and Kim, J. (2017). Writing, erasing and reading histone lysine methylations. Experimental & molecular medicine *49*, e324.

Ikegami, K., Iwatani, M., Suzuki, M., Tachibana, M., Shinkai, Y., Tanaka, S., Greally, J.M., Yagi, S., Hattori, N., and Shiota, K. (2007). Genome-wide and locus-specific DNA hypomethylation in G9a deficient mouse embryonic stem cells. Genes to cells : devoted to molecular & cellular mechanisms *12*, 1-11.

Intlekofer, A.M., and Younes, A. (2014). Precision therapy for lymphoma--current state and future directions. Nature reviews Clinical oncology *11*, 585-596.

Jaffe, J.D., Wang, Y., Chan, H.M., Zhang, J., Huether, R., Kryukov, G.V., Bhang, H.E., Taylor, J.E., Hu, M., Englund, N.P.*, et al.* (2013). Global chromatin profiling reveals NSD2 mutations in pediatric acute lymphoblastic leukemia. Nature genetics *45*, 1386-1391.

Jares, P., and Campo, E. (2008). Advances in the understanding of mantle cell lymphoma. British journal of haematology *142*, 149-165.

Jares, P., Colomer, D., and Campo, E. (2012). Molecular pathogenesis of mantle cell lymphoma. The Journal of clinical investigation *122*, 3416-3423.

Jiang, Y., Loh, Y.E., Rajarajan, P., Hirayama, T., Liao, W., Kassim, B.S., Javidfar, B., Hartley, B.J., Kleofas, L., Park, R.B.*, et al.* (2017). The methyltransferase SETDB1 regulates a large neuron-specific topological chromatin domain. Nature genetics *49*, 1239-1250.

Johnson, W.L., Yewdell, W.T., Bell, J.C., McNulty, S.M., Duda, Z., O'Neill, R.J., Sullivan, B.A., and Straight, A.F. (2017). RNA-dependent stabilization of SUV39H1 at constitutive heterochromatin. eLife *6*.

Jones, P.A., Issa, J.P., and Baylin, S. (2016). Targeting the cancer epigenome for therapy. Nature reviews Genetics *17*, 630-641.

Jones, R.J., Gocke, C.D., Kasamon, Y.L., Miller, C.B., Perkins, B., Barber, J.P., Vala, M.S., Gerber, J.M., Gellert, L.L., Siedner, M.*, et al.* (2009). Circulating clonotypic B cells in classic Hodgkin lymphoma. Blood *113*, 5920-5926.

Karimi, M.M., Goyal, P., Maksakova, I.A., Bilenky, M., Leung, D., Tang, J.X., Shinkai, Y., Mager, D.L., Jones, S., Hirst, M.*, et al.* (2011). DNA methylation and SETDB1/H3K9me3 regulate predominantly distinct sets of genes, retroelements, and chimeric transcripts in mESCs. Cell stem cell *8*, 676-687.

Khanal, P., Kim, G., Lim, S.C., Yun, H.J., Lee, K.Y., Choi, H.K., and Choi, H.S. (2013). Prolyl isomerase Pin1 negatively regulates the stability of SUV39H1 to promote tumorigenesis in breast cancer. FASEB journal : official publication of the Federation of American Societies for Experimental Biology *27*, 4606-4618.

Kipps, T.J., Stevenson, F.K., Wu, C.J., Croce, C.M., Packham, G., Wierda, W.G., O'Brien, S., Gribben, J., and Rai, K. (2017). Chronic lymphocytic leukaemia. Nature reviews Disease primers *3*, 17008.

Klier, M., Anastasov, N., Hermann, A., Meindl, T., Angermeier, D., Raffeld, M., Fend, F., and Quintanilla-Martinez, L. (2008). Specific lentiviral shRNA-mediated knockdown of cyclin D1 in mantle cell lymphoma has minimal effects on cell survival and reveals a regulatory circuit with cyclin D2. Leukemia *22*, 2097-2105.

Kluin-Nelemans, H.C., Hoster, E., Hermine, O., Walewski, J., Trneny, M., Geisler, C.H., Stilgenbauer, S., Thieblemont, C., Vehling-Kaiser, U., Doorduijn, J.K.*, et al.* (2012). Treatment of older patients with mantle-cell lymphoma. The New England journal of medicine *367*, 520-531.

Koide, S., Oshima, M., Takubo, K., Yamazaki, S., Nitta, E., Saraya, A., Aoyama, K., Kato, Y., Miyagi, S., Nakajima-Takagi, Y.*, et al.* (2016). Setdb1 maintains hematopoietic stem and progenitor cells by restricting the ectopic activation of nonhematopoietic genes. Blood *128*, 638-649.

Koues, O.I., Oltz, E.M., and Payton, J.E. (2015). Short-Circuiting Gene Regulatory Networks: Origins of B Cell Lymphoma. Trends in genetics : TIG *31*, 720-731.

Kridel, R., Meissner, B., Rogic, S., Boyle, M., Telenius, A., Woolcock, B., Gunawardana, J., Jenkins, C., Cochrane, C., Ben-Neriah, S.*, et al.* (2012). Whole transcriptome sequencing reveals recurrent NOTCH1 mutations in mantle cell lymphoma. Blood *119*, 1963-1971.

Kuppers, R. (2005). Mechanisms of B-cell lymphoma pathogenesis. Nature reviews Cancer *5*, 251-262.

Kurosaki, T., Shinohara, H., and Baba, Y. (2010). B cell signaling and fate decision. Annual review of immunology *28*, 21-55.

Lachner, M., O'Carroll, D., Rea, S., Mechtler, K., and Jenuwein, T. (2001). Methylation of histone H3 lysine 9 creates a binding site for HP1 proteins. Nature *410*, 116-120.

Lajmanovich, A., Ribeyron, J.B., Florin, A., Fournier, A., Pasquier, M.A., Duley, S., Chauvet, M., Plumas, J., Bonnefoix, T., Gressin, R.*, et al.* (2009). Identification, characterisation and regulation by

CD40 activation of novel CD95 splice variants in CD95-apoptosis-resistant, human, B-cell non-Hodgkin's lymphoma. Experimental cell research *315*, 3281-3293.

Lakshmikuttyamma, A., Scott, S.A., DeCoteau, J.F., and Geyer, C.R. (2010). Reexpression of epigenetically silenced AML tumor suppressor genes by SUV39H1 inhibition. Oncogene *29*, 576-588.

Lampreia, F.P., Carmelo, J.G., and Anjos-Afonso, F. (2017). Notch Signaling in the Regulation of Hematopoietic Stem Cell. Current stem cell reports *3*, 202-209.

Lander, E.S., Linton, L.M., Birren, B., Nusbaum, C., Zody, M.C., Baldwin, J., Devon, K., Dewar, K., Doyle, M., FitzHugh, W.*, et al.* (2001). Initial sequencing and analysis of the human genome. Nature *409*, 860-921.

Langmead, B., Trapnell, C., Pop, M., and Salzberg, S.L. (2009). Ultrafast and memory-efficient alignment of short DNA sequences to the human genome. Genome biology *10*, R25.

Lawson, K.A., Teteak, C.J., Gao, J., Li, N., Hacquebord, J., Ghatan, A., Zielinska-Kwiatkowska, A., Song, G., Chansky, H.A., and Yang, L. (2013). ESET histone methyltransferase regulates osteoblastic differentiation of mesenchymal stem cells during postnatal bone development. FEBS letters *587*, 3961-3967.

Le Gouill, S., Thieblemont, C., Oberic, L., Moreau, A., Bouabdallah, K., Dartigeas, C., Damaj, G., Gastinne, T., Ribrag, V., Feugier, P.*, et al.* (2017). Rituximab after Autologous Stem-Cell Transplantation in Mantle-Cell Lymphoma. The New England journal of medicine *377*, 1250-1260.

Lefrere, F., Delmer, A., Suzan, F., Levy, V., Belanger, C., Djabarri, M., Arnulf, B., Damaj, G., Maillard, N., Ribrag, V.*, et al.* (2002). Sequential chemotherapy by CHOP and DHAP regimens followed by high-dose therapy with stem cell transplantation induces a high rate of complete response and improves event-free survival in mantle cell lymphoma: a prospective study. Leukemia *16*, 587-593.

Lehnertz, B., Ueda, Y., Derijck, A.A., Braunschweig, U., Perez-Burgos, L., Kubicek, S., Chen, T., Li, E., Jenuwein, T., and Peters, A.H. (2003). Suv39h-mediated histone H3 lysine 9 methylation directs DNA methylation to major satellite repeats at pericentric heterochromatin. Current biology : CB *13*, 1192-1200.

Lei, H., Oh, S.P., Okano, M., Juttermann, R., Goss, K.A., Jaenisch, R., and Li, E. (1996). De novo DNA cytosine methyltransferase activities in mouse embryonic stem cells. Development (Cambridge, England) *122*, 3195-3205.

Leshchenko, V.V., Kuo, P.Y., Shaknovich, R., Yang, D.T., Gellen, T., Petrich, A., Yu, Y., Remache, Y., Weniger, M.A., Rafiq, S.*, et al.* (2010). Genomewide DNA methylation analysis reveals novel targets for drug development in mantle cell lymphoma. Blood *116*, 1025-1034.

Leux, C., Maynadie, M., Troussard, X., Cabrera, Q., Herry, A., Le Guyader-Peyrou, S., Le Gouill, S., and Monnereau, A. (2014). Mantle cell lymphoma epidemiology: a population-based study in France. Annals of hematology *93*, 1327-1333.

Levy, C., Frecha, C., Costa, C., Rachinel, N., Salles, G., Cosset, F.L., and Verhoeyen, E. (2010). Lentiviral vectors and transduction of human cancer B cells. Blood *116*, 498-500; author reply 500.

Lin, Y.C., Benner, C., Mansson, R., Heinz, S., Miyazaki, K., Miyazaki, M., Chandra, V., Bossen, C., Glass, C.K., and Murre, C. (2012). Global changes in the nuclear positioning of genes and intra- and interdomain genomic interactions that orchestrate B cell fate. Nature immunology *13*, 1196-1204.

Liu, J., Magri, L., Zhang, F., Marsh, N.O., Albrecht, S., Huynh, J.L., Kaur, J., Kuhlmann, T., Zhang, W., Slesinger, P.A.*, et al.* (2015). Chromatin landscape defined by repressive histone methylation during oligodendrocyte differentiation. The Journal of neuroscience : the official journal of the Society for Neuroscience *35*, 352-365.

Lovec, H., Grzeschiczek, A., Kowalski, M.B., and Moroy, T. (1994). Cyclin D1/bcl-1 cooperates with myc genes in the generation of B-cell lymphoma in transgenic mice. The EMBO journal *13*, 3487-3495.

Loyola, A., Bonaldi, T., Roche, D., Imhof, A., and Almouzni, G. (2006). PTMs on H3 variants before chromatin assembly potentiate their final epigenetic state. Molecular cell *24*, 309-316.

Loyola, A., Tagami, H., Bonaldi, T., Roche, D., Quivy, J.P., Imhof, A., Nakatani, Y., Dent, S.Y., and Almouzni, G. (2009). The HP1alpha-CAF1-SetDB1-containing complex provides H3K9me1 for Suv39-mediated K9me3 in pericentric heterochromatin. EMBO reports *10*, 769-775.

Lu, C., Ward, P.S., Kapoor, G.S., Rohle, D., Turcan, S., Abdel-Wahab, O., Edwards, C.R., Khanin, R., Figueroa, M.E., Melnick, A.*, et al.* (2012). IDH mutation impairs histone demethylation and results in a block to cell differentiation. Nature *483*, 474-478.

Machanick, P., and Bailey, T.L. (2011). MEME-ChIP: motif analysis of large DNA datasets. Bioinformatics *27*, 1696-1697.

Maison, C., Bailly, D., Quivy, J.P., and Almouzni, G. (2016). The methyltransferase Suv39h1 links the SUMO pathway to HP1alpha marking at pericentric heterochromatin. Nature communications *7*, 12224.

Maison, C., Bailly, D., Roche, D., Montes de Oca, R., Probst, A.V., Vassias, I., Dingli, F., Lombard, B., Loew, D., Quivy, J.P.*, et al.* (2011). SUMOylation promotes de novo targeting of HP1alpha to pericentric heterochromatin. Nature genetics *43*, 220-227.

Mal, A.K. (2006). Histone methyltransferase Suv39h1 represses MyoD-stimulated myogenic differentiation. The EMBO journal *25*, 3323-3334.

Manilay, J.O., and Zouali, M. (2014). Tight relationships between B lymphocytes and the skeletal system. Trends in molecular medicine *20*, 405-412.

Martin-Subero, J.I., and Oakes, C.C. (2017). Charting the dynamic epigenome during B-cell development. Seminars in cancer biology.

Martin, P., Ghione, P., and Dreyling, M. (2017). Mantle cell lymphoma - Current standards of care and future directions. Cancer treatment reviews *58*, 51-60.

Martin, P., Maddocks, K., Leonard, J.P., Ruan, J., Goy, A., Wagner-Johnston, N., Rule, S., Advani, R., Iberri, D., Phillips, T.*, et al.* (2016). Postibrutinib outcomes in patients with mantle cell lymphoma. Blood *127*, 1559-1563.

Martinez-Garcia, E., Popovic, R., Min, D.J., Sweet, S.M., Thomas, P.M., Zamdborg, L., Heffner, A., Will, C., Lamy, L., Staudt, L.M.*, et al.* (2011). The MMSET histone methyl transferase switches global histone methylation and alters gene expression in t(4;14) multiple myeloma cells. Blood *117*, 211-220.

Matoba, S., Liu, Y., Lu, F., Iwabuchi, K.A., Shen, L., Inoue, A., and Zhang, Y. (2014). Embryonic development following somatic cell nuclear transfer impeded by persisting histone methylation. Cell *159*, 884-895.

Matthias, P., and Rolink, A.G. (2005). Transcriptional networks in developing and mature B cells. Nature reviews Immunology *5*, 497-508.

Meissner, B., Kridel, R., Lim, R.S., Rogic, S., Tse, K., Scott, D.W., Moore, R., Mungall, A.J., Marra, M.A., Connors, J.M.*, et al.* (2013). The E3 ubiquitin ligase UBR5 is recurrently mutated in mantle cell lymphoma. Blood *121*, 3161-3164.

Morin, R.D., Mendez-Lago, M., Mungall, A.J., Goya, R., Mungall, K.L., Corbett, R.D., Johnson, N.A., Severson, T.M., Chiu, R., Field, M.*, et al.* (2011). Frequent mutation of histone-modifying genes in non-Hodgkin lymphoma. Nature *476*, 298-303.

Mozos, A., Royo, C., Hartmann, E., De Jong, D., Baro, C., Valera, A., Fu, K., Weisenburger, D.D., Delabie, J., Chuang, S.S.*, et al.* (2009). SOX11 expression is highly specific for mantle cell lymphoma and identifies the cyclin D1-negative subtype. Haematologica *94*, 1555-1562.

Muller-Tidow, C., Klein, H.U., Hascher, A., Isken, F., Tickenbrock, L., Thoennissen, N., Agrawal-Singh, S., Tschanter, P., Disselhoff, C., Wang, Y.*, et al.* (2010). Profiling of histone H3 lysine 9 trimethylation levels predicts transcription factor activity and survival in acute myeloid leukemia. Blood *116*, 3564-3571.

Mungamuri, S.K., Qiao, R.F., Yao, S., Manfredi, J.J., Gu, W., and Aaronson, S.A. (2016). USP7 Enforces Heterochromatinization of p53 Target Promoters by Protecting SUV39H1 from MDM2-Mediated Degradation. Cell reports *14*, 2528-2537.

Musgrove, E.A., Caldon, C.E., Barraclough, J., Stone, A., and Sutherland, R.L. (2011). Cyclin D as a therapeutic target in cancer. Nature reviews Cancer *11*, 558-572.

Nagasawa, T. (2006). Microenvironmental niches in the bone marrow required for B-cell development. Nature reviews Immunology *6*, 107-116.

Nestorov, P., Tardat, M., and Peters, A.H. (2013). H3K9/HP1 and Polycomb: two key epigenetic silencing pathways for gene regulation and embryo development. Current topics in developmental biology *104*, 243-291.

Nielsen, S.J., Schneider, R., Bauer, U.M., Bannister, A.J., Morrison, A., O'Carroll, D., Firestein, R., Cleary, M., Jenuwein, T., Herrera, R.E.*, et al.* (2001). Rb targets histone H3 methylation and HP1 to promoters. Nature *412*, 561-565.

Notarangelo, L.D., Kim, M.S., Walter, J.E., and Lee, Y.N. (2016). Human RAG mutations: biochemistry and clinical implications. Nature reviews Immunology *16*, 234-246.

O'Carroll, D., Scherthan, H., Peters, A.H., Opravil, S., Haynes, A.R., Laible, G., Rea, S., Schmid, M., Lebersorger, A., Jerratsch, M.*, et al.* (2000). Isolation and characterization of Suv39h2, a second histone H3 methyltransferase gene that displays testis-specific expression. Molecular and cellular biology *20*, 9423-9433.

Okano, M., Bell, D.W., Haber, D.A., and Li, E. (1999). DNA methyltransferases Dnmt3a and Dnmt3b are essential for de novo methylation and mammalian development. Cell *99*, 247-257.

Onder, T.T., Kara, N., Cherry, A., Sinha, A.U., Zhu, N., Bernt, K.M., Cahan, P., Marcarci, B.O., Unternaehrer, J., Gupta, P.B.*, et al.* (2012). Chromatin-modifying enzymes as modulators of reprogramming. Nature *483*, 598-602.

Orkin, S.H., and Zon, L.I. (2008). Hematopoiesis: an evolving paradigm for stem cell biology. Cell *132*, 631-644.

Pasquarella, A., Ebert, A., Pereira de Almeida, G., Hinterberger, M., Kazerani, M., Nuber, A., Ellwart, J., Klein, L., Busslinger, M., and Schotta, G. (2016). Retrotransposon derepression leads to activation of the unfolded protein response and apoptosis in pro-B cells. Development (Cambridge, England) *143*, 1788-1799.

Peng, J., and Wysocka, J. (2008). It takes a PHD to SUMO. Trends in biochemical sciences *33*, 191-194.

Peters, A.H., O'Carroll, D., Scherthan, H., Mechtler, K., Sauer, S., Schofer, C., Weipoltshammer, K., Pagani, M., Lachner, M., Kohlmaier, A.*, et al.* (2001). Loss of the Suv39h histone methyltransferases impairs mammalian heterochromatin and genome stability. Cell *107*, 323-337.

Petti, E., Jordi, F., Buemi, V., Dinami, R., Benetti, R., Blasco, M.A., and Schoeftner, S. (2015). Altered telomere homeostasis and resistance to skin carcinogenesis in Suv39h1 transgenic mice. Cell cycle (Georgetown, Tex) *14*, 1438-1446.

Pileri, S.A., and Falini, B. (2009). Mantle cell lymphoma. Haematologica *94*, 1488-1492.

Porro, A., Feuerhahn, S., Delafontaine, J., Riethman, H., Rougemont, J., and Lingner, J. (2014). Functional characterization of the TERRA transcriptome at damaged telomeres. Nature communications *5*, 5379.

Queiros, A.C., Beekman, R., Vilarrasa-Blasi, R., Duran-Ferrer, M., Clot, G., Merkel, A., Raineri, E., Russinol, N., Castellano, G., Bea, S.*, et al.* (2016). Decoding the DNA Methylome of Mantle Cell Lymphoma in the Light of the Entire B Cell Lineage. Cancer cell *30*, 806-821.

Quinlan, A.R., and Hall, I.M. (2010). BEDTools: a flexible suite of utilities for comparing genomic features. Bioinformatics *26*, 841-842.

Raaphorst, F.M., Otte, A.P., and Meijer, C.J. (2001). Polycomb-group genes as regulators of mammalian lymphopoiesis. Trends in immunology *22*, 682-690.

Rahal, R., Frick, M., Romero, R., Korn, J.M., Kridel, R., Chan, F.C., Meissner, B., Bhang, H.E., Ruddy, D., Kauffmann, A.*, et al.* (2014). Pharmacological and genomic profiling identifies NF-kappaB-targeted treatment strategies for mantle cell lymphoma. Nature medicine *20*, 87-92.

Ramirez, F., Ryan, D.P., Gruning, B., Bhardwaj, V., Kilpert, F., Richter, A.S., Heyne, S., Dundar, F., and Manke, T. (2016). deepTools2: a next generation web server for deep-sequencing data analysis. Nucleic acids research *44*, W160-165.

Raurell-Vila, H., Bosch-Presegue, L., Gonzalez, J., Kane-Goldsmith, N., Casal, C., Brown, J.P., Marazuela-Duque, A., Singh, P.B., Serrano, L., and Vaquero, A. (2017). An HP1 isoform-specific feedback mechanism regulates Suv39h1 activity under stress conditions. Epigenetics *12*, 166-175.

Rea, S., Eisenhaber, F., O'Carroll, D., Strahl, B.D., Sun, Z.W., Schmid, M., Opravil, S., Mechtler, K., Ponting, C.P., Allis, C.D.*, et al.* (2000). Regulation of chromatin structure by site-specific histone H3 methyltransferases. Nature *406*, 593-599.

Reed-Inderbitzin, E., Moreno-Miralles, I., Vanden-Eynden, S.K., Xie, J., Lutterbach, B., Durst-Goodwin, K.L., Luce, K.S., Irvin, B.J., Cleary, M.L., Brandt, S.J.*, et al.* (2006). RUNX1 associates with histone deacetylases and SUV39H1 to repress transcription. Oncogene *25*, 5777-5786.

Regina, C., Compagnone, M., Peschiaroli, A., Lena, A., Annicchiarico-Petruzzelli, M., Piro, M.C., Melino, G., and Candi, E. (2016). Setdb1, a novel interactor of DeltaNp63, is involved in breast tumorigenesis. Oncotarget *7*, 28836-28848.

Reimann, M., Lee, S., Loddenkemper, C., Dorr, J.R., Tabor, V., Aichele, P., Stein, H., Dorken, B., Jenuwein, T., and Schmitt, C.A. (2010). Tumor stroma-derived TGF-beta limits myc-driven lymphomagenesis via Suv39h1-dependent senescence. Cancer cell *17*, 262-272.

Rickert, R.C. (2013). New insights into pre-BCR and BCR signalling with relevance to B cell malignancies. Nature reviews Immunology *13*, 578-591.

Ripperger, T., von Neuhoff, N., Kamphues, K., Emura, M., Lehmann, U., Tauscher, M., Schraders, M., Groenen, P., Skawran, B., Rudolph, C.*, et al.* (2007). Promoter methylation of PARG1, a novel candidate tumor suppressor gene in mantle-cell lymphomas. Haematologica *92*, 460-468.

Rodriguez-Cortez, V.C., Martinez-Redondo, P., Catala-Moll, F., Rodriguez-Ubreva, J., Garcia-Gomez, A., Poorani-Subramani, G., Ciudad, L., Hernando, H., Perez-Garcia, A., Company, C.*, et al.* (2017). Activation-induced cytidine deaminase targets SUV4-20-mediated histone H4K20 trimethylation to class-switch recombination sites. Scientific reports *7*, 7594.

Rodriguez-Paredes, M., Martinez de Paz, A., Simo-Riudalbas, L., Sayols, S., Moutinho, C., Moran, S., Villanueva, A., Vazquez-Cedeira, M., Lazo, P.A., Carneiro, F.*, et al.* (2014). Gene amplification of the histone methyltransferase SETDB1 contributes to human lung tumorigenesis. Oncogene *33*, 2807-2813.

Romaguera, J.E., Fayad, L., Rodriguez, M.A., Broglio, K.R., Hagemeister, F.B., Pro, B., McLaughlin, P., Younes, A., Samaniego, F., Goy, A.*, et al.* (2005). High rate of durable remissions after treatment of newly diagnosed aggressive mantle-cell lymphoma with rituximab plus hyper-CVAD alternating with rituximab plus high-dose methotrexate and cytarabine. Journal of clinical oncology : official journal of the American Society of Clinical Oncology *23*, 7013-7023.

Rosenwald, A., Wright, G., Wiestner, A., Chan, W.C., Connors, J.M., Campo, E., Gascoyne, R.D., Grogan, T.M., Muller-Hermelink, H.K., Smeland, E.B.*, et al.* (2003). The proliferation gene expression signature is a quantitative integrator of oncogenic events that predicts survival in mantle cell lymphoma. Cancer cell *3*, 185-197.

Rowe, H.M., Jakobsson, J., Mesnard, D., Rougemont, J., Reynard, S., Aktas, T., Maillard, P.V., Layard-Liesching, H., Verp, S., Marquis, J.*, et al.* (2010). KAP1 controls endogenous retroviruses in embryonic stem cells. Nature *463*, 237-240.

Roy, D.M., Walsh, L.A., and Chan, T.A. (2014). Driver mutations of cancer epigenomes. Protein & cell *5*, 265-296.

Royo, C., Salaverria, I., Hartmann, E.M., Rosenwald, A., Campo, E., and Bea, S. (2011). The complex landscape of genetic alterations in mantle cell lymphoma. Seminars in cancer biology *21*, 322-334.

Rui, L., Emre, N.C., Kruhlak, M.J., Chung, H.J., Steidl, C., Slack, G., Wright, G.W., Lenz, G., Ngo, V.N., Shaffer, A.L.*, et al.* (2010). Cooperative epigenetic modulation by cancer amplicon genes. Cancer cell *18*, 590-605.

Ryu, H., Lee, J., Hagerty, S.W., Soh, B.Y., McAlpin, S.E., Cormier, K.A., Smith, K.M., and Ferrante, R.J. (2006). ESET/SETDB1 gene expression and histone H3 (K9) trimethylation in Huntington's disease. Proceedings of the National Academy of Sciences of the United States of America *103*, 19176-19181.

Sander, B., Quintanilla-Martinez, L., Ott, G., Xerri, L., Kuzu, I., Chan, J.K., Swerdlow, S.H., and Campo, E. (2016). Mantle cell lymphoma--a spectrum from indolent to aggressive disease. Virchows Archiv : an international journal of pathology *468*, 245-257.

Sarkozy, C., Terre, C., Jardin, F., Radford, I., Roche-Lestienne, C., Penther, D., Bastard, C., Rigaudeau, S., Pilorge, S., Morschhauser, F., *et al.* (2014). Complex karyotype in mantle cell lymphoma is a strong prognostic factor for the time to treatment and overall survival, independent of the MCL international prognostic index. Genes, chromosomes & cancer *53*, 106-116.

Sarraf, S.A., and Stancheva, I. (2004). Methyl-CpG binding protein MBD1 couples histone H3 methylation at lysine 9 by SETDB1 to DNA replication and chromatin assembly. Molecular cell *15*, 595-605.

Scarola, M., Comisso, E., Pascolo, R., Chiaradia, R., Marion, R.M., Schneider, C., Blasco, M.A., Schoeftner, S., and Benetti, R. (2015). Epigenetic silencing of Oct4 by a complex containing SUV39H1 and Oct4 pseudogene lncRNA. Nature communications *6*, 7631.

Schultz, D.C., Ayyanathan, K., Negorev, D., Maul, G.G., and Rauscher, F.J., 3rd (2002). SETDB1: a novel KAP-1-associated histone H3, lysine 9-specific methyltransferase that contributes to HP1-mediated silencing of euchromatic genes by KRAB zinc-finger proteins. Genes & development *16*, 919-932.

Scott, D.W., and Gascoyne, R.D. (2014). The tumour microenvironment in B cell lymphomas. Nature reviews Cancer *14*, 517-534.

Seifert, M., Sellmann, L., Bloehdorn, J., Wein, F., Stilgenbauer, S., Durig, J., and Kuppers, R. (2012). Cellular origin and pathophysiology of chronic lymphocytic leukemia. The Journal of experimental medicine *209*, 2183-2198.

Shaffer, A.L., Rosenwald, A., and Staudt, L.M. (2002). Lymphoid malignancies: the dark side of B-cell differentiation. Nature reviews Immunology *2*, 920-932.

Shaknovich, R., Cerchietti, L., Tsikitas, L., Kormaksson, M., De, S., Figueroa, M.E., Ballon, G., Yang, S.N., Weinhold, N., Reimers, M., *et al.* (2011). DNA methyltransferase 1 and DNA methylation patterning contribute to germinal center B-cell differentiation. Blood *118*, 3559-3569.

Shi, Y., Lan, F., Matson, C., Mulligan, P., Whetstine, J.R., Cole, P.A., Casero, R.A., and Shi, Y. (2004). Histone demethylation mediated by the nuclear amine oxidase homolog LSD1. Cell *119*, 941-953.

Shirai, A., Kawaguchi, T., Shimojo, H., Muramatsu, D., Ishida-Yonetani, M., Nishimura, Y., Kimura, H., Nakayama, J.I., and Shinkai, Y. (2017). Impact of nucleic acid and methylated H3K9 binding activities of Suv39h1 on its heterochromatin assembly. eLife *6*.

Snowden, A.W., Gregory, P.D., Case, C.C., and Pabo, C.O. (2002). Gene-specific targeting of H3K9 methylation is sufficient for initiating repression in vivo. Current biology : CB *12*, 2159-2166.

Soufi, A., Donahue, G., and Zaret, K.S. (2012). Facilitators and impediments of the pluripotency reprogramming factors' initial engagement with the genome. Cell *151*, 994-1004.

Spensberger, D., and Delwel, R. (2008). A novel interaction between the proto-oncogene Evi1 and histone methyltransferases, SUV39H1 and G9a. FEBS letters *582*, 2761-2767.

Sridharan, R., Gonzales-Cope, M., Chronis, C., Bonora, G., McKee, R., Huang, C., Patel, S., Lopez, D., Mishra, N., Pellegrini, M.*, et al.* (2013). Proteomic and genomic approaches reveal critical functions of H3K9 methylation and heterochromatin protein-1gamma in reprogramming to pluripotency. Nature cell biology *15*, 872-882.

Staller, P. (2010). Genetic heterogeneity and chromatin modifiers in renal clear cell carcinoma. Future oncology (London, England) *6*, 897-900.

Stewart, M.D., Li, J., and Wong, J. (2005). Relationship between histone H3 lysine 9 methylation, transcription repression, and heterochromatin protein 1 recruitment. Molecular and cellular biology *25*, 2525-2538.

Su, I.H., Basavaraj, A., Krutchinsky, A.N., Hobert, O., Ullrich, A., Chait, B.T., and Tarakhovsky, A. (2003). Ezh2 controls B cell development through histone H3 methylation and Igh rearrangement. Nature immunology *4*, 124-131.

Sun, L., and Fang, J. (2016). E3-Independent Constitutive Monoubiquitination Complements Histone Methyltransferase Activity of SETDB1. Molecular cell *62*, 958-966.

Sun, Q.Y., Ding, L.W., Xiao, J.F., Chien, W., Lim, S.L., Hattori, N., Goodglick, L., Chia, D., Mah, V., Alavi, M.*, et al.* (2015). SETDB1 accelerates tumourigenesis by regulating the WNT signalling pathway. The Journal of pathology *235*, 559-570.

Tachibana, K., Gotoh, E., Kawamata, N., Ishimoto, K., Uchihara, Y., Iwanari, H., Sugiyama, A., Kawamura, T., Mochizuki, Y., Tanaka, T.*, et al.* (2015). Analysis of the subcellular localization of the human histone methyltransferase SETDB1. Biochemical and biophysical research communications *465*, 725-731.

Takahashi, K., Tanabe, K., Ohnuki, M., Narita, M., Ichisaka, T., Tomoda, K., and Yamanaka, S. (2007). Induction of pluripotent stem cells from adult human fibroblasts by defined factors. Cell *131*, 861-872.

Tan, S.L., Nishi, M., Ohtsuka, T., Matsui, T., Takemoto, K., Kamio-Miura, A., Aburatani, H., Shinkai, Y., and Kageyama, R. (2012). Essential roles of the histone methyltransferase ESET in the epigenetic control of neural progenitor cells during development. Development (Cambridge, England) *139*, 3806-3816.

Timms, R.T., Tchasovnikarova, I.A., Antrobus, R., Dougan, G., and Lehner, P.J. (2016). ATF7IP-Mediated Stabilization of the Histone Methyltransferase SETDB1 Is Essential for Heterochromatin Formation by the HUSH Complex. Cell reports *17*, 653-659.

Torres, I.O., and Fujimori, D.G. (2015). Functional coupling between writers, erasers and readers of histone and DNA methylation. Current opinion in structural biology *35*, 68-75.

Trojer, P., and Reinberg, D. (2007). Facultative heterochromatin: is there a distinctive molecular signature? Molecular cell *28*, 1-13.

Ugarte, F., Sousae, R., Cinquin, B., Martin, E.W., Krietsch, J., Sanchez, G., Inman, M., Tsang, H., Warr, M., Passegue, E.*, et al.* (2015). Progressive Chromatin Condensation and H3K9 Methylation Regulate the Differentiation of Embryonic and Hematopoietic Stem Cells. Stem cell reports *5*, 728-740.

van der Lugt, N.M., Domen, J., Linders, K., van Roon, M., Robanus-Maandag, E., te Riele, H., van der Valk, M., Deschamps, J., Sofroniew, M., van Lohuizen, M.*, et al.* (1994). Posterior transformation, neurological abnormalities, and severe hematopoietic defects in mice with a targeted deletion of the bmi-1 proto-oncogene. Genes & development *8*, 757-769.

van Steensel, B., and Belmont, A.S. (2017). Lamina-Associated Domains: Links with Chromosome Architecture, Heterochromatin, and Gene Repression. Cell *169*, 780-791.

Vandel, L., Nicolas, E., Vaute, O., Ferreira, R., Ait-Si-Ali, S., and Trouche, D. (2001). Transcriptional repression by the retinoblastoma protein through the recruitment of a histone methyltransferase. Molecular and cellular biology *21*, 6484-6494.

Vaquero, A., Scher, M., Erdjument-Bromage, H., Tempst, P., Serrano, L., and Reinberg, D. (2007). SIRT1 regulates the histone methyl-transferase SUV39H1 during heterochromatin formation. Nature *450*, 440-444.

Vegliante, M.C., Palomero, J., Perez-Galan, P., Roue, G., Castellano, G., Navarro, A., Clot, G., Moros, A., Suarez-Cisneros, H., Bea, S.*, et al.* (2013). SOX11 regulates PAX5 expression and blocks terminal B-cell differentiation in aggressive mantle cell lymphoma. Blood *121*, 2175-2185.

Vegliante, M.C., Royo, C., Palomero, J., Salaverria, I., Balint, B., Martin-Guerrero, I., Agirre, X., Lujambio, A., Richter, J., Xargay-Torrent, S.*, et al.* (2011). Epigenetic activation of SOX11 in lymphoid neoplasms by histone modifications. PloS one *6*, e21382.

Velazquez Camacho, O., Galan, C., Swist-Rosowska, K., Ching, R., Gamalinda, M., Karabiber, F., De La Rosa-Velazquez, I., Engist, B., Koschorz, B., Shukeir, N.*, et al.* (2017). Major satellite repeat RNA stabilize heterochromatin retention of Suv39h enzymes by RNA-nucleosome association and RNA:DNA hybrid formation. eLife *6*.

Vert, J.P., Foveau, N., Lajaunie, C., and Vandenbrouck, Y. (2006). An accurate and interpretable model for siRNA efficacy prediction. BMC bioinformatics *7*, 520.

Vose, J.M. (2017). Mantle cell lymphoma: 2017 update on diagnosis, risk-stratification, and clinical management. American journal of hematology *92*, 806-813.

Wang, D., Zhou, J., Liu, X., Lu, D., Shen, C., Du, Y., Wei, F.Z., Song, B., Lu, X., Yu, Y.*, et al.* (2013a). Methylation of SUV39H1 by SET7/9 results in heterochromatin relaxation and genome instability. Proceedings of the National Academy of Sciences of the United States of America *110*, 5516-5521.

Wang, H., An, W., Cao, R., Xia, L., Erdjument-Bromage, H., Chatton, B., Tempst, P., Roeder, R.G., and Zhang, Y. (2003). mAM facilitates conversion by ESET of dimethyl to trimethyl lysine 9 of histone H3 to cause transcriptional repression. Molecular cell *12*, 475-487.

Wang, L.D., and Wagers, A.J. (2011). Dynamic niches in the origination and differentiation of haematopoietic stem cells. Nature reviews Molecular cell biology *12*, 643-655.

Wang, M.L., Rule, S., Martin, P., Goy, A., Auer, R., Kahl, B.S., Jurczak, W., Advani, R.H., Romaguera, J.E., Williams, M.E.*, et al.* (2013b). Targeting BTK with ibrutinib in relapsed or refractory mantle-cell lymphoma. The New England journal of medicine *369*, 507-516.

Wang, Y., and Ma, S. (2014). Risk factors for etiology and prognosis of mantle cell lymphoma. Expert review of hematology *7*, 233-243.

Williamson, C.T., Kubota, E., Hamill, J.D., Klimowicz, A., Ye, R., Muzik, H., Dean, M., Tu, L., Gilley, D., Magliocco, A.M.*, et al.* (2012). Enhanced cytotoxicity of PARP inhibition in mantle cell lymphoma harbouring mutations in both ATM and p53. EMBO molecular medicine *4*, 515-527.

Wrangle, J., Wang, W., Koch, A., Easwaran, H., Mohammad, H.P., Vendetti, F., Vancriekinge, W., Demeyer, T., Du, Z., Parsana, P.*, et al.* (2013). Alterations of immune response of Non-Small Cell Lung Cancer with Azacytidine. Oncotarget *4*, 2067-2079.

Xie, H., Ye, M., Feng, R., and Graf, T. (2004). Stepwise reprogramming of B cells into macrophages. Cell *117*, 663-676.

Yamaguchi, T., Cubizolles, F., Zhang, Y., Reichert, N., Kohler, H., Seiser, C., and Matthias, P. (2010). Histone deacetylases 1 and 2 act in concert to promote the G1-to-S progression. Genes & development *24*, 455-469.

Yu, G., Wang, L.G., and He, Q.Y. (2015). ChIPseeker: an R/Bioconductor package for ChIP peak annotation, comparison and visualization. Bioinformatics *31*, 2382-2383.

Yu, T., Wang, C., Yang, J., Guo, Y., Wu, Y., and Li, X. (2017). Metformin inhibits SUV39H1-mediated migration of prostate cancer cells. Oncogenesis *6*, e324.

Yuan, P., Han, J., Guo, G., Orlov, Y.L., Huss, M., Loh, Y.H., Yaw, L.P., Robson, P., Lim, B., and Ng, H.H. (2009). Eset partners with Oct4 to restrict extraembryonic trophoblast lineage potential in embryonic stem cells. Genes & development *23*, 2507-2520.

Zang, C., Schones, D.E., Zeng, C., Cui, K., Zhao, K., and Peng, W. (2009). A clustering approach for identification of enriched domains from histone modification ChIP-Seq data. Bioinformatics *25*, 1952-1958.

Zhang, J., Jima, D., Moffitt, A.B., Liu, Q., Czader, M., Hsi, E.D., Fedoriw, Y., Dunphy, C.H., Richards, K.L., Gill, J.I.*, et al.* (2014). The genomic landscape of mantle cell lymphoma is related to the epigenetically determined chromatin state of normal B cells. Blood *123*, 2988-2996.

Zhang, T., Cooper, S., and Brockdorff, N. (2015). The interplay of histone modifications - writers that read. EMBO reports *16*, 1467-1481.

Zotos, D., and Tarlinton, D.M. (2012). Determining germinal centre B cell fate. Trends in immunology *33*, 281-288.

Annexe

biomedicines

MDPI

Review

BET Family Protein BRD4: An Emerging Actor in NFκB Signaling in Inflammation and Cancer

Azadeh Hajmirza [1], Anouk Emadali [1,2], Arnaud Gauthier [1], Olivier Casasnovas [3], Rémy Gressin [4] and Mary B. Callanan [1,5,*]

1 INSERM U1209, CNRS UMR 5309, Institute for Advanced Biosciences, Université de Grenoble-Alpes, F-38042 Grenoble, France; azadeh.hajmirza@univ-grenoble-alpes.fr (A.H.); anouk.emadali@univ-grenoble-alpes.fr (A.E.); agauthier@chu-grenoble.fr (A.G.)
2 Pôle Recherche, Grenoble-Alpes University Hospital, F-38043 Grenoble, France
3 Département d'Hématologie Clinique, Dijon University Hospital, F-21000 Dijon, France; olivier.casasnovas@chu-dijon.fr
4 Département d'Hématologie Clinique, Grenoble-Alpes University Hospital, F-38043 Grenoble, France; RGressin@chu-grenoble.fr
5 Centre for Innovation in Cancer Genetics and Epigenetics, Dijon University Hospital, F-21000 Dijon, France
* Correspondance: mary.callanan@chu-dijon.fr

Received: 16 October 2017; Accepted: 1 February 2018; Published: 6 February 2018

Abstract: NFκB (Nuclear Factor-κ-light-chain-enhancer of activated B cells) signaling elicits global transcriptional changes by activating cognate promoters and through genome-wide remodeling of cognate regulatory elements called "super enhancers". BET (Bromodomain and Extra-Terminal domain) protein family inhibitor studies have implicated BET protein member BRD4 and possibly other BET proteins in NFκB-dependent promoter and super-enhancer modulation. Members of the BET protein family are known to bind acetylated chromatin to facilitate access by transcriptional regulators to chromatin, as well as to assist the activity of transcription elongation complexes via CDK9/pTEFb. BET family member BRD4 has been shown to bind non-histone proteins and modulate their activity. One such protein is RELA, the NFκB co-activator. Specifically, BRD4 binds acetylated RELA, which increases its transcriptional transactivation activity and stability in the nucleus. In aggregate, this establishes an intimate link between NFκB and BET signaling, at least via BRD4. The present review provides a brief overview of the structure and function of BET family proteins and then examines the connections between NFκB and BRD4 signaling, using the inflammatory response and cancer cell signaling as study models. We also discuss the potential of BET inhibitors for relief of aberrant NFκB signaling in cancer, focusing on non-histone, acetyl-lysine binding functions.

Keywords: NFκB; BET inhibition; transcription; chromatin looping; acetylation B cell non-Hodgkin lymphoma

1. Introduction

Epigenetic signaling refers to the chromatin-dependent mechanisms that directly or indirectly control genome activity. Essentially, this refers to the chemical modifications on DNA or chromatin (histone proteins) that, together with topological organization of the chromatin fiber in the nucleus, regulate chromatin compaction. This allows the formation of functionally distinct, dynamically reversible chromatin states called euchromatin and heterochromatin, respectively [1]. The former is characterized by loosely packed nucleosomes, while in heterochromatin nucleosomes are densely packed. Nucleosomes are the basic functional unit of chromatin and are comprised of an octamer of the core histones, H2A, H2B, H3, and H4 (two copies of each). DNA methylation and post-translational

histone modifications allow regulation of genome function by the modulation of chromatin compaction- and thereby access to DNA by transcription, replication, and repair factors- by serving as docking platforms for specific chromatin-associated signaling complexes [1]. Enzymes that mediate chemical modifications of DNA or chromatin are referred to as "writers" of epigenetic information, while those proteins that dock or erase these chemical modifications are referred to as "readers" and "erasers" or epigenetic information, respectively [1].

Bromodomain and extra-terminal domain (BET) proteins constitute a novel class of epigenetic "readers" that is involved in the control of genome activity through the ability to bind acetylated lysine residues in both histone and non-histone proteins, including transcription factors. The mechanism by which BET proteins are recruited to acetylated lysine is discussed below. How this links to transcriptional control by NFκB signaling is reviewed.

BET proteins have emerged as key regulators of transcriptional control in development and cellular differentiation and have been identified as critical actors of disordered transcription in transformed cells, thereby rendering them hypersensitive to small molecule inhibition of BET protein activity [2,3]. Mechanisms of action are complex but rely on the capacity of these proteins to bind acetylated histone and non-histone proteins via their double bromodomains (Figure 1) [2].

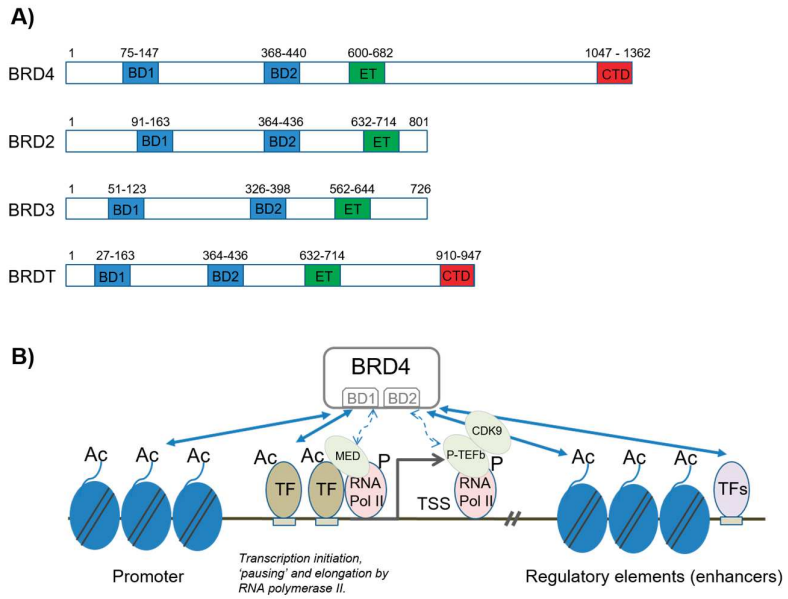

Figure 1. Schematic of domain organization of BET (bromodomain and extra-terminal domain) family proteins and the function of BRD4 in the regulation of promoter and enhancer activity. (**A**) Domain organization of human BET family members BRD4, BRD2, BRD3, and BRDT, as indicated. BET proteins contain two bromodomains (BD1 and BD2, respectively) and an extra-terminal domain (ET). BRD4 (long form) contains a carboxyterminal domain (CTD) that is not present in the other BET family members; (**B**) Schematic representation of the functions of BET family member BRD4 in the regulation of promoter and enhancer function (includes "super-enhancers"; see text for details). Through its BD1 and BD2 domains, BRD4 binds to acetylated lysines (Ac) in histones or transcription factors (TF). The binding of acetylated histones by BRD4, at transcription start sites (TSS), mediates transcriptional co-activation and elongation via RNA polymerase II (RNA pol II) and Mediator (Med) and pTEFb signaling complexes, respectively (see text for details). BRD4 can also bind acetylated lysines in histones or TF in enhancer elements, thereby contributing to long-range control of gene activity (see text for details). TF binding sites are depicted as horizontal rectangles.

2. Structure and Function of BET Proteins

The BET family of proteins comprises BRD2, BRD3, BRD4 (ubiquitously expressed), and BRDT (testis-specific expression). BET proteins are characterized by the presence of two conserved *N*-terminal

bromodomains (BD1 and BD2) and a C-terminal "extra-terminal" domain (Figure 1). The bromodomain structure contains four alpha helices separated by a variable loop region that together allow the formation of a hydrophobic cavity that recognizes acetyl-lysine residues [4,5]. Structural data have established that acetylated lysine is recognized in this central hydrophobic pocket, by anchoring to a conserved asparagine residue. The BET bromodomain proteins can bind to two acetylated lysine histone marks that are simultaneously recognized by the same bromodomain module [5]. This property is shared by all members of the BET subclass of bromodomains. High-resolution co-crystal structures showed that the first acetylated lysine mark of histone H4 docks directly onto the conserved asparagine (Asn140 in the first bromodomain of BRD4). A network of hydrogen bonds within the acetyl-lysine binding cavity link to the second acetylated lysine mark thus stabilizing the peptide complex [4,5]. The largely hydrophobic nature of the central acetylated lysine binding pocket of the bromodomain, which is necessary to accommodate the charge-neutralized acetylated lysine, and the comparably weak interaction with its target sequences make these modules particularly attractive for the development of inhibitors targeting this protein–protein interaction. The interaction of BET proteins with mono-acetylated lysine seems to be of weak affinity compared to the interactions that occur at multiple closely spaced acetylated lysines [4,5].

As well as interacting with acetylated lysine in histones, BET proteins also interact with members of the transcription elongation complex and with other transcription factors. In the latter case, this can be through lysine acetylation-dependent or -independent mechanisms. As such, BET proteins are key "readers" of epigenetic information in both normal and transformed cells. The interaction of BDs at acetylated chromatin either at gene promoters or in long range *cis* regulatory elements called enhancers allows chromatin-dependent signaling to connect to transcription regulation [6].

2.1. BRD4 in Transcriptional Regulation by NFκB

BRD4 is a particularly well-studied member of the BET protein family. BRD4 contains two bromodomains associated to an extra-terminal domain (Figure 1A). As explained above, the BD domains allow BRD4 to interact with acetylated lysine in histone or non-histone proteins. How this property is involved in transcriptional regulation is discussed. New findings relating to BET proteins and pro-inflammatory- or cancer cell-specific NFκB signaling [7] are also reviewed.

2.1.1. Transcription Initiation and Elongation

BRD4 participates in the activation and elongation of transcription via interactions with transcription initiation and elongation complexes Mediator and pTEFb (positive transcription elongation factor B), respectively. The pTEFb complex is composed of the cyclin-dependent kinase, CDK9, and a regulatory subunit, Cyclin T1 or T2. The kinase activity of CDK9 inhibits negative regulators of RNA polymerase II activity while stimulating its elongation activity by phosphorylation [8]. At least two different regions of BRD4 interact directly with pTEFb. The C-terminal region interacts with Cyclin T1 and CDK9 and the BD2 region interacts with the acetylated region of Cyclin T1. The BRD4/pTEFb interaction plays a central role in the rapid initiation of transcription after the exit from mitosis [8].

The extra-terminal (ET) domain is involved in transcriptional regulation through interactions with histone modifiers such as JMJD6 (jmjC domain-containing protein 6), an arginine demethylase, and NSD3, a lysine methyltransferase [9,10]. Furthermore, the ET domain can associate with ATP-dependent chromatin remodelers such as the SWI-SNF and CHD2 [10]. These interactions are thought to allow BRD4 to remodel chromatin locally, although the regulatory significance of these events is not well understood. One possibility is that this allows the release of paused RNA pol II activity [9].

NFκB-dependent transcriptional control is regulated at multiple levels, including cytoplasmic signaling events leading to the nuclear translocation of NFκB, the binding of nuclear NFκB to various transcriptional factors or regulators, and the post-transcriptional modifications of histones and NFκB itself [7]. Within the nucleus, NFκB recognizes the cognate NFκB sites on the enhancer or promoter

regions of its target genes and directs the binding of co-regulators to form the transcriptional machinery for target gene expression. In the setting of NFκB signaling, it has been found that pTEFb can be recruited by BRD4 to NFκB-dependent acetylated histones—a mechanism that is crucial for the transcription of primary response genes [6], and possibly pathological NFκB signaling in cancer cells, although the latter has not been investigated in any detail as yet.

2.1.2. Enhancer Regulation by BRD4 and Its Role in NFκB Signaling

The genome-wide distribution of BRD4 has been studied by chromatin immunoprecipitation and deep sequencing (ChIP-seq). These experiments have shown that BRD4 binds multiple promoters as well as intergenic regions, particularly enhancer sequences. The Mediator complex (MED), composed of 26 subunits in mammals, plays a key role in transcription initiation and elongation downstream of numerous signaling cascades as well as in the functional regulation of enhancer elements. BRD4 and MED have been found to co-occupy subsets of enhancers called "super-enhancers" [11], which are large enhancer regions that stimulate the transcription of growth-promoting and lineage-specific survival genes [6]. Super-enhancers are also co-enriched for histone H3 acetylated at lysine 27. Supporting a functional interaction of BRD4 and MED at super-enhancers, BET bromodomain inhibition releases the mediator complex from select *cis*-regulatory elements, at least in leukemia cells [12]. It is interesting to note that MED complex activity at super-enhancers involves reversible association with a subunit containing the cyclin dependent kinase CDK8 and the cofactors CCNC (CYCLIN C), MED12, and MED13. Mutations in the gene encoding MED12 have been described in chronic lymphocytic leukemia [13]. Furthermore, the MED complex contains both activating and inhibiting CDKs, the latter of which appear to constrain tumor suppressor and lineage identity gene-associated super-enhancers, which raises interest in combining BET and MED complex negative regulatory CDK inhibitors for anti-cancer treatment [14].

Numerous oncogenes have been shown to be under the control of super-enhancer elements in various cancer types. Remarkable examples are the deregulation of MYC in B cell non-Hodgkin lymphoma and multiple myeloma [15,16], EVI1 in acute myeloid leukemia with the inversion of chromosome 3q [17], and mutational processes that are predicted to alter super-enhancer activity in breast cancer [18]. The recruitment of BRD4 to enhancer regions seems to depend, at least in part, on the activity of specific transcription factors and on histone acetyl-transferases such as p300/CBP [19]. The recruitment of BRD4 is essential to the activity of numerous hematopoietic transcription factors such as PU.1, FLI1, ERG, C/EBPα, C/EBPβ, and MYB [19] and to the activity of NFκB at cognate enhancers, downstream of inflammatory responses in endothelial cells and macrophages [20]. Although the precise mechanism for BRD4 co-recruitment with the NFκB subunit RELA/p65 to pro-inflammatory genes is not yet deciphered, it may relate to both BRD4-dependent histone lysine acetylation docking as well as to the ability of BRD4 to bind acetylated p65/RELA, as discussed in detail below [21].

NFκB-dependent enhancer remodeling during pro-inflammatory responses has been shown to implicate the synthesis of enhancer RNA (eRNA) and local chromatin acetylation, followed by progressive H3 lysine 4 mono and di-methylation [22]. This process requires composite binding with other tissue-specific transcription factors. eRNAs belong to the non-coding RNAs and their transcripts are directed by enhancers, which is thought to favor the spatial repositioning ('chromatin looping') of distal enhancers close to their cognate promoters via RNA pol II. Thus, NFκB acts as a key modulator of de novo enhancer remodeling in the setting of pro-inflammatory signaling by modulating eRNA transcription [23].

In keeping with the above findings, BET inhibitors effectively suppress inflammatory responses mediated by NFκB, in particular at super-enhancers [20]. Likewise, the NFκB pathway is activated by LPS (lipopolysaccharide), and the pan-BET inhibitor I-BET762 has been shown to prevent or diminish the incidence of death in mice given lethal doses of lipopolysaccharide [24].

2.1.3. BRD4 Interaction with Acetylated RELA/p65; Impact on NFκB Signaling and Sensitivity to BET Inhibitors

BRD4/BET proteins have been shown to interact with acetylated lysines in non-histone proteins [6]. This facet of BRD4/BET activity has not been explored in detail in cancer, but is likely to underlie at least some of the clinical activity of BET inhibitors, in particular in relation to aberrant NFκB signaling. Indeed, BRD4 interacts with the NFκB subunit, p65/RELA, when the latter is acetylated at lysine 310 [21] (and references therein). Under NFκB activation conditions, this leads to the recruitment of pTEFb and stimulates the transcription of NFκB target genes [21], in a BRD4- and CDK9-dependent fashion. RELA/BRD4 co-recruitment to NFκB target promoters is observed under a variety of NFκB stimulation conditions and cell types, and is not observed at housekeeping genes, supporting a necessity for defined promoter features for this interaction. Mapping and amino acid exchange studies have identified RELA acetyl-lysine-310 as the key residue for this interaction. Indeed, lysine substitution by an arginine residue significantly reduces BRD4 co-recruitment to an NFκB target promoter, as measured by ChIP assays [21]. Importantly, this does not alter the recruitment of either CBP/p300 or non-acetylated RELA, while acetylated RELA recruitment is lost. Taken together, this points to a critical role for acetylated RELA lysine-310 in BRD4 recruitment at NFκB response promoters. The acetylation of RELA lysine 310 is mediated by p300/CBP (Figure 2).

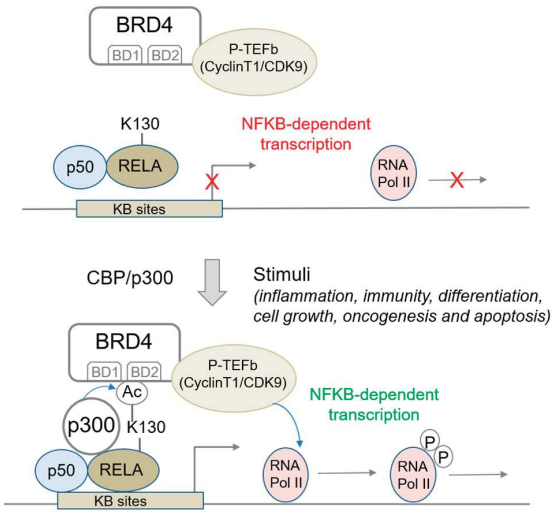

Figure 2. Schematic model for the binding of BRD4 to acetylated lysine-310 of RELA/p65 and the role of this interaction in the transcriptional activation of NFκB. Stimulus-dependent acetylation of RELA at lysine-310 by p300 induces the recruitment of BRD4 to the promoter via its bromodomains. BRD4 further activates CDK9 to phosphorylate the CTD (*C*-terminal domain) of RNA polymerase II and to facilitate the RNA pol II-mediated transcription of NFκB target genes. The p50 factor is a processed form of the REL family member p105 (NFκB1) that heterodimerizes with RELA/p65 and that is required for its transcriptional activation functions.

Of note, both bromodomains of BRD4 are necessary for the interaction with lysine-310-acetylated RELA, as evidenced by pull down assays using bromodomain deletion mutants, and in vivo immunoprecipitation assays. Moreover, loss of this interaction results in the inability of BRD4 to co-activate NFκB-dependent transcription. Structural studies have confirmed this by showing that both BD1 and BD2 bind to acetyl-lysine-310 peptide, and that this occurs through the conserved Asn140 in BD1 and Asn433 in BD2, respectively [25]. Consistent with this result, the dual bromodomain inhibitor JQ1 blocks the interaction between BRD4 and acetylated RELA, coincident with the suppression of NFκB-induced transcriptional responses [25]. Treatment with the BET inhibitor JQ1 releases RELA for ubiquitination and proteasome-mediated degradation. RELA transcript levels are not affected. In contrast, the levels of a second subunit of the NFκB signaling complex that binds RELA, p50,

are unaltered. In this regard, it is worth noting that MS417, a derivative of the triazolo-thienodiazepine compound class, also prevents BRD4 binding to acetylated NFκB, thus reducing the transcriptional activity of this factor [26].

Previous studies have shown that the RELA/BRD4 interaction is favored by the phosphorylation of RELA/p65 at serines 276 and 536, which allows recruitment of histone acetyl-transferase p300/CBP [27]. Interestingly, enhanced STAT3-dependent RELA phosphorylation has been shown to increase RELA acetylation by p300/CBP and has been implicated in constitutive NFκB activity in human and murine tumors [25,28].

Of note, the mono-methylation of RELA lysine 310 by SETD6 has been identified and shown to couple NFκB activity to that of histone methyltransferase EHMT1/GLP (Euchromatic histone-lysine *N*-methyltransferase 1) at chromatin, thereby leading to the tonic repression of NFκB signaling at target promoters [29]. RELA/p65 lysine 310 mono-methylation is blocked by activation-dependent phosphorylation at Ser311, by protein kinase C-ζ(PKC-ζ). How this impacts subsequent lysine 310 acetylation is not known in detail.

In aggregate, the above data underscore the feasibility and potential clinical interest of targeting BRD4 interactions with non-histone acetylated lysines in anti-cancer therapy. Targeting the BRD4/acetylated RELA axis should be of value in NFκB-dependent cancers, such as lymphoma, where aberrant NFκB signaling is frequent, including through genetic mechanisms [30].

3. BET Inhibition as an Anti-Cancer Therapy and Perspectives for Use in NFκB-Dependent Cancers

Numerous studies indicate that BET inhibition is an attractive therapeutic strategy in hematological and solid cancers. Single or dual agent therapy is showing promise pre-clinically [1,3,6,31,32]. Inhibitors are mostly small molecule inhibitors that are thought to mediate anti-cancer activity through the interruption of interactions between BET proteins and acetylated lysine in histones at promoters and enhancers. A number of these inhibitors are being tested in early phase clinical trials, in hematological and solid cancers, as either single agents or in combination with other treatments (Table 1; and https://clinicaltrials.gov/ for further details on BET inhibitor trials). Although published clinical data remain sparse, one BET inhibitor, OTX015, has shown efficacy in patients with refractory or relapsed hematological cancers [33,34].

Table 1. Summary of BET inhibitor clinical trials (open Dec. 2017).

Compound	Company	Indications	Phases	Completion Date	NCT Number
FT-1101	Forma Therapeutics, Inc. (Watertown, MA, USA)	Acute Myeloid Leukemia/Acute Myelogenous Leukemia/Myelodysplastic Syndrome	Phase 1	August 2018	NCT02543879
RO6870810 *	Hoffmann-La Roche (Basel, Switzerland)	Multiple Myeloma	Phase 1	15 January 2020	NCT03068351
CPI-0610	Constellation Pharmaceuticals (Cambridge, MA, USA)	Lymphoma	Phase 1	July 2018	NCT01949883
		Multiple Myeloma	Phase 1	March 2019	NCT02157636
		Acute Myeloid Leukemia/Myelodysplastic Syndrome (MDS)/ Myelodysplastic/Myeloproliferative Neoplasm, Unclassifiable/Myelofibrosis	Phase 1	January 2019	NCT02158858
		Peripheral Nerve Tumors	Phase 2	March 2020	NCT02986919
GSK525762	GSK (Brentford, UK)	Cancer	Phase 1	24 February 2020	NCT01943851
		Carcinoma, Midline	Phase 1	9 September 2019	NCT01587703
ZEN003694 **	Zenith Epigenetics (San Francisco, CA, USA)	Metastatic Castration-Resistant Prostate Cancer	Phase 1	April 2018	NCT02711956
BMS-986158	Bristol-Myers Squibb (New York, NY, USA)	Multiple Indications Cancer	Phase 1/Phase 2	17 December 2018	NCT02419417

* Alone or in combination with Daratumumab; ** in combination with Enzalutamide.

In this review, by focusing on BRD4-mediated regulation of NFκB signaling via acetylated RELA, we make a case for a second avenue of investigation for the development of therapeutic strategies utilizing BET inhibitors. Specifically, we propose that BRD4-dependent signaling via non-histone acetyl-lysine interactions will be of interest. Experimental data indicate that small molecule inhibition of the RELA-BRD4 interaction offers promise for the disruption of pathological NFκB signaling in cancer, a process which has been attributed to the inability of cancer cells to homeostatically control NFκB function [35]. Functional and chemical genomics approaches should allow progress in the identification and/or design of additional agents for pre-clinical testing in NFκB-dependent cancers such as lymphoma.

Acknowledgments: Mary B. Callanan acknowledges research support from the l'INCa 'épigénétique et cancer' program (2014–2017) and institutional support from Grenoble and Dijon University hospitals, Université Grenoble-Alpes, Université Bourgogne-Franche Comté, INSERM, and CNRS. Azadeh Hajmirza has been the recipient of doctoral funding from the Société Française d'Hématologie. Arnaud Gauthier was supported by the Auvergne-Rhone-Alpes region, under the program 'Année Recherche' (Masters 2 research training at Bart's Cancer Institute, Jude Fitzgibbon).

Author Contributions: Azadeh Hajmirza, Anouk Emadali, Arnaud Gauthier, Olivier Casasnovas, Rémy Gressin and Mary B. Callanan co-wrote the manuscript and approved the final version.

Conflicts of Interest: The authors declare no conflict of interest.

References

1. Dawson, M.A. The cancer epigenome: Concepts, challenges, and therapeutic opportunities. *Science* **2017**, *355*, 1147–1152. [CrossRef] [PubMed]
2. Basheer, F.; Huntly, B.J. BET bromodomain inhibitors in leukemia. *Exp. Hematol.* **2015**, *43*, 718–731. [CrossRef] [PubMed]
3. Shi, J.; Vakoc, C.R. The mechanisms behind the therapeutic activity of BET bromodomain inhibition. *Mol. Cell* **2014**, *54*, 728–736. [CrossRef] [PubMed]
4. Dhalluin, C.; Carlson, J.E.; Zeng, L.; He, C.; Aggarwal, A.K.; Zhou, M.M. Structure and ligand of a histone acetyltransferase bromodomain. *Nature* **1999**, *399*, 491–496. [PubMed]
5. Moriniere, J.; Rousseaux, S.; Steuerwald, U.; Soler-Lopez, M.; Curtet, S.; Vitte, A.L.; Govin, J.; Gaucher, J.; Sadoul, K.; Hart, D.J.; et al. Cooperative binding of two acetylation marks on a histone tail by a single bromodomain. *Nature* **2009**, *461*, 664–668. [CrossRef] [PubMed]
6. Filippakopoulos, P.; Knapp, S. Targeting bromodomains: Epigenetic readers of lysine acetylation. *Nat. Rev. Drug Discov.* **2014**, *13*, 337–356. [CrossRef] [PubMed]
7. Smale, S.T. Hierarchies of NF-kB target-gene regulation. *Nat. Immunol.* **2011**, *12*, 689–694. [CrossRef] [PubMed]
8. Zhou, Q.; Li, T.; Price, D.H. RNA polymerase II elongation control. *Annu. Rev. Biochem.* **2012**, *81*, 119–143. [CrossRef] [PubMed]
9. Liu, W.; Ma, Q.; Wong, K.; Li, W.; Ohgi, K.; Zhang, J.; Aggarwal, A.; Rosenfeld, M.G. Brd4 and JMJD6-associated anti-pause enhancers in regulation of transcriptional pause release. *Cell* **2013**, *155*, 1581–1595. [CrossRef] [PubMed]
10. Rahman, S.; Sowa, M.E.; Ottinger, M.; Smith, J.A.; Shi, Y.; Harper, J.W.; Howley, P.M. The Brd4 extraterminal domain confers transcription activation independent of pTEFb by recruiting multiple proteins, including NSD3. *Mol. Cell. Biol.* **2011**, *31*, 2641–2652. [CrossRef] [PubMed]
11. Loven, J.; Hoke, H.A.; Lin, C.Y.; Lau, A.; Orlando, D.A.; Vakoc, C.R.; Bradner, J.E.; Lee, T.I.; Young, R.A. Selective inhibition of tumor oncogenes by disruption of super-enhancers. *Cell* **2013**, *153*, 320–334. [CrossRef] [PubMed]
12. Bhagwat, A.S.; Roe, J.S.; Mok, B.Y.L.; Hohmann, A.F.; Shi, J.; Vakoc, C.R. BET Bromodomain Inhibition Releases the Mediator Complex from Select cis-Regulatory Elements. *Cell Rep.* **2016**, *15*, 519–530. [CrossRef] [PubMed]
13. Damm, F.; Mylonas, E.; Cosson, A.; Yoshida, K.; Della Valle, V.; Mouly, E.; Diop, M.; Scourzic, L.; Shiraishi, Y.; Chiba, K.; et al. Acquired initiating mutations in early hematopoietic cells of CLL patients. *Cancer Discov.* **2014**, *4*, 1088–1101. [CrossRef] [PubMed]

14. Pelish, H.E.; Liau, B.B.; Nitulescu, I.I.; Tangpeerachaikul, A.; Poss, Z.C.; Da Silva, D.H.; Caruso, B.T.; Arefolov, A.; Fadeyi, O.; Christie, A.L.; et al. Mediator kinase inhibition further activates super-enhancer-associated genes in AML. *Nature* **2015**, *526*, 273–276. [CrossRef] [PubMed]
15. Chapuy, B.; McKeown, M.R.; Lin, C.Y.; Monti, S.; Roemer, M.G.; Qi, J.; Rahl, P.B.; Sun, H.H.; Yeda, K.T.; Doench, J.G.; et al. Discovery and characterization of super-enhancer-associated dependencies in diffuse large B cell lymphoma. *Cancer Cell* **2013**, *24*, 777–790. [CrossRef] [PubMed]
16. Delmore, J.E.; Issa, G.C.; Lemieux, M.E.; Rahl, P.B.; Shi, J.; Jacobs, H.M.; Kastritis, E.; Gilpatrick, T.; Paranal, R.M.; Qi, J.; et al. BET bromodomain inhibition as a therapeutic strategy to target c-Myc. *Cell* **2011**, *146*, 904–917. [CrossRef] [PubMed]
17. Groschel, S.; Sanders, M.A.; Hoogenboezem, R.; de Wit, E.; Bouwman, B.A.M.; Erpelinck, C.; van der Velden, V.H.J.; Havermans, M.; Avellino, R.; van Lom, K.; et al. A single oncogenic enhancer rearrangement causes concomitant EVI1 and GATA2 deregulation in leukemia. *Cell* **2014**, *157*, 369–381. [CrossRef] [PubMed]
18. Glodzik, D.; Morganella, S.; Davies, H.; Simpson, P.T.; Li, Y.; Zou, X.; Diez-Perez, J.; Staaf, J.; Alexandrov, L.B.; Smid, M.; et al. A somatic-mutational process recurrently duplicates germline susceptibility loci and tissue-specific super-enhancers in breast cancers. *Nat. Genet.* **2017**, *49*, 341–348. [CrossRef] [PubMed]
19. Roe, J.S.; Mercan, F.; Rivera, K.; Pappin, D.J.; Vakoc, C.R. BET Bromodomain Inhibition Suppresses the Function of Hematopoietic Transcription Factors in Acute Myeloid Leukemia. *Mol. Cell* **2015**, *58*, 1028–1039. [CrossRef] [PubMed]
20. Brown, J.D.; Lin, C.Y.; Duan, Q.; Griffin, G.; Federation, A.; Paranal, R.M.; Bair, S.; Newton, G.; Lichtman, A.; Kung, A.; et al. NF-κB directs dynamic super enhancer formation in inflammation and atherogenesis. *Mol. Cell* **2014**, *56*, 219–231. [CrossRef] [PubMed]
21. Huang, B.; Yang, X.D.; Zhou, M.M.; Ozato, K.; Chen, L.F. Brd4 coactivates transcriptional activation of NF-kappaB via specific binding to acetylated RelA. *Mol. Cell. Biol.* **2009**, *29*, 1375–1387. [CrossRef] [PubMed]
22. Kaikkonen, M.U.; Spann, N.J.; Heinz, S.; Romanoski, C.E.; Allison, K.A.; Stender, J.D.; Chun, H.B.; Tough, D.F.; Prinjha, R.K.; Benner, C.; et al. Remodeling of the enhancer landscape during macrophage activation is coupled to enhancer transcription. *Mol. Cell* **2013**, *51*, 310–325. [CrossRef] [PubMed]
23. Hah, N.; Benner, C.; Chong, L.W.; Yu, R.T.; Downes, M.; Evans, R.M. Inflammation-sensitive super enhancers form domains of coordinately regulated enhancer RNAs. *Proc. Natl. Acad. Sci. USA* **2015**, *112*, E297–E302. [CrossRef] [PubMed]
24. Nicodeme, E.; Jeffrey, K.L.; Schaefer, U.; Beinke, S.; Dewell, S.; Chung, C.W.; Chandwani, R.; Marazzi, I.; Wilson, P.; Coste, H.; et al. Suppression of inflammation by a synthetic histone mimic. *Nature.* **2010**, *468*, 1119–1123. [CrossRef] [PubMed]
25. Zou, Z.; Huang, B.; Wu, X.; Zhang, H.; Qi, J.; Bradner, J.; Nair, S.; Chen, L.F. Brd4 maintains constitutively active NF-κB in cancer cells by binding to acetylated RelA. *Oncogene* **2014**, *33*, 2395–2404. [CrossRef] [PubMed]
26. Zhang, G.; Liu, R.; Zhong, Y.; Plotnikov, A.N.; Zhang, W.; Zeng, L.; Rusinova, E.; Gerona-Nevarro, G.; Moshkina, N.; Joshua, J.; et al. Down-regulation of NFκB transcriptional activity in HIV-associated kidney disease by BRD4 inhibition. *J. Biol. Chem.* **2012**, *287*, 28840–28851. [CrossRef] [PubMed]
27. Brasier, A.R.; Tian, B.; Jamaluddin, M.; Kalita, M.K.; Garofalo, R.P.; Lu, M. RelA Ser276 phosphorylation-coupled Lys310 acetylation controls transcriptional elongation of inflammatory cytokines in respiratory syncytial virus infection. *J. Virol.* **2011**, *85*, 11752–11769. [CrossRef] [PubMed]
28. Lee, H.; Herrmann, A.; Deng, J.H.; Kujawski, M.; Niu, G.; Li, Z.; Forman, S.; Jove, R.; Pardoll, D.M.; Yu, H. Persistently activated Stat3 maintains constitutive NF-kappaB activity in tumors. *Cancer Cell* **2009**, *15*, 283–293. [CrossRef] [PubMed]
29. Levy, D.; Kuo, A.J.; Chang, Y.; Schaefer, U.; Kitson, C.; Cheung, P.; Espejo, A.; Zee, B.M.; Liu, C.L.; Tangsombatvisit, S.; et al. Lysine methylation of the NF-kB subunit RelA by SETD6 couples activity of the histone methyltransferase GLP at chromatin to tonic repression of NF-kB signaling. *Nat. Immunol.* **2011**, *12*, 29–36. [CrossRef] [PubMed]
30. Nagel, D.; Vincendeau, M.; Eitelhuber, A.C.; Krappmann, D. Mechanisms and consequences of constitutive NF-κB activation in B-cell lymphoid malignancies. *Oncogene* **2014**, *33*, 5655–5665. [CrossRef] [PubMed]

31. Emadali, A.; Rousseaux, S.; Bruder-Costa, J.; Rome, C.; Duley, S.; Hamaidia, S.; Betton, P.; Debernardi, A.; Leroux, D.; Bernay, B.; et al. Identification of a novel BET bromodomain inhibitor-sensitive, gene regulatory circuit that controls Rituximab response and tumour growth in aggressive lymphoid cancers. *EMBO Mol. Med.* **2013**, *5*, 1180–1195. [CrossRef] [PubMed]
32. Emadali, A.; Hoghoughi, N.; Duley, S.; Hajmirza, A.; Verhoeyen, E.; Cosset, F.L.; Bertrand, P.; Roumier, C.; Roggy, A.; Suchaud-Martin, C.; et al. Haploinsufficiency for NR3C1, the gene encoding the glucocorticoid receptor, in blastic plasmacytoid dendritic cell neoplasms. *Blood* **2016**, *127*, 3040–3053. [CrossRef]
33. Berthon, C.; Raffoux, E.; Thomas, X.; Vey, N.; Gomez-Roca, C.; Yee, K.; Taussig, D.C.; Rezai, K.; Roumier, C.; Herait, P.; et al. Bromodomain inhibitor OTX015 in patients with acute leukaemia: A dose-escalation, phase 1 study. *Lancet Haematol.* **2016**, *3*, e186–e195. [CrossRef]
34. Amorim, S.; Stathis, A.; Gleeson, M.; Iyengar, S.; Magarotto, V.; Leleu, X.; Morschhauser, F.; Karlin, L.; Broussais, F.; Rezai, K.; et al. Bromodomain inhibitor OTX015 in patients with lymphoma or multiple myeloma: A dose-escalation, open-label, pharmacokinetic, phase 1 study. *Lancet Haematol.* **2016**, *3*, e196–e204. [CrossRef]
35. Baltimore, D. NF-κB is 25. *Nat. Immunol.* **2011**, *12*, 683–685. [CrossRef] [PubMed]

Regular Article

blood

MYELOID NEOPLASIA

Haploinsufficiency for *NR3C1*, the gene encoding the glucocorticoid receptor, in blastic plasmacytoid dendritic cell neoplasms

Anouk Emadali,[1,*] Neda Hoghoughi,[1,*] Samuel Duley,[1,*] Azadeh Hajmirza,[1] Els Verhoeyen,[2-4] Francois-Loic Cosset,[2,3] Philippe Bertrand,[5] Christophe Roumier,[6] Anne Roggy,[7] Céline Suchaud-Martin,[8] Martine Chauvet,[1,8] Sarah Bertrand,[1] Sieme Hamaidia,[1,8] Sophie Rousseaux,[1] Véronique Josserand,[1] Julie Charles,[1,9] Isabelle Templier,[9] Takahiro Maeda,[10] Juliana Bruder-Costa,[1,11] Laurence Chaperot,[1,11] Joel Plumas,[1,11] Marie-Christine Jacob,[1,12] Thierry Bonnefoix,[1] Sophie Park,[13] Remy Gressin,[1,13] Cornelis P. Tensen,[14] Cristina Mecucci,[15] Elizabeth Macintyre,[16] Dominique Leroux,[1,8] Elisabeth Brambilla,[1] Florence Nguyen-Khac,[17] Isabelle Luquet,[18] Dominique Penther,[5] Christian Bastard,[5] Fabrice Jardin,[5] Christine Lefebvre,[1,8] Francine Garnache,[7,†] and Mary B. Callanan[1,8,†]

[1]INSERM U1209, CNRS UMR 5309, Faculté de Médecine, Université Grenoble Alpes, Institut Albert Bonniot, Grenoble, France; [2]International Center for Infectiology Research, Université de Lyon 1, Lyon, France; [3]INSERM U1111, CNRS UMR 5308, Ecole Normale Supérieure de Lyon, Lyon, France; [4]INSERM U1065, Centre Méditerranéen de Médecine Moléculaire, Nice, France; [5]INSERM U918, Département d'Hématologie, Université de Rouen, Centre Henri Becquerel, Rouen, France; [6]Institut d'Hématologie, Centre Hospitalier Régional Universitaire de Lille, Lille, France; [7]INSERM U645, Etablissement français du sang, Université de Franche-Comté, Besançon, France; [8]Labortoire de Génétique Onco-Hématologique and [9]Departement de Dermatologie, Centre Hospitalier et Universitaire de Grenoble-Alpes, Grenoble, France; [10]Department of Community Medicine, Nagasaki University Graduate School of Biomedical Sciences, Nagasaki, Japan; [11]Etablissement français du sang Rhône-Alpes, Laboratoire de recherche et développement, Grenoble, France; [12]Laboratoire d'Immunologie and [13]Departement d'Hématologie Clinique, Centre Hospitalier et Universitaire de Grenoble-Alpes, Grenoble, France; [14]Department of Dermatology, Leiden University Medical Center, Leiden, The Netherlands; [15]Department of Medicine, Perugia University, Perugia, Italy; [16]Laboratory of Oncohematology, Assistance Publique–Hôpitaux de Paris, Hôpital Necker Enfants-Malades, University Paris Descartes Sorbonne Cité, Institut Necker-Enfants Malades, INSERM U1151, Paris, France; [17]Unité Fonctionnelle de Cytogénétique Hématologique, Groupe Hospitalier Pitié-Salpêtrière, Paris, France; and [18]Laboratoire d'Hématologie, Pôle de biologie, Centre Hospitalier et Universitaire de Toulouse, Toulouse, France

Key Points

- *NR3C1* haploinsufficiency is found in patients with a plasmacytoid dendritic cell neoplasm characterized by very poor clinical outcome.
- Overexpression of *lincRNA-3q* is a consistent feature of malignant cells in these patients and can be abrogated by BET protein inhibition.

Blastic plasmacytoid dendritic cell neoplasm (BPDCN) is a rare and highly aggressive leukemia for which knowledge on disease mechanisms and effective therapies are currently lacking. Only a handful of recurring genetic mutations have been identified and none is specific to BPDCN. In this study, through molecular cloning in an index case that presented a balanced t(3;5)(q21;q31) and molecular cytogenetic analyses in a further 46 cases, we identify monoallelic deletion of *NR3C1* (5q31), encoding the glucocorticoid receptor (GCR), in 13 of 47 (28%) BPDCN patients. Targeted deep sequencing in 36 BPDCN cases, including 10 with *NR3C1* deletion, did not reveal *NR3C1* point mutations or indels. Haploinsufficiency for *NR3C1* defined a subset of BPDCN with lowered GCR expression and extremely poor overall survival ($P = .0006$). Consistent with a role for GCR in tumor suppression, functional analyses coupled with gene expression profiling identified corticoresistance and loss-of-EZH2 function as major downstream consequences of *NR3C1* deletion in BPDCN. Subsequently, more detailed analyses of the t(3;5)(q21;q31) revealed fusion of *NR3C1* to a long noncoding RNA (lncRNA) gene (*lincRNA-3q*) that encodes a novel, nuclear, noncoding RNA involved in the regulation of leukemia stem cell programs and G1/S transition, via E2F. Overexpression of *lincRNA-3q* was a consistent feature of malignant cells and could be abrogated by bromodomain and extraterminal domain (BET) protein inhibition. Taken together, this work points to *NR3C1* as a haploinsufficient tumor suppressor in a subset of BPDCN and identifies BET inhibition, acting at least partially via lncRNA blockade, as a novel treatment option in BPDCN. (*Blood*. 2016;127(24):3040-3053)

Introduction

Blastic plasmacytoid dendritic cell neoplasm (BPDCN) is a rare and clinically aggressive disorder that shows dismal prognosis whatever the treatment.[1] Median overall survival is less than 2 years, even with high-dose chemotherapy, although longer-term, albeit short-lived, remissions have been observed in allotransplanted patients.[2-4]

BPDCN derives from malignant transformation of plasmacytoid dendritic cell (pDC) precursors[5-7] and is currently classified with acute myeloid leukemia (AML) and related precursor neoplasms in the 2008 World Health Organization classification of hematologic malignancies.[1] Tumor cells infiltrate skin, bone marrow, peripheral blood, and

Submitted September 18, 2015; accepted March 25, 2016. Prepublished online as *Blood* First Edition paper, April 8, 2016; DOI 10.1182/blood-2015-09-671040.

*A.E., N.H., and S.D. contributed equally to this study.

†F.G. and M.B.C. are co-senior authors.

The online version of this article contains a data supplement.

The publication costs of this article were defrayed in part by page charge payment. Therefore, and solely to indicate this fact, this article is hereby marked "advertisement" in accordance with 18 USC section 1734.

lymph nodes and show the characteristic immunophenotypic profile $CD4^+$ $CD56^+$ HLA-DR^{hi} $CD123^+$ lineage $(Lin)^-$, although atypical profiles are reported.[8,9]

BPDCN presents heterogeneous genetic features characterized by chromosomal losses and deletions[10,11] and a mutational landscape that overlaps with other hematologic malignancies without evidence of unique, disease-specific, driver genetic lesions.[12-14] As in myeloid and lymphoid malignancies, mutations in key epigenetic modifier-encoding genes, such as *TET2*, *ASXL1*, and *EZH2*, have been described in a proportion of BPDCN cases, thus supporting a role for deregulation of epigenetic signaling in disease pathogenesis.[12-14] Gene expression profiling (GEP), although performed in relatively few cases, has shown a distinctive transcriptional program in BPDCN characterized by predominant expression of genes that are typical of the pDC lineage[15,16] and evidence of aberrant activation of the NF-κB pathway.[16]

Deletion of chromosome 5q, commonly seen in myelodysplastic syndrome (MDS) and AML, is frequent in BPDCN.[10,11] Deletion 5q (outside of the 5q− syndrome) is associated with increased risk of leukemic transformation in MDS[17] and with very poor prognosis in AML.[18,19] This is attributed to haploinsufficiency for critical 5q gene(s), which in cooperation with additional signaling networks, drives malignant transformation and clonal evolution in these disorders.[20-22] In keeping with this, treatments that are effective in 5q-deleted myeloid malignancies have been shown to directly target critical haploinsufficient 5q genes and their signaling networks.[20]

Based on the latter findings,[20-22] we hypothesized that similar 5q gene haploinsufficiency mechanisms are likely to operate in BPDCN and that identification of the relevant 5q target genes might lead to new insight into disease biology and therapy. In this setting, we have used molecular cloning coupled with molecular cytogenetics and next-generation sequencing to characterize 5q alterations in BPDCN. Our work points to *NR3C1*, encoding the glucocorticoid receptor (GCR), as a haploinsufficient tumor suppressor in this disorder. *NR3C1* loss defines a subset of highly aggressive BPDCN characterized by a loss-of-EZH2 function gene expression signature. In addition, we extend previous observations that identified a potential role for epigenetic modifier gene mutations in BPDCN pathogenesis by providing the first evidence of a key role for nuclear long noncoding RNA (lncRNA) deregulation in the pathogenesis of this disorder.

Methods

BPDCN patients and cell lines

BPDCN patients investigated in this study were recruited retrospectively between 2008 and 2014 through 2 French study groups, the Groupe Francophone de Cytogénétique Hématologique and the French BPDCN network (identified as cohorts A and B, respectively, in supplemental Table 1, available on the *Blood* Web site). After centralized review of clinical and biological criteria for BPDCN diagnosis,[8] and on the basis of available cytogenetic/molecular cytogenetic data, 47 patients (median age, 66 years; range, 7-82 years) were enrolled in the current study (supplemental Tables 1-4). All patient data were obtained at diagnosis. All patients provided written informed consent. The study was approved by the institutional review boards of the participating centers. For 2 patients, derived cell lines that displayed the same cytogenetic characteristics as the original patient blasts were used for analyses (unique patient number 1 [UPN 1]: GEN2.2 and UPN 2: CAL-1).[23,24] BPDCN cell lines were cultured in RPMI 1640 medium supplemented with 10% fetal calf serum.[23,24] Murine stromal cell support was provided for GEN2.2 cells, as previously described.[23]

Cytogenetics, FISH, molecular analyses, and aCGH

R-banded karyotyping, fluorescence in situ hybridization (FISH) analyses, and array comparative genomic hybridization (aCGH) were performed by standard methods, as previously described.[10,25] All cytogenetic and aCGH data were centrally reviewed by the Groupe Francophone de Cytogénétique Hématologique and the French BPDCN network. Karyotypes were described according to the International System for Human Cytogenetic Nomenclature. Bacterial artificial chromosome and fosmid probes for FISH mapping are listed in supplemental Table 5. Additional molecular analyses (see below) used reagents given in supplemental Tables 6-12.

NR3C1, *EZH2*, and *ASXL1* mutation screening

For mutation screening of the coding regions of *NR3C1*, a custom, targeted next-generation sequencing panel covering all 9 exons of the *NR3C1* gene (total panel size, 3.3 kb; 31 amplicons) was designed using the Ampliseq Designer software (Thermo Fisher Scientific). Ion Ampliseq DNA libraries were prepared using 10 ng of amplified genomic DNA (for a list of the cases studied and the tissue source of DNA, see supplemental Table 2). Libraries were submitted to emulsion polymerase chain reaction (PCR) with the Ion PGM Hi-Q OneTouch 2 template kit v2. The generated ion sphere particles were enriched with the Ion OneTouch Enrichment System, loaded, and sequenced with the Ion PGM Hi-Q Sequencing 200 Kit on Ion 316 v2 chips (Thermo Fisher Scientific). Torrent Suite version 5.0 software (Thermo Fisher Scientific) was used to perform primary analysis, including signal processing, base calling, sequence alignment to the reference genome (hg19), and generation of binary alignment/map files. Binary alignment/map files were used by Torrent Suite Variant Caller to detect point mutations and short indels using the PGM Somatic Low Stringency profile. Variant Call Format files generated by Variant Caller were annotated using Variant Effect Predictor.[26] Samples were considered of sufficient quality when >90% of targeted bases were read with a base call accuracy of at least Q20 (success rate, 100%). The average coverage was 1800× (range, 400-4000×). Variants present in single nucleotide polymorphism databases and absent in COSMIC (version 64) were discarded, as were variants with a predictive SIFT (sorting intolerant from tolerant) score >0.05.[26]

EZH2 (all coding exons) and *ASXL1* (exon 12) mutation screening was performed in a subset of BPDCN patients (those undergoing GEP; supplemental Table 2) by using primers and PCR cycling conditions, as previously described.[27,28] Purified PCR products were directly sequenced in both directions, using BigDye Terminator Mix (Applied Biosystems), on the Applied Biosystems 3130xl Genetic Analyzer. Data were analyzed with the SeqScanner software version 1.0 (Applied Biosystems).

LD-PCR and fusion transcript cloning

Long-distance PCR (LD-PCR) cloning of the t(3;5)(q21;q31) genomic breakpoint was performed using the Expand Long Template PCR system (Sigma) and LD-PCR primers, TA cloning of PCR products, and sequencing (supplemental Table 6). For RNA analysis, total RNA was prepared by TRIzol reagent, according to the manufacturer's instructions. Rapid amplification of complementary DNA (cDNA) ends (RACE)-PCR (5′ and 3′) was used to clone the t(3;5)-encoded fusion transcript and was performed using the SMARTer RACE cDNA Amplification Kit (Clontech), according to the manufacturer's instructions. RACE primers are listed in supplemental Table 7. For functional studies, GCR fusion protein (GCR-FP) cDNA was cloned into pcDNA3.1 and pEGFP-C1 and subcloned as a green fluorescent protein (GFP)-tagged isoform into a modified pHIV-SFFV-mRFP-WPRE lentiviral vector, using primers described in supplemental Table 8. CAL-1 cell lines stably expressing GFP alone or GFP-tagged GCR-FP were obtained by lentiviral transduction and cell sorting (BD FACSAria). Successful transduction was confirmed by flow cytometry and western blotting.

RT-qPCR, Northern blotting, and GEP

Total RNA was obtained from whole cells or from subcellular fractions (nuclear and cytoplasmic), reverse transcribed (RT) by using the SuperScript III First-Strand Synthesis SuperMix (Invitrogen), and subjected to quantitative PCR (qPCR) by using SYBR Green PCR Master Mix (Applied Biosystems) and

the primers shown in supplemental Table 7, according to the manufacturers' instructions. The *ABL* gene was used as a control for normalization of gene expression data. qPCR was performed on an MX3000P machine (Stratagene). Northern blotting used *NR3C1* cDNA probe (see supplemental Methods and supplemental Table 9 for details). Affymetrix GEP was performed as described previously by using total RNA and Affymetrix U133 2.0 chips.[29] GEP data normalization and bioinformatics analysis were performed as described previously (see supplemental Methods for details).[29]

IHC and western blotting

For GCR expression analysis in formalin-fixed paraffin-embedded tissue, sections of 3-μm thickness were stained with an anti-human polyclonal GCR antibody (SC-1003; Santa Cruz Biotechnology; polyclonal E20), at an optimized dilution of 1:800. Immunohistochemistry (IHC) was performed on a Benchmark XT autostainer (Ventana Medical Systems) using standard antigen retrieval (1 hour at 98°C) in Cell Conditioning Solution (CC1; Ventana Medical Systems). Primary antibody was incubated for 1 hour at room temperature, and the signal was visualized by diaminobenzidine with the OptiView DAB IHC Detection Kit (Ventana Medical Systems). Sections were counterstained with hematoxylin. The H-Score method was used for evaluation of the immunostaining by multiplying the intensity of the staining (0, no staining; 1, weak; 2, moderate; and 3, strong staining) by the percentage of the tumor stained. The minimum score was 0 and the maximum was 300.

For western blotting, whole cell lysates, obtained by sonication of cell pellets in Laemmli buffer, were resolved by sodium dodecyl sulfate–polyacrylamide gel electrophoresis and transferred onto nitrocellulose membranes for blotting with anti-N-terminal GCR (polyclonal E-20), anti-GFP (clone B2; Santa Cruz Biotechnology), anti-H3K27me3 (Millipore), anti-histone H3 (Upstate), anti-E2F1 (clone KH95; Santa Cruz Biotechnology), and anti-ACTIN (Sigma) antibodies. After treatment with blocking solution (1× phosphate-buffered saline, 8% skimmed milk, and 0.1% Tween 20), membranes were incubated with primary antibody (anti-GCR [0.4 mg/mL] and anti-H3K27me3, anti-histone H3, and anti-ACTIN [0.5 mg/mL] in phosphate-buffered saline, 3% skimmed milk, and 0.1% Tween 20), washed, and incubated with anti-rabbit or anti-mouse immunoglobulin G–horseradish peroxidase (Thermo Fisher Scientific) before incubation in enhanced chemiluminescent SuperSignal West Pico Chemiluminescent Substrate (Thermo Fisher Scientific). Images were captured using autoradiography films.

Gene silencing

Nontargeting (control; Ctrl), GCR-targeting, and lincRNA-3q-targeting short hairpin RNA (shRNA) sequences were designed using the DSIR (designer of small interfering RNA [siRNA]) algorithm (http://biodev.cea.fr/DSIR/DSIR.html).[30] Hairpin sequences are provided in supplemental Table 10. Short hairpin sequences were cloned into the pLKO-1 lentiviral vector (Addgene) and packaged, as described previously.[31] Cell lines stably expressing shCtrl, shGCR, and shlincRNA-3q were established under puromycin selection.

Glucocorticoid response element and E2F reporter assays and RNA interference

Transient transfection assays using the glucocorticoid response element luciferase reporter plasmid (gift from J. Cidlowski, National Institute of Environmental Health Sciences, National Institutes of Health, Durham, NC) were performed in COS7 cells using Lipofectamine (Invitrogen), according to the manufacturer's instructions. Transient transfection assays with the E2F reporter system were performed in H1299 cells using X-tremeGENE (Roche) following the manufacturer's instructions. Luciferase activity was measured using the Dual-Luciferase Reporter Assay System (Promega). siRNAs were ordered from Eurogentec (supplemental Table 10) and transfected using Lipofectamine RNAiMAX (Invitrogen) according to the manufacturer's instructions.

Evaluation of drug sensitivity

For drug sensitivity testing, 5×10^5 cells per milliliter were treated for the desired time and drug dose (dexamethasone at 100 nM or 10 μM, etoposide at 10 μM, and JQ1 at 1 μM). Dexamethasone was provided by the pharmacy at Grenoble University Hospital. Etoposide was purchased from Sigma. JQ1 was synthesized, as described previously.[29] Cell viability was evaluated by AnnexinV/propidium iodide (Beckman Coulter) or propidium iodide staining and flow cytometry analysis (BD LSR II). Specific cell death was calculated as (% drug-induced cell death − % control cell death) ÷ (100 − % control cell death) × 100, as described previously.[32]

ChIP

Chromatin immunoprecipitation (ChIP) experiments were performed as described by Fournier et al[25] (native chromatin) or using the Magna ChIP kit (Millipore; cross-linked chromatin), following the manufacturer's instructions. Briefly, all ChIP assays were performed in triplicate in at least 2 independent chromatin preparations. For qPCR analyses of immunoprecipitated chromatin fractions at sequences of interest, a SYBR Green PCR Kit (Applied Biosystems) was used with primer pairs, as listed in supplemental Table 11. The qPCR data obtained on immunoprecipitated fractions were normalized to input chromatin ($\%\ \text{Input} = 2^{\Delta Ct} = 2^{[Ct(\text{Immunoprecipitation}) - Ct(\text{Input})]}$). Background precipitation was evaluated with a mock immunoprecipitation.

Clonogenicity and xenotransplantation assays

Clonogenic cell frequencies were estimated by a method[33] checking that the limiting dilution data do not include false-negative outcomes and conform to the single-hit Poisson model. Statistical differences of clonogenic cell frequency estimates between assays were analyzed by a likelihood ratio test developed for limiting dilution assays.[34] Animal studies are described in supplemental Methods.

Statistics

Excel 2010 (Microsoft), JMP 10.0.0 (SAS Institute), Stata/IC 10.1 (StataCorp), and GraphPad (Prism) software programs were used for graphical representations and to perform statistical analysis across all experiments. Survival curves were built according to the Kaplan-Meier method. Comparison of Kaplan-Meier survival estimates was performed using the log-rank test. Univariate and multivariate survival analyses were performed using Cox proportional hazards regression to identify statistically significant predictors of overall survival and to obtain hazard ratio estimates as well as corresponding 95% confidence intervals. Multivariate models were constructed by including all variables with $P < .2$ in univariate analysis. The Wald test was used to assess the significance of variables in models. The Wilcoxon nonparametric method or the 2-sided Student *t* test were used for statistical analysis, as indicated. Histograms represent the average for each group, and error bars represent standard deviation or standard error on the mean, as indicated.

Results

5q Anomalies in BPDCN confer adverse clinical outcome

To uncover 5q-linked disease mechanisms in BPDCN, we screened 47 BPDCN patients at diagnosis for the presence of 5q alterations/chromosome 5 loss, by conventional metaphase karyotyping (39/47 cases), coupled with aCGH (25/47 cases), and/or locus-specific FISH (23/47 cases) when material was available (supplemental Tables 1 and 2; Figure 1). Overall, 5q alterations, including a single case of balanced 5q translocation [UPN 1; t(3;5)(q21;q31); supplemental Figure 1A] and 1 case with chromosome 5 loss, were observed in 17 of 47 patients (36%) (Figure 1A). In agreement with our previous findings,[10,11] a majority of 5q abnormalities occurred in the context of complex karyotypes, in either founder clones (13 cases) or subclones at diagnosis (4 cases) (supplemental Table 2). Consistent with a role in leukemia initiation and/or clonal evolution, and as seen in other myeloid cancers,

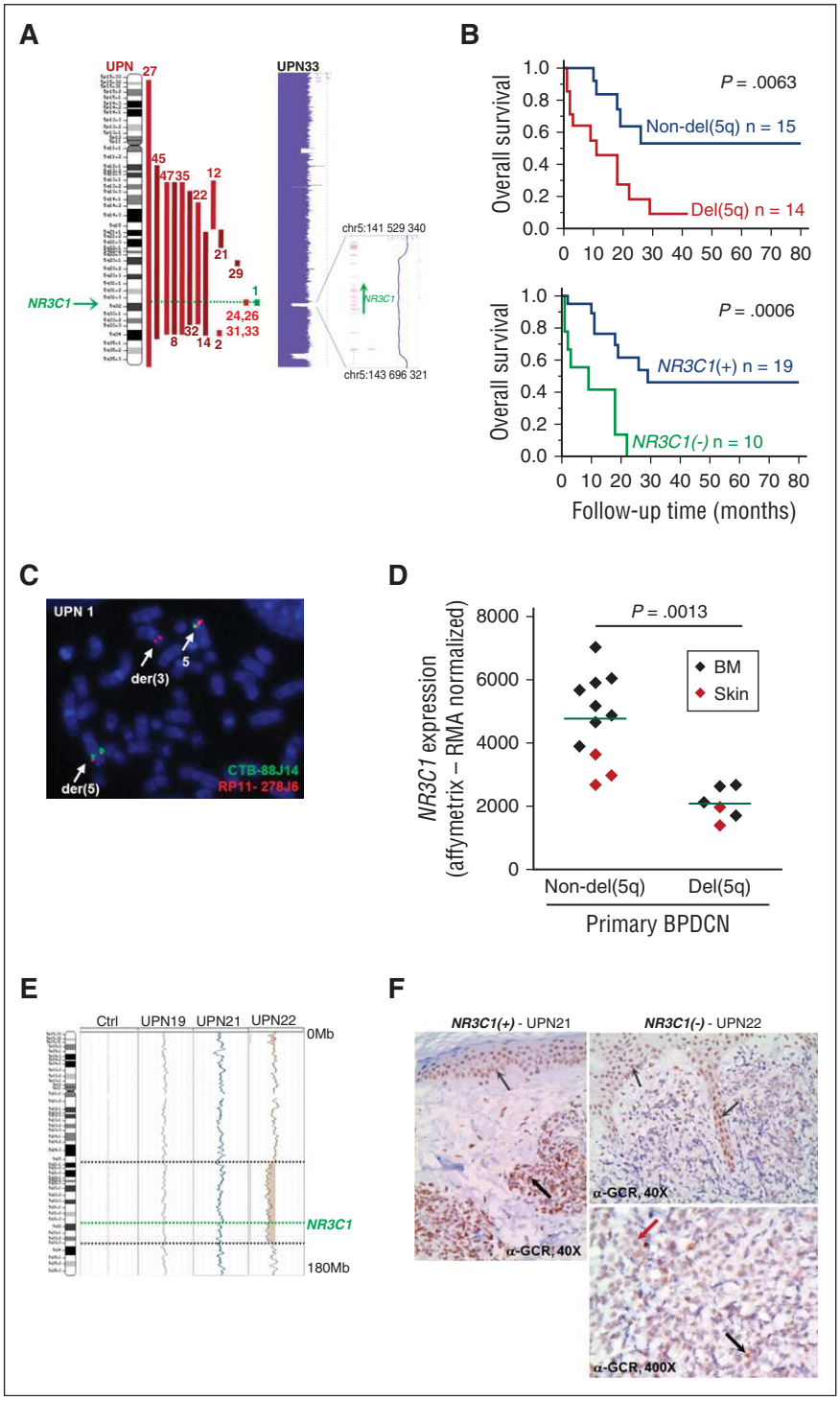

Figure 1. Targeting of the *NR3C1* gene by 5q deletion/translocation in BPDCN. (A) Schematic representation of 5q alterations in BPDCN patients (n = 17/47), as indicated (left). aCGH image of case UPN 33 showing focal deletion of the *NR3C1* gene (right). (B) Kaplan-Meier cumulative survival curves in BPDCN according to 5q alteration status (for simplicity, this is labeled del(5q) [UPNs 1, 2, 8, 12, 14, 21, 22, 24, 26, 27, 29, 31, 35, and 45] and non-del(5q) [UPNs 3, 9, 10, 16-19, 25, 27, 36, 37, and 40-42]; upper) and to *NR3C1* deletion status (UPNs 1, 8, 14, 22, 24, 26, 27, 31, 35, and 45) (lower), determined by FISH or aCGH; *ΔNR3C1*). *P* values were determined by log-rank test. (C) FISH analysis of the t(3;5)(q21;q31) in the BPDCN cell line GEN2.2 (UPN 1) with chromosome 5q probes CTB-88J14 (green) and RP11-278J6 (red) (supplemental Table 2). Note a split signal for RP11-278J6 (*NR3C1*) on the der(3) and der(5) chromosomes. (D) Affymetrix-derived *NR3C1* expression in BPDCN patients presenting del(5q) targeting *NR3C1* or not. *P* value was determined by Wilcoxon test. (E) aCGH image showing 5q/*NR3C1* deletion in DNA from a skin biopsy sample with leukemic infiltrate (UPN 22) compared with control DNA (Ctrl), and analysis in 2 BPDCN cases without 5q/*NR3C1* deletion (UPNs 19 and 21). (F) Overview of immunostaining (diaminobenzidine and hematoxylin) of GCR on BPDCN dermal localization in a del(5q) case: *NR3C1*(+) (left) and a del(5q)/*NR3C1* case: *NR3C1*(−) (upper right). Epidermal squamous cells showing positive nuclear staining are marked with thin gray arrows; leukemia infiltrate cells are marked with thick black arrows. A higher magnification of the clonal infiltrate in dermis of the same case as the upper right image shows mainly negative tumor cells (red arrow) and some positive cells (thick black arrow) (lower right). BM, bone marrow.

the presence of 5q anomalies in BPDCN was associated with very poor prognosis (*P* = .0063) (Figure 1B, top).

Targeting of *NR3C1* by 5q anomalies in BPDCN

As an entry point to identification of pathogenically relevant 5q genes in BPDCN, we next focused our attention on molecular cytogenetic characterization of the balanced t(3;5)(q21;q31) identified in UPN 1 (supplemental Table 2; supplemental Figure 1A).[11] Involvement of chromosomal arm 3q was of added interest because 3q aberrations are known to confer extremely poor prognosis, at least in AML and MDS.[17-19,35] Remarkably, FISH mapping of the t(3;5)(q21;q31) in UPN 1 metaphases identified the *NR3C1* gene, encoding the GCR, a ligand-dependent transcription factor of the nuclear hormone receptor family,[36] as the 5q target gene. Subsequently, aCGH and/or FISH analysis with an *NR3C1*-specific probe in our cohort of BPDCN showed *NR3C1* deletion to occur in 13 of 17 5q-rearranged cases (76%), of which 4 occurred in subclones detected at diagnosis (Figure 1A; supplemental Tables 1 and 2). Strikingly, 1 case with normal cytogenetics (UPN 33) presented a focal, morphologically

cryptic *NR3C1* deletion (chromosome 5:141,529,340 to 143,696,321), thus defining a minimally deleted 5q region in our BPDCN patient series (Figure 1A, right). It is of note that focal deletions of *NR3C1* have previously been implicated in B-cell acute lymphoblastic leukemia (B-ALL),[37,38] but not in myeloid malignancies. No further *NR3C1* translocations were identified. Targeted deep sequencing in 36 cases, including 10 of the 13 cases with *NR3C1* translocation/deletion (UPNs 1, 8, 14, 22, 24, 26, 27, 31, 32, 33), did not detect *NR3C1* point mutations or indels (see supplemental Table 12 for *NR3C1* amplicon primers). This finding suggested that haploinsufficiency for *NR3C1* is a pathogenically relevant event in BPDCN with 5q/*NR3C1* alteration. In keeping with this, GEP in bone marrow and skin biopsy tissue from cases with *NR3C1* deletion showed lower *NR3C1* expression in a subset of *NR3C1*-deleted BPDCN cases compared with nondeleted cases (Figure 1D).

We next examined GCR protein expression levels according to *NR3C1* deletion status in leukemia-infiltrated skin biopsy tissue from 2 BPDCN cases, 1 with *NR3C1* deletion (UPN 22) and 1 without (UPN 21) (Figure 1E-F). Material was not available for GCR protein expression analysis in any other cases. Quite strikingly, IHC with the anti-GCR antibody (clone A20) revealed markedly diminished GCR protein levels in the *NR3C1*-deleted case (UPN 22) compared with the nondeleted case (UPN 21; H-Score, 300) (Figure 1F). In the latter, GCR protein expression was high and localized to the nucleus of the leukemia cells, indicating engagement of GCR signaling. BPDCN cells in the *NR3C1* haploinsufficient case appeared mostly negative for GCR immunostaining (H-Score, 0), although we suspect that IHC may not be sufficiently sensitive to detect very low level GCR expression. In the few GCR-positive leukemic cells seen in the *NR3C1*-deleted case (UPN 22), GCR expression was nuclear, indicative of active, nuclear GCR signaling.

Taken together, these results show that *NR3C1* deletion impacts *NR3C1* expression at the RNA and protein levels in BPDCN. Nuclear GCR signaling is engaged in BPDCN and appears attenuated in *NR3C1*-deleted BPDCN.

Haploinsufficiency for *NR3C1* defines a very high risk subset of BPDCN

We next wished to determine the clinical impact of monoallelic *NR3C1* deletion in BPDCN. We first analyzed the impact on overall survival of variables, including 5q/*NR3C1* deletion, in univariate and multivariate Cox proportional hazards regression models (supplemental Table 3). By univariate analysis, patient age (>66 years) ($P = .03$), lack of allogeneic bone marrow transplant (allo-BMT) ($P = .008$), presence of del(5q) ($P = .013$), and *NR3C1* gene alterations ($P = .004$) were significant hazards for death. Age was significantly linked to allo-BMT ($P < .0001$ by standard χ^2 test), and del(5q) significantly linked to *NR3C1* alterations ($P < .0001$), suggesting that allo-BMT and *NR3C1* alterations, rather than age and del(5q), were the main factors of interest. Accordingly, allo-BMT and *NR3C1* alteration were investigated for their impact on survival by multivariate analysis. Although allo-BMT did not reach statistical significance ($P = .08$), the analysis suggests that lack of allo-BMT and monoallelic loss of *NR3C1* ($P = .022$) are independent factors that negatively impact survival in BPDCN (supplemental Table 3). Thus, haploinsufficiency for *NR3C1* appears to define a very high risk subgroup of BPDCN patients. Of note, none of the 3 chemotherapy regimens was statistically significantly related to favorable or unfavorable outcome in univariate analysis (supplemental Table 3).

Molecular characterization of a novel t(3;5)(q21;q31) in BPDCN reveals fusion of the *NR3C1* gene to a lncRNA-encoding gene in 3q21

To further explore the pathological relevance of *NR3C1* rearrangement in BPDCN, we performed detailed molecular and functional characterization of the t(3;5)(q21;q31) observed in the primary cells and in the derived cell line GEN2.2 of patient UPN 1 (Figure 1C; supplemental Figure 1A; supplemental Table 2). RACE-PCR and sequencing revealed the t(3;5)(q21;q31) to encode a single chimeric transcript comprising exons 1 and 2 of the *NR3C1* gene fused to an antisense sequence deriving from a novel *lincRNA* gene located in 3q21 (named here, *lincRNA-3q*) (Figure 2A; supplemental Figure 1C-D). LD-PCR genomic breakpoint cloning identified this transcript to result from fusion of *NR3C1* intron 2 (chromosome 5:142,732,115) to *lincRNA-3q* intron 3 on the der(3) chromosome (chromosome 3: 129,837,689) (supplemental Figure 1D). No further abnormal transcripts were detectable by Northern blotting across the *NR3C1* gene, thus ruling out *NR3C1* reciprocal fusion transcripts deriving from the der(5) chromosome (supplemental Figure 1B). Sequencing predicted the *NR3C1-lincRNA-3q* fusion gene transcript to encode a GCR fusion protein comprising the GCR N-terminal activation domain AF1 (amino acids 1-393) fused to 18 amino acids derived from transcriptional read-through into the *lincRNA-3q* locus (Figure 2B, left). In keeping with this, western blotting in t(3;5)-positive GEN2.2 cells, using an anti-N-terminal GCR antibody (clone E20), detected a single abnormal GCR protein isoform (~52 kDa, hereafter referred to as GCR-FP), in addition to the wild-type GCR (90 kDa) (Figure 2B, right).

NR3C1 translocation/deletion drives altered GCR signaling and drug resistance in BPDCN

NR3C1 gene alterations have been described in a subset of relapsing B-ALL, suggesting a role in therapy resistance.[37,38] We thus investigated responses to drug therapy in CAL-1 cells after stable overexpression of a GFP-tagged isoform of GCR-FP (CAL-1 GCR-FP[+]; Figure 2C; supplemental Figure 2A-B) or after stable GCR knockdown (CAL-1 shGCR1 and 2; Figure 2D) designed to mimic haploinsufficiency for *NR3C1* as seen in patients compared with control cells (ie, CAL-1 cells expressing GFP alone [CAL1 GCR-FP(−)] or CAL-1 shCtrl cells, respectively). Strikingly, responses to combination therapy with high-dose synthetic GCR ligand (dexamethasone at 10 μM) and etoposide (10 μM) were markedly reduced in CAL-1 GCR-FP-overexpressing cells compared with controls (Figure 2E). Cell death after dexamethasone (10 μM) or etoposide (10 μM) treatment alone was unchanged, at least under these conditions (Figure 2E). Similarly, GCR depletion by short hairpin markedly reduced cell death responses to single-agent dexamethasone or to combination therapy by etoposide–dexamethasone compared with controls, but did not affect cell death response to etoposide alone (Figure 2F).

The next step was to analyze more globally the potential impact of GCR haploinsufficiency on ligand-dependent GCR transcriptional regulatory activity in BPDCN. We first used luciferase reporter assays to test the impact of GCR-FP on wild-type GCR activity in the absence (dimethyl sulfoxide) or presence of dexamethasone (Figure 3A). As expected, this revealed GCR-FP dose-dependent attenuation of GCR transcriptional transactivation activity (Figure 3A). We next performed GEP in GCR-FP-overexpressing or shGCR-treated CAL-1 cells (designed to mimic haploinsufficiency; Figure 2D), in the absence (dimethyl sulfoxide) or presence of dexamethasone (100 nM, 6 hours) (Figure 3B). Low-dose, as opposed to high-dose (therapeutic-level) dexamethasone, was used in order to simulate the conditions in which *NR3C1* alterations might be expected to undergo clonal selection in treatment-naive leukemia cells in vivo (ie, physiological glucocorticoid concentrations). Strikingly, this analysis revealed specific, hormone-dependent deregulation of 2332 (1205 down; 1127 up) and 3205 genes (1456 down; 1749 up) in CAL-1 shGCR and CAL-1 GCR-FP dexamethasone-treated cells, respectively,

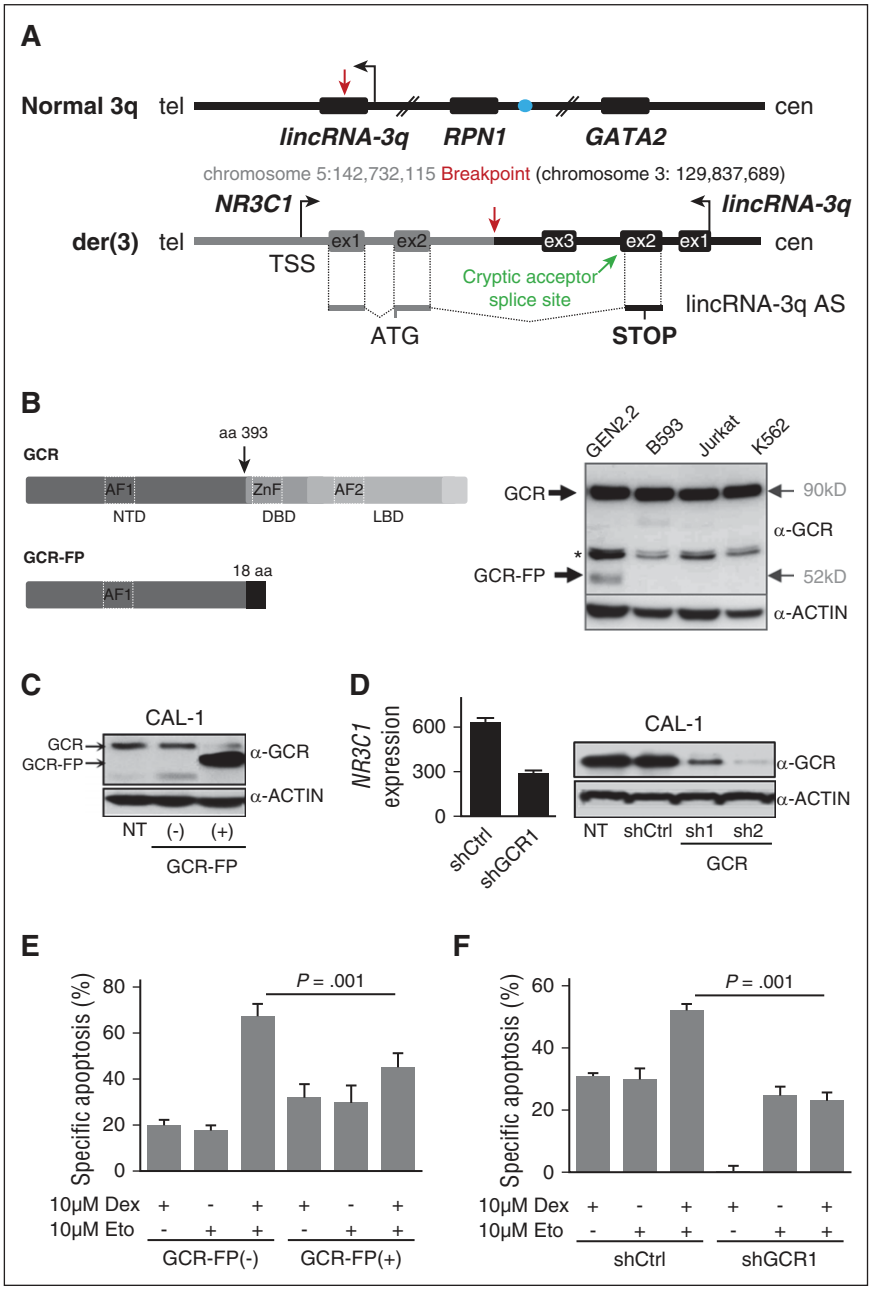

Figure 2. The t(3;5)-encoded GCR-lincRNA-3q fusion protein is associated with glucocorticoid resistance. (A) Schematic representation of the genomic organization surrounding the normal 3q and der(3) breakpoint regions, indicating the resulting fusion transcript NR3C1-lincRNA-3q. The blue filled circle denotes the GATA2 superenhancer. In black, 3q sequences. In gray, 5q sequences. The NR3C1-lincRNA-3q fusion transcript likely derives from a splicing event between *NR3C1* exon 2 and a cryptic splice acceptor site located in the antisense orientation in *lincRNA-3q* exon 2 (chromosome 3:129,832,478). (B) Schematic representation of the structure of wild-type GCR (top left) and predicted GCR-FP (bottom left). GCR and ACTIN western blot analyses showing expression of an abnormal GCR isoform (GCR-FP) exclusively in GEN2.2 cells compared with t(3;5)-negative cell lines, as indicated (right); * denotes nonspecific band. (C) Western blot using anti-GCR and anti-ACTIN antibodies in the parent CAL-1 cell line (nontransduced; NT) compared with CAL-1 cells transduced with empty GFP vector (−) or with the GFP-tagged GCR-FP expression vector (+), as indicated (n = 2). (D) Western blot using anti-GCR and anti-ACTIN antibodies in the parent CAL-1 cell line (NT) compared with CAL-1 cells transduced with shCtrl or shGCR (n = 2 independent hairpins, shGCR1 and 2), as indicated (right). Affymetrix NR3C1 messenger RNA expression in shGCR1 compared with shCtrl-transduced cells (experimental haploinsufficiency, n = 3) (left). (E) Evaluation of drug sensitivity of CAL-1 cells overexpressing GCR-FP compared with control CAL-1 cells after 16 hours of treatment with 10 μM etoposide (Eto), 72 hours of treatment with 10 μM dexamethasone (Dex), or a combination of both treatments. Specific apoptosis was measured by AnnexinV/propidium iodide staining and flow cytometry, and calculated as follows: (% drug-induced cell death − % control cell death) ÷ (100 − % control cell death) × 100. *P* value determined by Wilcoxon test; n = 3. (F) Evaluation of drug sensitivity of CAL-1 cells shGFP compared with shCtrl as described in panel E. aa, amino acid; AF, activation function domain; cen, centromere; DBD, DNA binding domain; LBD, ligand binding domain; ex, exon; NTD, N-terminal domain; tel, telomere; TSS, transcription start site; ZnF, zinc finger domain.

compared with CAL-1 control cells. Further analysis revealed a common subset of 264 deregulated genes (139 down; 125 up) (Figure 3B; supplemental Table 13), which included known GCR target genes such as *PFKB2* (encoding 6-phosphofructo-2-kinase) and genes encoding nuclear factors that have been implicated in normal (IKZF2/Helios) or leukemic (ZEB2) T lymphoid[39,40] or dendritic cell lineage development (*SPIB*).[41] Supporting the clinical relevance of the latter findings, deregulated expression of *IKZF2*, *ZEB2*, and *SPIB* was also observed by GEP in primary patient cells with *NR3C1* deletion compared with nondeleted control cases (supplemental Figure 3A).

Loss-of-EZH2 function is a hallmark of 5q alterations that target *NR3C1* in BPDCN

To further explore the pathological relevance of 5q alterations targeting *NR3C1* and related gene expression changes in BPDCN, we used GSEA to identify, in an unbiased manner, common dexamethasone-dependent gene signatures that are abnormally modulated upon overexpression of the t(3;5)-encoded GCR-FP or experimental *NR3C1* haploinsufficiency in CAL-1 BPDCN cells. Consistent with our functional studies (Figure 2E-F), this analysis revealed enrichment of prednisone resistance gene signatures that have previously been described in B-ALL[42,43] in dexamethasone-treated CAL-1-GCR-FP-expressing cells and CAL-1 shGCR cells compared with controls (supplemental Figure 2C). Of note, 1 of these resistance signatures[43] was also enriched in *NR3C1*-deleted primary BPDCN cells compared with nondeleted cases, thus further reinforcing the notion that *NR3C1* deletion contributes to treatment failure in BPDCN, as in B-ALL[37,38] (supplemental Figure 2C). Strikingly, this analysis also revealed marked enrichment for signatures related to loss-of-EZH2 function in cancer cells, including gene expression programs that are functionally linked to *HOXA* locus derepression in myeloid leukemia[44,45]

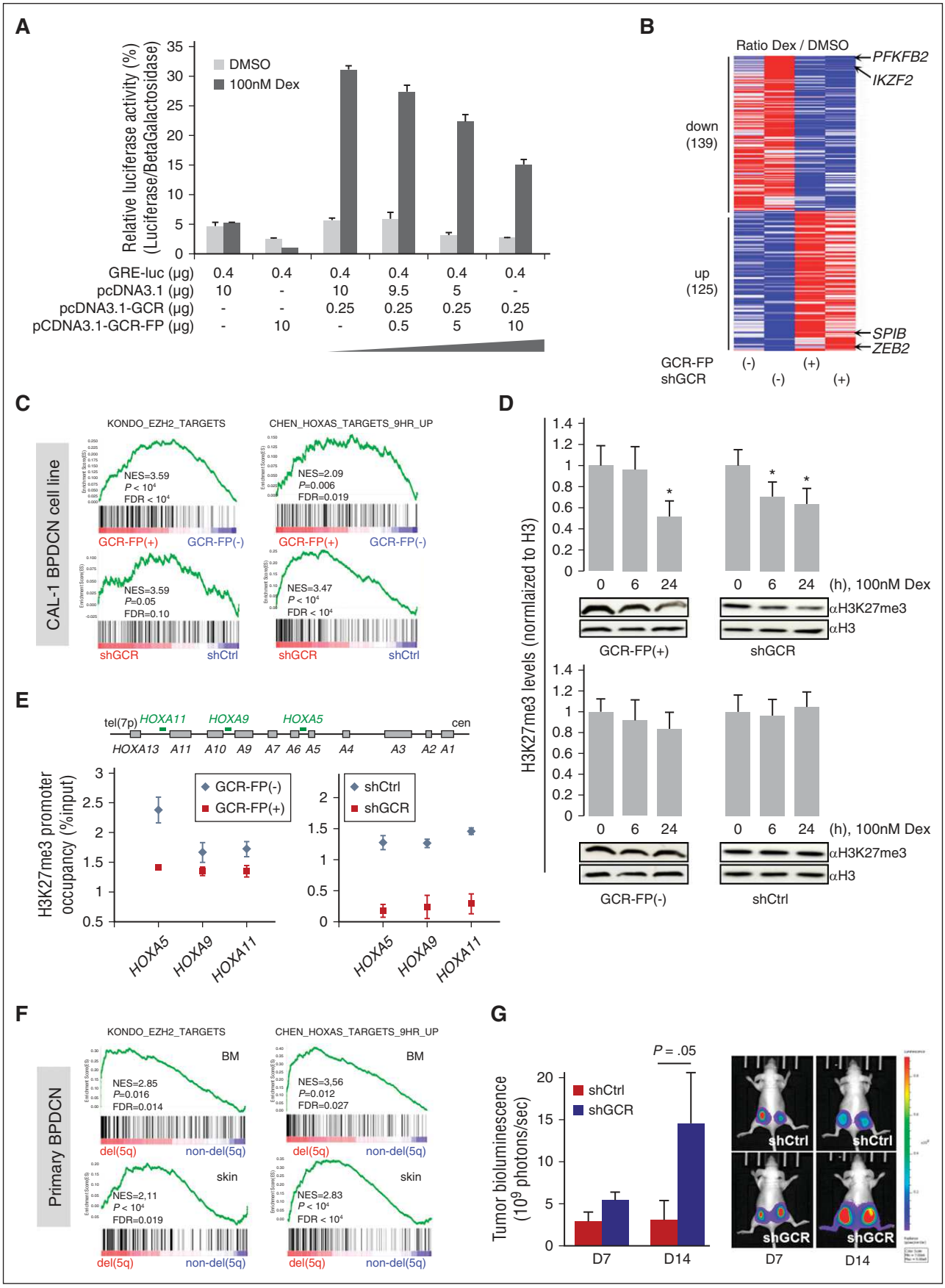

(Figure 3C). This prompted us to examine the impact of attenuated GCR signaling on global H3K27me3 levels in BPDCN. For this, we used CAL-1 cells overexpressing GCR-FP or undergoing GCR knockdown to assess global H3K27me3 levels after low-dose dexamethasone treatment compared with control conditions. Consistent with our GEP experiments, western blot analyses revealed global loss of H3K27me3 under attenuated GCR signaling (Figure 3D; supplemental Figure 3D). Further analysis by site-specific anti-H3K27me3 ChIP confirmed reduced H3K27me3 levels at the *HOXA* locus, a major downstream target of the polycomb-repressive complex 2 (PRC2) complex in the hematopoietic lineage, specifically at the *HOXA5*, *HOXA9*, and *HOXA11B* gene promoters, in dexamethasone-treated GCR-FP overexpressing CAL-1 cells and in CAL-1 shGCR cells compared with controls (Figure 3E). In keeping with the clinical pertinence of these findings, GEP in primary *NR3C1*-deleted BPDCN leukemia cells compared with nondeleted cases from bone marrow (UPNs 32-42) or skin (UPNs 43-47) also identified EZH2 loss-of-function signatures (Figure 3F; supplemental Figure 3B). Genomic DNA sequencing was performed to check whether *ASXL1* and *EZH2* mutations might be responsible for the observed loss-of-EZH2 function signatures. This is important because mutations in these genes have been described in BPDCN.[14] We screened the 2 BPDCN cell lines (UPNs 1 and 2) and the bone marrow or blood-derived DNA from the 12 patients for which GEP was used for GSEA (UPNs 31-42, including 4 cases with *NR3C1* monoallelic loss [UPNs 31-33 and UPN 35]). Sequencing identified 2 BPDCN cases with deleterious *ASXL1* exon 12 mutations (UPNs 34 and 40) (supplemental Table 4; supplemental Figure 3C) and 1 case (UPN 36) with a heterozygous *EZH2* mutation. UPN 40 showed 2 different *ASXL1* mutations (supplemental Table 4). In 5 cases (ie, 3 non-del(5q) [UPNs 38, 39, and 41] and 2 5q/*NR3C1* deletion [UPNs 32 and 33]), the region spanning the G-rich region chromosome 20:31,022,184 to 31,022,744 of *ASXL1* exon 12 could not be fully sequenced because of insufficient DNA. Of note however, mutations in this region appear rare in BPDCN (1/25 reported cases).[14] When GSEA was performed, without the GEP data from the *EZH2* and *ASXL1* mutant cases (UPN 36 and UPNs 34 and 40, respectively), *NR3C1* deletion remained significantly associated with multiple loss-of-EZH2 function signatures (Figure 3F; bone marrow, top; skin, bottom). Although this does not exclude other, yet-to-be-determined factors, in the emergence of the loss-of-EZH2 function signature in our *NR3C1*-deleted BPDCN cases, gene mutations affecting *ASXL1* and *EZH2* are unlikely to be responsible for the observed phenotype. In keeping with the relevance of these findings to BPDCN pathogenesis, knockdown of GCR significantly accelerates leukemia growth in a xenotransplant assay utilizing CAL-1 BPDCN cells (Figure 3G; supplemental Figure 3E-F). Of note, the loss-of-EZH2 function GEP signatures did not include PRC2 factor or H3K27me3 demethylase encoding genes, suggesting that altered PRC2 activity, rather than deregulated expression of individual PRC2 components per se, is responsible for the observed phenotypes. Taken together, these findings point to the existence of a novel cellular mechanism by which GCR and EZH2 signaling collaborate to reprogram EZH2 targets in leukemia.

LincRNA-3q is overexpressed in BPDCN and AML and encodes a nuclear noncoding RNA that regulates cell proliferation and leukemic stem cell gene expression programs

We next wished to assess the pathological relevance of the lncRNA gene identified at the 3q21 breakpoint in the t(3;5)(q21;q31) observed in BPDCN case UPN 1 (Figure 2A). For this, we first measured expression levels of lincRNA-3q in normal pDC, BPDCN cell lines, and primary BPDCN leukemia samples by RT-qPCR (Figure 4A). This revealed evidence of illegitimate *lincRNA-3q* activation in primary BPDCN cases compared with normal pDC. Deregulation of *lincRNA-3q* was also evident in AML (Figure 4A), B-cell lymphoma, and solid cancers (supplemental Figure 4A-B). In normal tissues, *lincRNA-3q* was predominantly expressed in fetal brain, bone marrow, and testis (supplemental Figure 4A). We next assessed the subcellular localization of lincRNA-3q by cell fractionation and qRT-PCR analysis in CAL-1 and U937 AML cells (Figure 4B). lincRNA-3q was found to be predominantly nuclear, suggestive of a role in chromatin signaling.[46] Quite strikingly, lincRNA-3q knockdown in CAL-1 and U937 cells induced a G1/S arrest (Figure 4C and supplemental Figure 4C, respectively), without inducing cell death (supplemental Figure 4D). In view of this phenotype, GEP, followed by GSEA, was performed in the same cells (Figure 4D and supplemental Figure 4E, respectively). Short hairpin-mediated lincRNA-3q depletion was associated with differential expression of 371 (174 up; 197 down) and 904 genes (428 up; 476 down) in CAL-1 and U937 cells, respectively, thus suggestive of a cell context–dependent role for lincRNA-3q in both gene activation and repression. Among the lincRNA-3q regulated genes in BPDCN CAL-1 cells were *TCL1B*,[47] *HOXB4*,[48] and *TP53INP1*, a tumor suppressor gene[49] (Figure 4D). Similarly, E2F family members (E2F7 and E2F8) known to negatively regulate E2F transcriptional activity were modulated by lincRNA-3q knockdown in U937 cells[50] (supplemental Figure 4E). Consistent with G1/S arrest in lincRNA-3q-depleted leukemia cells, E2F-regulated gene expression signatures were markedly reduced upon lincRNA-3q depletion in both CAL-1 and U937 cells compared with controls (Figure 4D and supplemental Figure 4E, respectively), thus suggesting a role for lincRNA-3q in the regulation of E2F transcriptional transactivation functions. In keeping with this, lincRNA-3q depletion by siRNA transient transfection in H1299 cells led to G1/S arrest coincident to markedly reduced E2F activity, as measured by a cyclin E–luciferase reporter assay, in the same cells compared with control conditions (Figure 4E; supplemental Figure 5A-E). Knockdown of lincRNA-3q in CAL-1 and U937 AML cells was found to downregulate normal and/or leukemic hematopoietic stem cell gene expression programs[48,51] (Figure 4D and supplemental Figure 4E, respectively), suggestive of a role in the normal hematopoietic/leukemic stem cell compartment, which is consistent with high-level

Figure 3. Misregulated GCR and EZH2 signaling as a consequence of *NR3C1* alterations in BPDCN. (A) Luciferase reporter assay for glucocorticoid transcriptional transactivation activity in COS7 cells transduced with empty pcDNA3.1 vector, pcDNA3.1-GCR, and pcDNA3.1-GCR-FP, as indicated, after a 6-hour treatment with either dimethyl sulfoxide (DMSO) or 100 nM dexamethasone (n = 3). (B) Heatmap representation of the common differentially expressed genes among CAL-1-GCR-FP (GCR-FP[+]), CAL-1 control cells (GCR-FP[−]), and shGCR-transduced cells (shGCR[+]) compared with controls (shGCR[−]) after treatment with 100 nM dexamethasone for 6 hours (n = 3 for each group). Black arrows indicate genes cited in the text. (C) GSEA plots showing gene regulatory circuits that are differentially expressed between dexamethasone-treated CAL-1-GCR-FP or shGCR compared with respective control CAL-1 cells (CAL-1-GFP or CAL-1 shCtrl). (D) Western blot analysis and quantification of global H3K27me3 levels in CAL-1-GCR-FP (GCR-FP[+]) and CAL-1 shGCR (upper) and respective CAL-1 control cells (CAL-1 GFP [GCR-FP(−)] and CAL-1 shCtrl) (lower) upon 6-hour or 24-hour treatment with 100 nM dexamethasone (n = 3). (E) ChIP for H3K27me3 followed by qPCR analysis for enrichment on *HOXA* gene promoters, as indicated, in CAL-1-GCR-FP (GCR-FP[+]), CAL-1 shGCR, and respective CAL-1 control cells (CAL-1 GFP [GCR-FP(−)] and CAL-1 shCtrl) treated for 24 hours with 100 nM dexamethasone (n = 3). (F) GSEA plots showing gene regulatory circuits that are differentially expressed between BPDCN patients presenting, or not, del(5q) abnormalities that target *NR3C1* (bone marrow or skin, as indicated; unmutated EZH2 and ASXL1 cases only). (G) Tumor bioluminescence (7 and 14 days postinjection) for xenotransplanted nude mice bearing tumors derived from CAL-1 shCtrl and shGCR cell lines (left). *P* value determined by Wilcoxon test; n = 6 for each group. Bioluminescence imaging for representative mouse (right). D, day; GSEA, gene set enrichment analysis.

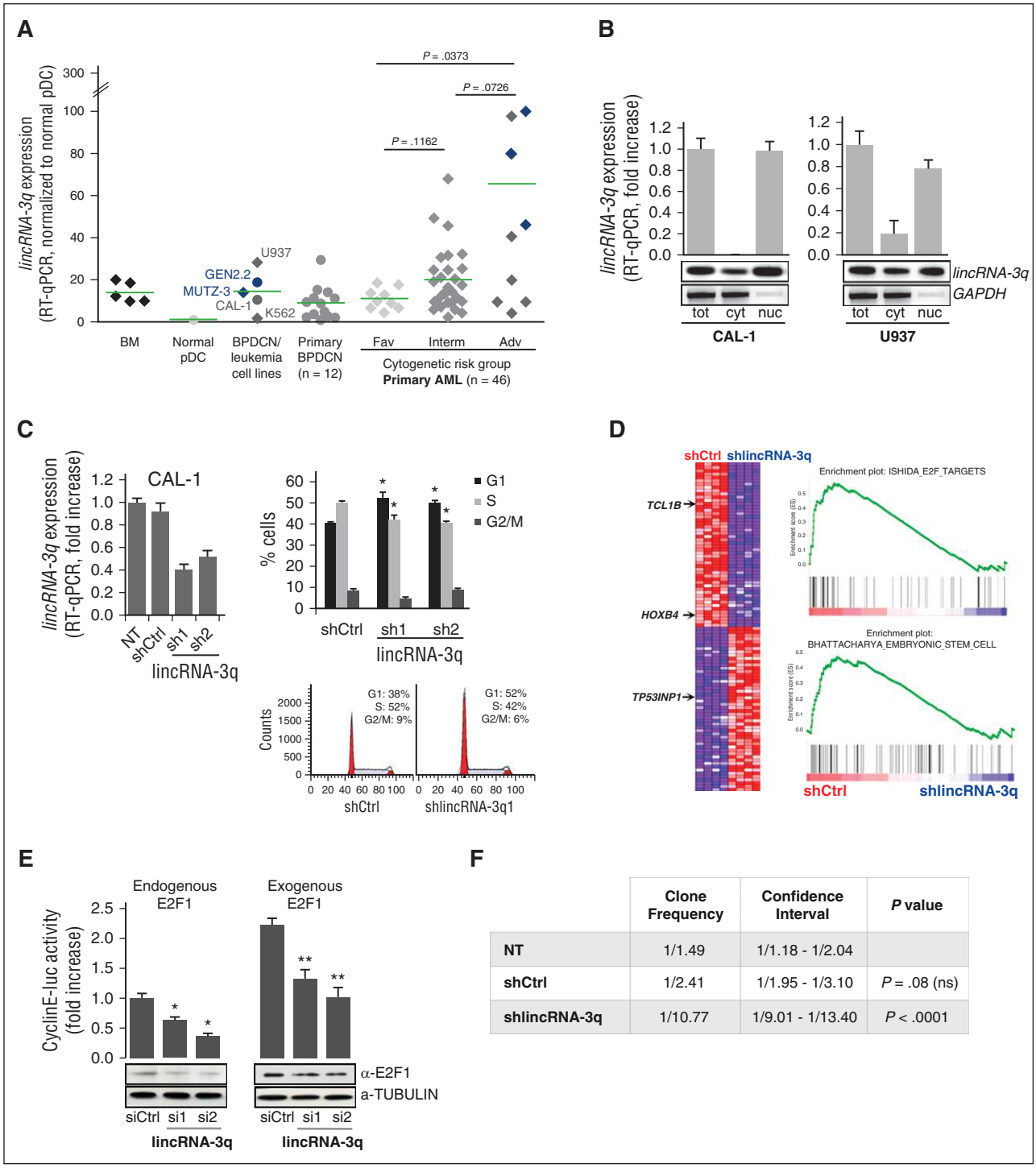

	Clone Frequency	Confidence Interval	*P* value
NT	1/1.49	1/1.18 - 1/2.04	
shCtrl	1/2.41	1/1.95 - 1/3.10	*P* = .08 (ns)
shlincRNA-3q	1/10.77	1/9.01 - 1/13.40	*P* < .0001

Figure 4. *lincRNA-3q* overexpression in BPDCN and AML drives G1/S and leukemia-driver gene expression programs. (A) RT-qPCR-derived *lincRNA-3q* expression profiles in normal bone marrow; normal pDC; BPDCN (CAL-1, GEN2.2), AML (U937, MUTZ-3), and chronic myeloid leukemia cell lines (K562); and in BPDCN and AML patient samples. AML patients are classified according to cytogenetic risk group. Cases presenting chromosome 3q abnormalities are identified in blue. (B) RT-qPCR and RT-PCR analysis of the subcellular localization of lincRNA-3q in CAL-1 BPDCN cells and U937 AML cells. RNA extracted from whole-cell and subcellular fractions (n = 2). Glyceraldehyde-3-phosphate dehydrogenase (GAPDH) was used as a control. (C) RT-qPCR-derived *lincRNA-3q* expression in CAL-1 cells transduced with control (shCtrl) or lincRNA-3q-targeting short hairpin constructs (sh1 and 2) (left). Cell cycle analysis in CAL-1 cells transduced with control (shCtrl) or lincRNA-3q sh1 and 2 constructs (upper right). **P* < .05 by Wilcoxon test; n = 6. Representative histogram representation of percentage of cells in cell cycle phases (n = 4) (lower right). (D) GSEA plots obtained by comparing gene expression profiles of CAL-1 cells transduced with control (shCtrl) or lincRNA-3q-targeting short hairpin (shlincRNA-3q) (right) and associated heatmap (n = 4 for each group) (left). Genes mentioned in the text are marked with an arrow. (E) E2F cyclin E–luciferase (luc) reporter assay in H1299 cells transiently transfected with control or siRNA targeting lincRNA-3q with or without addition of exogenous E2F1 (100 ng) (upper). **P* < .05, ***P* < .01 by Wilcoxon test; n = 6. Western blot using anti-E2F1 antibody in H1299 cells transduced with siCtrl or silincRNA-3q, as indicated (n = 2) (lower). (F) Table presenting clone frequency and associated statistics derived from in vitro limiting dilution clonogenicity for CAL-1 either nontransduced (NT) or transduced with control (shCtrl) or lincRNA-3q-targeting (shlincRNA-3q) shRNA. Adv, adverse; cyt, cytosolic fraction; Fav, favorable; Interm, intermediate; nuc, nuclear fraction; tot, whole cell extract.

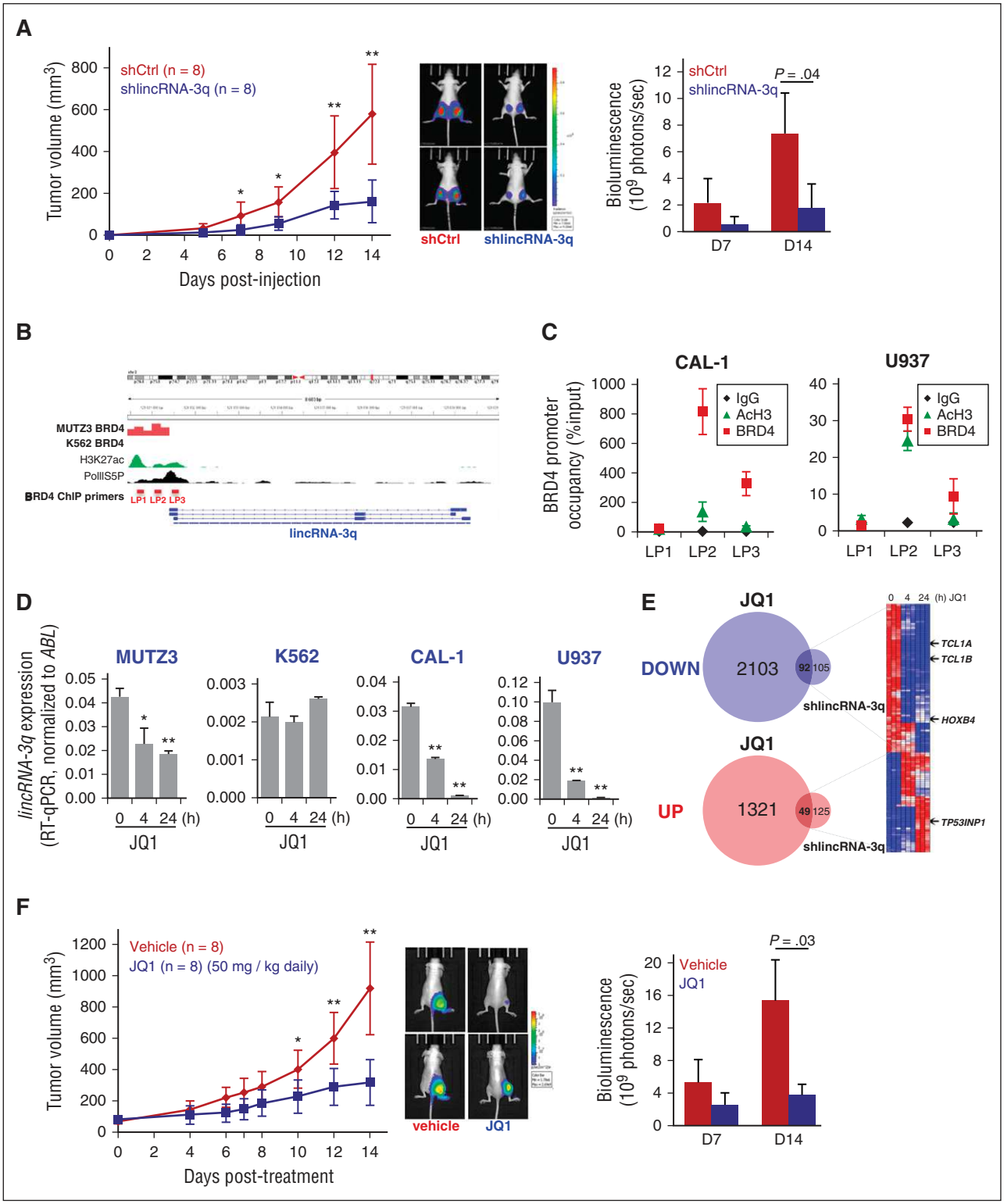

Figure 5. Abrogation of *lincRNA-3q* activity by BET inhibition in BPDCN and AML leukemia cells. (A) Tumor growth kinetics measured in nude mice engrafted with shCtrl or shlincRNA-3q-transduced CAL-1 cells (left); bioluminescence imaging for 2 representative mice (day 14) (middle); and quantification of tumor bioluminescence (7 and 14 days postinjection) for each group (right). $^*P < .05$, $^{**}P < .01$ by Student *t* test; n = 8 for each group. (B) Genomic organization of the *lincRNA-3q* locus and BRD4 ChIP-sequencing analysis (ArrayExpress accession number ERP004614) showing promoter occupancy by BRD4 in MUTZ-3 cell line (3q rearrranged AML) compared with K562 cell line (no 3q rearrangement). ENCODE data showing positions of active chromatin marks and phospho-RNA polymerase II (Pol II) binding, as indicated. (C) Anti-BRD4 and anti-AcH3 ChIP at the promoter region of *lincRNA-3q* in CAL-1 and U937 cells, as indicated. (D) RT-qPCR-derived *lincRNA-3q* expression in MUTZ3, K562, U937, and CAL-1 cells treated with 1 μM JQ1 at the time indicated. $^*P < .05$, $^{**}P < .01$ by Wilcoxon test; n = 3. (E) Venn diagrams (left) and heatmap (right) showing time course of differential gene expression of lincRNA-3q targets upon JQ1 treatment in CAL-1, as indicated. (F) Tumor growth kinetics measured in nude mice bearing tumors derived from CAL-1 cell lines after control or JQ1 treatment (left); bioluminescence imaging for 2 representative mice (day 14) (middle); and quantification of tumor bioluminescence (7 and 14 days posttreatment) for each group (right). $^*P < .05$, $^{**}P < .01$ by Student *t* test; n = 6 for each group. AcH3, acetylated histone H3; BET, bromodomain and extraterminal domain; Ig, immunoglobulin; LP, lincRNA ChIP Primer.

lincRNA-3q expression in normal bone marrow samples (Figure 4A). This was borne out by in vitro limiting dilution clonogenicity assays in CAL-1 cells, which showed dramatically reduced clonogenic potential upon lincRNA-3q depletion compared with controls (Figure 4F). Concordant with this, lincRNA-3q knockdown markedly impaired CAL-1 leukemia growth in an in vivo xenotransplantation assay (Figure 5A; supplemental Figure 4F). Thus, *lincRNA-3q* displays features of a bona fide leukemic driver that warrants assessment for therapeutic intervention.

BET inhibition abrogates lincRNA-3q overexpression and signaling in BPDCN

Numerous cancer genes,[29,52,53] including the cancer-related lncRNA gene *HOTAIR*,[54] have been shown to critically depend on proteins of the BET domain family for their expression. Because high-level overexpression of lincRNA-3q was detected in 3q-rearranged AML in which BET proteins (bromodomain-containing protein 4 [BRD4]) have been implicated in deregulation of a critical 3q oncogene (*EVI1*), we asked whether BRD4 might also play a role in the regulation of *lincRNA-3q*. To address this question, we interrogated BRD4 ChIP sequencing data sets[52] derived from MUTZ3 (3q-rearranged AML cell line) compared with K562 (no 3q rearrangement) leukemia cells (ArrayExpress accession number ERP004614). This revealed marked enrichment of BRD4 across the promoter region of the linc-RNA-3q gene in MUTZ3 cells, but not K562 cells (Figure 5B). Site-specific anti-BRD4 ChIP subsequently revealed BRD4 occupancy of the *lincRNA-3q* promoter in CAL-1 and U937 cells (Figure 5C). In aggregate, this indicated that BRD4 directly regulates *linc-RNA-3q* in CAL-1, U937, and MUTZ-3 cells, but not K562 cells (no detectable occupancy of the *lincRNA-3q* promoter by BRD4) and that BET inhibition might constitute a means to reverse abnormal *lincRNA-3q* expression in leukemia cells. In keeping with this, treatment with one such BET inhibitor (JQ1) led to suppression of lincRNA-3q levels in a time-dependent manner in MUTZ-3, U937, and CAL-1 BPDCN cells, but not in K562 cells (Figure 5D). In view of this, we next assessed the consequences on global gene expression profiles of JQ1 treatment BET-sensitive lincRNA-3q-overexpressing CAL-1 cells compared to those obtained upon depletion of lincRNA-3q in the same cells. Quite strikingly, JQ1 treatment in CAL-1 cells modulated a common subset of lincRNA-3q targets (92 down; 49 up), including downregulation of known leukemic driver genes (eg, *TCL1A*, *TCL1B*, and *HOXB4*, of which the former 2 are of relevance to BPDCN), as well as enhanced expression of candidate tumor suppressor genes such as *TP53INP1* (Figures 4D and 5E, arrows; supplemental Table 14). As expected for BET inhibition, numerous additional genes not coregulated by lincRNA-3q were also identified (Figure 5E). Thus, BET inhibition would be expected to counteract at least some of the oncogenic signaling properties of lincRNA-3q in BPDCN and AML. To test this in vivo, we performed a JQ1 treatment protocol in a CAL-1 xenotransplantation assay, which revealed significant suppression of CAL-1 leukemia growth in the treatment (50 mg/kg daily for 14 days) compared with the control arm (vehicle alone) (Figure 5F) at kinetics that closely mirrored those seen in lincRNA-3q-depleted compared with control tumors (Figure 5A; supplemental Figure 4F), indicating that BET inhibition is a potent therapeutic strategy in BPDCN.

Discussion

A remarkable finding from our focused genetic screen was the identification of the GCR-encoding gene, *NR3C1*, as a candidate 5q-linked haploinsufficient tumor suppressor in BPDCN. Based on functional studies coupled with GEP and survival analyses in BPDCN patients, we provide novel evidence of a role for *NR3C1* haploinsufficiency in corticoresistance and functional antagonism of gene silencing via EZH2 in a subset of BPDCN. In addition, this report contains the first description of an *NR3C1* fusion gene translocation in human leukemia, thereby raising the necessity for screening for balanced structural aberrations at this locus in BPDCN.

That corticoresistance could be driven by haploinsufficiency for GCR expression in BPDCN is in line with recent findings that identify diminished GCR protein levels as a major determinant of de novo corticoresistance in B-ALL.[55] *NR3C1* haploinsufficiency in BPDCN is associated with gene expression programs that characterize corticoresistance in B-ALL, suggestive of the existence of common cellular mechanisms for resistance to glucocorticoid-induced apoptosis in BPDCN and B-ALL.[42,43] In the specific case of BPDCN, most cases initially respond well clinically to corticotherapy-based regimens, suggesting that glucocorticoid resistance may arise initially at the subclinical level as a consequence of the persistence of residual resistant cells that are haploinsufficient for *NR3C1*. Larger prospective studies will be required to address the relationship, if any, between *NR3C1* haploinsufficiency, residual disease, and the presence of central nervous system involvement at diagnosis which has been implicated in rapid disease recurrence in BPDCN patients.[56] As proposed recently,[55] restoring normal GCR levels from the intact *NR3C1* allele might represent a route to overcoming glucocorticoid-based therapy failure in *NR3C1*-haploinsufficient BPDCN. Of note in this context is the finding that thalidomide appears to specifically benefit patients presenting with multiple myeloma and low GCR expression.[57]

The present study has revealed a previously unsuspected connection between GCR signaling and EZH2 activity in human leukemia. EZH2 activity seems to be acutely sensitive to GCR signaling thresholds. Attenuated GCR signaling was associated with profound reductions in H3K27me3, including at the *HOXA* locus, which is a target for derepression in leukemia. We speculate that under conditions in which GCR is limiting, such as in haploinsufficiency for *NR3C1*, GCR-ligand binding elicits dynamic GCR recruitment to high affinity sites in chromatin where either transcriptional activation or repression, depending on the regulatory context of nearby promoters or enhancers, occurs.[58,59] Enhanced GCR recruitment to high affinity sites would occur at the expense of GCR recruitment to lower-affinity sites across the genome, including at loci that may encode hormone-sensitive, developmentally regulated, and/or lineage-specific transcriptional regulatory factors that are direct PRC2 targets or that control deployment of PRC2 to other critical downstream targets such as the *HOXA* locus in BPDCN. In an alternative, but not mutually exclusive scenario, GCR binding to chromatin increases active marks such as H3K4me2/3 and H3K27ac,[60] which are known to antagonize H3K27me3 by PRC2.[61,62]

We propose that hormone-dependent, epigenetic reprogramming is the ultimate consequence of *NR3C1* haploinsufficiency in BPDCN (Figure 6). This hypothesis is supported by our clinical and functional analysis in vitro and in vivo and by reports in other cancers showing that low *NR3C1*/GCR expression is linked to poor prognosis[57,63,64] and tumor progression.[65] This postulate is also consistent with analyses showing increased tumor incidence in *Nr3c1* haploinsufficient mice.[64]

A second striking finding in this work resulted from the detailed characterization of the *NR3C1* fusion partner in our index case presenting the balanced t(3;5)(q21;q31). Molecular cloning of this case identified a novel nuclear lncRNA-encoding gene as the partner gene in 3q21. Significantly, ectopic expression of this lncRNA was linked to

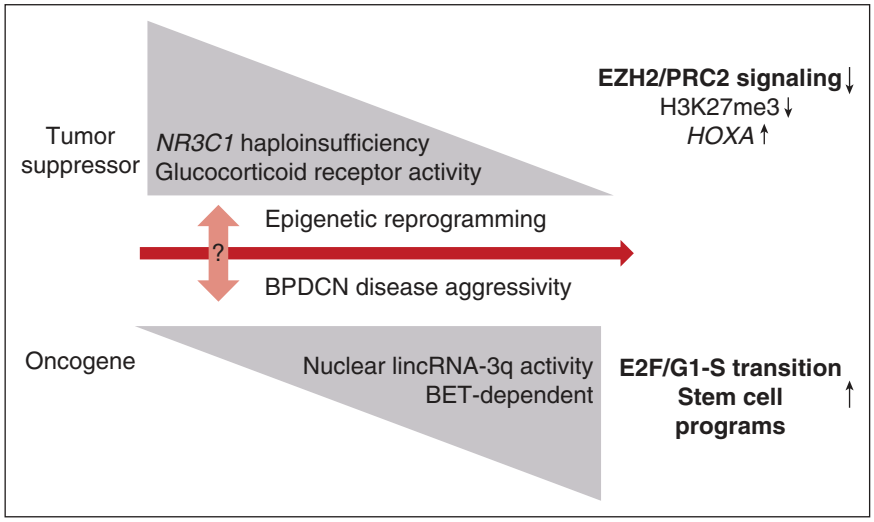

Figure 6. A model illustrating how *NR3C1* haploinsufficiency and *lincRNA-3q* misregulation contribute to BPDCN pathogenesis. We postulate that attenuated GCR signaling and *lincRNA-3q* malfunction drive BPDCN disease pathogenesis through epigenetic reprogramming. This is proposed to favor emergence of clinically aggressive disease and predicted to occur progressively by 2 routes. In the first, altered GCR signaling drives a loss-of-EZH2 phenotype that rewires key downstream PRC2 targets (eg, the *HOXA* locus) and drives deregulation of pDC differentiation pathways and treatment resistance in BPDCN. In the second, BET-dependent desilencing of oncogenic lncRNA genes (*lincRNA-3q*) may occur as "collateral damage" downstream of altered GCR and EZH2 activity or through other mechanisms. Abnormal activity of the affected nuclear lncRNA (in this case, lincRNA-3q) would engage further rounds of epigenetic reprogramming, leading to misregulation of E2F activity and activation of leukemia stem cell programs.

enrichment of the BET protein BRD4 to the promoter region. BET-inhibitor treatment rapidly abrogated *lincRNA-3q* expression only in leukemia cells showing BRD4 binding to the *lincRNA-3q* promoter, suggestive of a critical role for BET proteins in the maintenance of high-level lincRNA-3q expression in BPDCN and AML. We speculate that BRD4 recruitment to the *lincRNA-3q* promoter may depend on the activity of upstream (oncogenic) transcription factors, including possibly the GCR itself, that direct BRD4 to the *lincRNA-3q* promoter region or to neighboring "superenhancers." The latter are known to mediate long-range dysregulation of key oncogenes in hematologic cancers[52] and to coordinate activity of key hematopoietic transcription factors in leukemia.[66] Alternatively, disruption of BRD4 interaction with transcription and elongation factors (eg, polymerase II, positive transcription elongation factor b, Mediator, and Activator) may be part of the mechanism by which JQ1 inhibits *lincRNA-3q* expression. Finally, intrinsic histone acetylase activity of BRD4 itself may play a role.[67] Our findings indicate that lncRNA function constitutes a novel BET-inhibitor target in human leukemia.

In conclusion, our focused, functional genomics analysis has identified attenuated GCR signaling and unscheduled activation of a novel nuclear lncRNA as important drivers of deregulated epigenetic signaling, treatment resistance, and malignant reprogramming in the dendritic cell lineage (Figure 6). Further studies will be required to fully leverage these findings for treatment innovation in BPDCN and potentially other myeloid and lymphoid cancers that share biological features with this disease. One avenue of investigation is BET protein inhibition.

Acknowledgments

The authors thank members of the Groupe Francophone de Cytogénétique Hématologique for enrollment of BPDCN cases and for centralized review of karyotype and FISH data; Veronique Pantesco at the Microarray Core Facility of the Institute of Research on Biotherapy, Centre Hospitalier Régional Universitaire de Montpellier, INSERM Université Montpellier 1, for performing Affymetrix microarrays; Amandine Chatagnon for advice on next-generation sequencing (NGS), NGS core facility Grenoble University Hospital; Nicolas Lemaitre of the Plateforme de Pathologie Moléculaire in situ, Grenoble University Hospital, for IHC analysis; Céline Villenet, Frédéric Leprêtre, and Martin Figeac of the Plateforme de génomique fonctionnelle et structurale, Université de Lille, for performing and analyzing aCGH; Mylene Pezet and Alexandra Debernardi for expert advice on flow cytometry and bioinformatics, respectively (Flow cytometry and EpiMed core facilities, INSERM U1209, CNRS 5309, Université Grenoble Alpes); Beatrice Eymin for providing the E2F activity reporter system; Patricia Betton-Fraisse and staff in the cytogenetics and molecular genetics laboratory and at the Centre de Resources Biologiques–Grenoble University Hospital for additional technical assistance; André Verdel, Ramin Shiekhattar, Saadi Khochbin, Carlo Petosa, Alexandra Traverse-Glehen, and Tony Petrella for helpful discussions during the course of this work.

This study was supported by the Ligue Nationale Contre le Cancer (comités de l'Isère et de la Haute Savoie) (M.B.C.) and by the French Ministry for Higher Education and Research and the Société Française d'Hématologie (N.H.; doctoral funding). Additional funding in the M.B.C. laboratory is from the Institut National du Cancer "Epigénétique et Cancer Programme." NGS diagnostics in oncology/hematology at Grenoble University Hospital is funded through the Institut National du Cancer "NGS à visé diagnostique" program via the "Plateforme de génétique moléculaire des cancers " of Grenoble Hospital (P. Hainaut).

Authorship

Contributions: A.E. analyzed the data and jointly coordinated the research; N.H., S.D., A.H., S.B., S.H., M.C., and J.B.-C. performed all molecular and cell biology experiments and analyzed the data; C.S.-M. performed the targeted deep sequencing; E.B. interpreted the IHC and pathology; V.J. performed the bioluminescence imaging in vivo and analyzed the data; E.V. and F.-L.C. provided advice on the lentiviral constructs, supplied all lentiviral stocks, and analyzed the data; T.B. coordinated the flow cytometry and the limiting dilution analysis and performed the patient survival analysis; S.R. performed the bioinformatics analysis; P.B., C.R., A.R., J.C., I.T., T.M., L.C., J.P., M.-C.J., S.P., R.G., C.P.T., C.M., E.M., D.L., F.N.-K., I.L., D.P., C.B., F.J., C.L., and F.G. provided

the patient samples, clinical and molecular cytogenetic/transcriptome data, and expert analysis on BPDCN (through the French BPDCN network and Groupe Francophone de Cytogénétique Hématologique); and M.B.C. conceived and coordinated the research, analyzed the data, and wrote the paper. All authors contributed to manuscript preparation, writing, and final approval.

Conflict-of-interest disclosure: The authors declare no competing financial interests.

Correspondence: Mary B. Callanan, Centre de Recherche, INSERM U1209, CNRS UMR 5309, Université Grenoble Alpes, Site Santé, IAB, BP 170, La Tronche, 38042 Grenoble Cedex 9, France; e-mail: mary.callanan@univ-grenoble-alpes.fr.

References

1. Fachetti F, Jones DM, Petrella T. Blastic plasmacytoid dendritic cell neoplasm. In: Press W, ed. WHO Classification of Tumours of Haematopoietic and Lymphoid Tissues. 4th ed. Lyon, France: IARC; 2008:145-147.
2. Feuillard J, Jacob MC, Valensi F, et al. Clinical and biologic features of CD4(+)CD56(+) malignancies. *Blood.* 2002;99(5):1556-1563.
3. Ramanathan M, Cerny J, Yu H, Woda BA, Nath R. A combination treatment approach and cord blood stem cell transplant for blastic plasmacytoid dendritic cell neoplasm. *Haematologica.* 2013; 98(3):e36.
4. Roos-Weil D, Dietrich S, Boumendil A, et al; European Group for Blood and Marrow Transplantation Lymphoma, Pediatric Diseases, and Acute Leukemia Working Parties. Stem cell transplantation can provide durable disease control in blastic plasmacytoid dendritic cell neoplasm: a retrospective study from the European Group for Blood and Marrow Transplantation. *Blood.* 2013;121(3):440-446.
5. Chaperot L, Bendriss N, Manches O, et al. Identification of a leukemic counterpart of the plasmacytoid dendritic cells. *Blood.* 2001;97(10): 3210-3217.
6. Osaki Y, Yokohama A, Saito A, et al. Characterization of CD56+ dendritic-like cells: a normal counterpart of blastic plasmacytoid dendritic cell neoplasm? *PLoS One.* 2013;8(11): e81722.
7. Petrella T, Comeau MR, Maynadié M, et al. 'Agranular CD4+ CD56+ hematodermic neoplasm' (blastic NK-cell lymphoma) originates from a population of CD56+ precursor cells related to plasmacytoid monocytes. *Am J Surg Pathol.* 2002;26(7):852-862.
8. Garnache-Ottou F, Feuillard J, Ferrand C, et al; GOELAMS and GEIL study. Extended diagnostic criteria for plasmacytoid dendritic cell leukaemia. *Br J Haematol.* 2009;145(5):624-636.
9. Marafioti T, Paterson JC, Ballabio E, et al. Novel markers of normal and neoplastic human plasmacytoid dendritic cells. *Blood.* 2008;111(7): 3778-3792.
10. Jardin F, Callanan M, Penther D, et al. Recurrent genomic aberrations combined with deletions of various tumour suppressor genes may deregulate the G1/S transition in CD4+CD56+ haematodermic neoplasms and contribute to the aggressiveness of the disease. *Leukemia.* 2009; 23(4):698-707.
11. Leroux D, Mugneret F, Callanan M, et al. CD4(+), CD56(+) DC2 acute leukemia is characterized by recurrent clonal chromosomal changes affecting 6 major targets: a study of 21 cases by the Groupe Français de Cytogénétique Hématologique. *Blood.* 2002;99(11):4154-4159.
12. Alayed K, Patel KP, Konoplev S, et al. TET2 mutations, myelodysplastic features, and a distinct immunoprofile characterize blastic plasmacytoid dendritic cell neoplasm in the bone marrow. *Am J Hematol.* 2013;88(12):1055-1061.
13. Jardin F, Ruminy P, Parmentier F, et al. TET2 and TP53 mutations are frequently observed in blastic plasmacytoid dendritic cell neoplasm. *Br J Haematol.* 2011;153(3):413-416.
14. Menezes J, Acquadro F, Wiseman M, et al. Exome sequencing reveals novel and recurrent mutations with clinical impact in blastic plasmacytoid dendritic cell neoplasm. *Leukemia.* 2014;28(4):823-829.
15. Dijkman R, van Doorn R, Szuhai K, Willemze R, Vermeer MH, Tensen CP. Gene-expression profiling and array-based CGH classify CD4+ CD56+ hematodermic neoplasm and cutaneous myelomonocytic leukemia as distinct disease entities. *Blood.* 2007;109(4):1720-1727.
16. Sapienza MR, Fuligni F, Agostinelli C, et al; AIRC 5xMille consortium 'Genetics-driven targeted management of lymphoid malignancies' and the Italian Registry on Blastic Plasmacytoid Dendritic Cell Neoplasm. Molecular profiling of blastic plasmacytoid dendritic cell neoplasm reveals a unique pattern and suggests selective sensitivity to NF-kB pathway inhibition. *Leukemia.* 2014; 28(8):1606-1616.
17. Jerez A, Gondek LP, Jankowska AM, et al. Topography, clinical, and genomic correlates of 5q myeloid malignancies revisited. *J Clin Oncol.* 2012;30(12):1343-1349.
18. Grimwade D, Walker H, Harrison G, et al; Medical Research Council Adult Leukemia Working Party. The predictive value of hierarchical cytogenetic classification in older adults with acute myeloid leukemia (AML): analysis of 1065 patients entered into the United Kingdom Medical Research Council AML11 trial. *Blood.* 2001;98(5): 1312-1320.
19. Byrd JC, Mrózek K, Dodge RK, et al; Cancer and Leukemia Group B (CALGB 8461). Pretreatment cytogenetic abnormalities are predictive of induction success, cumulative incidence of relapse, and overall survival in adult patients with de novo acute myeloid leukemia: results from Cancer and Leukemia Group B (CALGB 8461). *Blood.* 2002;100(13):4325-4336.
20. Krönke J, Fink EC, Hollenbach PW, et al. Lenalidomide induces ubiquitination and degradation of CK1α in del(5q) MDS. *Nature.* 2015;523(7559):183-188.
21. Schneider RK, Ademà V, Heckl D, et al. Role of casein kinase 1A1 in the biology and targeted therapy of del(5q) MDS. *Cancer Cell.* 2014;26(4): 509-520.
22. Varney ME, Niederkorn M, Konno H, et al. Loss of Tifab, a del(5q) MDS gene, alters hematopoiesis through derepression of Toll-like receptor-TRAF6 signaling. *J Exp Med.* 2015;212(11):1967-1985.
23. Chaperot L, Blum A, Manches O, et al. Virus or TLR agonists induce TRAIL-mediated cytotoxic activity of plasmacytoid dendritic cells. *J Immunol.* 2006;176(1):248-255.
24. Maeda T, Murata K, Fukushima T, et al. A novel plasmacytoid dendritic cell line, CAL-1, established from a patient with blastic natural killer cell lymphoma. *Int J Hematol.* 2005;81(2): 148-154.
25. Fournier A, McLeer-Florin A, Lefebvre C, et al. 1q12 Chromosome translocations form aberrant heterochromatic foci associated with changes in nuclear architecture and gene expression in B cell lymphoma. *EMBO Mol Med.* 2010;2(5):159-171.
26. McLaren W, Pritchard B, Rios D, Chen Y, Flicek P, Cunningham F. Deriving the consequences of genomic variants with the Ensembl API and SNP Effect Predictor. *Bioinformatics.* 2010;26(16): 2069-2070.
27. Ernst T, Chase AJ, Score J, et al. Inactivating mutations of the histone methyltransferase gene EZH2 in myeloid disorders. *Nat Genet.* 2010; 42(8):722-726.
28. Gelsi-Boyer V, Trouplin V, Adélaïde J, et al. Mutations of polycomb-associated gene ASXL1 in myelodysplastic syndromes and chronic myelomonocytic leukaemia. *Br J Haematol.* 2009; 145(6):788-800.
29. Emadali A, Rousseaux S, Bruder-Costa J, et al. Identification of a novel BET bromodomain inhibitor-sensitive, gene regulatory circuit that controls Rituximab response and tumour growth in aggressive lymphoid cancers. *EMBO Mol Med.* 2013;5(8):1180-1195.
30. Vert JP, Foveau N, Lajaunie C, Vandenbrouck Y. An accurate and interpretable model for siRNA efficacy prediction. *BMC Bioinformatics.* 2006;7:520.
31. Lévy C, Frecha C, Costa C, et al. Lentiviral vectors and transduction of human cancer B cells. *Blood.* 2010;116(3):498-500, author reply 500.
32. Lajmanovich A, Ribeyron JB, Florin A, et al. Identification, characterisation and regulation by CD40 activation of novel CD95 splice variants in CD95-apoptosis-resistant, human, B-cell non-Hodgkin's lymphoma. *Exp Cell Res.* 2009; 315(19):3281-3293.
33. Bonnefoix T, Callanan M. Accurate hematopoietic stem cell frequency estimates by fitting multicell Poisson models substituting to the single-hit Poisson model in limiting dilution transplantation assays. *Blood.* 2010;116(14):2472-2475.
34. Hu Y, Smyth GK. ELDA: extreme limiting dilution analysis for comparing depleted and enriched populations in stem cell and other assays. *J Immunol Methods.* 2009;347(1-2):70-78.
35. Grimwade D, Hills RK, Moorman AV, et al; National Cancer Research Institute Adult Leukaemia Working Group. Refinement of cytogenetic classification in acute myeloid leukemia: determination of prognostic significance of rare recurring chromosomal abnormalities among 5876 younger adult patients treated in the United Kingdom Medical Research Council trials. *Blood.* 2010;116(3):354-365.
36. Nicolaides NC, Galata Z, Kino T, Chrousos GP, Charmandari E. The human glucocorticoid receptor: molecular basis of biologic function. *Steroids.* 2010;75(1):1-12.
37. Mullighan CG, Phillips LA, Su X, et al. Genomic analysis of the clonal origins of relapsed acute lymphoblastic leukemia. *Science.* 2008; 322(5906):1377-1380.
38. Kuster L, Grausenburger R, Fuka G, et al. ETV6/RUNX1-positive relapses evolve from an ancestral clone and frequently acquire deletions of genes implicated in glucocorticoid signaling. *Blood.* 2011;117(9):2658-2667.
39. Holmfeldt L, Wei L, Diaz-Flores E, et al. The genomic landscape of hypodiploid acute lymphoblastic leukemia. *Nat Genet.* 2013;45(3): 242-252.
40. Goossens S, Radaelli E, Blanchet O, et al. ZEB2 drives immature T-cell lymphoblastic leukaemia

development via enhanced tumour-initiating potential and IL-7 receptor signalling. *Nat Commun.* 2015;6:5794.

41. Schotte R, Nagasawa M, Weijer K, Spits H, Blom B. The ETS transcription factor Spi-B is required for human plasmacytoid dendritic cell development. *J Exp Med.* 2004;200(11): 1503-1509.
42. Holleman A, Cheok MH, den Boer ML, et al. Gene-expression patterns in drug-resistant acute lymphoblastic leukemia cells and response to treatment. *N Engl J Med.* 2004;351(6):533-542.
43. Rhein P, Scheid S, Ratei R, et al. Gene expression shift towards normal B cells, decreased proliferative capacity and distinct surface receptors characterize leukemic blasts persisting during induction therapy in childhood acute lymphoblastic leukemia. *Leukemia.* 2007; 21(5):897-905.
44. Kondo Y, Shen L, Cheng AS, et al. Gene silencing in cancer by histone H3 lysine 27 trimethylation independent of promoter DNA methylation. *Nat Genet.* 2008;40(6):741-750.
45. Takeda A, Goolsby C, Yaseen NR. NUP98-HOXA9 induces long-term proliferation and blocks differentiation of primary human CD34+ hematopoietic cells. *Cancer Res.* 2006;66(13): 6628-6637.
46. Ulitsky I, Bartel DP. lincRNAs: genomics, evolution, and mechanisms. *Cell.* 2013;154(1): 26-46.
47. Hashimoto M, Suizu F, Tokuyama W, et al. Protooncogene TCL1b functions as an Akt kinase co-activator that exhibits oncogenic potency in vivo. *Oncogenesis.* 2013;2:e70.
48. Wang Z, Iwasaki M, Ficara F, et al. GSK-3 promotes conditional association of CREB and its coactivators with MEIS1 to facilitate HOX-mediated transcription and oncogenesis. *Cancer Cell.* 2010;17(6):597-608.
49. Chaluvally-Raghavan P, Zhang F, Pradeep S, et al. Copy number gain of hsa-miR-569 at 3q26.2 leads to loss of TP53INP1 and aggressiveness of epithelial cancers. *Cancer Cell.* 2014;26(6): 863-879.
50. Chen HZ, Tsai SY, Leone G. Emerging roles of E2Fs in cancer: an exit from cell cycle control. *Nat Rev Cancer.* 2009;9(11):785-797.
51. Georgantas RW III, Tanadve V, Malehorn M, et al. Microarray and serial analysis of gene expression analyses identify known and novel transcripts overexpressed in hematopoietic stem cells. *Cancer Res.* 2004;64(13):4434-4441.
52. Gröschel S, Sanders MA, Hoogenboezem R, et al. A single oncogenic enhancer rearrangement causes concomitant EVI1 and GATA2 deregulation in leukemia. *Cell.* 2014;157(2): 369-381.
53. Lovén J, Hoke HA, Lin CY, et al. Selective inhibition of tumor oncogenes by disruption of super-enhancers. *Cell.* 2013;153(2):320-334.
54. Pastori C, Kapranov P, Penas C, et al. The bromodomain protein BRD4 controls HOTAIR, a long noncoding RNA essential for glioblastoma proliferation. *Proc Natl Acad Sci USA.* 2015; 112(27):8326-8331.
55. Paugh SW, Bonten EJ, Savic D, et al. NALP3 inflammasome upregulation and CASP1 cleavage of the glucocorticoid receptor cause glucocorticoid resistance in leukemia cells. *Nat Genet.* 2015; 47(6):607-614.
56. Martín-Martín L, Almeida J, Pomares H, et al. Blastic plasmacytoid dendritic cell neoplasm frequently shows occult central nervous system involvement at diagnosis and benefits from intrathecal therapy [published online ahead of print January31, 2016]. *Oncotarget.*
57. Heuck CJ, Szymonifka J, Hansen E, et al. Thalidomide in total therapy 2 overcomes inferior prognosis of myeloma with low expression of the glucocorticoid receptor gene NR3C1. *Clin Cancer Res.* 2012;18(19):5499-5506.
58. John S, Sabo PJ, Thurman RE, et al. Chromatin accessibility pre-determines glucocorticoid receptor binding patterns. *Nat Genet.* 2011;43(3): 264-268.
59. Nixon M, Andrew R, Chapman KE. It takes two to tango: dimerisation of glucocorticoid receptor and its anti-inflammatory functions. *Steroids.* 2013; 78(1):59-68.
60. Wu JN, Pinello L, Yissachar E, Wischhusen JW, Yuan GC, Roberts CW. Functionally distinct patterns of nucleosome remodeling at enhancers in glucocorticoid-treated acute lymphoblastic leukemia. *Epigenetics Chromatin.* 2015;8:53.
61. Schmitges FW, Prusty AB, Faty M, et al. Histone methylation by PRC2 is inhibited by active chromatin marks. *Mol Cell.* 2011;42(3):330-341.
62. Tie F, Banerjee R, Stratton CA, et al. CBP-mediated acetylation of histone H3 lysine 27 antagonizes Drosophila Polycomb silencing. *Development.* 2009;136(18):3131-3141.
63. Pan D, Kocherginsky M, Conzen SD. Activation of the glucocorticoid receptor is associated with poor prognosis in estrogen receptor-negative breast cancer. *Cancer Res.* 2011;71(20):6360-6370.
64. Matthews LC, Berry AA, Morgan DJ, et al. Glucocorticoid receptor regulates accurate chromosome segregation and is associated with malignancy. *Proc Natl Acad Sci USA.* 2015; 112(17):5479-5484.
65. Yemelyanov A, Czwornog J, Chebotaev D, et al. Tumor suppressor activity of glucocorticoid receptor in the prostate. *Oncogene.* 2007;26(13): 1885-1896.
66. Roe JS, Mercan F, Rivera K, Pappin DJ, Vakoc CR. BET bromodomain inhibition suppresses the function of hematopoietic transcription factors in acute myeloid leukemia. *Mol Cell.* 2015;58(6): 1028-1039.
67. Devaiah BN, Case-Borden C, Gegonne A, et al. BRD4 is a histone acetyltransferase that evicts nucleosomes from chromatin [published online ahead of print May 9, 2016]. *Nat Struct Mol Biol.* doi:10.1038/nsmb.3228.

2016 127: 3040-3053
doi:10.1182/blood-2015-09-671040 originally published online April 8, 2016

Haploinsufficiency for *NR3C1*, the gene encoding the glucocorticoid receptor, in blastic plasmacytoid dendritic cell neoplasms

Anouk Emadali, Neda Hoghoughi, Samuel Duley, Azadeh Hajmirza, Els Verhoeyen, Francois-Loic Cosset, Philippe Bertrand, Christophe Roumier, Anne Roggy, Céline Suchaud-Martin, Martine Chauvet, Sarah Bertrand, Sieme Hamaidia, Sophie Rousseaux, Véronique Josserand, Julie Charles, Isabelle Templier, Takahiro Maeda, Juliana Bruder-Costa, Laurence Chaperot, Joel Plumas, Marie-Christine Jacob, Thierry Bonnefoix, Sophie Park, Remy Gressin, Cornelis P. Tensen, Cristina Mecucci, Elizabeth Macintyre, Dominique Leroux, Elisabeth Brambilla, Florence Nguyen-Khac, Isabelle Luquet, Dominique Penther, Christian Bastard, Fabrice Jardin, Christine Lefebvre, Francine Garnache and Mary B. Callanan

Blood (print ISSN 0006-4971, online ISSN 1528-0020), is published weekly by the American Society of Hematology, 2021 L St, NW, Suite 900, Washington DC 20036.

Thérapie épigénétique "nouvelle génération"

Mécanismes d'action des inhibiteurs des protéines BET

Next generation epigenetic therapy

Mechanisms of action of BET proteins inhibitors

A. Hajmirza[1, 2, 3], E. Gimenez[1, 2, 3], S. Duley[1, 2], A. Emadali[1, 2, 3], R. Gressin[1, 2, 4], M. Callanan[1, 2, 5]

résumé

Les facteurs de régulation épigénétique ont émergé récemment comme de nouvelles cibles des traitements anticancéreux. Parmi ceux-ci, les protéines BET (protéines à *Bromodomain and ExtraTerminal domain*), qui reconnaissent les histones acétylées pour réguler l'activité génique, soulèvent un vif intérêt. Les protéines BET sont au nombre de 4 : BRD2, BRD3, BRD4 et BRDT. Ces protéines ont en commun la présence d'un double bromodomaine N-terminal (B) et d'un domaine C-terminal dit "extraterminal". Les protéines BET sont impliquées dans la régulation génique via des interactions avec la chromatine acétylée, soit au niveau des promoteurs de gènes, soit au niveau d'éléments *enhancers* responsables de la régulation transcriptionnelle tissu-spécifique à distance. Les protéines BET ont une expression et/ou une activité dérégulée dans les cancers dans lesquels elles sont des acteurs majeurs dans le maintien du phénotype transformé et la résistance thérapeutique. L'introduction récente de petites molécules inhibitrices des protéines BET offre la possibilité d'abroger leurs fonctions oncogéniques. Cet article présente les principaux mécanismes responsables de l'activité antitumorale de cette nouvelle classe de thérapie épigénétique. Les mécanismes de résistance aux inhibiteurs BET, qui commencent à être décrits, seront également évoqués.

Mots-clés : Inhibiteurs BET – Hémopathies malignes – Régulation épigénétique – Signalisation cellulaire.

summary

Epigenetic regulation factors have recently emerged as new antitumoral targets. Among them, BET proteins (with bromodomain and extraterminal domain), recognizing acetylated histones to regulate transcriptional activity, have raised great interest. There are four BET proteins, BRD2, BRD3, BRD4 and BRDT. They share the presence of a double N-terminal bromodomain (B) and a C-extraterminal domain. BET proteins are involved in genic regulation via interactions with acetylated chromatin, either at the level of gene promoters or at the level of enhancers responsible for tissue-specific transcriptional regulation at distance. BET proteins expression or activity is dysregulated in cancers where they are major actors to maintain the transformed phenotype and resistance to therapy. The recent irruption of small molecules inhibiting BET proteins allows to abrogate their oncogenic properties. In this review, the major mechanisms responsible for the anti-tumoral activity of this new epigenetic treatment class are presented. Resistance mechanisms to BET inhibitors, which begin to be described, are also evoked.

Keywords: BET inhibitors – Hematological malignancies –Epigenetic regulation – Cell signaling.

[1] *Université de Grenoble.*
[2] *Inserm U823, institut Albert-Bonniot, Grenoble.*
[3] *Pôle de recherche, CHU de Grenoble.*
[4] *Département d'hématologie clinique, CHU de Grenoble.*
[5] *Unité de génétique onco-hématologique, plateforme hospitalière de génétique moléculaire des cancers, pôle de biologie, CHU de Grenoble.*

L'information épigénétique correspond à toute information génétique qui n'est pas directement codée par la séquence d'ADN. L'essentiel de l'information épigénétique est codé par des modifications chimiques de l'ADN – méthylation ou hydroxyméthylation, par exemple – ou par des modifications post-traductionnelles des histones. Ces modifications chimiques agissent ensemble pour constituer des compartiments fonctionnels distincts au niveau de la chromatine, respectivement l'euchromatine et l'hétérochromatine. L'euchromatine est constituée de chromatine "ouverte" hypéracétylée, tandis que l'hétérochromatine est composée de chromatine "fermée" hypoacétylée. L'hyperacétylation de la chromatine est corrélée à la transcription des gènes, alors que l'hypoacétylation est liée à la répression génique *(1)*. En définitive, les modifications post-traductionnelles des histones, comme l'acétylation et la méthylation, pour n'en citer que deux, constituent un "code histone" qui est écrit, lu et effacé par des facteurs spécifiques pour arriver à une régulation fine des fonctions nucléaires (transcription, réplication et réparation) au cours du développement et de la différenciation cellulaire. Cette régulation étroite est corrompue

dans les cancers, d'où l'intérêt particulier du ciblage thérapeutique des mécanismes de régulation épigénétique dans les traitements anticancéreux *(1)*. Dans ce cadre, on connaît déjà les inhibiteurs des histones déacétylases et les agents hypométhylants de l'ADN. Les protéines BET (protéines à *Bromodomain and ExtraTerminal domain*) émergent comme des facteurs pivots dans la transformation maligne, la progression tumorale et la résistance aux traitements *(2, 3)*. Les mécanismes sous-jacents sont complexes et font intervenir l'ensemble de leurs activités de régulation de la transcription ***(figure)*** *[2]*.

Fonctions des protéines BET

La famille des protéines BET comprend 3 protéines d'expression ubiquitaire – BRD2, BRD3 et BRD4 – et une protéine d'expression restreinte au testicule, BRDT. Leur fonction est la régulation génique en *cis* ou en *trans*. Les protéines BET ont 2 bromodomaines communs, BD1 et BD2, en N-terminal, et un domaine C-terminal dit "extraterminal" ***(figure)***. La structure des bromodomaines comporte 4 hélices alpha séparées par une région variable en boucle. L'ensemble forme une cavité hydrophobe qui reconnaît l'acétyl-lysine *(4, 5)*. Les bromodomaines sont des zones d'interaction de très forte affinité pour la chromatine acétylée, soit au niveau des promoteurs de gènes, soit au niveau de régions régulatrices agissant à distance, telles que les éléments *enhancers*. L'interaction des protéines BET avec les lysines mono-acétylées semble de faible affinité comparativement aux interactions observées sur des lysines poly-acétylées et/ou rapprochées.
Outre cette interaction avec la chromatine acétylée, les protéines BET interagissent avec les facteurs d'élongation de la transcription et avec des facteurs de transcription au niveau des promoteurs de gènes, mais aussi au sein d'éléments régulateurs *en cis*. Ainsi, les protéines BET constituent des protéines "lectrices", clés de l'interprétation de l'information épigénétique dans les cellules normales ou transformées *(3)*.

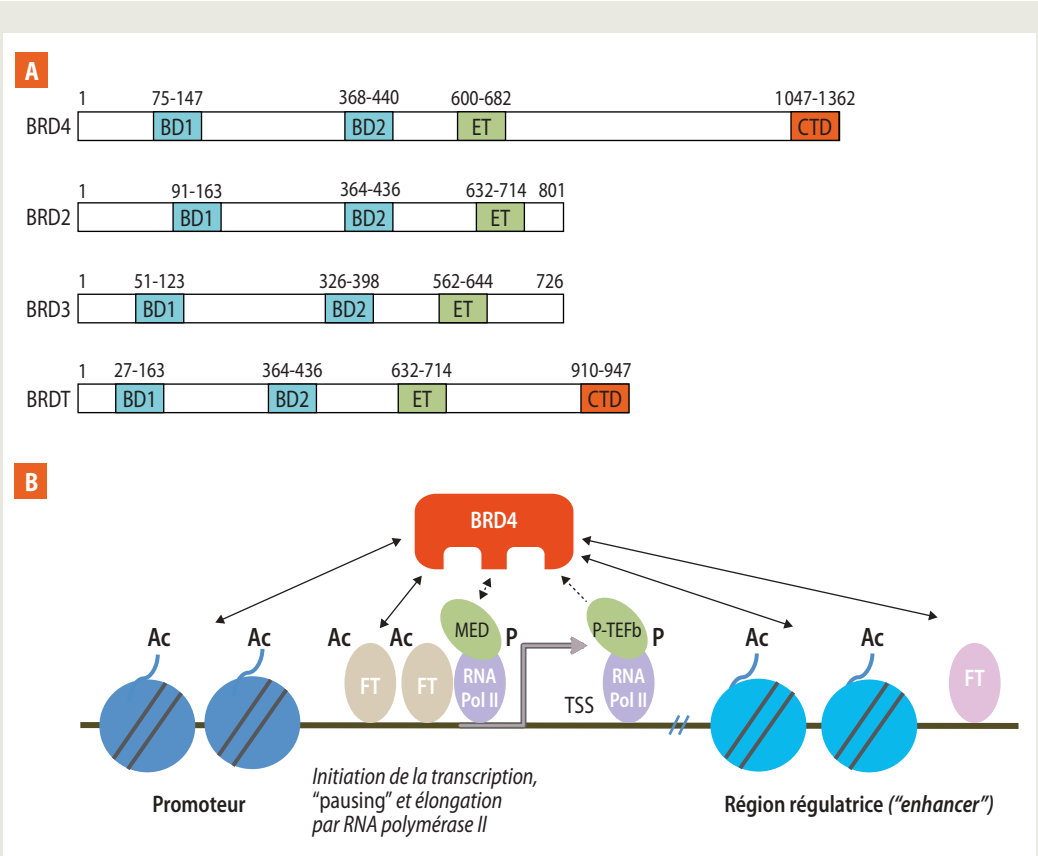

Figure. Schéma récapitulant l'organisation en domaines **(A)** et les principaux mécanismes de régulation transcriptionnelle médiée par les protéines BET **(B)**.

BRD4 et régulation transcriptionnelle

BRD4 est un membre particulièrement bien étudié de la famille des protéines BET. BRD4 interagit avec les complexes d'initiation et d'élongation de la transcription, respectivement Mediator (MED) et P-TEFb. Le complexe MED, composé de 26 sous-unités chez les mammifères, joue un rôle essentiel dans l'initiation de la transcription, en aval des cascades de signalisation, ainsi que dans la régulation fonctionnelle d'éléments *enhancers*. Le complexe P-TEFb est composé de la kinase dépendant des cyclines, CDK9, et d'une de ses sous-unités régulatrices, la cycline T1 ou la cycline T2. L'activité kinase de CDK9 inhibe la fonction de régulateurs négatifs de l'activité ARN pol II et stimule l'élongation d'ARN pol II par phosphorylation *(6)*. Au moins 2 régions différentes de BRD4 interagissent directement avec P-TEFb : la région C-terminale avec la cycline T1 et CDK9, et la région BD2 avec la zone acétylée de la cycline T1. L'interaction BRD4/P-TEFb joue un rôle central dans l'initiation rapide de la transcription après la fin de la mitose.

Le domaine ET est impliqué dans la régulation transcriptionnelle via son interaction avec des facteurs de modification des histones tels que JMJD6, une arginine déméthylase, et NSD3, une lysine méthyltransférase *(7, 8)*. De plus, le domaine ET est capable de s'associer avec les enzymes de remodelage de la chromatine ATP dépendantes, SWI-SNF et CHD2 *(8)*. Ces interactions permettraient à BRD4 de moduler localement l'état de la chromatine, mais la signification régulatrice de ces événements n'est pas encore élucidée. Cependant, un rôle dans le déblocage d'une "pause" de l'activité ARN polymérase II est suggéré *(7)*.

La distribution de la protéine BRD4 a été étudiée en détail dans le génome par les techniques d'immunoprécipitation de la chromatine et de séquençage nouvelle génération (NGS). Ces travaux montrent une large distribution de BRD4 au travers du génome, avec un enrichissement au niveau des régions promotrices des gènes, sites d'initiation de la transcription. BRD4 est aussi présente au niveau des régions intergéniques, en particulier au sein de séquences d'ADN régulatrices appelées *enhancers*, qui agissent à distance pour stimuler l'activité génique *(9)*.

L'interaction de BRD4 avec les éléments *enhancers* coïncide avec celle du complexe Mediator (sous-unité M1) et avec un enrichissement en histone H3 acétylée sur la lysine 27 (H3K27) qui constitue un marqueur épigénétique actif. Parmi les éléments *enhancers* régulés par BRD4/BET, on distingue les *superenhancers,* caractérisés par un corecrutement étendu, par des taux élevés de BRD4 et de MED1, et par la marque H3K27 acétylée. Il est intéressant de noter que l'activité du complexe MED au niveau des *superenhancers* implique son association réversible avec un module contenant CDK8 et les cofacteurs CCNC, MED12 et MED13. Pour mémoire, des mutations de MED2 sont décrites dans les leucémies lymphoïdes chroniques (LLC) *[10]*. La colocalisation des complexes MED-CDK8 avec BRD4 au niveau des *superenhancers* soulève un vif intérêt dans les cancers, car elle offre des possibilités de ciblage thérapeutique via des inhibiteurs BET et/ou de CDK8. Une preuve de concept a récemment été obtenue dans les leucémies aiguës myéloblastiques (LAM) *[11]*.

Le recrutement de BRD4 sur les régions *enhancers* des gènes semble au moins en partie dépendre de l'interaction préalable de facteurs de transcription spécifiques et de l'activité d'histones acétyltransférases comme p300/CBP *(12)*. Le recrutement de BRD4 dans ce contexte est essentiel à l'activité fonctionnelle de nombreux facteurs de transcription hématopoïétiques tels que PU.1, FLI1, ERG, C/EBPα, C/EBPβ et MYB *(12)*. Les *superenhancers*, qui peuvent être considérés comme un regroupement d'*enhancers* conventionnels, sont impliqués dans la régulation de gènes codant des facteurs de contrôle des programmes transcriptionnels de l'identité cellulaire. La présence des protéines BET au niveau des *enhancers* et des *superenhancers* est aussi directement impliquée dans la dérégulation de nombreux proto-oncogènes. C'est par exemple le cas pour la dérégulation du gène *MYC* avec la t(8;14) qui rapproche *MYC* du *superenhancer* du gène codant les chaînes lourdes des immunoglobulines dans le lymphome B de Burkitt ou le myélome multiple (MM) *[13-16]*, ou pour le gène *EVI1* dans les LAM présentant une inversion du chromosome 3q *(17)*.

La protéine BRD4 est également capable d'interagir directement, de manière dépendante ou non de son bromodomaine, avec d'autres facteurs de transcription, régulant ainsi leur activité de liaison à l'ADN. Le rôle de cette fonction reste peu étudié dans les hémopathies malignes, mais serait très certainement important pour l'activité thérapeutique des inhibiteurs BET. Par criblage biochimique, il a été montré que la région régulatrice C-terminale de p53 interagit avec BRD4 de manière indépendante des bromodomaines *(18)*. Cette interaction nécessite la phosphorylation de BRD4 par la caséine kinase II (CK2) et régule l'activité de liaison à l'ADN de p53. En l'absence de phosphorylation, BRD4 interagit avec p53 au sein d'un complexe inactif, incapable d'interagir avec l'ADN. La phosphorylation de BRD4 lève aussi l'auto-inhibition du deuxième bromodomaine, ce qui permet son inter-

action avec la chromatine acétylée. Dans la même étude, d'autres facteurs de transcription sont décrits comme interagissant avec BRD4 : YY1, c-Jun, AP2, et l'hétérodimère MYC/MAX *(18)*.
Une autre étude a montré une interaction dépendante des bromodomaines entre BRD4 et la sous-unité RelA du facteur de transcription hétérodimérique, NF-κB. Cette interaction dépend de l'acétylation de RelA et serait essentielle pour l'activité de régulation transcriptionnelle de NF-κB *(19)*. La signalisation NF-κB joue un rôle central dans le système immunitaire et dans les cancers, en particulier les lymphomes. En effet, cette signalisation est engagée suite à la stimulation de récepteurs de surface tels que les *Toll-like receptors* (TLR) *[20]*.

Protéines BET comme cibles thérapeutiques : les inhibiteurs de BET

Les fonctions multiples des protéines BET dans la régulation épigénétique de la cellule sont au cœur de leur activité oncogénique dans de nombreux cancers, allant de la leucémie aiguë aux lymphomes et aux tumeurs solides *(3)*.
La résolution de la structure cristallographique de l'interaction entre un domaine BD et une lysine acétylée a permis le développement des premières petites molécules inhibitrices des protéines BET *(21, 22)*. En entrant en compétition avec les lysines acétylées, ces molécules inhibitrices, JQ1 et I-BET, bloquent les fonctions des protéines BET. Une activité antitumorale a été démontrée très tôt avec JQ1 dans des cancers *MYC*-dépendants comme le lymphome de Burkitt et le MM *(13, 14)*. Le traitement des cellules de lymphome de Burkitt par JQ1 induit un arrêt du cycle en G1/S et la répression du gène *MYC*, coïncidant avec la perte de BRD4 et CDK9 au niveau du promoteur du gène *MYC*. Dans les lignées de MM, des effets similaires ont été observés. De plus, le traitement par JQ1 induit la sénescence des cellules de MM, ce qui évoque des activités dépendant du contexte cellulaire pour les inhibiteurs BET. Il faut noter que les MM présentent de manière fréquente des amplifications partielles du chromosome 19p, alors que le gène de BRD4 est localisé en 19p13. Très rapidement, l'efficacité antileucémique des inhibiteurs de BET a été démontrée dans les LAM avec réarrangement *MLL (22, 23)*. En particulier, la molécule I-BET (GSK1210151A - I-BET151) provoque un arrêt du cycle et une induction d'apoptose dans un large spectre de LAM avec réarrangement *MLL*. Ces effets peuvent être attribués à l'inhibition de gènes clés comme *BCL2*, *C-MYC* et *CDK6*, en raison de la capacité de l'inhibiteur de BET à déloger BRD3/4 et des protéines spécifiques de régulation de l'élongation transcriptionnelle qui sont des partenaires de fusion fréquents de *MLL* dans les LAM *(24)*. Il a depuis été montré que les LAM présentant une mutation de *NPM1* ont une sensibilité accrue aux inhibiteurs de BET *(25)*. Cela serait en relation avec la capacité de NPM à interagir avec BRD4 et à bloquer ses fonctions. Dans les LAM mutées contenant une protéine NPM cytoplasmique, ce blocage est levé, ce qui conduit à l'induction par BRD4 d'un programme transcriptionnel spécifique essentiel à la prolifération des cellules leucémiques. Le traitement par un inhibiteur de BET permet de bloquer ce programme *(25)*. L'efficacité des inhibiteurs de BET a également été démontrée dans les leucémies aiguës lymphoblastiques (LAL) B et T *(2)* et dans les lymphomes diffus à grandes cellules B (LDGCB) *[26, 27]*.

Tableau. Essais cliniques avec inhibiteurs des protéines BET dans les hémopathies malignes.

NCT numéro de l'essai clinique	Inhibiteur de bromodomaine	Phase	Pathologie	Population cible
NCT01713582	OTX015	I	LAM, LAL, LMNH, MM	Rechute/réfractaire
NCT01949883	CPI-0610	I	LMNH, MH	Réfractaire
NCT02157636	CPI-0610	I	MM	Rechute
NCT02158858	CPI-0610	I	LAM, SMD, SMP	Rechute
NCT01587703	GSK525762	I/II	*NUT midline carcinoma*, autres tumeurs solides, MM	Au diagnostic
NCT01943851	GSK525762	I/II	LAM, SMP, LMNH, MH, MM	Rechute/réfractaire
NCT02308761	TEN-010	I	LAM, SMD	Rechute/réfractaire
NCT02369029	BAY1238097	I	LAM, LMNH, MM, tumeurs solides	Réfractaire

LAM : leucémie aiguë myéloïde ; LAL : leucémie aiguë lymphoblastique ; LMNH : lymphome malin non hodgkinien ; MM : myélome multiple ; MH : maladie de Hodgkin ; SMD : syndrome myélodysplasique ; SMP : syndrome myéloprolifératif.

Les traitements combinés incluant des inhibiteurs de BET présentent un intérêt non négligeable. En effet, des phénomènes de résistance de novo ou acquise à un traitement BET inhibiteur seul commencent à être décrits dans les LAM *(28)*. Ces résistances impliquent la perte ou le gain de certaines voies de régulation génique, PRC2 et la voie WNT, respectivement.

Dans ce contexte, notre équipe a identifié, par une approche protéomique, un nouveau circuit de régulation faisant intervenir la protéine CYCLON en collaboration avec MYC. L'activité de ce circuit définit un sous-groupe de lignées cellulaires de LDGCB sensibles à un traitement combiné par inhibiteurs de BET et anticorps anti-CD20 (rituximab). En revanche, la surexpression seule (en l'absence de MYC) de CYCLON définit un sous-groupe de LDGCB résistants à ce traitement combiné. Ainsi, CYCLON serait un biomarqueur de l'activité antilymphomateuse d'un traitement combinant anti-CD20 et inhibiteurs de BET *(27)*.

Développement clinique

Les résultats précliniques encourageants ont déjà incité certains investigateurs à mettre en place des essais précoces dans les hémopathies malignes *(tableau, p. 57)* [données actualisées sur le site Internet du National Cancer Institute en novembre 2015). Les résultats de ces essais, combinés à ceux des études précliniques, vont permettre de mieux identifier les patients susceptibles de répondre à un traitement par inhibiteurs de BET. À l'avenir, les stratégies thérapeutiques vont sûrement reposer sur des traitements combinés adaptés aux mécanismes physiopathologiques pertinents (génétiques et épigénétiques) de chaque pathologie. ■

Les auteurs n'ont pas précisé leurs éventuels liens d'intérêts.

Remerciements

Les auteurs remercient l'Institut national du cancer "programme épigénétique et cancer" et la délégation à la recherche clinique et à l'innovation du CHU de Grenoble pour leur soutien financier des travaux de recherche de l'équipe "Génétique et épigénétique des cancers lymphoïdes". M. Callanan remercie Sieme Hamaidia, Patricia Betton, Sarah Bertrand, Céline Suchaud-Martin, Isabelle Putaud et Martine Chauvet pour la qualité de leur contribution aux travaux de recherche et d'innovation diagnostique de l'équipe.

Références

1. *Chi P, Allis CD, Wang GG. Covalent histone modifications--miswritten, misinterpreted and mis-erased in human cancers. Nat Rev Cancer 2010;10(7):457-69.*

2. *Basheer F, Huntly BJ. BET bromodomain inhibitors in leukemia. Exp Hematol 2015;43(8):718-31.*

3. *Shi J, Vakoc CR. The mechanisms behind the therapeutic activity of BET bromodomain inhibition. Mol Cell 2014;54:728-36.*

4. *Dhalluin C, Carlson JE, Zeng L, He C, Aggarwal AK, Zhou MM. Structure and ligand of a histone acetyltransferase bromodomain. Nature 1999;399(6735):491-6.*

5. *Morinière J, Rousseaux S, Steuerwald U et al. Cooperative binding of two acetylation marks on a histone tail by a single bromodomain. Nature 2009;461(7264):664-8.*

6. *Zhou Q, Li T, Price DH. RNA polymerase II elongation control. Ann Rev Biochem 2012;81:119-43.*

7. *Liu W, Ma Q, Wong K et al. Brd4 and JMJD6-associated anti-pause enhancers in regulation of transcriptional pause release. Cell 2013;155(7):1581-95.*

8. *Rahman S, Sowa ME, Ottinger M et al. The Brd4 extraterminal domain confers transcription activation independent of pTEFb by recruiting multiple proteins, including NSD3. Mol Cell Biol 2011;31(13):2641-52.*

9. *Loven J, Hoke HA, Lin CY et al. Selective inhibition of tumor oncogenes by disruption of super-enhancers. Cell 2013;153(2):320-34.*

10. *Damm F, Mylonas E, Cosson A et al. Acquired initiating mutations in early hematopoietic cells of CLL patients. Cancer Discov 2014;4(9):1088-101.*

11. *Pelish HE, Liau BB, Nitulescu II et al. Mediator kinase inhibition further activates super-enhancer-associated genes in AML. Nature 2015;526(7572):273-6.*

12. *Roe JS, Mercan F, Rivera K, Pappin DJ, Vakoc CR. BET bromodomain inhibition suppresses the function of hematopoietic transcription factors in acute myeloid leukemia. Mol Cell 2015;58(6):1028-39.*

13. *Delmore JE, Issa GC, Lemieux ME et al. BET bromodomain inhibition as a therapeutic strategy to target c-Myc. Cell 2011;146(6):904-17.*

14. *Mertz JA, Conery AR, Bryant BM et al. Targeting MYC dependence in cancer by inhibiting BET bromodomains. Proc Natl Acad Sci U S A 2011;108(40):16669-74.*

15. *Roderick JE, Tesell J, Shultz LD et al. c-Myc inhibition prevents leukemia initiation in mice and impairs the growth of relapsed and induction failure pediatric T-ALL cells. Blood 2014;123(7):1040-50.*

16. *Tolani B, Gopalakrishnan R, Punj V, Matta H, Chaudhary PM. Targeting Myc in KSHV-associated primary effusion lymphoma with BET bromodomain inhibitors. Oncogene 2014;33(22):2928-37.*

17. *Gröschel S, Sanders MA, Hoogenboezem R et al. A single oncogenic enhancer rearrangement causes concomitant EVI1 and GATA2 deregulation in leukemia. Cell 2014;157(2):369-81.*

18. *Wu SY, Lee AY, Lai HT, Zhang H, Chiang CM. Phospho switch triggers Brd4 chromatin binding and activator recruitment for gene-specific targeting. Mol Cell 2013;49(5):843-57.*

19. *Huang B, Yang XD, Zhou MM, Ozato K, Chen LF. Brd4 coactivates transcriptional activation of NF-kappaB via specific binding to acetylated RelA. Mol Cell Biol 2009;29(5):1375-87.*

20. *Hayden MS, Ghosh S. NF-kappaB, the first quarter-century: remarkable progress and outstanding questions. Genes Dev 2012;26(3):203-34.*

21. *Filippakopoulos P, Qi J, Picaud S et al. Selective inhibition of BET bromodomains. Nature 2010;468(7327):1067-73.*

22. *Nicodeme E, Jeffrey KL, Schaefer U et al. Suppression of inflammation by a synthetic histone mimic. Nature 2010;468(7327):1119-23.*

23. *Dawson MA, Prinjha RK, Dittmann A et al. Inhibition of BET recruitment to chromatin as an effective treatment for MLL-fusion leukaemia. Nature 2011;478(7370):529-33.*

24. *Zuber J, Shi J, Wang E et al. RNAi screen identifies Brd4 as a therapeutic target in acute myeloid leukaemia. Nature 2011;478(7370):524-8.*

25. *Dawson MA, Gudgin EJ, Horton SJ et al. Recurrent mutations, including NPM1c, activate a BRD4-dependent core transcriptional program in acute myeloid leukemia. Leukemia 2014;28(2):311-20.*

26. *Chapuy B, McKeown MR, Lin CY et al. Discovery and characterization of super-enhancer-associated dependencies in diffuse large B cell lymphoma. Cancer Cell 2013;24(6):777-90.*

27. *Emadali A, Rousseaux S, Bruder-Costa J et al. Identification of a novel BET bromodomain inhibitor-sensitive, gene regulatory circuit that controls Rituximab response and tumour growth in aggressive lymphoid cancers. EMBO Mol Med 2013;5(8):1180-95.*

28. *Rathert P, Roth M, Neumann T et al. Transcriptional plasticity promotes primary and acquired resistance to BET inhibition. Nature 2015;525(7570):543-7.*